2 Cys Bulk

FACILITY FORM 602

N66-15266
(ACCESSION NUMBER)

(THRU)

244
(PAGES)

1
(CODE)

CR 69236
(NASA CR OR TMX OR AD NUMBER)

31
(CATEGORY)

GPO PRICE $ _____

CFSTI PRICE(S) $ _____

Hard copy (HC) 3.00

Microfiche (MF) 1.50

ff 653 July 65

JET PROPULSION LABORATORY
CALIFORNIA INSTITUTE OF TECHNOLOGY
PASADENA, CALIFORNIA

RE-ORDER NO. 64-522

CONCEPTUAL DESIGN STUDIES OF AN ADVANCED MARINER SPACECRAFT

Volume II
Systems Analysis

Prepared by

RESEARCH AND ADVANCED DEVELOPMENT DIVISION
AVCO CORPORATION
Wilmington, Massachusetts

RAD-TR-64-36
Contract 950896

This work was performed for the Jet Propulsion Laboratory, California Institute of Technology, sponsored by the National Aeronautics and Space Administration under Contract NAS7-100.

Prepared for

CALIFORNIA INSTITUTE OF TECHNOLOGY
JET PROPULSION LABORATORY
4800 Oak Grove Drive
Pasadena, California

228 PAGES INCLUDE (15 ROMAN NUMERIAL)

1 of

RE-ORDER No. 64-522

This document consists of 230 pages,
200 copies, Series A

CONCEPTUAL DESIGN STUDIES OF AN ADVANCED MARINER SPACECRAFT

Volume II
Systems Analysis

Prepared by

RESEARCH AND ADVANCED DEVELOPMENT DIVISION
AVCO CORPORATION
Wilmington, Massachusetts

RAD-TR-64-36
Contract 950896

Prepared for

CALIFORNIA INSTITUTE OF TECHNOLOGY
JET PROPULSION LABORATORY
4800 Oak Grove Drive
Pasadena, California

II

RE-ORDER No. 64-522

SUMMARY

This report presents the results of a 4-month parametric analysis and conceptual design study conducted by the Research and Advanced Development Division of Avco Corporation for the Jet Propulsion Laboratory. The study objectives included a parametric analysis of the unmanned Flyby Bus/Lander concept for scientific investigation of Mars during the 1969 and 1971 launch opportunities, a conceptual design of the selected configuration, and a development and cost plan indicating the program leading to development and first flight of the Advanced Mariner Vehicle in 1969.

The Flyby/Lander concept utilizes a 1493 pound spacecraft launched on an Atlas Centaur launch vehicle. The scientific capability of the lander and flyby bus vehicles were determined to obtain a balance between scientific data and overall systems complexity commensurate with the first landing mission to Mars.

The lander vehicle separates from the flyby bus vehicle prior to planet encounter, enters the planetary atmosphere, and descends to the surface on a parachute. During atmospheric entry parachute descent, and surface operations, the lander analyzes the Martian atmosphere; and for five hours after impact determines wind velocity as well as performing a simple life detection experiment. The information is transmitted to Earth via both a direct transmission link to the D. S. I. F. and is also relayed through the flyby bus which has been placed on a delayed flyby trajectory for this purpose. The flyby bus also collects interplanetary data and maps the planet. The lander vehicle has been designed to accommodate the minimum projected atmosphere for Mars (11 millibar surface pressure) and surface winds gusting to 200 ft/sec resulting in impact loads of up to 1500 g for a landed payload protected by crushable material. The lander is to be dry-heat sterilized to avoid contamination of Mars with Earth organisms while the flyby bus is placed on a biased trajectory providing a small probability of entering the planetary atmosphere and therefore is not required to be sterilized.

The development plan shows that a minimum of three launch attempts are necessary to achieve an 84 percent chance of a successful mission in the 1969 and 1971 launch opportunities requiring that hardware development begin in early 1965 to meet a 1969 launch date.

RE-ORDER No. 64-522

CONTENTS

RE-ORDER No.64-522

ILLUSTRATIONS

RE-ORDER No. 64-522

ILLUSTRATIONS (Cont'd)

RE-ORDER No. 64-522.

ILLUSTRATIONS (Cont'd)

RE-ORDER No. 64-522.

ILLUSTRATIONS (Cont'd)

RE-ORDER No. 64-522

ILLUSTRATIONS (Cont'd)

RE-ORDER No. 64-522

ILLUSTRATIONS (Cont'd)

RE-ORDER No. 64-522.

ILLUSTRATIONS (Cont'd)

RE-ORDER No. 64-522

ILLUSTRATIONS (Concl'd)

RE-ORDER No. 64-522

TABLES

RE-ORDER No. 64-522

TABLES (Concl'd)

RE-ORDER No. 64-522

1.0 INTRODUCTION

The systems analysis volume presents the results of mission analysis, trajectory analysis and payload studies accomplished for the Advanced Mariner Study Program. A factory to launch and mission sequence is included together with a definition of the anticipated environments to outline the sequential steps throughout the assembly; test, launch, and mission phases of the program. A mission plan is developed to indicate the number and type of spacecraft required to attain a reasonable probability of success in accomplishing the total mission objectives.

The trajectory data presented detail the anticipated departure, transit, approach, encounter, and post encounter parameters of importance with particular emphasis on launch window selection and flyby bus/lander separation analysis. The data presented in this volume are used extensively in developing the flyby bus and lander parametric analyses and conceptual designs presented in volumes III and IV.

RE-ORDER No. 64-522

2.0 MISSION ANALYSIS

2.1 MISSION OBJECTIVES

The Advanced Mariner Study Program provided a five-month parametric evaluation and conceptual design of the Flyby bus/Lander mission for the 1969 and 1971 launch opportunities to Mars. In order to proceed with the study program, mission objectives and constraints were established. These serve to direct and restrain the spacecraft design into the size, weight and performance class appropriate for the first unmanned lander mission to another planet. The Jet Propulsion Laboratory specified a set of mission objectives at the initiation of the study program. These were:

1. Demonstrate the capability of successful landing and survival on the planetary surface for several hours.

2. Successfully perform a simple biological experiment on the planet's surface for a period of five hours.

3. Extend the lifetime of the above biological experiment.

Implied in these objectives is successful operation of the flyby bus vehicle through completion of its lander support mission, lander separation, and any subsequent operations necessary for relay communications from the lander through the flyby bus to Earth.

In order to synthesize reasonable lander scientific payloads for the parametric evaluation and conceptual design studies, the first JPL mission objective was modified to include such diagnostic data as is necessary to evaluate spacecraft performance in compliance with the "land and survive" objective.

The third JPL objective was implemented by attempting to augment the simple biological experiment with a second simple biological experiment operating on a different life detection principle while extending the surface lifetime to 24 and 48 hours.

A fourth mission objective was added by Avco:

4. Obtain scientific and engineering data in support of future lander missions to Mars.

This objective includes data concerning the atmospheric properties; density profile, temperature profile, pressure profile, scale height, wind velocity, and atmospheric composition as well as surface topographical and geological data. This data should be sufficient to resolve at least partially the many uncertainties concerning the Martian atmospheric and surface properties which

RE-ORDER No. 64-522

presently force an extremely conservative approach to the design of a lander vehicle. The design of future landers in the Voyager and Manned Martian lander classes is heavily dependent upon good information concerning the entry, descent, impact, and surface operation phases of these more complex and costly vehicles which are necessarily more sensitive to anomalies in the atmospheric and surface properties of the planet.

2. 2. FACTORY TO LAUNCH SEQUENCE

Figure 1 shows a general hardware flow plan from initial assembly of the spacecraft subsystems through typical significant operations to launch. It is intended that various classes of clean room facilities or protective packaging will be utilized from the original manufacture of the piece parts, their assembly into subsystems, throughout all test operations and operations at the launch site. These clean room techniques will be most beneficial in maintaining the highest standards of total spacecraft assembly, and will increase the probability of adequate Lander sterilization by minimizing any biological contamination before the final heat sterilization.

The test and checkout procedures shown in the flow plan consider sterilization and final test site to be remote from the assembly and test site, due to the explosive nature of the lander pyrotechnics during the high temperatures of sterilization. The transfer and shipping criteria between any of the facilities from assembly to launch will require definition to establish the type protective ground support and handling equipment needed.

The concept presented assumes a majority of the spacecraft, subsystems are prepackaged and are adaptable to automatic checkout procedures to minimize all the checkout tests, but most important, to minimize the launch pad handling and operations.

2. 3 FLIGHT SEQUENCE

The Advanced Mariner flight sequence as shown in table 1 follows as closely as possible the Mariner 64 flight sequence. However the new launch vehicle, and the addition of the lander force, some significant changes. These changes are particularly apparent in the launch sequence, in the flyby bus/lander separation-flyby bus slowdown maneuver sequence. In addition, a completely new sequence, table 2, has been added for the lander after separation from the flyby bus. Several less apparent modifications have been necessary to accommodate the lander, such as trickle charging of the lander battery during the spacecraft cruise mode, powering of lander thermal control heaters from the flyby bus during the cruise mode, and receipt of relay communications from the lander during the encounter phase of the mission.

Particular attention has been applied to synthesis of the flyby bus/lander separation sequence. The sequence finally selected represents extensive analysis

RE-ORDER No. 64-522

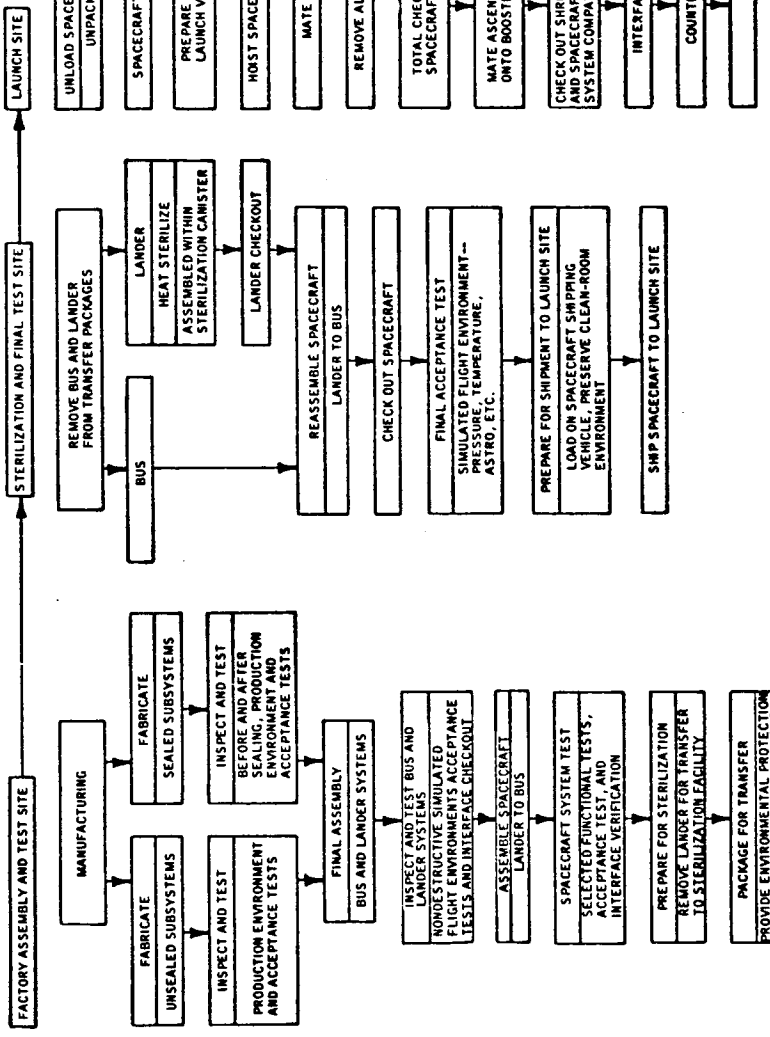

Figure 1 FACTORY TO LAUNCH SEQUENCE

TABLE 1

SPACECRAFT FLIGHT SEQUENCE

Event	Time	Source	Destination	Comments
1. Subsystem Checkout	T-120 min.	GCE	All systems	
2. Update CC and S Stored Data	T-10 min.	GCE	CC and S	Update all timed events which vary with trajectory (launch date and time)
3. Switch to Internal Power	T-5 min.	GCE	Power	
4. Release CC and S Lockout	T-3 min.	GCE	CC and S	Enable launch sequence
5. Initiate CC and S Clock	T-1 min.	GCE	CC and S	Initiate launch sequence
6. Atlas Engine ignite	T-18 sec.	Engine	Atlas	
6A. Release spacecraft umbilical		GCE	Pyrotechnics	Emergency control available through booster umbilical
7. Liftoff	T-0	Event		
8. Programmed Pitchover	T + 15 sec.	Atlas G and C	Atlas TVC	Attitude maneuver for proper parking orbit
9. Booster engine cut off (BECO)	T + 143 sec.	Atlas G and C	Atlas engine	
10. Booster package staging	T + 146 sec.	Atlas G and C	Atlas pyrotechnics	
11. Insulation package staging	T + 170 sec.	Atlas G and C	Atlas pyrotechnics	Remove ascent heat protection
12. Nose fairing	T + 206 sec.	Atlas G and C	Atlas pyrotechnics	Remove ascent heat protection
12A. RF power on (Data Mode 2 preset)			Power	
12B. Cruise mode science on		Centaur G and C		

Data Mode 1-Maneuvers
Data Mode 2-Launch, acquisition, cruise
Data Mode 3-Lander Preseparation
Data Mode 4-Encounter
Data Mode 5-Post Encounter

RE-ORDER No. 64-522

TABLE 1 (Cont'd)

Event	Time	Source	Destination	Comments
13. Sustainer engine cut off (SECO)	T + 238 sec.	Atlas G and C	Atlas propulsion	
14. Vernier engine cut off (VECO)	T + 247.5 sec.	Atlas G and C	Atlas propulsion	
15. Centaur ignition	T + 248 sec.	Centaur G and C	Centaur propulsion	
16. Atlas-Centaur separation	T + 248.6 sec.	Atlas G and C	Centaur pyrotechnics	
17. Parking orbit injection	T + 567 sec.	Event		
18. Centaur cut off		Centaur G and C	Centaur propulsion	
19. Centaur attitude maneuver		Centaur G and C	Centaur A/C	Prevents excessive propellant boil-off
20. End Centaur attitude maneuver		Centaur G and C	Centaur A/C	Selects proper transfer trajectory
21. Centaur ignition	T + 2500 sec. (typ.)	Centaur G and C	Centaur propulsion	
22. Centaur cut off		Centaur G and C	Centaur propulsion	
23. Spacecraft injection	I-O	Event		
24. Spacecraft separation	s = I + 3 min. (T + 2800 sec., nom)	Centaur G and C		
24A. RF Power on		Separation Switch	Power	Backup to events 12A and 12B
24B. Cruise mode science on			Power	
24C. Enable CC and S master sequence			CC and S	
24D. Close pyrotechnics arming switch			Pyrotechnics	
24E. Start separation initiated timer				
25A. Arm pyrotechnic system	s + 25 sec.	SIT	Pyrotechnics	

RE-ORDER No. 64-522-

TABLE 1 (Cont'd)

Event	Time	Source	Destination	Comments
25B. Event marker	s + 60 sec.	SIT	Data Encoder	Indicates separation.
26A. Deploy solar panels	s + 80 sec.	SIT	Pyrotechnics	
26B. Activate ACS		SIT	ACS	
27. Deploy solar panels	T + 50 min. s + 2 min.	CC and S	Pyrotechnics	Backup to event 26A
28. Activate attitude control system	T + 52 min. s + 4 min.	CC and S	A/C	Backup to event 26B
29. Acquire Sun	0 to 7 min.	Event		Pitch and yaw attitude reference.
30. Acquire Canopus	0 to 20 min.	Event		Roll attitude reference.
31. Trajectory verification	T + 1 day	Event		DSIF tracking.
32. Transmit trajectory correction commands	T + 1 day			Commands may be for pitch and yaw angles and ΔV magnitude or pitch and yaw turn duration and polarity and burn duration.
32A. Pitch angle		QC - 1a		
32B. Yaw angle		QC - 1b DSIF	CC and S	
32C. Velocity magnitude (burn time)		QC - 1c		
33. Maneuver start command	m - O	DC - 27, DSIF	CC and S	
34. Activate gyros for warmup	m + 0 to 1 min.	CC and S	A/C	
34A. Switch to data mode 1.		CC and S	DAS	Backup: DC 1.
35. Switch spacecraft from cruise mode to inertial control	m + 60 min.	CC and S	A/C	
35A. Deactivate Canopus tracker		CC and S	A/C	
35B. Activate autopilot		CC and S	A/C	
35C. Transfer pitch command	m + 66 min(max)	CC and S	A/C	
35D. Start pitch turn		CC and S	A/C	
36. Stop pitch turn		CC and S	A/C	Magnitude inserted prior to maneuver initiation.

RE-ORDER No. 64-532

TABLE 1 (Cont'd)

Event	Time	Source	Destination	Comments
36A. Transfer yaw command		CC and S	A/C	
36B. Start yaw turn		CC and S	A/C	
37. Stop yaw turn	m + 73 min. (max.)	CC and S	A/C	Magnitude inserted prior to maneuver initiation.
38. Ignite midcourse motor	m + 73 min.	CC and S	Propulsion	Relay pulsed
39. Stop midcourse motor	m + 76 min. (1st midcourse)	CC and S	Propulsion	Relay pulsed. Magnitude inserted prior to maneuver initiation.
40. Switch to reference acquisition mode	m + 76 min. (1st midcourse)	CC and S	A/C	
41. Acquire Sun	0 to 6 min.	CC and S	A/C	
42. Acquire Canopus	0 to 20 min.	CC and S	A/C	
42A. Confirm reacquisition of Sun and Canopus		CC and S	A/C	
42B. Switch to data mode 2		CC and S	DAS	
43. Repeat events 31 through 42 for second midcourse correction, if required.	T + 10 days	QE - 1 a, QE - 1 b, QC - 1 c, DC - 27 DSIF	CC and S	
44. Set Canopus sensor cone angle 1	P - 262 days	CC and S	A/C	
45. Set Canopus sensor cone angle 2	P - 249 days	CC and S	A/C	
46. Set Canopus sensor cone angle 3	P - 237 days	CC and S	A/C	
47. Set Canopus sensor cone angle 4	P - 266 days	CC and S	A/C	
48. Set Canopus sensor cone angle 5	P - 216 days	CC and S	A/C	
49. Set Canopus sensor cone angle 6	P - 205 days	CC and S	A/C	
50. Set Canopus sensor cone angle 7	P - 193 days	CC and S	A/C	
51. Set Canopus sensor cone angle 8	P - 179 days	CC and S	A/C	

RE-ORDER NO. 64-532.

TABLE 1 (Cont'd)

Event	Time	Source	Destination	Comments
52. Set Canopus sensor cone angle 9	P - 161 days	CC and S	A/C	
53. Set Canopus sensor cone angle 10	P - 128 days	CC and S	A/C	
54. Switch to high gain antenna	P - 177 days	CC and S master timer	Radio subsystem	Maintain bit rate.
55. Set Canopus sensor cone angle 11	P - 84 days	CC and S	A/C	
56. Set Canopus sensor cone angle 12	P - 42 days	CC and S	A/C	
57. Set Canopus sensor cone angle 13	P - 14 days	CC and S	A/C	
58. Trajectory verification complete.		Event		
59. Transmit lander separation and bus slow-down commands.	A - 10 days (nom.)		CC and S	Separation command sequence stored by CC and S and updated via the DSIF.
59A. Separation pitch angle		QC - 2a		
59B. Separation yaw angle		QC - 2b		
59C. Cruise mode return delay		QC - 2c		
59D. Select data mode 3, monitor lander p. c. u. return to data mode 2		QC - 3a (DSIF)	Data bus encoder Lander pcu	
59E. Insert lander engine and atmospheric entry timing commands		QC - 3e-i		
59F. Repeat 59D		CC and S	Bus data encoder	
60. Transmit bus slowdown commands				
60A. Slowdown pitch angle		QC - 1a		
60B. Slowdown yaw angle		QC - 1b (DSIF)	CC and S	
60C. Slowdown burn time		QC - 1c		
61. Activate lander systems	S - 2 hrs.	QC - 3d, DSIF	Power	For precheck warmup, turn on bus power to lander.
62. Confirm lander systems checkout		CC and S	Lander systems checkout logic in CC and S	From lander pcu
		QC - 3a, DSIF	Data encoder	For data mode 3 to DSIF.

RE-ORDER No. 64-522

TABLE 1 (Cont'd)

Event	Time	Source	Destination	Comments
62A. IF systems go - arm lander pyrotechnics		CC and S logic	Lander pyro-technics	
63. Maneuver start command	M + 0 min.	DC - 28, DSIF	CC and S.	
64. Activate gyros for warmup	M to 1 min.		A/C	
65. Switch to data mode 3		CC and S	Data encoder	Backup for event 62.
66. Switch spacecraft from cruise mode to inertial control	M + 60 min.	CC and S	A/C	
66A. Deactivate Canopus tracker		CC and S	A/C	
66B. Activate autopilot		CC and S	A/C	
66C. Transfer pitch command		CC and S	A/C	
66D. Start pitch turn		CC and S	A/C	
67. Stop pitch turn	M + 66 min. (max.)	CC and S	A/C	
67A. Transfer yaw command		CC and S	A/C	
67B. Start yaw turn		CC and S	A/C	
68. Stop yaw turn	M + 72.5 min. (max.)	CC and S	A/C	
69. Arm separation system		CC and S	Pyrotechnics	When tiedowns and umbilical are cut, springs propel the lander from the bus at a relative velocity of 1.7 fps.
70. Fire separation pyrotechnics	S - 0	CC and S, S and ST	Pyrotechnics	To eject lander.
70A. Verify separation	S + 10 sec.	Event monitor	CC and S Event Marker	Monitor separation event.
70B. Transfer to maneuver sequence timer pitch command	S + 1 min. (M + 75 min.)			Stored for later transmission to DSIF.
71. Transfer pitch command		CC and S	A/C	
71A. Start pitch turn		CC and S	A/C	To orient bus for slowdown.

RE-ORDER NO. 64-1322.

TABLE 1 (Cont'd)

Event	Time	Source	Destination	Comments
72. Stop pitch turn	S + 6 min.	CC and S	A/C	Magnitude was preset.
72A. Transfer yaw command		CC and S	A/C	
72B. Start yaw turn		CC and S	A/C	To orient bus for slowdown retro.
73. Stop yaw turn	S + 12 min.	CC and S	A/C	Magnitude was preset.
74. Ignite propulsion system		CC and S	Propulsion	To slow down spacecraft to obtain proper approach geometry for relay.
75. Stop propulsion system	S + 27 Min.	CC and S	Propulsion	Timer preset by QC - 1c.
76. Switch to reference acquisition mode	M + 100 min. (nom.)	CC and S	A/C	To reacquire references. Also backup by timer in CC and S set by QC - 2c, delay time after lander separation to return to acquisition mode.
76A. Acquire Sun	0 to 6 min.	CC and S	A/C	Pitch and yaw attitude reference.
76B. Acquire Canopus	0 to 20 min.	CC and S	A/C	Roll attitude reference.
77. Confirm reacquisition of Sun and Canopus	M + 126 min. (e - 68 hrs.)			
77A. Turn on lander receiver and recorder		CC and S	Radio subsystem Power	Stays on for 2 hours.
77B. Switch to data Mode 2		CC and S	DAS	
78A. Receive, store lander pre-entry transmission	e - 68 hrs. (S + 1 hr.)	Lander	Bus telemetry	Relay later to DSIF.
78B. Turn off lander recorder	S + 2 hrs.	CC and S Master Timer	Power	
79A. Remove science covers and unlatch planetary scan platform and begin scan.	P - 17-2/3 hrs.	CC and S Master Timer	Pyrotechnics	Backup for DC - 25 from DSIF. Also starts wide angle planetary acquisition and tracking by planetary scan system.
79B. Encounter science on, tape recorder electronics on	P - 14-1/3 hrs.	CC and S Master Timer	Power	Preset before launch.

RE-ORDER No. 64-522

TABLE 1 (Concl'd)

Event	Time	Source	Destination	Comments
80. Planetary acquisition		PHP	DAS	
81. Switch to data mode 4	P - 11 hrs.	DAS	Data encoder	Real time transmission of encounter science to Earth.
82A. Turn on lander recorder on bus	e - 2 hrs.	CC and S Master Timer	Power	P - 7-2/3 hrs.
82B. Turn on encounter science recorder	P - 7-2/3 hrs.	CC and S Master Timer	Power	
83. Receive and store lander pre-entry transmission.	e - 2.0 hrs.	Lander	Lander recorder on bus	Store for later transmission to DSIF.
84. Lander atmospheric entry	e	Event		800,000 ft. altitude (P - 5-2/3 hrs.)
85. Receive and store lander descent transmission	e + 1 min. (min.)	Lander	Lander recorder on bus	Store for later transmission to DSIF.
86. Lander planetary impact	I		Event	e + 3 min. (min.)
87. Receive and record lander surface transmissions	I + 6 min.	Lander	DSIF.	
88. Start recording closest approach science data	P - 1.0 hrs.	CC and S Master Timer	Tape recorder.	
89. Periapsis passage	P	Event		
90. Stop recording	P +			When record takeup is full.
91. Switch to data mode 2	P + 2-1/3 hrs.	CC and S Master Timer	Encoder	
91A. Turn off encounter science	P + 2-1/3 hrs.	CC and S Master Timer	Power	
92. Switch to data mode 5	P + 5-2/3 hrs.	Encoder	Power	
92A. Turn off cruise science				
93. Set Canopus Sensor Cone Angle 14		CC and S	A/C	
94. End playback	P + 8 days			End of tape.
95. Switch to data mode 2		Encoder		After satisfactory playout.
95A. Turn on cruise science	P + 10 days	CC and S	Power	

RE-ORDER NO. 64-522-

TABLE 2

LANDER FLIGHT SEQUENCE

Event	Time	Source	Communication Mode*	Destination	Comments
1. Begin Lander thermal control		CC and S		Bus power supply	At time of event 24, spacecraft flight sequence.
2. Trickle charge lander batteries		CC and S		Bus power supply	As required.
3. Check out lander status		CC and S		Lander program control unit (pcu)	Commanded and confirmed through bus umbilical and bus communications system during interplanetary flight.
4. Command lander spacecraft separation timer, update lander programmer clock settings.		QC-3e to i, DSIF		Lander pcu	Commands are sent at time of event 59, spacecraft flight sequence, to update lander programmer controlling lander mission.
5. Verify commands		QC-3a, DSIF		Lander pcu	Through bus umbilical and bus communications system.
6. Activate lander systems		CC and S		Lander systems	
7. Confirm lander operational status a) Activate Mode I subsystems	S-2 hours	CC and S		Lander systems	Through bus umbilical and communications system.

*Mode I - Separation to Entry Data
Mode II - Entry to Impact Data
Mode III - Surface Data

RE-ORDER No. 64-522

28

TABLE 2 (Cont'd)

Event	Time	Source	Communication Mode	Destination	Comments
8. Activate pre-entry relay lander transmitter (10 percent RF power)	S-30 sec.	CC and S		Lander communications	Warm up transmitter.
9. Separate lander a) Start timer b) Monitor separation event	S-0 (Event)	CC and S		Separation subsystem	Physical separation activates separation timer and programmer.
10. Activate spin rockets a) Monitor event	S + 1 sec.	Lander pcu	Mode I	Lander communications	Sterilization shroud is split in four sections and spun off centrifugally.
11. Switch pre-entry relay transmitter to full power	S + 90 sec.	Lander pcu	Mode I	Lander communications	To acquire carrier link.
12. Activate axial accelerometer	S + 100 sec.	Lander pcu	Mode I	Lander accelerometer	To monitor magnitude of rocket impulse.
13. Transmit lander status (2 cycles)	S + 180 sec.	Lander pcu		Relay Bus	
14. Ignite lander rocket a) Monitor event	S + 200 sec.	Lander pcu	Mode I	Lander rocket	To alter lander trajectory.
15. Rocket thrust terminates a) Monitor event b) Obtain ΔV magnitude	S + 210 sec.		Mode I	 Lander communications	For control of magnitude of ΔV By breakwire circuit. By integrating accelerometer output.

RE-ORDER No. 64-522

TABLE 2 (Cont'd)

Event	Time	Source	Communication Mode	Destination	Comment
16. Activate despin system a) Monitor event	S + 220 sec.	Lander pcu	Mode I	Lander pyrotechnics	
17. Jettison ΔV rocket assembly a) Monitor event	S + 230 sec.	Lander pcu	Mode I	Lander pyrotechnics	Mechanical and electrical disconnect.
18. Turn off all systems	S + 240 sec.	Lander pcu	Mode I	Lander systems	
19. Timer times out; activates accutron	S + 2.3 days (max.)	Lander pcu	Mode I	Lander pcu	
20. Activate recorder	e-124 min.	Lander pcu	Mode I	Recorder	To monitor pre-entry event data.
21. Turn on pre-entry relay transmitter (10 percent RF power)	e-122 min.	Lander pcu	Mode I	Lander communications	For warmup.
a) Switch transmitter to full power		Lander pcu		Lander communications	To acquire carrier link.
22. Transmit lander status (2 cycles)	e-120 min.	Lander pcu	Mode I	Relay bus	
23. Turn off pre-entry relay transmitter	e-119 min.	Lander pcu	Mode I	Lander communications	
24. Entry a) Turn on descent transmitter (10 percent RF power)	e Event at time of 0.01 g ascending	g-actuated		Lander communications	

RE-ORDER No. 64-5222

TABLE 2 (Cont'd)

Event	Time	Source	Communication Mode	Destination	Comment
25. Activate Mode II subsystems and record data	At time of 0.1 g ascending	g-actuated	Mode II	Lander entry instruments	
26. Deploy drogue chute	e + 45 sec.	g-actuated timer	Mode II	Parachute systems	Barometric backup.
27. Jettison lander afterbody	e + 49 sec.	timer	Mode II	Pyrotechnic system	
28. Deploy main chute	e + 49 sec.	afterbody deployment	Mode II	Parachute system	Barometric backup.
29. Switch descent relay transmitter to full power	e + 49 sec.	Lander pcu	Mode II	Lander communications	For acquisition of carrier link.
30. Play out Mode II recorded data (2 cycles)	e + 59 sec.	Lander data system	Mode II	Lander DAS Relay bus	
31. Impact (Event)	e + 159 sec L = 0				
32. Activate Mode III subsystems, Record event data	L - 0	Lander pcu	Mode III	Lander systems	
33. Jettison crushup and deploy bio collector	L + 3 min.	Lander pcu	Mode III	Lander pyrotechnics	
34. Record science and engineering data	L + 3 min.	Lander pcu	Mode III	Lander DAS	

RE-ORDER No. 64-522

TABLE 2 (Cont'd)

Event	Time	Source	Communication Mode	Destination	Comment
35. Turn on surface transmitter (10 percent RF power)	L + 6.5 min.	Lander pcu	Mode III	Lander communications	To warm up transmitter.
36. Switch transmitter to full power	L + 8.5 min.	Lander pcu	Mode III	Lander communications	To acquire carrier link.
37. Start transmission of stored and new lander data	L + 10.0 min.	Lander communications	Mode III	Relay to Bus Direct to DSIF	
38. Turn off transmitter a) Record lander data	L + 24.0 min.	Lander pcu	Mode III	Lander communications	
39. Turn on surface transmitter (10 percent RF power)	L + 90.5 min.	Lander pcu	Mode III	Lander communications	Warmup.
40. Switch transmitter to full power	L + 92.5 min.	Lander pcu	Mode III	Lander communications	To acquire carrier link.
41. Start second transmission of landed data	L + 94 min.	Lander communications	Mode III	Relay to Bus Direct to DSIF	
42. Turn off transmitter	L + 95.8 min.	Lander pcu	Mode III	Lander communications	
43. Turn on surface transmitter (10 percent RF power)	L + 286.5 min.	Lander pcu	Mode III	Lander communications	Warmup.

RE-ORDER No. 64-522

TABLE 2 (Concl'd)

Event	Time	Source	Communication Mode	Destination	Comment
44. Switch transmitter to full power	L + 288.5 min.	Lander pcu	Mode III	Lander communications	To acquire carrier link.
45. Start third transmission of landed data Continue to transmit until battery power is depleted.	L + 290 min.	Lander communications	Mode III	Relay to Bus Direct to DSIF	

RE-ORDER No. 64-522

of many alternate approaches. The influence of flyby bus operations on the success of the lander mission was carefully considered and the constraints placed upon the flyby bus mission by the addition of the lander were analyzed in detail. The selected sequence appears to have the best overall operating characteristics, however, as an alternate sequence, the flyby bus could return to its reference SunCanopus orientation between the lander separation and flyby bus slowdown maneuvers. This sequence would allow the present "command control and sequencer" to remain unchanged as each of the four maneuver sequences could use the existing command sequence structure. A small penalty would result in the flyby bus thermal control and in the weight of battery required to accommodate the maneuver power requirements, since the maneuver sequence at lander separation would be lengthened, and sufficient time would not be available for battery recharge before flyby bus slowdown.

The lander mission sequence outlines the sequence of events and operations from lander separation through the five-hour mission on the planetary surface. Both relay and direct link communications have been included for redundancy and to explore the impact of both systems upon the spacecraft design. The lander mission as it is shown could be modified to extend its lifetime to 24 hours or to considerably increase the relay link data output without exceeding the Advanced Mariner capability. These alternate missions have not been explored in detail.

2.4 ENVIRONMENTAL REQUIREMENTS

The effect of the total environment on the flight hardware, with its subsequent influence on the associated aerospace ground equipment throughout the entire mission sequence, is one of the earliest design considerations. In many cases the Earth handling and test requirements will establish the design criteria. As an example, the Advanced Mariner design for the lander heat sterilization will probably be the most severe design constraint. In developing this conceptual design, these environmental influences were studied in two representative categories, Factory to Launch and Launch to Mission.

1. Factory to Launch Environmental Requirements

The criteria for design of the ground support equipment used throughout the Factory to Launch Sequence of operations is based on the environments encountered throughout this phase, as shown in table 3, whereby the major aspects of this handling equipment would be to maintain the spacecraft in the factory clean room environment throughout most of its Earth storage and life. Past studies of these expected environments have been updated for the Advanced Mariner mission sequences as presented herein. It was presumed that the transfer from the factory to the sterilization and test site will be by special air or truck transportation. This same criteria would also be applied for the transfer to the Launch site. These same shipping and handling equipment and techniques developed to accommodate

TABLE 3

FACTORY TO LAUNCH ENVRIONMENTAL REQUIREMENTS

Item	Phase 1	Phase 2	Phase 3	Phase 4	Phase 5
	Factory	Transfer	Sterilization and Final Test Site	Transfer	Launch Site
Configuration and Duration	The components will be fabricated, inspected, assembled and tested in a clean room at the factory. The subsystems will then be assembled into a spacecraft for systems integration and testing. The spacecraft will then be disassembled and suitably packaged consistent with practical shipping limitations. Total duration of this phase will not exceed 8 weeks.	Special handling will be accorded the units. The shipping containers will be capable of maintaining the clean room environment when exploded to the environment below. Shipping time by air will not exceed 12 hours.	The assemblies will be received and stored in an environmentally controlled area. Possible storage time will not exceed 2 weeks. The capsule components will then be bacteriologically sterilized, wherever possible. Assembly, test and integration of vehicles into a sterilization shroud will take place in a controlled atmosphere. Total assembly, test and integration time will not exceed 3 months.	Same as phase 2.	The spacecraft will be mated to the Atlas-Centaur Booster and the ascent shroud installed. A gantry mounted controlled environment approaching a type I clean room will be utilized to protect the spacecraft from the launch site environment. Final checkout will then be performed.
Temperature	60° to 80°F	-35°F to 150°F (includes 25°F temperature rise caused by solar radiation)	60° to 80°F in receipt assembly and test area. Sterilization: dry heat method - 1 cycle of 275° for 24 hrs at low humidity.	Same as phase 2	30°F to 150°F (includes 25°F rise caused by solar radiation)
Pressure	Approx sea level ambient 29.9 in. Hg (normal)	Sea level to 50,000 feet 29.9 in Hg (normal) to 3.44 in. Hg.	Same as Phase 1	Same as Phase 2	Same as Phase 1
Humidity	Relative humidity range approx 40% to 50%	Relative humidity ranging from 0 to 100%	Relative humidity range receipt area: 0 to 90%. Assembly and test area: approx 40 to 50%	Same as Phase 2	Same as Phase 2
Sand and Dust	Negligible (Clean Room I-II)	Particle diameters ranging from 10^{-4} to 0.3 m.m. blown by 60 mph winds.	Receipt area: subject to settling dust. Assembly and test area: negligible.	Same as Phase 2	Same as Phase 2
Precipitation	Not applicable	Rain: maximum precipitation rate of 4 ± 1 in. /hr for 30 min Snow: Snow crystals with a diameter of 1 to 3 m.m. occurring for 30 minutes at a temperature of 0°F. Max. instantaneous rate is 3 in/hr. Hail: frozen water pellets of 1/2 to 5 m.m. (.02 to 0.6) diameter blown by 50 mph winds. Maximum instantaneous rate of 4 inches/hr for a duration of 15 minutes. Ice: conditions such that water frozen at a temperature surfaces to a thickness of 1/2 inch. Sleet: pellets .03 to.06 in. diameter blown by 40 mph winds at a temperature of 32°F. Maximum instantaneous rate of 4 inches/hr for a duration of 30 minutes.	Not applicable	Same as phase 2	Rain: maximum precipitation rate of 4 ± 1 in/hr for 30 minutes

RE-ORDER NO. 64-522

3.1

RE-ORDER No. 64-522

TABLE 3 (Cont'd)

Item	Phase 1	Phase 2	Phase 3	Phase 4	Phase 5
	Factory	Transfer	Sterilization and Final Test Site	Transfer	Launch Site
Corrosive Atmosphere	Not applicable	Salt fog of 20 parts salt by weight to 80 parts of water by weight with a specific gravity of 1.126 to 1.157 and a ph between 6.5 and 7.2 at a temperature of 95° F with a relative humidity of 85%.	Receipt area: Exposure to coastal salt sea atmosphere consisting of 5 parts salt by weight to 95 parts distilled water. Assembly and test area: negligible	Same as Phase 2	Same as Phase 2
Fungus	Negligible	Non fungus nurtient materials will be used.	Receipt area: Same as Phase 2. Assembly and test area: negligible	Same as Phase 2	Same as Phase 2
Wind	Not applicable	Maximum peak wind velocity shall be 60 mph.	Not applicable	Same as Phase 2	Same as Phase 2
Electromagnetic Radiation (Solar)	Not applicable	Radiation Intensity: Varying sinusoidally with a 24 hour period. Intensity varies from 0 to 105 Watts/ft^2. Spectrum consists of approximately 50% infra-red, 44% visible and 6% ultra-violet.	Not applicable	Same as Phase 2	Same as Phase 2
Particle Radiation	Negligible	Negligible	Negligible	Negligible	Negligible
Meteroids and Dust	Not applicable	Not applicable	Not applicable	Not applicable	Not applicable
Vibration	The maximum vibration levels that the spacecraft and components will experience will be as follows: Unpackaged Vibratory D. A. or Peak Acceleration (g-rms) / Freq. Range (cps) ± 3.5g / 2-50 ± 1.5g / 50-300 Packaged Vibratory D. A. or Peak Acceleration (g-rms) / Freq. Range (cps) ± 1.3g / 2-26 0.036 in. / 26-52 ± 5g / 52-300	Unpackaged: Not applicable Packaged: Same as Phase 1	Same as Phase 1	Same as Phase 2	Negligible
Shock	Unpackaged Major Assemblies As simulated by a 10G-11msec shock applied along 3 mutually perpendicular axes. If above simulation is impossible to perform because of test equipment limitations, 1 inch flat drops and 4 inch pivot drops may be used. Unpackaged Components and Small Component Assemblies As simulated by a 100G-6msec shock applied along 3 mutually perpendicular axes. Packaged Assemblies and Components Containers shall be designed to meet the requirements of MIL-P-7936.	Unpackaged Assemblies and Components: not applicable Packaged Assemblies and Components: Same as Phase 1.	Same as Phase 1	Same as Phase 1	Unpackaged: Same as Phase 1

TABLE 3 (Concl'd)

Item	Phase 1	Phase 2	Phase 3	Phase 4	Phase 5
	Factory	Transfer	Sterilisation and Final Test Site	Transfer	Launch Site
Sustained Acceleration Load	Not applicable	Not applicable	Not applicable	Not applicable	Not applicable
Acoustic Noise	Not applicable	Not applicable	Not applicable	Not applicable	Not applicable
Electromagnetic interference	Negligible	Negligible	Electro interference levels shall be considered to be as per MIL-I-26600 (RAD-E-59064) (probably to a lesser degree than Phase 5)	Same as Phase 4	Electrc Interference levels shall be considered to be as per MIL-I-26600 (RAD E-59064)

RE-ORDER No. 64-522

these major shipment phases can be utilized for shorter, less severe transfers, such as between the spacecraft assembly building and the launch pad while at the launch site.

2. Launch to Mission Environmental Requirements

Past studies of Earth to Mars environments have also been adapted to the Advanced Mariner mission from launch to lander operation on the surface of Mars and bus operation after planetary encounter. These environments will be updated as new data become available from continuing space studies and exploration.

2.5 MISSION SUCCESS PROFILE

During the conceptual design phase, the reliability profile for the Advanced Mariner mission was developed. This reliability profile shows the probabilities of successfully accomplishing major events in the mission. The key steps involved in this analysis were as follows:

1. Prediction of the system failure contributions
2. Preparation of the mission success diagram
3. Development of the mission mathematical model
4. Quantification of the mathematical model.

Since the development of the reliability profile required the prediction of the system failure contributions, a valuable output from the analysis was the estimate of system mission reliability. An indication of the degree of the reliability improvement needed in the program can be obtained by comparing these system reliability predictions with preliminary reliability goals allocated to these same systems.

In addition to providing success probabilities for the critical events occurring during the mission, the analysis resulted in an estimate of the probability of success for the overall flyby bus/lander mission. The latter reliability estimate was used to determine the probabilities of obtaining at least one successful mission out of "n" launch attempts.

Because of several important limitations, it was necessary to make some qualifying assumptions. These limitations and the related assumptions are described below.

1. Little is known of the effects of storage on equipment reliability during the transit phase of mission. However, the various parts, components, and subsystems will presumably be stored in a controlled environment; i.e.,

RE-ORDER No. 64-522

every attempt will be made to maintain an environment which approaches room ambient conditions. Therefore, it was assumed "that the problem of failures due to storage (of electronic equipment in particular) is not serious when compared to the problems of failures due to other sources ..."*, and hence, considered negligible.

2. Details concerning the reference system designs are not too complete at this time. It is recognized that significant deviations between the reference designs and later definitive designs could cause changes in the system reliability estimates. These variations, however, are expected to be compensating so that little difference will result in the reliability estimates. Hence, the reference system designs were assumed to closely approximate later definitive designs.

3. Since reliability is a time-dependent, probabilistic expression,** and a detailed mission profile for each system was not readily available, any significant change in the operating time of a system would modify its reliability estimate. As in the previous case, it was assumed that this effect on the overall mission reliability estimate would be minimum.

4. The availablity of failure rate information for most parts, components, and subsystems used in the space environment is quite limited. When available, these data often indicate wide variations in the failure rate experience of similar component types. To compensate for these deficiences, a number of failure rate sources were examined to assure the selection of the most realistic failure rates associated with off-the-shelf missile and space parts, components, and subsystems. Thus, it was assumed that this screening process minimized any gross errors in the reliability estimation.

5. There is little information concerning the effects of heat sterilization on equipment reliability. However, it is believed that the implementation of a design review program which assures the selection and application of heat resistant parts and materials will minimize reliability degradation attributed to heat sterilization. Hence, it was assumed that the effect of heat sterilization on equipment reliability will be negligible.

6. There are some parts, components, and subsystems which are inherently redundant or can be made redundant without difficulty. However, because of the incomplete nature of the design details, series operation was assumed for the various spacecraft systems and its elements, except in cases where redundancy was specifically indicated.

---

* This is the conclusion reached by Task Force 8 of the Advisory Group on Reliability of Electronic Equipment in a study to investigate the effects of storage on electronic reliability; included in the study was equipment stored for periods of from 3 to 5 years.

** Except in the case of one-shot items such as shaped charges and solid rockets.

TABLE 4

LAUNCH TO MISSION ENVIROMENTAL REQUIREMENTS

Item	Phase 1	Phase 2	Phase 3	Phase 4	Phase 5
	Powered flight/injection into interplanetary orbit.	Spacecraft Cruise	Atmospheric entry of lander	Lander on surface of Mars	Bus as it flys by Mars
Configuration and Duration	The spacecraft will be injected into interplanetary transfer orbit by Atlas-Centaur booster. Time from launch to injection is about 1 hour.	The spacecraft is in unpowered flight on the interplanetary trajectory. Propulsion system on Bus is activated twice for midcourse corrections and after separation of lander from bus. The lander is separated from the bus nominally 10^6 km from Mars. The flight time to Mars is approximately 300 days.	The lander is subjected to the high heat and acceleration loads associated with Martian atmospheric reentry. Additional loads are induced by the firing of the retrothrust rockets and deployment of parachutes. Total entry and descent time is from 10 to 20 minutes depending upon atmospheric model.	The payload is separated from the lander and protected by crush-up material after impact on Mars surface. Scientific experiments are operated for 5 hours after impact. Direct and relay communication transmits data during 3 playouts in 5 hours period.	The periapsis of the fly by bus with Mars is nominally 6328 a 3621 km. Lander relay transmission of data begins approximately 70 hours before periapsis and ends about periapsis. Bus data is tape recorded begining at periapsis and continuing for 5 to 10 minutes. Playback transmittal of this data to DSIG continuous for approximately 10 days.
Temperature	Temperature of internal equipment ranges from 0°F to 140°F.	Temperature of internal equipment ranges from 0°F to 140°F. Temperature of solar panels and sensors may be as high as 220°F.	Maximum backface temperature of lander will be 800°F.	Temperature on surface ranges from -135°F to 80°F.	Temperature of internal equipment ranges from 0°F to 140°F.
Pressure	Sea level to 90 nm (29.9 inches Hg to 10^{-6} Torr)	90 nm to outer space (10^{-6} Torr to 10^{-12} Torr)	Outer space to surface of Mars (10^{-12} Torr to .21 in. Hg)	4.1 in.Hg to .21 in.Hg (referenced to Earth) - 7 to 136 mill. bars	10^{-12} Torr
Humidity	The relative humidity shall be assumed to be 100 percent for all altitudes up to 20,000 feet.	None	None	None	None
Sand and Dust	Negligible	None	Sand and dust clouds blown by winds up to 200 fps.	Same as Phase 3	None
Precipitation	No requirements	None	Clouds of ice crystals and CO_2 crystals are usually present in Mars atmosphere. They are probably blown by winds up to 200 fps.	Hail storms generated by conditions in Phase 3 are sporadically present on surface of Mars.	
Corrosive Atmosphere	Negligible	None	Negligible	Probably not corrosive.	None
Fungus	None	None	None	Unknown	None
Wind	Wind velocity versus altitude profile as defined in ARDC Handbook of Geophysics.	None	Up to 200 fps.	Same as Phase 3	None

RE-ORDER No. 64-522

TABLE 4 (Cont'd)

Item	Phase 1	Phase 2	Phase 3	Phase 4	Phase 5
	Powered flight/injection into interplanetary orbit.	Spacecraft Cruise	Atmospheric entry of lander	Lander on surface of Mars	Bus as it flys by Mars
Electromagnetic Radiation (Solar)	Change occure from level in Phase 1 to level in Phase 4*. *The total solar electromagnetic energy flux at the parking orbit is 0.140 w/cm^2 distributed as shown in Phase 4. Earth's hemispherical reflectance (albedo) will increase the average intensity in the visible wavelength by a factor of between 1.36 to 1.39 with season changes from about 0.3 to 0.5. Estimates for the near infrared are about 0.3 and for the near ultraviolet about 0.5.	Energy distribution at Earths mean destance from the sun (1 a.u.) Up to Wave-Length A / Fraction to Total Energy / Energy at Sunspot max including fluxes erg/cm^2-yr 0.1 / 10^{-11} / 10^2 to 10^3* 1 / 10^{-11} / 10^2 to 10^3 10 / 10^{-8} / 10^5 to 10^6 100 / 10^{-6} / 10^7 to 10^8 500 / 10^{-6} / 10^8 1,000 / 10^{-5} / 10^8 1,500 / 10^{-5} / 10^9 2,000 / 10^{-4} / 4×10^9 2,500 / 1.3×10^{-3} / 6×10^{10} 3,000 / 1.2×10^{-2} / 5×10^{11} 4,000 / 9×10^{-2} / 4.0×10^{12} 5,000 / 0.24 / 1.1×10^{13} 6,000 / 0.37 / 1.6×10^{12} 7,000 / 0.49 / 2.2×10^{13} 8,000 / 0.58 / 2.6×10^{13} 9,000 / 0.65 / 2.9×10^{13} 10,000 / 0.71 / 3.2×10^{13} 15,000 / 0.88 / 3.9×10^{13} 20,000 / 0.94 / 4.2×10^{13} 30,000 / 0.98 / 4.3×10^{13} 70,000 / 0.999 / 4.4×10^{13} *10^9 to 10^{10} photons/cm^2 - yr shorter than 0.1 A. The intensity of this radiation varies inversely as the square of the distance from the sun. Light Pressure At 1 au from sun, the maximum light pressure is 2×10^{-3} lbs/ft^2. This varies inversely as the square of distance from the sun and decreases to about 9×10^{-8} lbs/ft^2. at the orbit of Mars.	At orbit of Mars the energy reduces to 0.4 times the values given in Phase 2. Mars albedo will increase the average intensity in the visibile wavelengths by a factor of 1.14. This increase varies from 0.04 at 3,000 to 4,000 A to 0.24 at 6,400 A.	There may be some attenuation of the short wavelength portion of the spectrum due to the atmosphere.	Same as Phase 3

RE-ORDER NO. 64-322

RE-ORDER No. 64-522

TABLE 4 (Cont'd)

Item	Phase 1	Phase 2	Phase 3	Phase 4	Phase 5
	Powered flight/injection into interplanetary orbit.	Spacecraft Cruise	Atmospheric entry of lander	Lander on surface of Mars	Bus as it flys by Mars
Particle Radiation	Negligible	Inner Van Allen Belt Altitude: 250/750 miles (depending on latitude) to 6,000 miles Latitude: 45° north to 45° south Highest Intensity Region: (2200 miles altitude at magnetic equator **Protons** flux energy level — density (protons/cm^2-sec) >1 kev — 10^8 >20 kev — 10^7 >10 mev — 3×10^4 to 2×10^5 >40 mev — 1×10^4 to 4×10^5 >650 mev — 10^2 **Electrons** flux energy levels — density (protons/cm^2-sec) >20 kev — 3×10^{10} >100 kev — 10^{10} >600 kev — 10^7 >1 mev — 10^5 Outer Van Allen Altitude: 6000 miles to 40,000/55,000 miles Peak Intensity: (10,000 to 14,000 miles altitude at magnetic equator) **Protons** flux energy levels — density (protons/cm^2-sec) >30 mev — <1 **Electrons*** flux energy levels — density (electrons/cm^2-sec) >20 kev — 10^{11} >1.5 mev — 10^6 >4 mev — 1 *During solar storms intensity may increase by a factor of 10 in the peak intensity region and by a factor of 100 at higher altitudes.	A. During Major Flare Activity: **Protons** flux energy level — density (protons/cm^2-sec) >20 mev — 10^4 >100 mev — 10^2 >500 mev — 10^0 **Electrons** flux energy level — density (electrons/cm^2-sec) 50 kev — 10^6 to 10^7 B. During Minor Flare Activity: **Protons** flux energy level — density (protons /cm^2-sec) .5 to 20 kev — 10^8 to 10^{12} **Electrons** flux energy level — density (electrons/cm^2-sec) .2 to 10 ev — 10^8 to 4×10^9 C. During Quiet Sun: **Protons** flux energy level — density (protons/cm^2-sec) <3 kev — $<10^9$ The protons make up over 90 percent of the total cosmic radiation. Alpha particles make up 7 percent of the total number while the rest are nuclei of heavier element of atomic numbers up to 26 to 27 (iron and cobalt) **Electrons** The necessary electrons to neutralize the positive particles may be present in a flux as high as 2×10^{10} electron/cm^2-sec but as energies below 2 ev. **Solar Wind** A pressure increase in the solar equatorial plane caused by ionized hydrogen gas emitted from sun. At 1 au from sun: Period — dynes/cm^2 Quiet sun — 10^{-7} Major flare activity — 10^{-3} Average conditions — 10^{-8}	Unknown	Same as Phase 3

TABLE 4 (Concl'd)

Item	Phase 1	Phase 2	Phase 3	Phase 4	Phase 5
	Powered flight/injection into interplanetary orbit.	Spacecraft Cruise	Atmospheric entry of lander	Lander on surface of Mars	Bus as it flys by Mars
Meteoroids	Whipple's 1963 estimate of near Earth flux.	Whipple's 1963 estimate of deep space flux used for nominal design case. Whipple's 1963 estimate of near Earth flux used for reliability calculations.	Negligible -- atmosphere assumed to retard most particles as near Earth.	Negligible -- same as Phase 3	Slightly greater than Phase 1 due to closer proximity to the asteroid belt.
Vibration	Vibration inputs to spacecraft to be determined for fundamental booster frequency from lift off to sustainer burnout and for both burn periods of centaur stage.	Negligible	Negligible	Negligible	Negligible
Shock	Shock input to spacecraft at black boxes to be determined when design is firm.	Negligible	See acceleration load	Impact -- 1500 g_e	Negligible
Acceleration Load	Axial load -- 5.8 g_e limit Lateral load -- ± 1 g_e limit	Negligible	Entry Deceleration Axial -- 110 g_e Max q -- 1005 psf Drogue Para. Deceleration Axial -- 27.02 g_e Main Para. Deceleration Axial -- 37.15 g_e	Vertical Descent Velocity -- 65 fps	Not Applicable
Acoustic Noise	To be determined for selected booster	Negligible	To be determined	Negligible	Negligible
Electromagnetic Interference	Per MIL-I-26600 (RAD E - 59064)	Same as Phase 1	Same as Phase 1	Same as Phase 1	Same as Phase 1

RE-ORDER No. 64-522

RE-ORDER No. 64-522

The method of approach used to derive the mission reliability profile is briefly described below.

The failure contribution of the systems comprising the flyby bus and lander was predicted in terms of their element failure rates. Basically, this was accomplished by (1) determining the elements (parts, components, and subsystems) within each system, † (2) assigning failure rates, extracted from a variety of appropriate failure rate sources, to these elements, and (3) statistically combining the element failure rates to determine the system failure contributions. The failure contribution of a series operating system, where failure of a single element results in a system malfunction, was obtained by summing the element failure rates. For a system with redundant elements, a more complex model was used.

An analysis was conducted to show the combination and sequence of major events which must occur to achieve mission success. This analysis made use of the information contained in the detailed flight sequence to establish the relationship between each system (or its elements) for successful execution of each major mission event. For example, to decelerate the Mars lander for planetary entry, it will be necessary to (1) deploy drogue chute, (2) jettison the lander structure, and (3) deploy the main chute. Each of these three subevents requires the successful operation, in proper sequence, of several systems.

A mathematical model which expresses the probability of mission sucess as a function of the successful accomplishment of the various mission events was developed which describes probabilistically the sequence and relationship of events (including launch) which occur throughout the mission. Since all events must be successfully executed to achieve total mission success, this probabilistic expression can be reduced to a simple series model.

The failure contribution of the various systems was then factored into the mission mathematical model. This was done by calculating the probability of success for each major event included in the model. * The computation involved three basic inputs: (1) the systems (or elements thereof) required to accomplish each event, taking into consideration the subevents occurring prior to the execution of each major event, (2) the failure contribution of each system employed, and (3) the operational time for each system. For each event, a system (or its elements) possessing a failure rate, λ, will be required to operate for some time, t. ** The reliability of that system can be given by the exponential failure distribution model, $R(t) = \exp(-\lambda t)$, where $R(t)$ is the reliability or probability of success for time, t.

† The term "part" refers to elements such as valves, filters, regulators, etc.; "components" refers to elements such as transmitters, receivers, inverters, etc.; "subsystems" refers to elements such as telemetry, data automation, command, etc.

* The reliability (0.75) of the Atlas-Centaur launch vehicle was estimated by extrapolating the achieved reliability of the Atlas and Atlas-Agena boosters.

** Except in the case of one-shot devices which are not time dependent.

RE-ORDER No. 64-522

Since several systems must usually operate failure-free to successfully accomplish a mission event, the success probability for that event is given as the product of the reliability estimates for those systems. The resultant quantitative expression of event success probabilities, as a function of time, yielded the reliability profile for the Advanced Mariner mission (see figure 2).

The development of the reliability profile resulted in estimates† of mission reliability for the various spacecraft systems. For comparative purposes, allocated system reliability goals are also given. These system goals are associated with a mission success objective of 0.50 and were allocated using the model described in the Voyager final report.††

In the Advanced Mariner program, multilaunches will be employed to enhance program success. From the above analysis, the probability of success for a single flyby bus/lander mission was estimated to be 0.452; i.e., the product of booster reliability (0.75) and spacecraft reliability (0.603). Cumulative binomial probability tables were then used to determine the probabilities of at least one successful mission out of n launch attempts. These results are shown graphically in figure 3. In conclusion, there is a better than 90 percent probability that with four launch attempts, there will be at least one successful flyby bus/lander mission in the Advanced Mariner program.

2.6 MISSION DATA REQUIREMENTS

In developing the bus mission and the payload for the lander vehicle a series of tradeoffs of equipment and instrumentation were necessary. The details of the results of these selections are discussed in volumes (3) and (4) wherein the parametric payload and selected payload analysis are shown. Tables 5, 6, 7 and 8 list the data requirements established to accomplish the selected conceptual design. The number of bits of data shown on these tables are representative of the selected design. Of the 31,051 total number of lander data bits shown, 26,470 are for science data and 4581 are in the engineering diagnostic and event category. This 85/15 percent split is typical of what can be expected throughout most of the payloads analyzed. The playout of 13,161 bits after landing is totally redundant through the relay link to the flyby/bus and directly to Earth via the DSIF link. Of these, 8165 bits are a replay of stored data taken during entry.

† These estimates obviously exclude the reliability of the booster.

†† This model, which is based on quantitative factors, is explained on pages 309 and 310 of Volume Three, "Systems Analysis," (part of the Voyager Design Studies, prepared by Avco Corporation under Contract No. NASw 697, 15 October 1963).

45

RE-ORDER No. 64-522

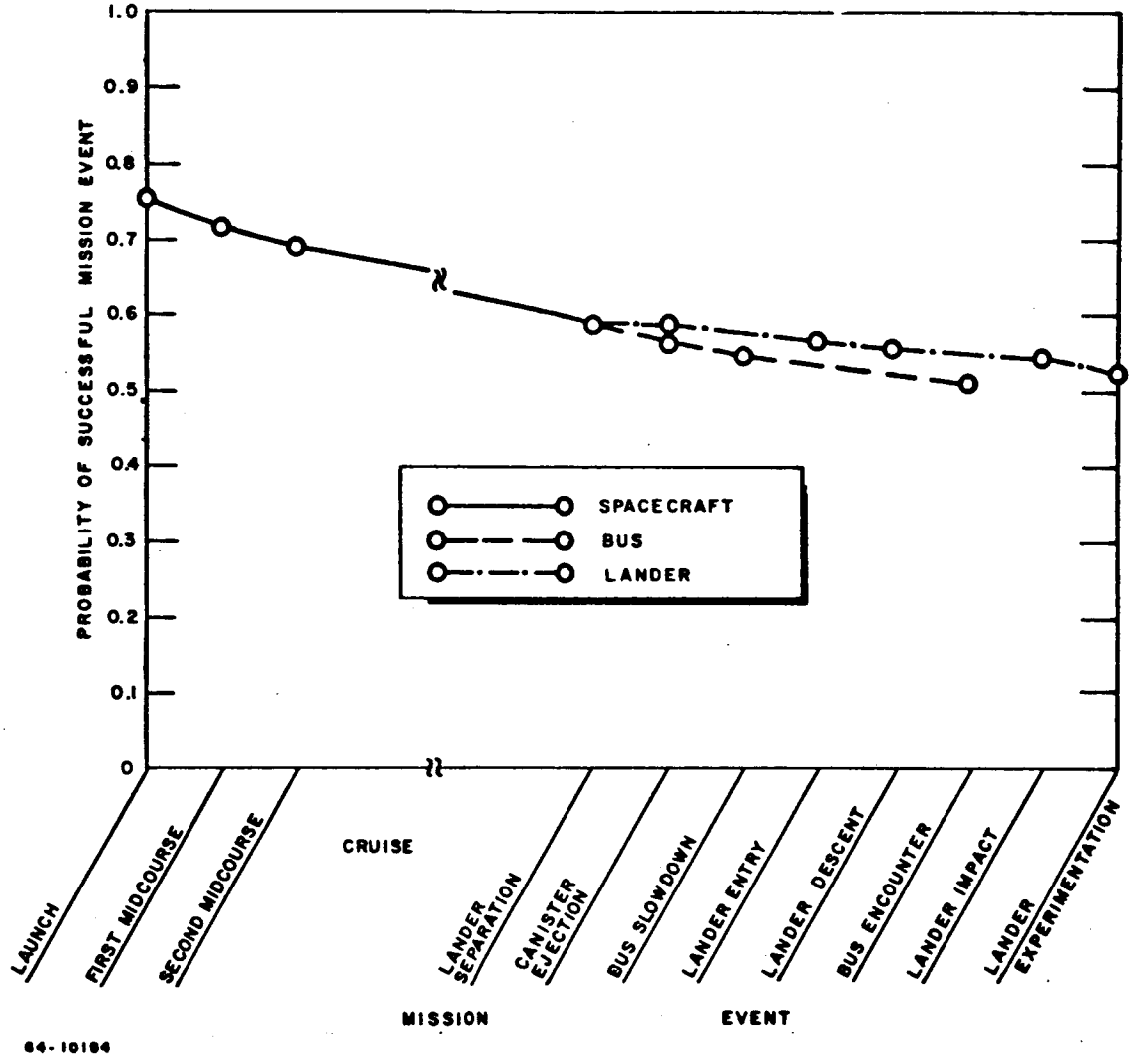

Figure 2 ADVANCED MARINER MISSION RELIABILITY PROFILE

RE-ORDER No. 64-522

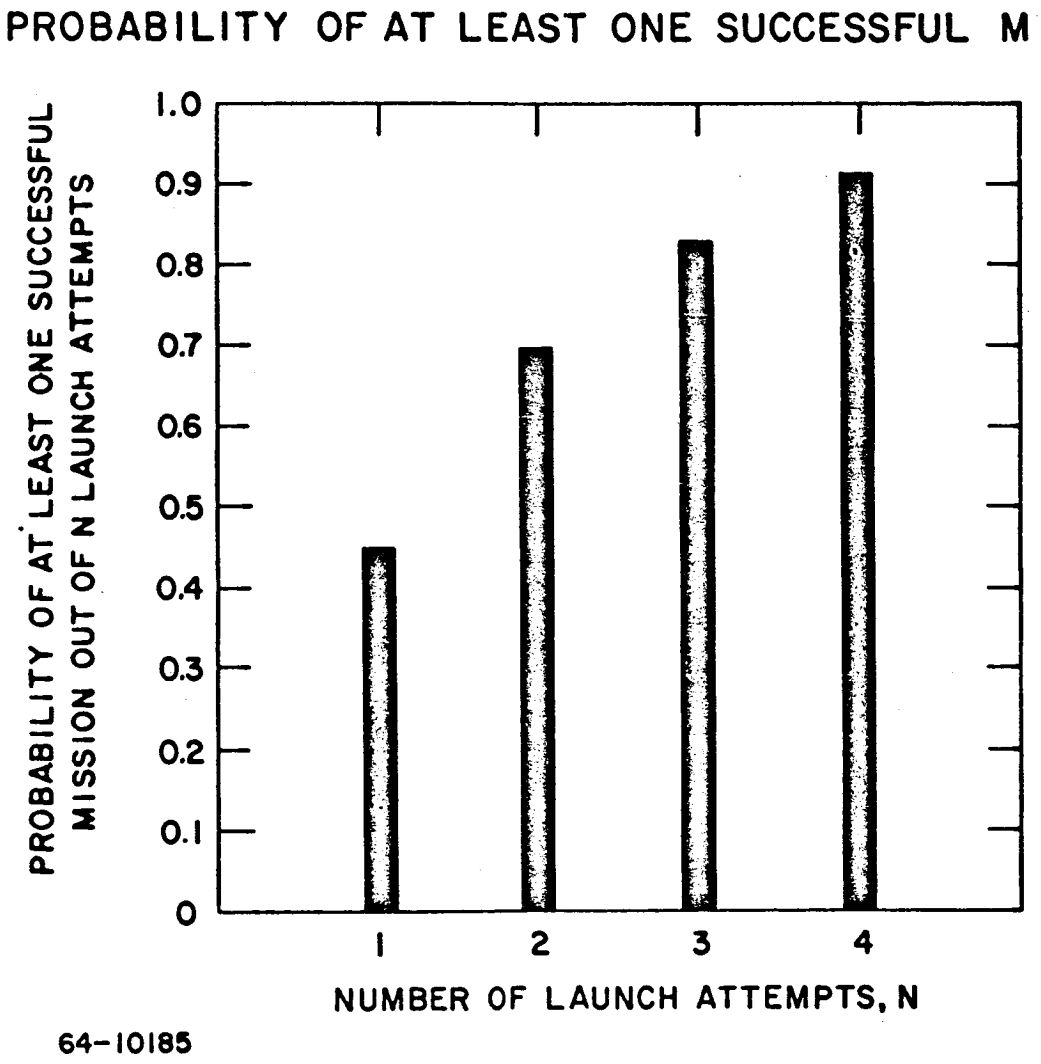

Figure 3 ADVANCED MARINER PROGRAM SUCCESS EVALUATION

RE-ORDER No. 64-522

TABLE 5

BUS DATA LIST

Scientific Instrument

Cosmic Dust Detector

Micrometeoroid Detector

Ion Chamber

Particle Flux Detector

Magnetometer

Infrared Spectrometer

TV Mapping System

Engineering Diagnostic and Event Data

Selected monitors on all operational equipment to determine equipment status.

Monitor sequence of events and timing marks to determine spacecraft status.

Relay Lander Data

Receive from Bus and retransmit to DSIF all data from the three phases of Lander operation.

RE-ORDER No. 64-522

TABLE 6

LANDER DATA LIST - 1

1560 BITS

Separation to Entry

First Playout - Post Separation (twice)

Second Playout - Pre Entry (twice)

Engineering Diagnostic Data

Battery Temperature

Battery Voltage

Current Drain

Calibration

Exciter Power Output

Amplitron Power Supply Voltage

Amplitron Power Supply Current

Amplitron Power Supply Recycle Indicator

VSWR

Science Temperatures (three)

Vehicle Temperatures(three)

Capsule ΔV

Rocket Temperature (Before Ignition)

Event Data

Separation

Spinup

Rocket Ignition

Rocket Jettison

Despin

RE-ORDER No. 64-522

TABLE 7

LANDER DATA LIST - 2

16,330 BITS

Entry to Impact

- Playout twice during main chute descent
  - Engineering Diagnostic Data
    - Battery Temperature
    - Battery Voltage
    - Exciter Power Output
    - Amplitron Power Supply Voltage
    - Amplitron Power Supply Current
    - Amplitron Power Supply Recycle Indicator
    - VSWR
    - Forebody Temperature
    - Afterbody Temperatures (three)
  - Event Data
    - 0.1 g_e ascending
    - 1.0 g_e ascending
    - 10.0 g_e ascending
    - Peak g_e
    - 10 g_e descending
  - Drogue Chute Deploy
  - Main Chute Deploy
  - Miscellaneous instrumentation markers

Science Data

- Axial Acceleration (a_x)
- Lateral Accelerations (a_y and a_z)
- Science Temperatures (three)
- Forebody Pressure
- Atmospheric Composition

RE-ORDER No. 64-522

TABLE 8

LANDER DATA LIST - 3

13, 161 BITS

On Surface

First Playout: Impact plus 6 minutes

Stored Entry to Impact Data (once)

Playout both science and Engineering Data

New Engineering Diagnostic and Event Data (Twice)

Same test points as prior playouts

Science Data (Twice)

Wind Velocity

Biological Determination

Pressure

Second Playout: Impact plus 90 minutes

Stored Landed Data - Repeat of 1st Playout (twice)

Updated Engineering Diagnostic and Event Data (twice)

Same test point as prior playouts

Updated Science Data (Twice)

Third Playout: Impact plus 5 hours

Stored landed Data - Repeat of 1st and 2nd Playout (twice)

Updated Engineering Diagnostic and Event Data (twice)

Same test points as prior playouts

Updated Science Data (twice)

Same test points as prior playouts.

2.7 MISSION TRADEOFFS

1. Introduction

During the Advanced Mariner Study Program several major mission tradeoffs were investigated. These tradeoff studies were heavily influenced by the mission objectives, mission and study constraints, launch window flight geometry and the payload capability of the Advanced Mariner Spacecraft. The results of these mission tradeoff studies were included in the final conceptual design for the flyby bus and lander.

a. Consideration was given to various methods of reference attitude orientation for the spacecraft in the cruise mode. The Sun-Canopus reference frame was selected.

b. The sterilization requirement forces a nonsterilized bus to a 1×10^{-4} probability of entering the planetary atmosphere. The bus can be directed at the planet until lander sepatation and then diverted to the flyby trajectory. The selected approach directed the flyby bus on a trajectory biased away from the planet, with a separate lander propulsion system to place the lander on an impact trajectory.

c. Several launch window-landing site combinations were considered for this mission. The emphasis on the life detection mission objective indicated selection of a launch window which allows lander impact on Syrtis Major, close to the height of the wave of darkening to allow the best chance of success for the mission objective.

d. Both relay and direct link communication systems were considered for pre-entry, descent, and post-impact communication requirements. For the selected mission a relay link was used for all pre-impact requirements, while totally redundant direct and relay communications are employed during the post-impact phase.

e. The flyby bus lander spacial time relationship during the encounter phase was analyzed to determine the lander speedup or bus slowdown requirement to accommodate the relay link. A bus slowdown of five hours was selected.

2. Spacecraft orientation

In making a selection of the reference attitude of the spacecraft, consideration must be given to the equipment of the craft which must be pointed in various directions and to the sources available to provide reference directions. The selection of solar energy as the source of power immediately identifies the solar panels as the primary object which must be pointed

toward the sun. The real engineering problems involved in mounting the panels on gimbals due to their large size, led to the selection of a Sun-oriented configuration. The second reference direction is provided by the star Canopus which is chosen because of its brightness and because of its location near the south ecliptic pole. The Canopus tracker is oriented so that a single gimballed mirror is all that is required for pointing, as the angle between the sun line and the star line changes during the interplanetary voyage. Thus the gimballing of the star tracker poses no difficulties with the Sun-Canopus orientation. When in planetocentric flyby, additional equipment must be pointed toward the planet. All planet-oriented science is mounted on a single gimballed platform which is attached to the periphery of the flyby bus. This allows convenient pointing of television cameras and other experiments as the spacecraft holds its fixed orientation and the platform turns about two axes. Pointing is accomplished by a horizon sensor mounted directly on the platform itself. Since the spacecraft is in a hyperbolic orbit, the mapping gimbal must rotate at a varying rate. This causes some expenditure of attitude control system fuel, but the amount is not excessive.

3. Flyby Trajectory Selection

Two techniques were considered for maintaining an unsterilized flyby bus for the Advanced Mariner mission, which requires that the probability of the flyby bus entering the planetary atmosphere be less than 10^{-4}. The flyby bus trajectory can be biased away from the planet by an amount commensurate with the anticipated dispersion in the flyby attitude; the bias is reduced at each subsequent maneuver as the anticipated dispersion is reduced. This approach requires a small propulsion system on the lander to place it on an impact trajectory subsequent to separation from the flyby bus. The second technique places the flyby bus on an impact trajectory from launch making the lander system much simpler. The flyby bus is then diverted to a flyby trajectory after lander separation. This approach required one additional burn of the flyby bus propulsion system.

The selection of the biased flyby bus trajectory was dictated primarily by the necessity to maintain a high probability of planetary miss for the flyby bus. While either technique will satisfy the sterilization criteria, the biased trajectory requires a complex sequence of malfunctions to cause the flyby bus to enter the planetary atmosphere and is therefore a more conservative approach to the sterilization problem.

4. Launch Window Selection

The launch window can be selected on the basis of optimizing, singly or in combination, any of the departure or approach trajectory parameters. Of particular significance are the injected payload, planetary approach asymptote direction, arrival date, and planetary approach asymptote

velocity magnitude. For the launch windows under consideration, the primary objective is the performance of the life detection experiment. This overriding consideration led to the selection of a launch window so as to arrive at Mars during the height of the wave of darkening to maximize the success probability of this experiment. Within this constraint the selection of launch window was further constrained by the desire to maintain a ZAP angle as close as possible to 90 degrees to provide a reasonable relay link geometry over the five-hour lander surface lifetime. These criteria indicated selection of launch windows which depart slightly from the minimum departure velocity or maximum payload launch windows for both 1969 and 1971.

5. Direct versus relay communications

The return of scientific information obtained by the lander requires an information channel to Earth. This can be provided with reasonable power either by a direct link or by relay through the flyby bus using a low-gain lander antenna and a high-gain antenna on the flyby bus. The disadvantage of the direct link is the difficulty in designing the lander which can be erected after impact so that the antenna can be pointed toward Earth. The design selected for the Mars lander utilizes a direct-link antenna in which the lander is designed to re-erect itself after landing.

The present lack of knowledge of the terrain of Mars makes it difficult to be sure that the re-erection mechanism will function under all possible circumstances. However, the benefit to be gained by eliminating the lander dependence on the flyby bus makes the attempt worthwhile. To minimize the risk, a capability is provided for using a relay link as well. The additional weight penalty which is incurred is nonexistent, since both links receive transmission from the same lander communication transmitter and antenna system. However, in the event of off-vertical lander re-erection, the relay link, which has considerable positive performance margin, can still operate satisfactorily.

6. Lead Time Requirements

Engineering and scientific measurements made by instruments on the lander during atmosphere entry and descent are recorded for later playback. These data are transmitted to the relay during a period before planet impact. Also five hours are required after impact for transmission of scientific data in real time. To obtain the necessary communication time, the lander must lead the flyby bus so that it remains within the lander antenna beam during the communication period.

The required lander lead time is determined from the geometric analysis. It is defined as the difference in time between nominal flyby perapsis passage and lander atmospheric entry. The amount of lead time required

to provide the necessary communication time is approximately five hours. The required lead time can be achieved by accelerating the lander or by slowing down the flyby bus. The magnitude of velocity change required along the flight path is a function of the lead time required, the separation range, and the approach velocity.

The method selected for obtaining lead time was to slow down the flyby bus and impart a velocity increment to the lander normal to the flight path in order to change it from a flyby to an impact trajectory. The following factors were considered in making the selection:

a. Accuracy of achieving desired landing site

Outside of the undertainty in vehicle position at separation due to guidance error, the most significant source of lander dispersion is the error in magnitude and direction (launch angle) of the velocity increment imparted to the lander. The dispersion due to uncertainty is the magnitude of the velocity increment and is therefore independent of the method of obtaining lead time. The dispersion due to launch-angle error is a function of the total velocity increment and the cosine of the launch angle. Since the required velocity increment along the flight path is much larger than the normal component, the launch angle would be close to 0 degree in the case of lander speedup. This would maximize the effect of launch-angle error. If no velocity increment is applied to the lander in the direction of the flight path but is applied only normal to the flight path, then the launch angle is 90 degrees and the dispersion due to launch angle error is reduced.

b. Effect on sterilization requirements

Applying a velocity change to the flyby bus may increase the probability of the unsterilized flyby bus impacting on the planet. However, an unlikely sequence of events must occur to cause flyby bus impact. The malfunction must be undetected prior to rocket firing. The velocity change due to the malfunction must be in the proper direction. The DSIF command to correct the trajectory error must fail to be carried out. If the probability of these events occurring is shown to be unacceptably high, the velocity change could be applied in smaller increments, allowing time between impulses to ensure by DSIF tracking that the resultant maneuver is being performed correctly.

RE-ORDER No. 64-522

3.0 TRAJECTORY ANALYSIS

3.1 LAUNCH WINDOW ANALYSIS

An integral portion of a preliminary design study for an interplanetary mission entails a comprehehensive analysis of the various daily trajectory characteristics to select the optimum launch window. In theory, an unlimited number of possible interplanetary trajectories exists for a given target planet as there are at least four trajectory paths per given departure velocity per day. This vast wealth of information can be reduced to within tolerable limits by the employment of realistic engineering constraints. An evaluation of the payload characteristics of presently conceived boost vehicles in conjunction with desirous mission payloads places an upper bound on the injection energy requirements. Additional engineering constraints which may be employed in the optimization of a launch window selection include:

a. Approach velocity

b. Approach geometry

c. Time of flight

d. Communication range

e. Launch azimuth

f. Target dispersion ellipse

g. Injected payload capability

An attempt to select a launch window that yields the lowest approach velocity consistent with a favorable range in the remaining parameters should be considered since the ramifications of this parameter on a lander, orbiter or flyby mission include:

a. Lander - structural and heat shield

b. Orbiter - planetocentric orbit establishment

c. Flyby - scientific dwell time in vicinity of planet

The desirous approach geometry is essentially a function of the mission, if there is a freedom of selection for a particular opportunity. For a lander mission, the optimum ZAP angle is around 90 degrees to permit daylight landing and direct Earth communication capability for up to 6 hours after impact depending upon the landing latitude while maintaining a steep entry angle.

During the initial phases of this study, the requirement for a sunrise landing at Syrtis Major was dictated by the desire for descent TV. This science objective was eliminated from the conceptual design, however, the requirement for a sunrise landing is still valid due to the fact that the earth line is essentially equidistant between the Mars Sunline and the terminator. Therefore, the optimum period for lander Earth direct communication is between sun-rise and noon. For ZAP angles between 90 and 180 degrees Earth occulation and the lander/flyby spatial time relationships are key areas that must also be considered in the selection of the launch window. With a flyby/bus photographic mission, the optimum ZAP angle is between 30-60 degrees from the sun line to achieve adequate relief in addition to favorable lighting conditions. Mission reliability may be enhanced if significant reductions in the time of flight can be achieved without detremental effects. The Mars-Earth distance at encounter determines the power requirement and transmission bit rate for the direct link communication system. The launch azimuth constraint eliminates from consideration those trajectories where the declination of the launch asymptote exceeds the maximum orbital inclination achievable with an AMR launch subject to range safety constraints. This constraint can be relaxed or entirely removed, with a subsequent severe payload penalty, by the employment of a dog-leg maneuver.

Subsequent to the injection of the payload on the departure hyperbola, one or more midcourse maneuvers are required to eliminate injection errors and insure acceptable target planet-probe passing distances. Tracking errors which introduce slight perturbations to the actual vehicle parameters prior to the midcourse maneuver and velocity uncertainties resulting from the maneuver propagate into a dispersion ellipse at encounter. While the selection of a launch window would not be based upon the size of the dispersion ellipse, certainly with all other factors being constant the least sensitive trajectory should be selected.

Since the cost per pound of scientific payload is extremely high for any interplanetary mission, a serious attempt should be made to maximize the useful payload. For a lander or flyby lander mission, this is accomplished by employing the daily minimum departure velocity and then selecting the launch window such that the payload is maximized. In the case of an orbiter mission, the payload in the desired planetocentric orbit is a function of both the departure and approach velocities and since, in general, these velocities are not simultaneously minimized a significantly different launch window may result for the same launch opportunity.

Therefore, the selection of an optimum launch window within any launch opportunity is directly dependent upon the selected mission configuration, and scientific objectives, and numerous trade-off studies exist to simultaneously achieve acceptable variations in all pertinent trajectory parameters.

RE-ORDER No. 64-522

1. 1969 Launch Opportunity

For the 1969 Advanced Mariner flyby-lander mission, with no major retropropulsion maneuvers in the vicinity of the target planet, the absolute minimum departure velocity window centered about 1 April 1969 affords an excellent starting location in the search for the optimum window.

The trajectory charácteristics associated with a 30-day launch window from 17 March to 16 April 1969 are presented in table 9. This window yields approach dates from 5 January to 10 February 1970 (2 to 3 months subsequent to the peak of the Southern Hemisphere wave of darkening) with the time of flight approximately constant at 300 days. This window is characterized by essentially having a constant departure velocity varying only between 2.82 and 2.87 km/sec. which results in a payload of between 1680 and 1697 pounds for an unfloxed Atlas/Centaur and 2360 to 2380 for 30 percent floxed Atlas/Centaur. The Atlas/Centaur payload capability for zero percent flox (minimum); 20 percent flox (nominal); and 30 percent flox (maximum is presented in figure 4. The approach velocity increases monotonically from 4.94 to 5.31 km/sec whereas the ZAP angle (the angle between the approach asymptote and the planet-sun line) decreases monotonically from 42.2 to 33.2 degrees. Since the time of flight is essentially constant, the 30-day launch window translates into approximately a 30-day encounter window. The communication distance at encounter is essentially the Mars-Earth distance. After each opposition, this distance increases by about 1 million kilometers per day for approximately 12 months until the planets are on opposite sides of the sun. Therefore, since opposition occurs around the middle of June 1969 with a Mars-Earth distance of 72 million kilometers, the encounter distance 7 to 8 months later varies between 240 and 279 million kilometers.

The dispersion elipse in the R-T plane at encounter is composed of two components. The semi-major axis of a dispersion ellipse due to a 0.1 m/sec spherically distributed midcourse velocity error is essentially 10,000 km and the semi-major axis of the dispersion ellipse due to tracking error after the first day varies between 1,300 km and 3,500 km.

Examination of these trajectory parameters reveals a relative constancy of the departure velocity coupled with monotonic trends exhibited by the other pertinent trajectory parameters which suggests that a more favorable launch window may be obtained at an earlier date without a significant payload penalty. To assist in the selection of a more favorable window, pertinent parameters were analyzed, for constant departure velocity windows, for departure velocities of 3.25, 3.5, 3.75 and 4 km/sec. The parameters presented in figures 5 to 7 exhibit the following advantageous trends for a launch window early in 1969:

TABLE 9

1969 MINIMUM DEPARTURE VELOCITY WINDOW

Launch Date	Arrival Date	Departure Velocity (km/sec)	Departure Velocity (km/sec)	Flight Time (days)	Payload 0 % Flox (pounds)	Decl. of Geo. Asymptote (degrees)	ZAP Angle (degrees)	GP Angle (degrees)	Communication Range (10^6 km)	Encounter Dispersion Ellipse					
										Midcourse Correction			Tracking Error		
										Semi-Major Axis 1σ (km)	Semi-Minor Axis 1σ (km)	Orientation (degrees)	Semi-Major Axis 1σ (km	Semi-Major Axis 1σ (km)	Orientation (degrees)
17 Mar '69	5 Jan '70	2.865	4.943	294	1681	-1.03	42.21	-15.58	240.4	9540	386	6.4	3516	22	10.1
19	7	2.855	4.969	294	1685	-1.25	41.71	-15.51	242.5	9551	383	6.1	3499	22	9.9
21	9	2.846	4.995	294	1688	-1.50	41.22	-15.42	244.6	9572	378	5.9	3479	24	9.7
23	13	2.838	5.044	296	1692	-3.62	39.92	-14.54	248.8	9717	373	5.3	3267	25	9.5
25	15	2.831	5.067	296	1695	-3.98	39.45	-14.41	250.9	9783	388	5.1	3312	26	9.6
27	17	2.825	5.090	296	1697	-4.39	38.98	-14.27	253.1	9743	355	4.9	3126	25	9.2
29	19	2.822	5.112	296	1699	-4.85	38.52	-14.12	255.2	9753	351	4.7	3040	26	9.0
31	23	2.819	5.154	298	1700	-7.11	37.32	-13.19	259.4	9875	344	4.1	2762	30	9.2
2 Apr	25	2.818	5.174	298	1700	-7.69	36.88	-12.99	261.6	9876	340	3.9	2661	29	9.1
	27	2.819	5.193	298	1700	-8.33	36.43	-12.77	263.7	9882	334	3.7	2534	30	9.1
6	29	2.822	5.212	298	1699	-9.01	35.99	-12.53	265.8	9889	327	3.5	2400	32	9.1
9	31	2.827	5.230	298	1697	-9.76	35.54	-12.28	268.0	9891	320	3.3	2255	34	9.2
10	4 Feb	2.834	5.264	300	1694	-12.21	34.46	-11.28	272.2	10000	311	2.7	1903	41	10.0
12	6	2.843	5.279	300	1689	-13.09	34.02	-10.97	274.4	10003	302	2.5	1722	43	10.4
14	8	2.854	5.295	300	1685	-14.04	33.59	-10.62	276.5	10002	293	2.3	1529	47	10.9
16	10	2.869	5.310	300	1680	-15.06	33.15	-10.25	278.6	10010	284	2.1	1321	52	11.8

RE-ORDER No. 64-5222.

RE-ORDER No. 64-522

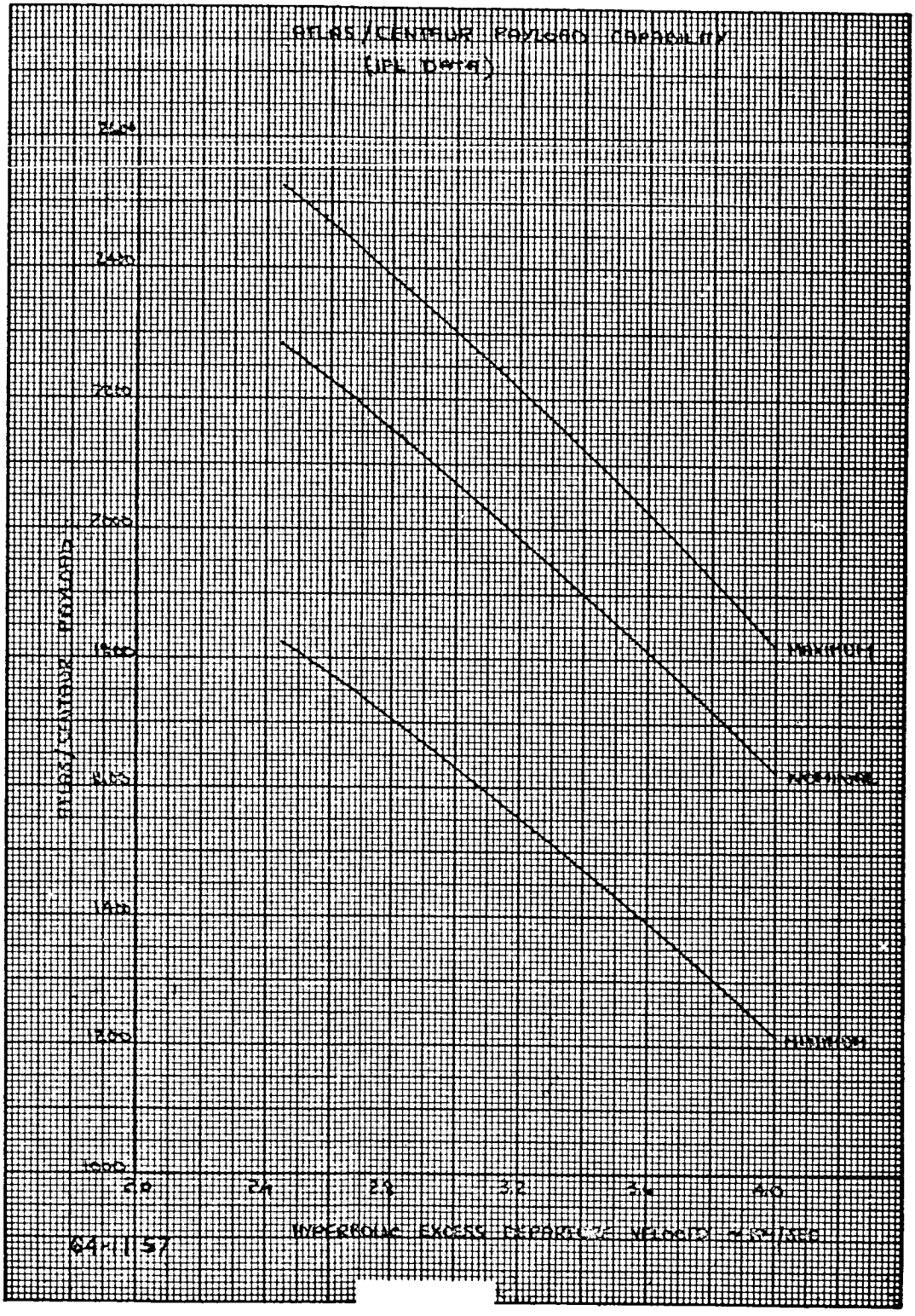

Figure 4 ATLAS/CENTAUR PAYLOAD CAPABILITY (JPL DATA)

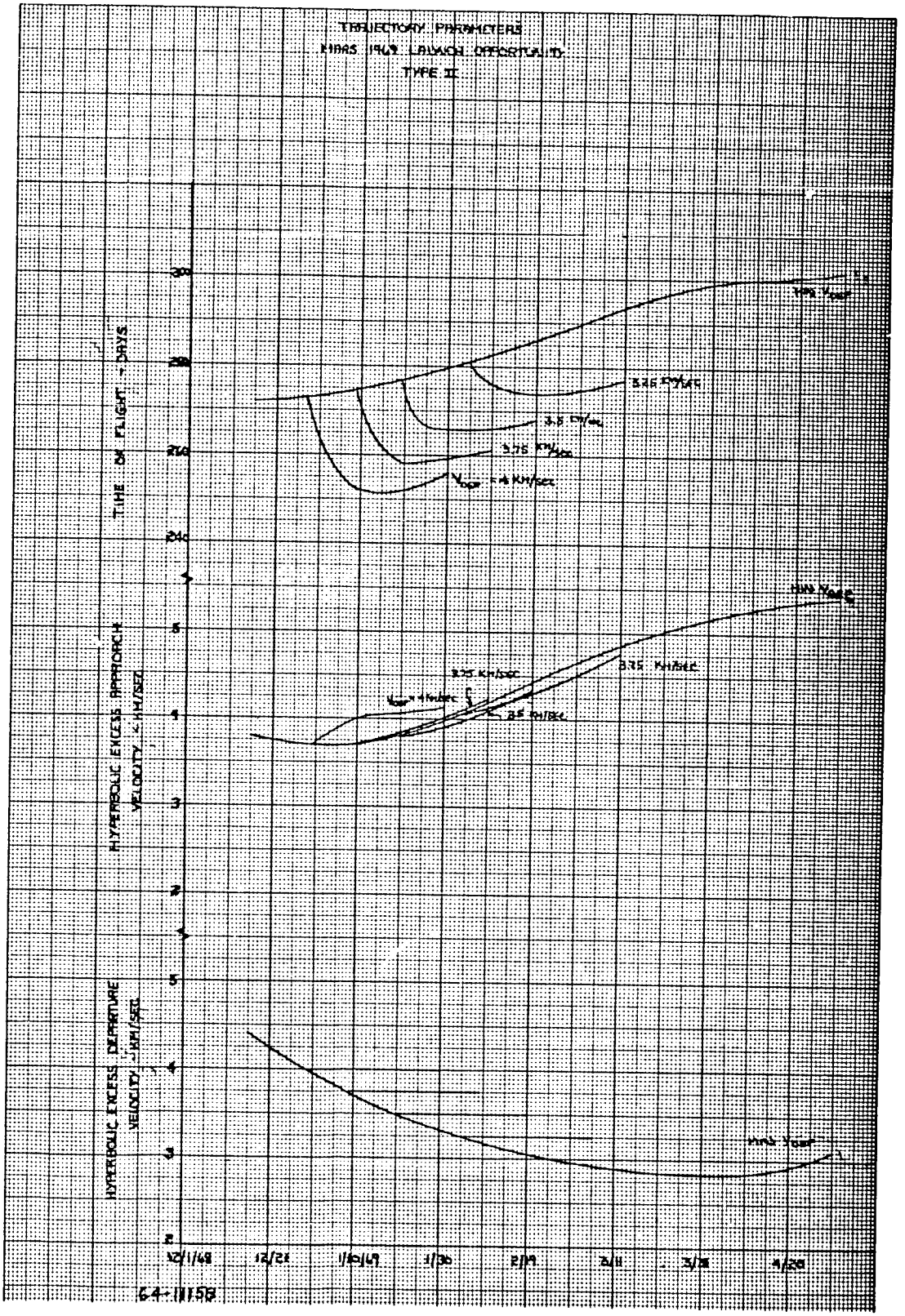

Figure 5 TRAJECTORY PARAMETERS MARS 1969 LAUNCH OPPORTUNITY TYPE II

RE-ORDER No. 64-522.

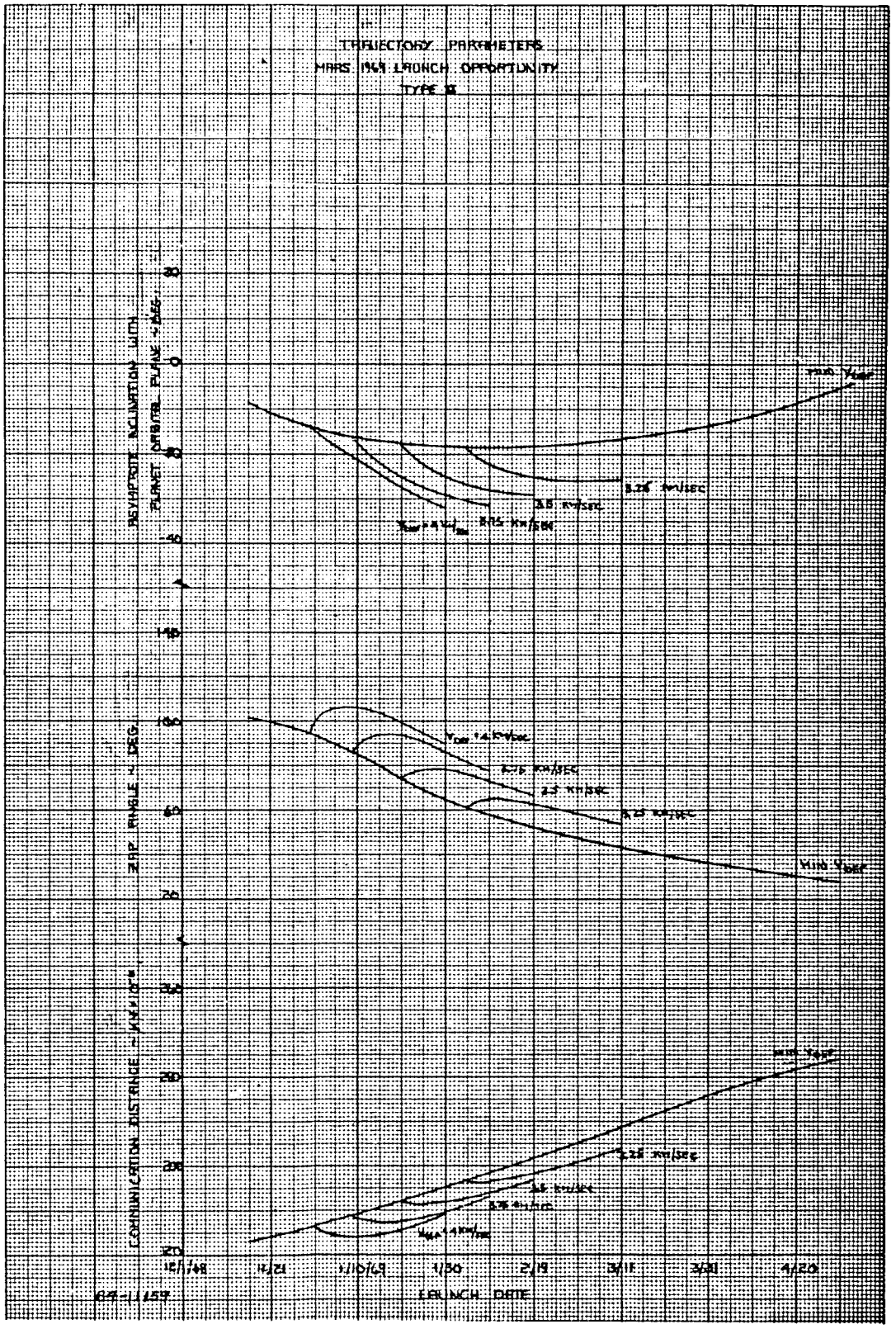

Figure 6 TRAJECTORY PARAMETERS MARS 1969 LAUNCH OPPORTUNITY TYPE II

RE-ORDER No. 64-522

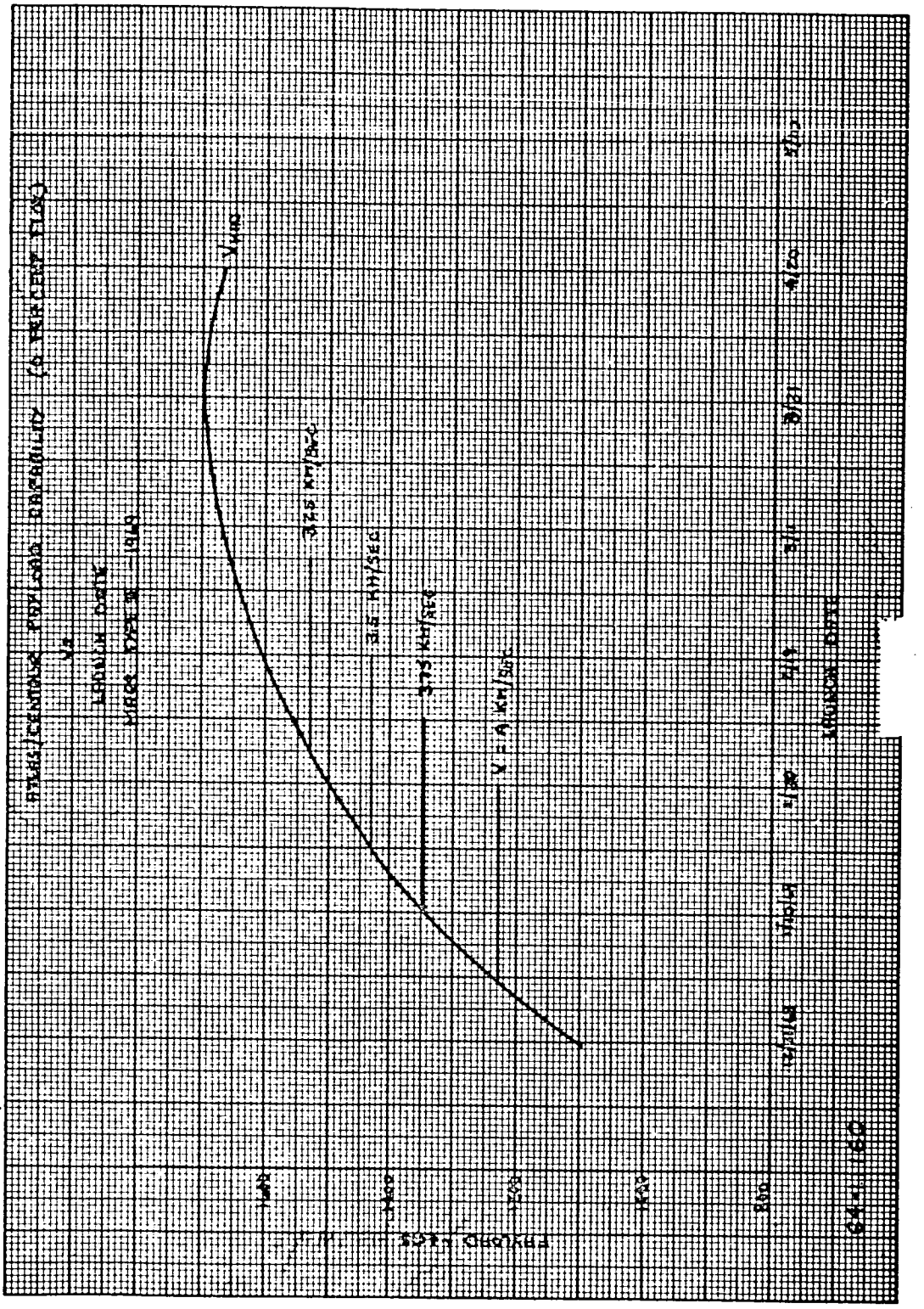

Figure 7 ATLAS/CENTAUR PAYLOAD CAPABILITY (0 PERCENT FLOX)
VERSUS LAUNCH DATE-MARS TYPE II-1969

RE-ORDER No. 64-522

a. Approach velocity is reduced by approximately 24 percent

b. Time of flight is decreased by approximately 10 percent as the minimum departure velocity is moved back to January 1969 with additional decreases resulting from the utilization of nonminimum departure velocities

c. Reduction in flight duration coupled with earlier launch dates results in a shifting of the approach window into a more favorable time; the peak of the southern hemisphere wave of darkening at Syrtis Major.

d. The reduction in flight duration coupled with the earlier launch date results in a reduction of 100 million kilometers in the communication range

e. ZAP angles of approximately 90 degrees are achievable thereby yielding a more favorable "Type 1" approach with sunrise landings.

The only disadvantage associated with earlier launch windows is the previously mentioned payload penalty. This penalty is approximately 350 pounds for a constant departure velocity of 3.75 km/sec with an associated launch window starting 10 January 1969. However, one of the primary functions of this mission is the biological experiments; there does not appear to be a severe penalty in shifting the arrival window to the peak of the wave of darkening where the probability of determining the existence of life is maximized. Also, the marked improvement in the remaining pertinent trajectory parameters will tend to reduce this penalty since the reduced approach velocity will result in reductions in the lander structural thermal and protection requirements.

Based upon this preliminary analysis, a tentative launch window between 10 January and 19 February was selected for further consideration. The variation in the trajectory parameters associated with this window are presented in table 10. The corresponding variations in the planetocentric latitude and longitude of the approach asymptote, Earth and sun lines are presented in figures 8 and 9. These data indicate that both the Earth and the sun are below the Martian equator while the probe is passing from north to south.

The next step in the selection of a more definite launch window was the analysis of pertinent trajectory characteristics associated with constant arrival date windows. Approach dates between 15 October and 20 December were considered at 6-day intervals providing information for about 1 month on either side of the optimum scientific arrival date, 15 November. The pertinent trajectory parameters are presented in table 11 for 28- 32-day launch

RE-ORDER No. 64-522

TABLE 10

COMPARISON OF TRAJECTORY PARAMETERS

FOR ADVANCED MARINER 1969 LAUNCH OPPORTUNITY*

Launch Window	16 Mar - 15 Apr	20 Jan - 19 Feb	10 Jan - 9 Feb
Conditions	Min. Dep. Velocity	Constant Dep. Velocity	Constant Dep. Vel.
Departure Velocity (km/sec)	2.82-2.87	3.50	3.75
Payload** (pounds)	1680-1698	1430	1345
Approach Velocity (km/sec)	4.94-5.31	3.80-4.34	3.70-4.22
Time of Flight (days)	294-300	266-277	258-274
Arrival Date	5 Jan - 10 Feb 1970	15 Oct - 12 Nov 1969	3 Oct - 26 Oct 1969
ZAP Angle (degrees	33-42	66-78	78-94
Communication Range (10^6 km)	240-279	166-188	149-172

*Spread in parameters indicates maximum excursion rather than extremes of window

**Data Based upon minimum payload capability (0 percent floxing)

RE-ORDER No. 64-522

TABLE 11

COMPARISON OF TRAJECTORY PARAMETERS

1969 LAUNCH OPPORTUNITY
Constant Arrival Dates (6 - Day Intervals)

Launch Date	Arrival Date	Departure Velocity (km/sec)	Payload (pounds)	Approach Velocity (km/sec)	Flight Time (days)	ZAP Angle (degrees)	Declination of Launch Asymptote (degrees)	Communication Range (10^6 km)
10 Jan	15 Oct	3.718	1340	3.744	278	79.80	1.57	159.6
14 Jan		3.628	1378	3.740	274	81.43	4.52	
18 Jan		3.571	1405	3.757	270	82.96	8.12	
22 Jan		3.562	1408	3.802	266	84.40	12.50	
26 Jan		3.626	1380	3.889	262	85.73	17.80	
30 Jan		3.805	1302	4.042	258	86.96	24.14	
3 Feb		4.180		4.316	254	88.07	31.64	
7 Feb		4.928		4.834	250	89.02	40.35	
10 Jan	21 Oct	3.752	1327	3.820	284	73.91	-.85	165.1
14 Jan		3.636	1372	3.796	280	75.50	1.67	
18 Jan		3.546	1413	3.788	276	77.04	4.74	
22 Jan		3.492	1435	3.802	272	78.51	8.46	
26 Jan		3.487	1437	3.844	268	79.91	12.95	
30 Jan		3.557	1410	3.929	264	81.27	18.35	
3 Feb		3.744	1330	4.082	260	82.60	24.78	
7 Feb		4.132		4.357	256	83.91	32.32	
11 Feb		4.903		4.886	252	85.25	41.07	
14 Jan	27 Oct	3.677	1360	3.892	286	69.94	-.95	170.6
18 Jan		3.561	1407	3.863	282	71.43	1.65	
22 Jan		3.472	1445	3.852	278	72.87	4.80	
26 Jan		3.419	1465	3.863	274	74.27	8.61	
30 Jan		3.416	1466	3.903	270	75.65	13.18	
3 Feb		3.490	1438	3.984	266	77.03	18.65	
7 Feb		3.684	1355	4.135	262	78.44	25.12	
11 Feb		4.081		4.410	258	79.95	32.71	
15 Feb		4.869		4.942	254	81.66	41.50	
18 Jan	2 Nov	3.610	1386	3.976	288	66.22	-1.17	176.2
22 Jan		3.493	1435	3.944	284	67.60	1.49	
26 Jan		3.404	1470	3.930	280	68.95	4.70	
30 Jan		3.351	1494	3.938	276	70.29	8.56	
3 Feb		3.350	1494	3.974	272	71.63	13.18	
7 Feb		3.426	1461	4.052	268	73.02	18.68	
11 Feb		3.623	1380	4.199	264	74.50	25.18	
15 Feb		4.025	1205	4.470	260	76.19	32.80	

66

TABLE 11 (Cont'd)

Launch Date	Arrival Date	Departure Velocity (km/sec)	Payload (pounds)	Approach Velocity (km/sec)	Flight Time (days)	ZAP Angle (degrees)	Declination of Launch Asymptote (degrees)	Communication Range (10^6 km)
18 Jan	8 Nov	3.689	1355	4.119	294	61.43	-3.74	181.9
22 Jan		3.549	1410	4.070	290	62.73	-1.50	
26 Jan		3.431	1460	4.036	286	64.02	1.20	
30 Jan		3.341	1498	4.019	282	65.28	4.43	
3 Feb		3.288	1518	4.022	278	66.56	8.31	
7 Feb		3.288	1518	4.055	274	67.87	12.94	
11 Feb		3.365	1495	4.129	270	69.25	18.45	
15 Feb		3.562	1408	4.271	266	70.79	24.96	
19 Feb		3.965	1231	4.536	262	72.61	32.59	
26 Jan	14 Nov	3.495	1435	4.171	292	59.50	-1.94	187.7
30 Jan		3.375	1485	4.134	288	60.69	.76	
3 Feb		3.284	1518	4.114	284	61.88	3.99	
7 Feb		3.230	1540	4.115	280	63.09	7.85	
11 Feb		3.229	1540	4.143	276	64.36	12.47	
15 Feb		3.304	1510	4.213	272	65.72	17.96	
19 Feb		3.500	1432	4.349	268	67.29	24.45	
23 Feb		3.900	1260	4.605	264	69.23	32.08	
27 Feb		4.698		5.117	260	71.85	41.02	
30 Jan	20 Nov	3.446	1453	4.278	294	56.50	-2.50	193.5
3 Feb		3.325	1502	4.238	290	57.61	.18	
7 Feb		3.232	1544	4.215	386	58.72	3.38	
11 Feb		3.176	1562	4.212	282	59.87	7.20	
15 Feb		3.173	1563	4.237	278	61.08	11.77	
19 Feb		3.246	1536	4.301	274	62.42	17.20	
23 Feb		3.436	1459	4.430	270	64.00	23.65	
27 Feb		3.829	1292	4.675	266	66.02	31.27	
3 Mar		4.617		5.171	262	68.86	40.28	
3 Feb	26 Nov	3.403	1470	4.386	296	53.74	-3.16	199.4
7 Feb		3.279	1522	4.344	292	54.76	-.53	
11 Feb		3.184	1558	4.319	288	55.80	2.61	
15 Feb		3.126	1581	4.313	284	56.88	6.36	
19 Feb		3.120	1584	4.334	280	58.03	10.84	
23 Feb		3.188	1557	4.393	276	59.33	16.20	
27 Feb		3.372	1485	4.513	272	60.90	22.57	
3 Mar		3.754	1326	4.745	268	62.97	30.15	
7 Mar		4.526		5.219	264	65.99	39.24	

RE-ORDER No. 64-522

TABLE 11 (Concl'd)

Launch Date	Arrival Date	Departure Velocity (km/sec)	Payload (pounds)	Approach Velocity (km/sec)	Flight Time (days)	ZAP Angle (degrees)	Declination of Launch Asymptote (degrees)	Communication Range (10^6 km)
7 Feb	2 Dec	3.365	1488	4.496	298	51.18	-3.92	205.3
11 Feb		3.239	1540	4.452	294	52.13	-1.36	
15 Feb		3.141	1576	4.424	290	53.09	1.69	
19 Feb		3.080	1600	4.415	286	54.10	5.34	
23 Feb		3.070	1604	4.432	282	55.19	9.70	
27 Feb		3.133	1580	4.485	278	56.44	14.93	
3 Mar		3.308	1510	4.596	274	57.99	21.19	
7 Mar		3.675	1360	4.812	270	60.08	28.73	
11 Mar		4.426		5.263	266	63.22	37.92	
11 Feb	8 Dec	3.331	1500	4.604	300	48.82	-4.76	211.4
15 Feb		3.203	1551	4.558	296	49.69	-2.30	
19 Feb		3.102	1591	4.528	292	50.58	.63	
23 Feb		3.038	1618	4.517	288	51.52	4.14	
27 Feb		3.024	1621	4.530	284	52.55	8.34	
3 Mar		3.079	1600	4.576	280	53.74	13.40	
7 Mar		3.243	1536	4.677	276	55.25	19.53	
11 Mar		3.593	1394	4.877	272	57.33	27.01	
15 Mar		4.317		5.302	268	60.54	36.31	
15 Feb	14 Dec	3.302	1511	4.711	302	46.64	-5.68	217.5
19 Feb		3.171	1565	4.663	298	47.44	-3.34	
23 Feb		3.068	1605	4.631	294	48.25	-.56	
27 Feb		3.000	1630	4.617	290	49.12	2.77	
3 Mar		2.981	1638	4.625	286	50.08	6.78	
7 Mar		3.029	1620	4.665	282	51.21	11.64	
11 Mar		3.180	1560	4.755	278	52.66	17.59	
15 Mar		3.090	1558	4.939	274	54.69	24.99	
19 Mar		4.202	1122	5.336	270	57.94	34.40	
19 Feb	20 Dec	3.278	1523	4.814	304	44.61	-6.66	223.7
23 Feb		3.144	1575	4.765	300	45.34	-4.47	
27 Feb		3.038	1618	4.731	296	46.09	-1.87	
3 Mar		2.966	1645	4.714	292	46.89	1.25	
7 Mar		2.942	1651	4.717	288	47.78	5.02	
11 Mar		2.982	1638	4.750	284	48.84	9.64	
15 Mar		3.120	1574	4.830	280	50.21	15.38	
19 Mar		3.426	1463	4.998	276	52.17	22.66	
23 Mar		4.081	1180	5.363	272	55.39	32.17	

RE-ORDER No. 64-522

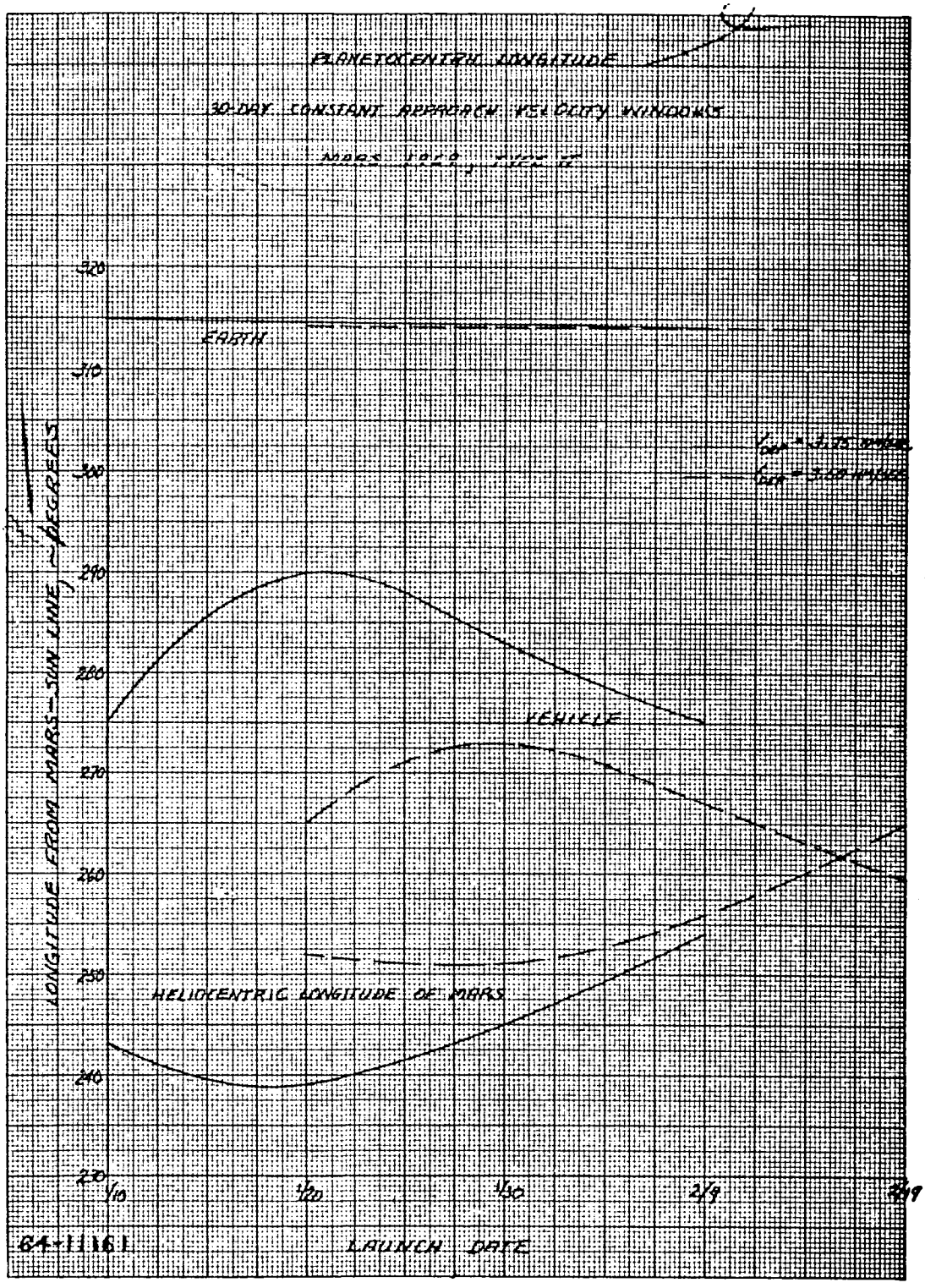

Figure 8 PLANETOCENTRIC LONGITUDE 30-DAY CONSTANT APPROACH VELOCITY WINDOWS MARS 1969, TYPE II

64

RE-ORDER No. 64-522

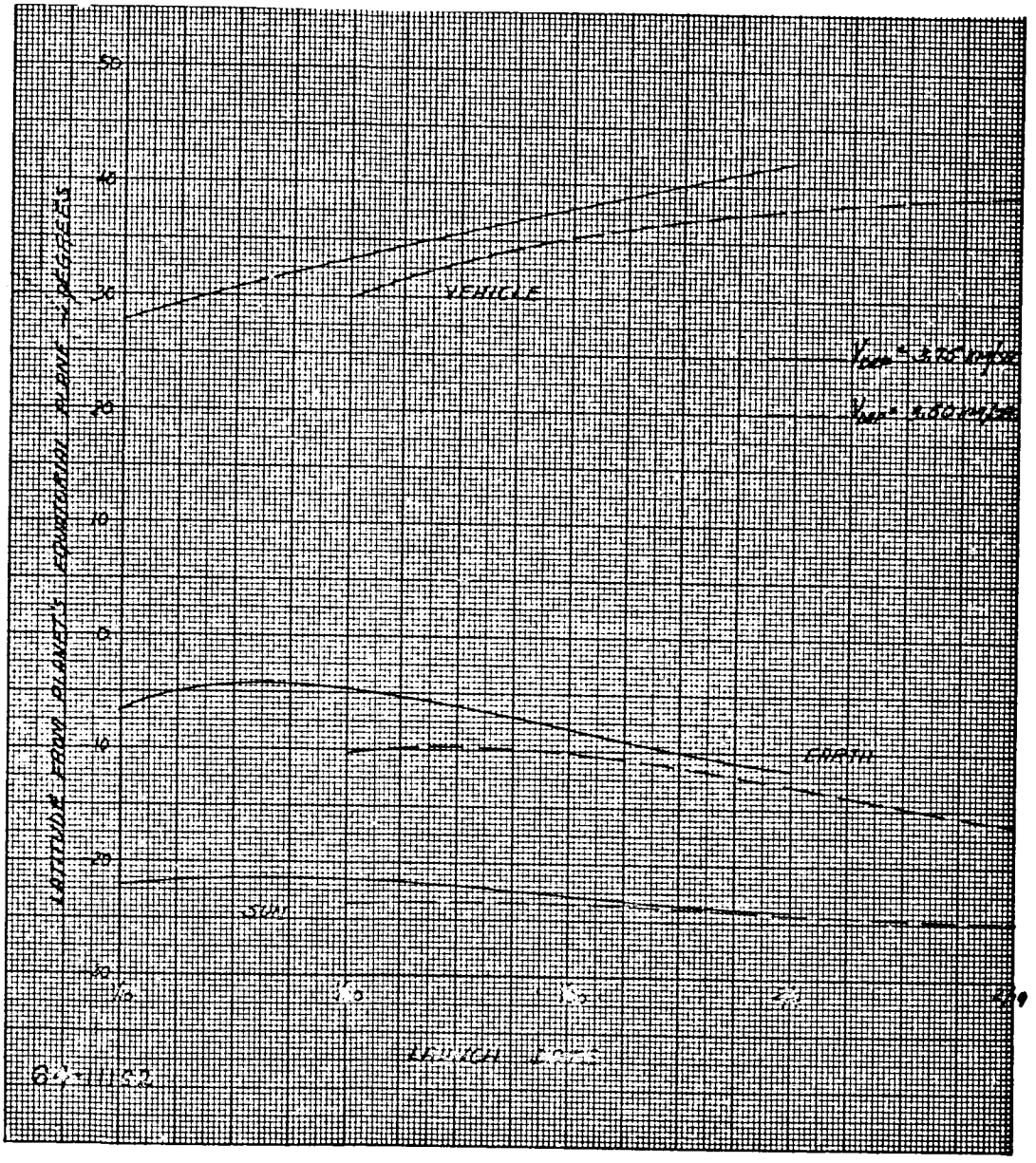

Figure 9 PLANETOCENTRIC LATTITUDE 30-DAY CONSTANT APPROACH VELOCITY WINDOWS MARS 1969, TYPE II

RE-ORDER No. 64-522.

windows. From these data it is immediately obvious that a single fixed arrival date is not feasible due to the rapid increase in the departure velocity required for the successively faster trips at the end of each window. Although these data are presented for fixed arrival date window, the information is also available to perform a similar analysis for fixed time of flight trajectories.

The minimum departure and arrival velocities associated with this fixed arrival date window occur within several days of each other. As the arrival date is moved back, the minimum departure velocity associated with the window is reduced, whereas, the minimum approach velocity is increased. This results from the fact that there is approximately a 4-month difference in launch date between the dates where the approach and departure velocities are minimized.

For a given fixed arrival date window there is a 12-degree variation in the ZAP angle with the ZAP angle increasing as the time of flight decreases. This variation is essentially independent of the window; however, the magnitude of the ZAP angle decreases about 5 degrees for each 6-day shift in the window. Therefore, in the initial selection of a launch window based upon the trajectory parameters, with little regard to the associated payload penalty, arrival dates during the later part of October result in the above mentioned ground rule of arriving within one month of the peak wave of darkening. Also due to the reduction in both ZAP angle and payload as the time of flight increases, launch dates prior to 10 January with a 15 October arrival were not considered.

In an attempt to achieve uniformity in both the payload and ZAP angle, 8-day launch windows were selected for each of the 4 fixed arrival dates, 15 October, 21 October, 27 October, and 2 November. Another factor considered in the selection of 4 fixed arrival dates is that two or more missions during the same opportunity would not conflict with each other during the encounter phase of each mission. A complete summary of the trajectory parameters associated with this window is presented in table 12. In addition to the trajectory parameters this table also contains the dispersion ellipse in the R-T plane resulting from 1 and 2 midcourse corrections. The 1 midcourse dispersion ellipse is based upon the assumptions that there is a spherically distributed velocity uncertainty of 0.1 m/sec and that the correction occurs about one day after injection. The second midcourse correction occurs at a sufficiently large distance from Earth so that the tracking ellipse errors are reduced to about 1,000 kilometers and the velocity uncertainty is reduced by a factor of 10 to 0.01 m/sec.

Therefore, the launch window presented in table 12 is only intended as a preliminary launch window based upon the optimization of pertinent trajectory parameters. A detailed analysis of various system studies must now be

TABLE 12

TRAJECTORY PARAMETERS
1969 LAUNCH OPPORTUNITY

Launch Date	Arrival Date	Departure Velocity (km/sec)	Approach Velocity (km/sec)	Flight Time (days)	Payload (pounds)	Declination of Launch Asymptote (degrees)	ZAP Angle (degrees)	Minimum Flyby Inclination (degrees)	Communication Range (10^6 km)	Encounter Dispersion Ellipse					
										1 Midcourse Correction			2 Midcourse Correction		
										Semi-Major Axis (km)	Semi-Minor Axis (km)	Orientation (degrees)	Semi-Major Axis (km)	Semi-Minor Axis (km)	Orientation (degrees)
10 Jan 1969	15 Oct 1969	3.718	3.744	278	1342	1.57	79.80	27.68	159.593	5512	537	25	1131	82	29
14 Jan 1969		3.628	3.740	274	1379	4.52	81.43	28.95		5455	538	30	1127	78	32
18 Jan 1969		3.571	3.757	270	1403	8.12	82.96	30.54		5475	565	34	1126	76	35
18 Jan 1969	21 Oct 1969	3.546	3.788	276	1418	4.74	77.04	29.69	165.069	6072	518	26	1155	78	28
22 Jan 1969		3.492	3.802	272	1435	8.46	78.51	31.31		6085	545	30	1153	75	31
26 Jan 1969		3.487	3.844	268	1437	12.95	79.91	33.34		6174	586	34	1154	76	33
26 Jan 1969	27 Oct 1969	3.419	3.863	274	1466	8.61	74.27	31.82	170.604	6648	514	26	1179	73	27
30 Jan 1969		3.416	3.903	270	1467	13.18	75.65	33.85		6728	554	29	1179	74	29
3 Feb 1969		3.490	3.984	266	1436	18.65	77.03	36.40		6913	625	33	1181	80	32
3 Feb 1969	2 Nov 1969	3.350	3.974	272	1494	13.18	71.63	34.07	176.210	7244	527	26	1203	72	26
7 Feb 1969		3.426	4.052	268	1463	18.68	73.02	36.60		7416	595	29	1203	77	28
11 Feb 1969		3.623	4.199	264	1381	25.18	74.90	39.79		7711	691	32	1207	86	31

RE-ORDER No. 64-522

conducted to determine the suitability of this window to direct and relay communication, lander-flyby geometry, lander entry angle and dispersion ellipse for Syrtis Major impact, occultation problem, etc. Upon completion of these studies a shift in the launch window may be required to satisfy certain criteria and this iteration process will continue until a final launch window satisfying both trajectory parameters and mission requirements is achieved.

The variation in the individual trajectory parameters associated with this launch window are presented in figures 10 to 12. With the exception of the inclination of the approach asymptote with respect to the Martian orbital plane, the trajectory parameters are fairly constant within each 8-day launch window. Over the entire 32-day window the ZAP angle variation is about 17 degrees and the approach velocity varies less the 0.5 km/sec.

The planetocentric latitude and longitude of the approach asymptote, the Earth line and the sun line are presented in figures 13 and 14.

For this window, the longitude of the approach asymptote with respect to the sun line is within ±6 degrees of the terminator, thereby minimizing the longitude excursion to achieve a sunrise landing. The longitude of the Earth line is about 315 degrees indicating that a direct link lander-Earth communication is feasible for about 6 hours, from sunrise to noon. The latitude of both the Earth line and sun line is in the southern hemisphere with the sun line at its southernmost declination; summer solstice in the southern hemisphere. The latitude of the approach asymptote varies between 28 and 40 degrees with the vehicle passing the planet from north to south. Therefore, a latitude excursion between 18 and 30 degrees is required to impact Syrtis Major even though the window was selected to minimize the longitude excursion. This latitude excursion indicates that the maximum entry angle for a Syrtis Major impact is between -66 and -74 degrees and this maximum angle is achievable only with a near polar lander orbit from separation to impact.

2. Look Angles

A spacecraft designed for interplanetary missions contains many sensors - solar panels, planet and star trackers, communication antennas, etc. - that must remain oriented toward the specific target for the duration of the mission except for possible short duration maneuver periods. In order to determine the optimum location, number of degrees of freedom and gimbaling requirements for each instrument, to insure satisfactory operation throughout the mission, it is necessary to determine the look angle requirements for each sensor. In this analysis it was assumed that the sun, Earth, Mars, and Canopus were the bodies of interest. A vehicle-centered coordinate system was established where one axis, e_3, is the vehicle-sun line;

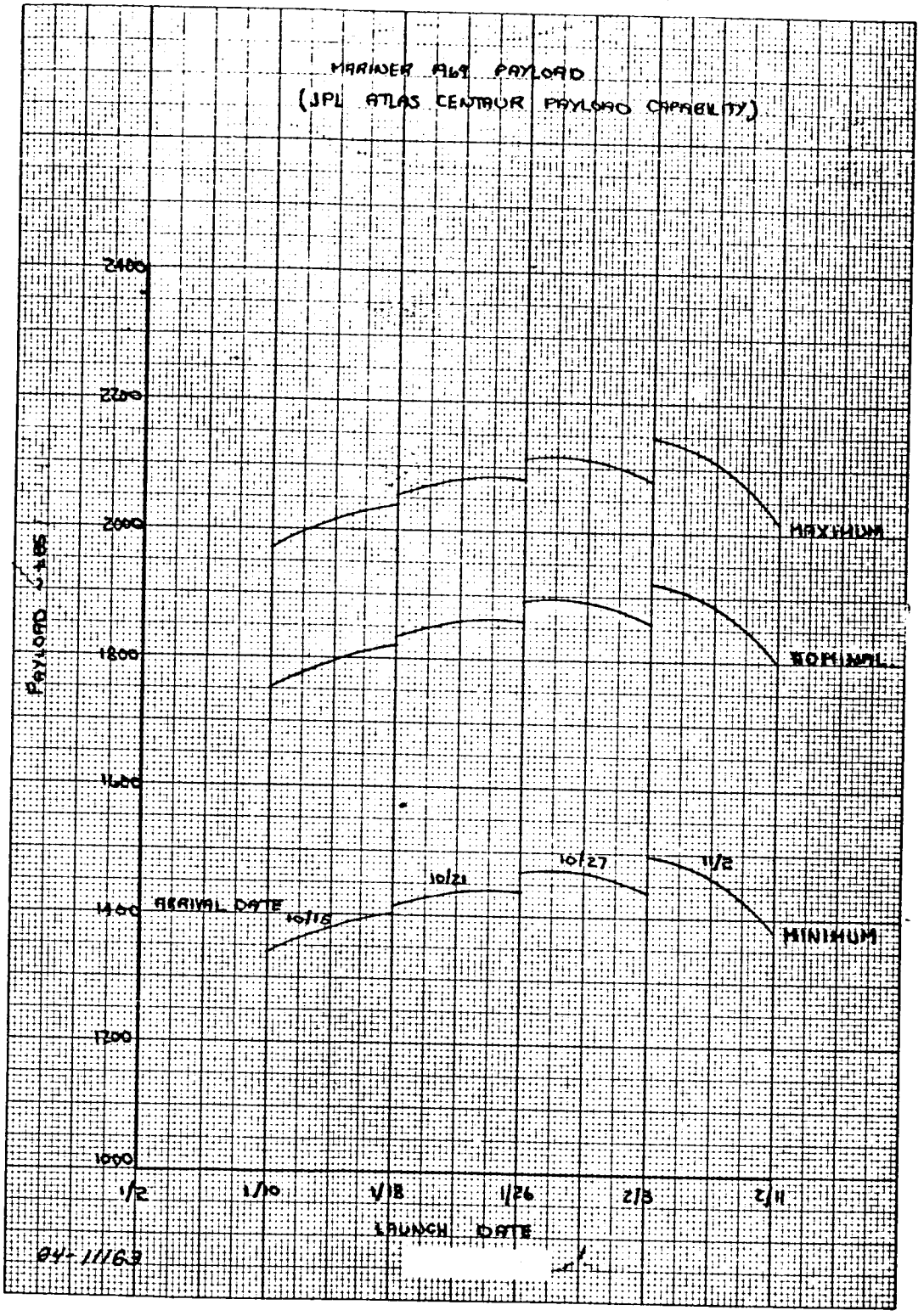

Figure 10 MARINER 1969 PAYLOAD

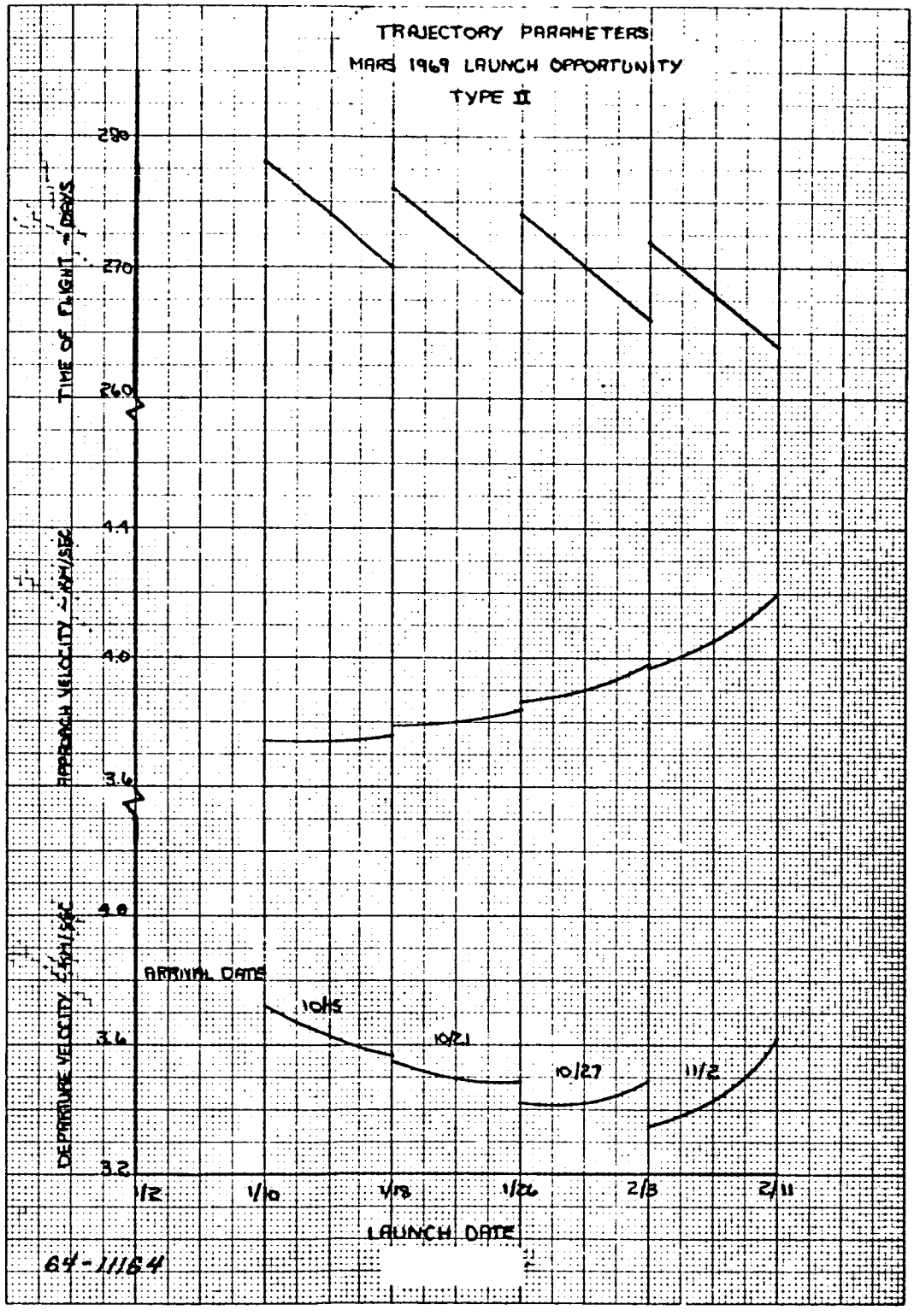

Figure 11 TRAJECTORY PARAMETERS MARS 1969 LAUNCH OPPORTUNITY TYPE II

RE-ORDER No. 64-522

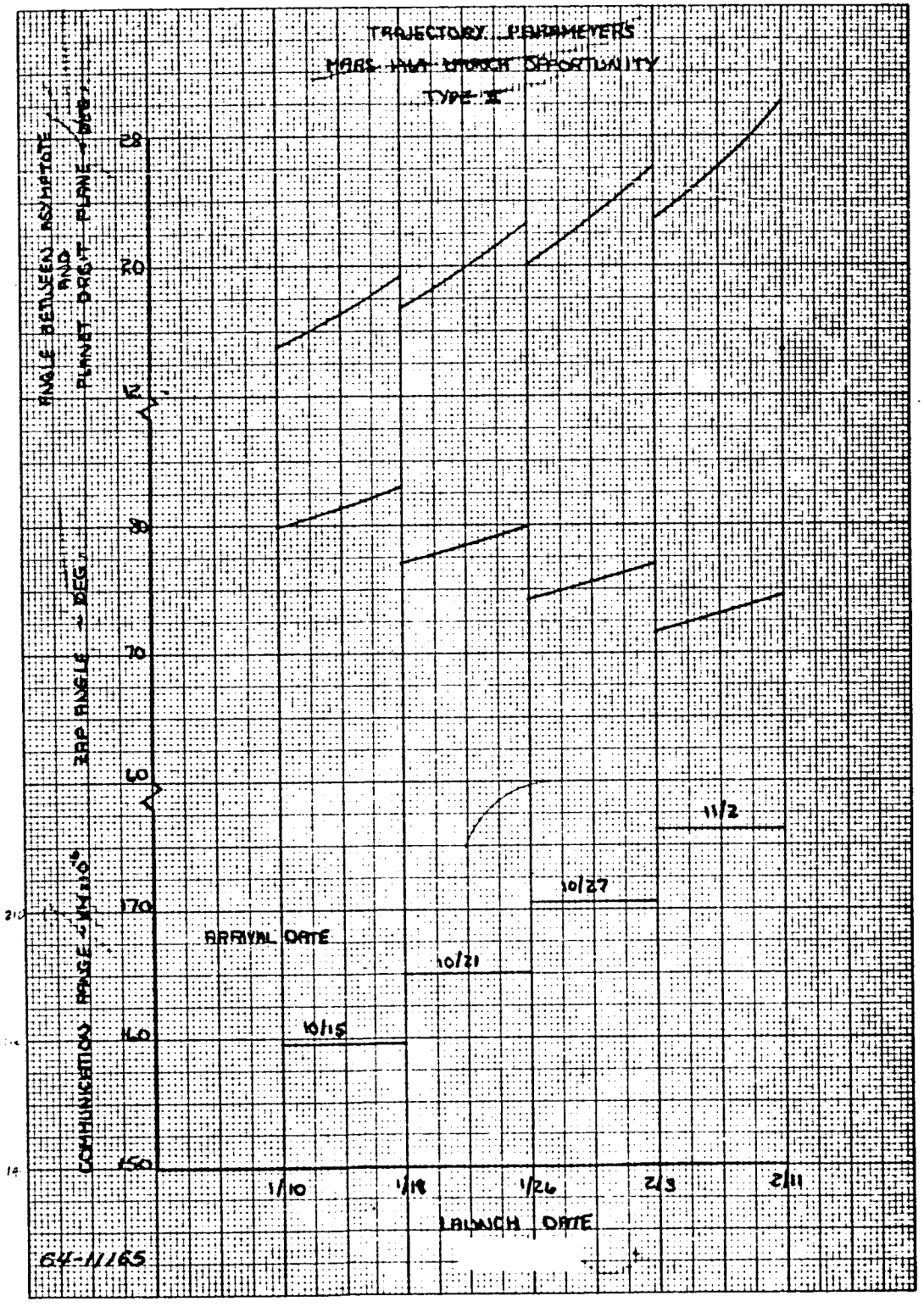

Figure 12 TRAJECTORY PARAMETERS MARS 1969 LAUNCH OPPORTUNITY TYPE II

RE-ORDER No. 64-522

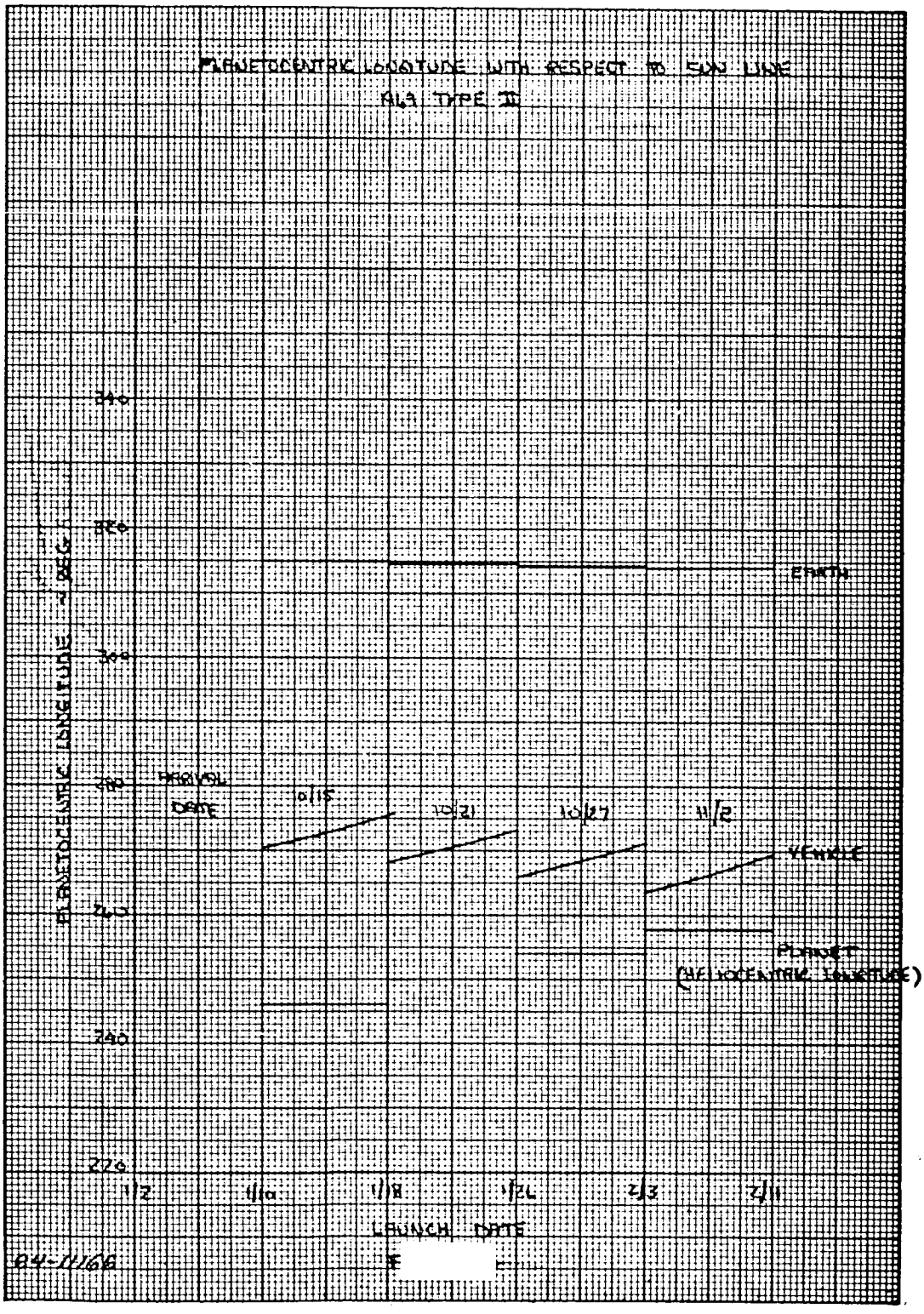

Figure 13 PLANETOCENTRIC LONGITUDE WITH RESPECT TO SUN LINE
1969 TYPE II

RE-ORDER No. 64-522

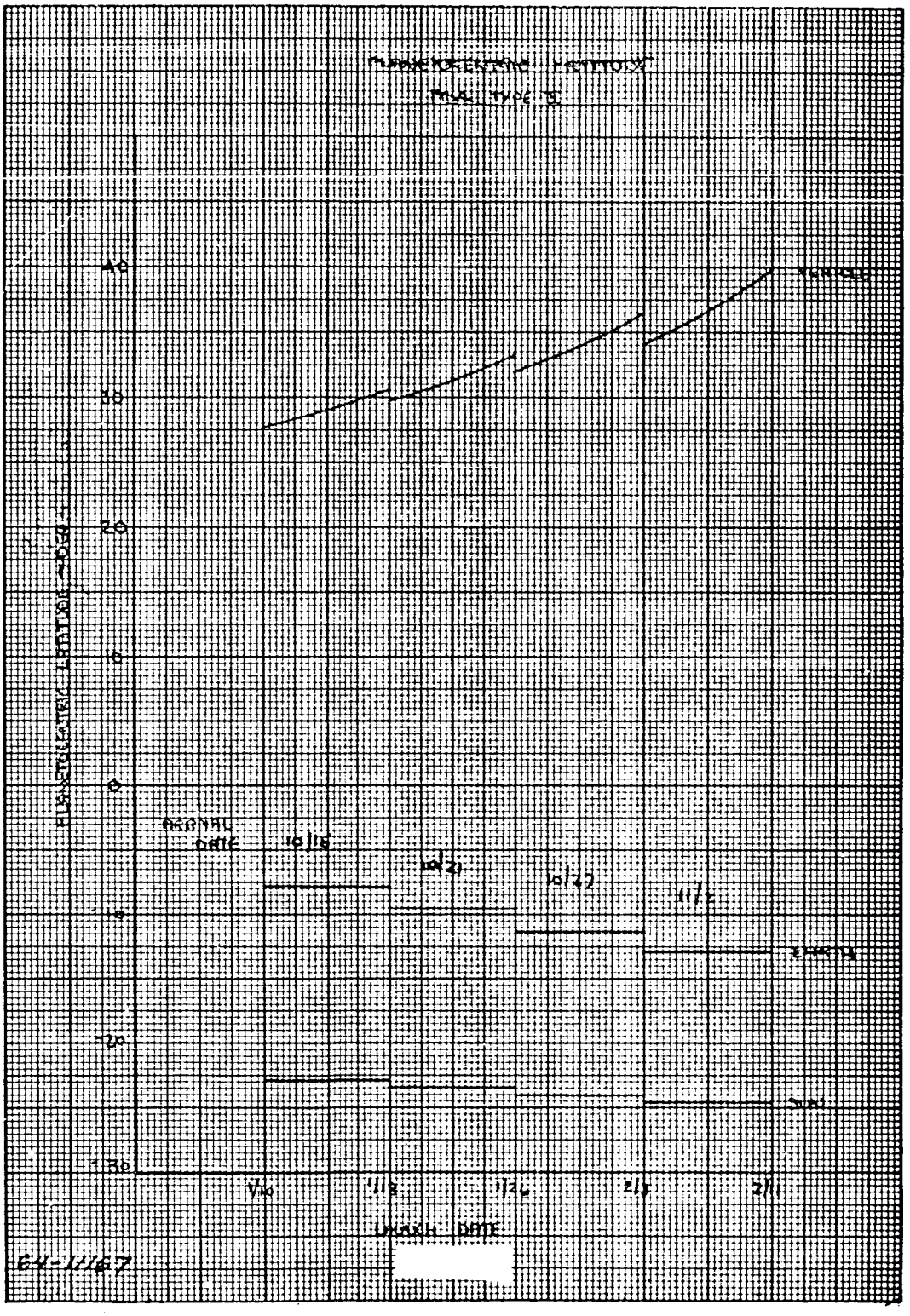

Figure 14 PLANETOCENTRIC LATTITUDE 1969 TYPE II

RE-ORDER No 64-522

the second axis, e_2, is normal to the vehicle-sun-Canopus plane; and the third axis, e_1, is in the vehicle-sun-Canopus plane normal to the vehicle-sun line. Expressed mathematically

$$\underline{e}_3 = \underline{1}_{vs}$$

$$\underline{e}_2 = \frac{\underline{e}_3 \times \underline{1}_{vs}}{|\underline{e}_3 \times \underline{1}_{vs}|}$$

$$\underline{e}_1 = \underline{e}_2 \times \underline{e}_3$$

In this vehicle centered coordiante system (which rotates as a function of time) the direction cosines or cone-clock angles (see figure 15) to the desired target can be obtained as a function of time. For the two separate phases of the mission-interplanetary and approach hyperbola-digital computer programs were developed during the course of the Voyager studies[3] to obtain the above mentioned angles.

For launch dates corresponding to the middle of each of the four constant arrival date windows, the cone-clock angles to Earth are presented as a function of time in table 13. Since the cone angle is measured in a probe centered system, the cone angle can be employed to determine those periods of time where the probe is inside (cone angle greater than 90 degrees) the orbit of the target body. Similiarly the clock angle gives the relative position of the probe and target body in the plane of motion. Clock angles between 0 and 180 degrees indicate the probe is ahead of the target body, whereas angles between 180 and 360 degrees indicate the probe is trailing the target body. Also clock angles in the first and fourth quadrants imply the probe is above the target body and clock angles in the second and third quadrants imply the probe is below the target body.

For the 1969 launch window under consideration the spacecraft is launched prior to perihelion of the transfer orbit and the probe passes inside the Earth's orbit initially as is indicated by the fact that the cone angle is greater than 90 degrees. Since the probe passes inside the Earth's orbit the probe is moving faster than the Earth and initially moves ahead of the Earth with clock angles between 0 and 90 degrees. Approximately 160 days after launch, the Earth cone-clock angles achieve a steady-state condition regardless of launch and arrival dates. For one representative trajectory the same cone-clock angles are presented as a function of the distance from Earth in figures 16 and 17. These results indicate that the steady-state condition is reached when the probe is about 50×10^6 km from Earth. This steady-state condition might be realized earlier if the trajectory were not inside the Earth's orbit for 40-50 days. Between 120-140 days after launch the clock angle is zero indicating that the Earth has caught up with the probe and is now in the probe-Sun-Canopus plane. At this time the cone angle also reaches a minimum;

[3] Voyager Design Studies, Vol. 3, 15 Oct 1963, pgs 130-140.

TABLE 13

INTERPLANETARY EARTH CONE-CLOCK ANGLE
MARS 1969 TYPE II

Time (days)	Launch Date: 14 Jan Arrival Date: 15 Oct		Launch Date: 22 Jan Arrival Date: 21 Oct		Launch Date: 30 Jan Arrival Date: 27 Oct		Launch Date: 7 Feb Arrival Date: 2 Nov	
	Cone Angle (degrees)	Clock Angle (degrees)	Cone Angle (degrees)	Clock Angle (degrees)	Cone Angle (degrees)	Clock Angle (degrees)	Cone Angle (degrees)	Clock Angle (degrees)
1	133.9	47.8	126.9	43.9	120.8	39.9	113.9	35.0
5	130.4	49.0	124.2	44.9	117.6	40.6	110.8	35.3
10	120.0	50.1	119.9	45.8	113.6	41.1	106.9	35.5
20	117.5	51.5	111.9	46.8	105.7	41.6	99.0	35.7
40	101.6	52.0	96.1	47.1	90.0	41.5	83.6	34.9
60	86.4	52.0	80.4	46.8	73.8	40.4	67.0	32.5
80	70.2	51.9	62.9	45.5	55.1	36.9	48.2	25.6
100	50.6	50.3	41.4	40.0	33.7	24.5	29.7	4.5
120	26.6	40.1	19.5	12.7	19.4	342.5	23.5	318.4
140	11.5	326.7	18.5	299.5	25.3	291.3	30.7	288.8
160	24.5	280.0	30.4	277.5	34.8	278.1	38.1	279.4
180	35.4	271.9	38.7	273.4	41.1	275.1	42.8	276.9
200	41.6	271.9	43.3	273.5	44.6	275.1	45.3	276.8
220	44.9	273.4	45.6	274.9	46.1	276.3	46.3	277.7
240	46.2	275.4	46.4	276.6	46.3	277.9	46.1	279.0
260	46.3	277.5	46.1	278.5	45.7	279.5	45.3	280.3
268	46.1	278.3	45.7	279.3	45.3	280.1	44.7	280.9
270	46.0	278.5	45.6	279.4	45.1	280.3		
272	45.9	278.7	45.6	279.6				
274	45.9	278.9						

RE-ORDER No. 64-522

RE-ORDER No. 64-522

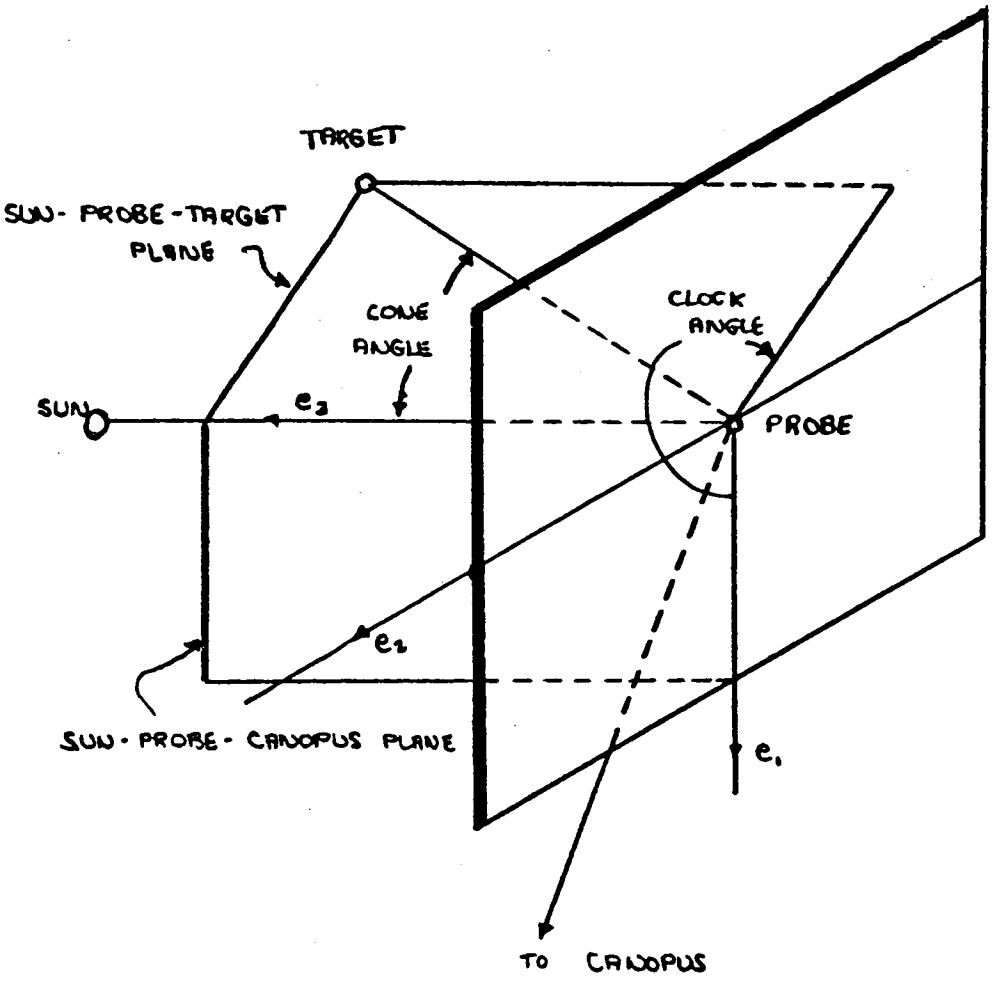

Figure 15 VEHICLE CENTERED COORDINATE SYSTEM

RE-ORDER No. 64-522

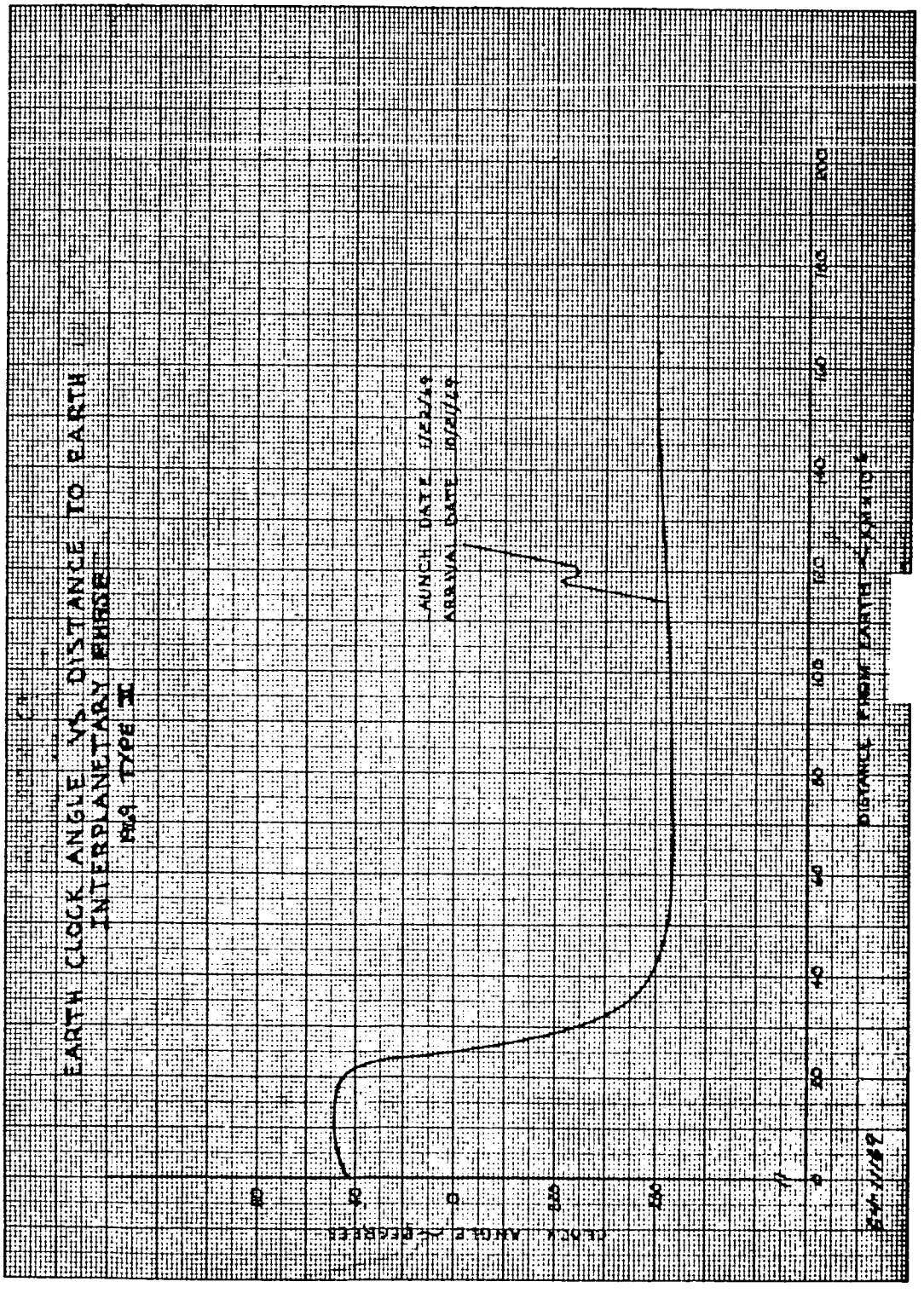

Figure 16 EARTH CLOCK ANGLE VERSUS DISTANCE TO EARTH INTERPLANETARY PHASE 1969 TYPE II

RE-ORDER No. 64-522

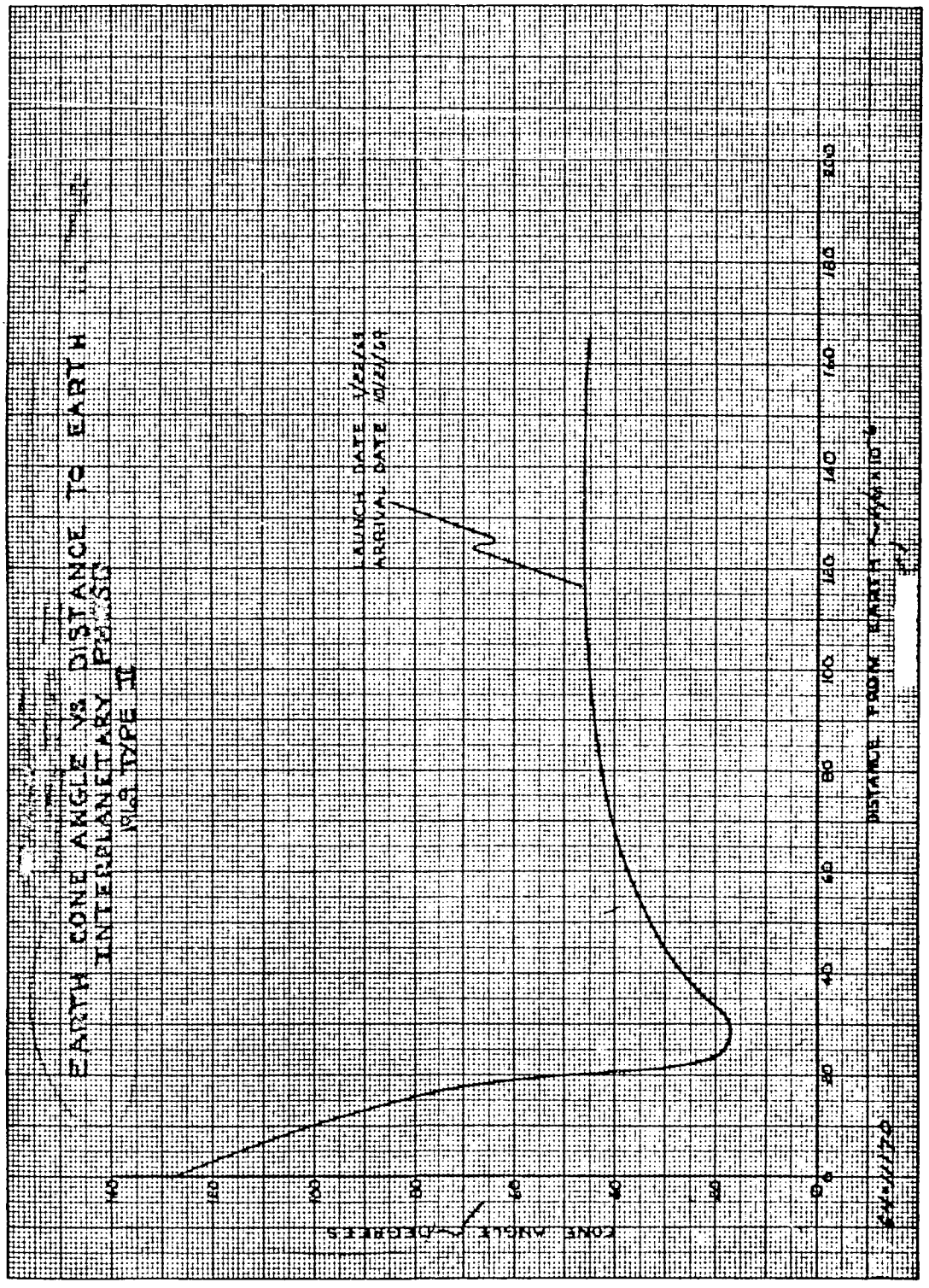

Figure 17 EARTH CONE ANGLE VERSUS DISTANCE TO EARTH INTERPLANETARY PHASE 1969 TYPE II

RE-ORDER No. 64-522

this minimum will be other than zero unless the probe is also in the ecliptic plane.

For the same launch dates the variation in the cone angle to Canopus is presented in table 14. By definition this clock angle is zero. These results indicate that the cone angle is about 90 ± 14 degrees resulting from the fact that Canopus is not at the celestial south pole.

During the approach phase, the cone-clock angles to the planet are of prime importance due to the presence on the probe of a planetary horizontal platform and can be employed to determine the gimbal orientation and the excursion of both gimbals. Since the duration of this phase is relatively short the look angles to Earth and Canopus are relatively constant. For one representative arrival date the look angles to Mars, Earth, and Canopus are presented in table 15 for the minimum flyby inclination and a 10,000 km passing altitude. For this phase of the flight the cone angle excursion is 180 degrees plus an additional angle to account for the bending of the flyby trajectory produced by the planet's gravitational field. For an approach velocity of 4 km/sec and a passing altitude of 10,000 km the trajectory experiences a total deflection of about 19 degrees, thereby adding an additional 19-degree excursion to the cone angle gimbal requirement. As the passing altitude is reduced the additional cone angle excursion increases due to the increased bending of the trajectory.

For a representative date on the launch window the cone-clock angles are presented as a function of distance from the planet in figures 18 and 19.

A similar analysis was also performed for a flyby inclination of 45 degrees. These results, presented in table 16 and figures 20 and 21, indicate that the cone angle excursion is essentially independent of inclination for the range of inclinations under consideration. The clock angle goes from the first to the third quadrants, as expected, indicating a change in the planets position from ahead and below to behind and above; in one case the clock angle excursion includes the second quadrant and in the other case it includes the fourth.

The discontinuity associated with these figures is introduced since the data are presented as a function of the distance from the center of the planet wher the vehicle is on the oncoming and departure asymptotes and therefore never passes closer than 10,000 km from the planet.

3. Occultation - Minimum Passing Altitude Analysis

A strong factor which may be influential in the selection of a numinal aim point in the R-T plane is the minimum passing altitude at which the occultation constraints are violated. In this analysis the occultation constraint,

TABLE 14

1969 INTERPLANETARY TRAJECTORIES
CANOPUS CONE ANGLE

Time (days)	Launch Date: 14 Jan Arrival Date: 15 Oct Cone Angle (degrees)	Launch Date: 22 Jan Arrival Date: 21 Oct Cone Angle (degrees)	Launch Date: 30 Jan Arrival Date: 27 Oct Cone Angle (degrees)	Launch Date: 7 Feb Arrival Date: 2 Nov Cone Angle (degrees)
0	104.0	103.5	102.8	101.8
5	103.4	102.8	101.8	100.
10	102.7	101.9	100.7	99.3
20	101.0	99.7	98.2	96.5
40	96.3	94.5	92.6	90.5
60	90.8	88.9	86.8	84.7
80	85.7	83.8	81.6	79.9
100	81.3	79.7	78.1	76.4
120	78.2	76.9	75.6	74.3
140	76.2	75.2	74.3	73.3
160	75.2	74.6	74.0	73.4
180	75.1	74.8	74.5	74.3
200	75.7	75.7	75.7	75.8
220	76.9	77.1	77.5	77.9
240	78.5	79.0	79.6	80.3
260	80.5	81.3	82.1	83.1
268			83.2	84.2
270	81.6	82.5	83.5	
272	81.8	82.8		
274	82.1			

RE-ORDER No. 64-522

85-1

RE-ORDER No.64-522

TABLE 15

ADVANCED MARINER1969
HYPERBOLIC APPROACH LOOK ANGLES

Launch 1/14/69, t_f = 274 days, i = 28.9 degrees, R_p = 13400 km

Time (days)	Planet		Earth		Canopus Cone	Range from Planet (km x 10^{-3})
	Cone	Clock	Cone	Clock		
	(deg)	(deg)	(deg)	(deg)	(deg)	
0	81.9	82.4	45.9	279.0	82.1	1000
1.0	81.9	82.3	45.8	279.0	82.2	676
2.0	82.5	81.9	45.8	279.1	82.3	351
2.5	84.4	81.1	45.7	279.2	82.4	188
2.8	89.1	79.3	45.7	279.2	82.4	91
3.0	113.1	69.8	45.7	279.2	82.4	25
3.02	123.5	64.7	45.7	279.2	82.4	19
3.04	140.1	52.6	45.7	279.2	82.5	16
3.05	150.6	37.8	45.7	279.2	82.5	15
3.06	158.8	5.7	45.7	279.2	82.5	13
3.07	157.2	321.0	45.7	279.2	82.5	13
3.08	147.8	295.0	45.7	279.2	82.5	15
3.10	129.0	276.5	45.7	279.2	82.5	18
3.15	106.4	265.2	45.7	279.2	82.5	33
3.27	92.3	259.8	45.7	279.3	82.5	72
3.57	85.6	257.3	45.7	279.3	82.5	170
4.07	83.4	256.4	45.6	279.3	82.6	334
5.12	82.6	256.0	45.6	279.4	82.7	676
6.12	82.6	256.0	45.5	279.5	82.9	1000
11.12	84.5	256.3	45.1	280.0	83.6	2612
21.12	89.2	256.9	44.2	280.7	85.0	5810
31.12	94.0	257.2	43.3	281.5	86.5	8945

RE-ORDER No. 64-522

TABLE 16

ADVANCED MARINER 1969
HYPERBOLIC APPROACH LOOK ANGLES

Launch 1/14/69, t_f = 274 days, R_p = 13400 km, i = 45 degrees

Time (days)	Planet		Earth		Canopus Cone	Range from Planet (km x 10^{-3})
	Cone	Clock	Cone	Clock		
	(deg)	(deg)	(deg)	(deg)	(deg)	
0	82.3	83.0	45.9	278.9	82.0	1000
1.0	82.2	83.1	45.8	279.0	82.2	676
2.0	82.9	83.5	45.8	279.1	82.3	351
2.5	84.8	84.1	45.7	279.1	82.3	188
2.8	89.5	85.5	45.7	279.2	82.4	91
3.0	114.5	92.7	45.7	279.2	82.4	25
3.02	125.2	96.7	45.7	279.2	82.4	19
3.04	142.8	106.3	45.7	279.2	82.4	16
3.05	154.3	119.6	45.7	279.2	82.4	15
3.06	164.0	155.7	45.7	279.2	82.4	13
3.07	161.4	212.7	45.7	279.2	82.4	13
3.08	150.1	237.8	45.7	279.2	82.4	15
3.10	129.9	252.7	45.7	279.2	82.4	18
3.15	106.3	261.1	45.7	279.2	82.4	33
3.27	91.8	265.2	45.7	279.2	82.4	72
3.57	84.9	267.1	45.7	279.2	82.5	170
4.07	82.6	267.9	45.6	279.3	82.5	334
5.126	81.8	268.4	45.6	279.4	82.6	676
6.126	81.9	268.6	45.5	279.5	82.8	1000
11.126	84.0	269.1	45.1	280.0	83.3	2612
21.126	89.1	269.8	44.2	280.9	84.6	5810
31.126	94.4	270.3	43.2	281.7	85.8	8945

RE-ORDER No. 64-522

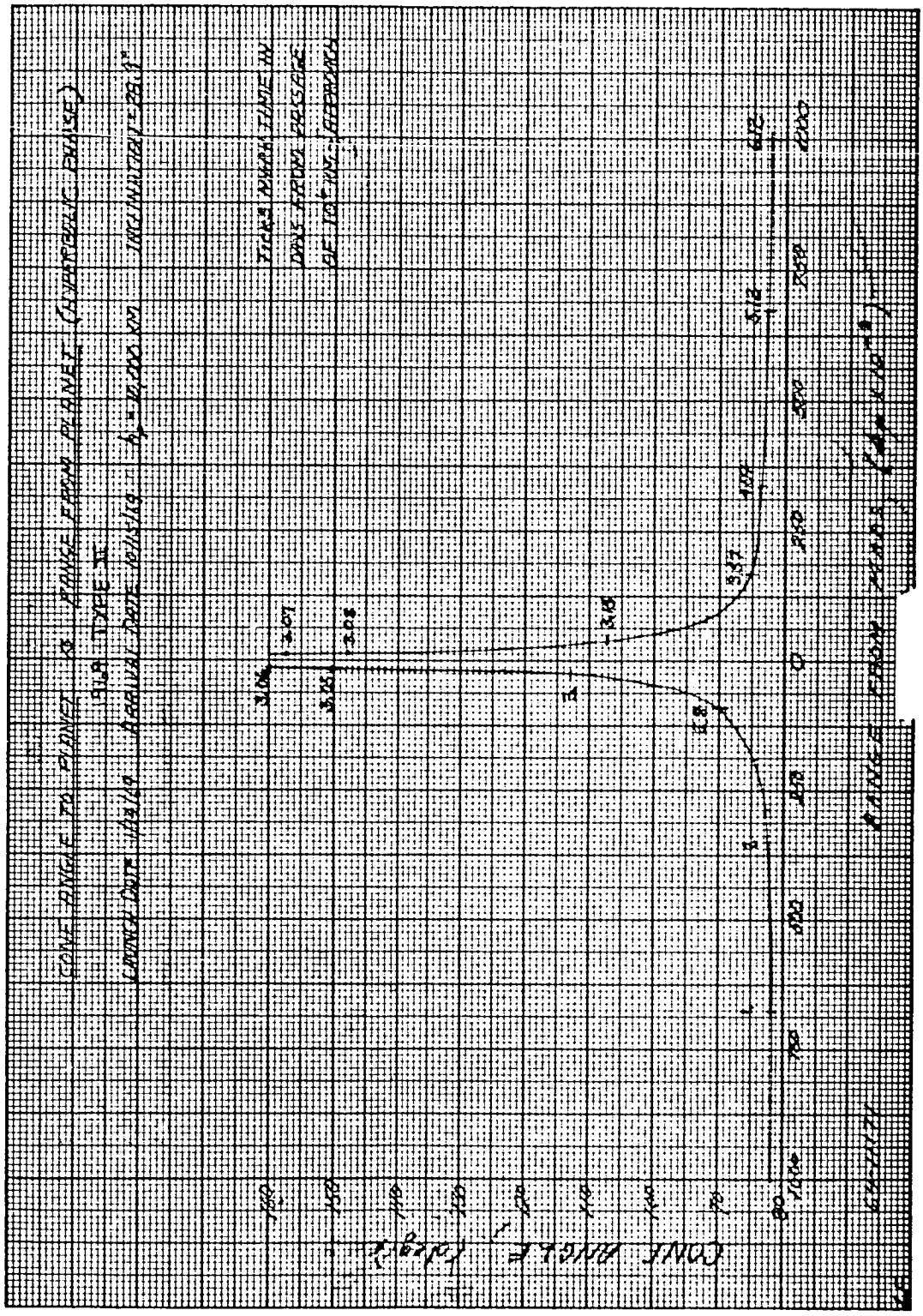

Figure 18 CONE ANGLE TO PLANET VERSUS RANGE FROM PLANET
(HYPERBOLIC PHASE) 1969 TYPE II

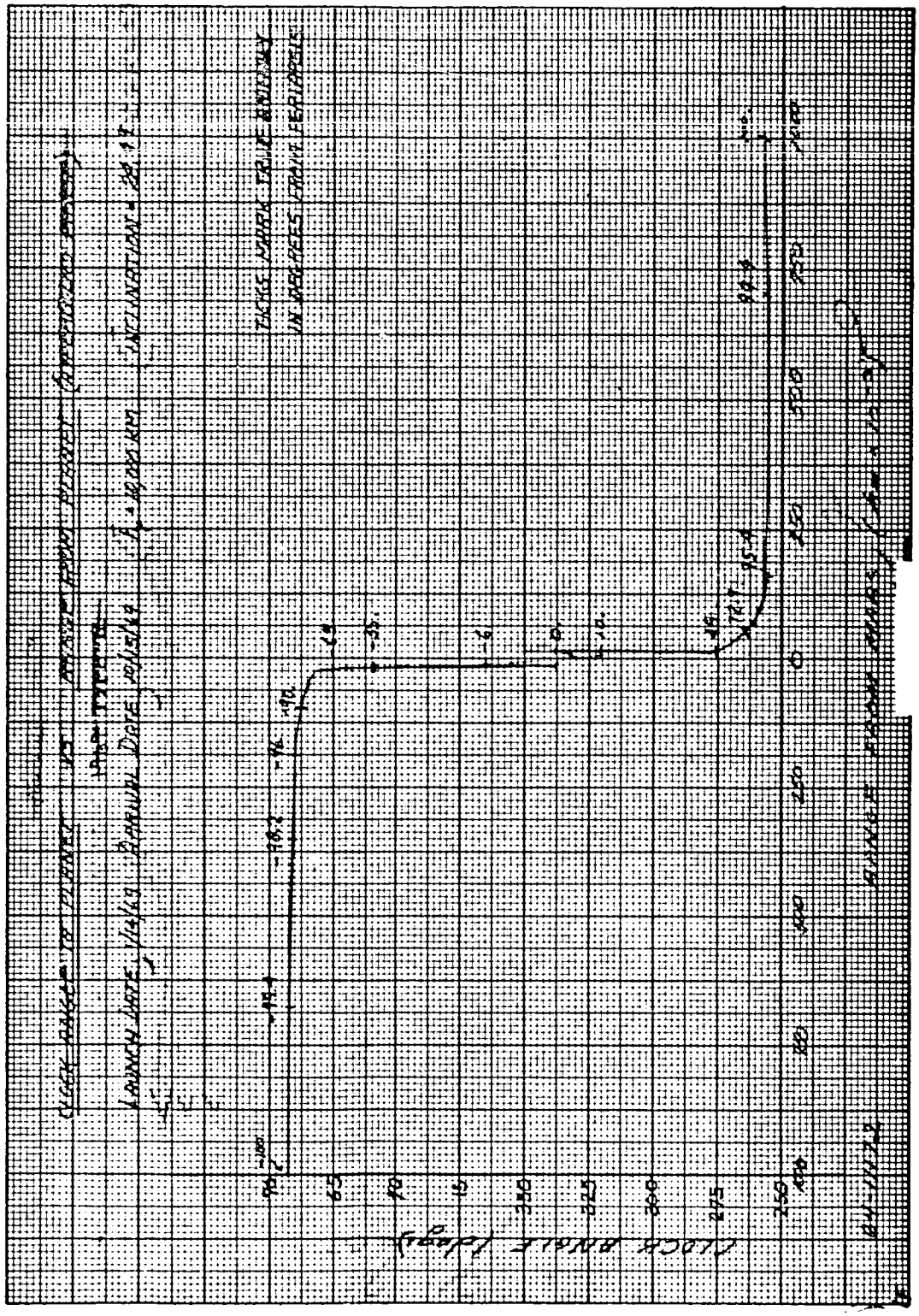

Figure 19 CLOCK ANGLE TO PLANET VERSUS RANGE FROM PLANET
(HYPERBOLIC PHASE) 1969 TYPE II

RE-ORDER No. 64-522

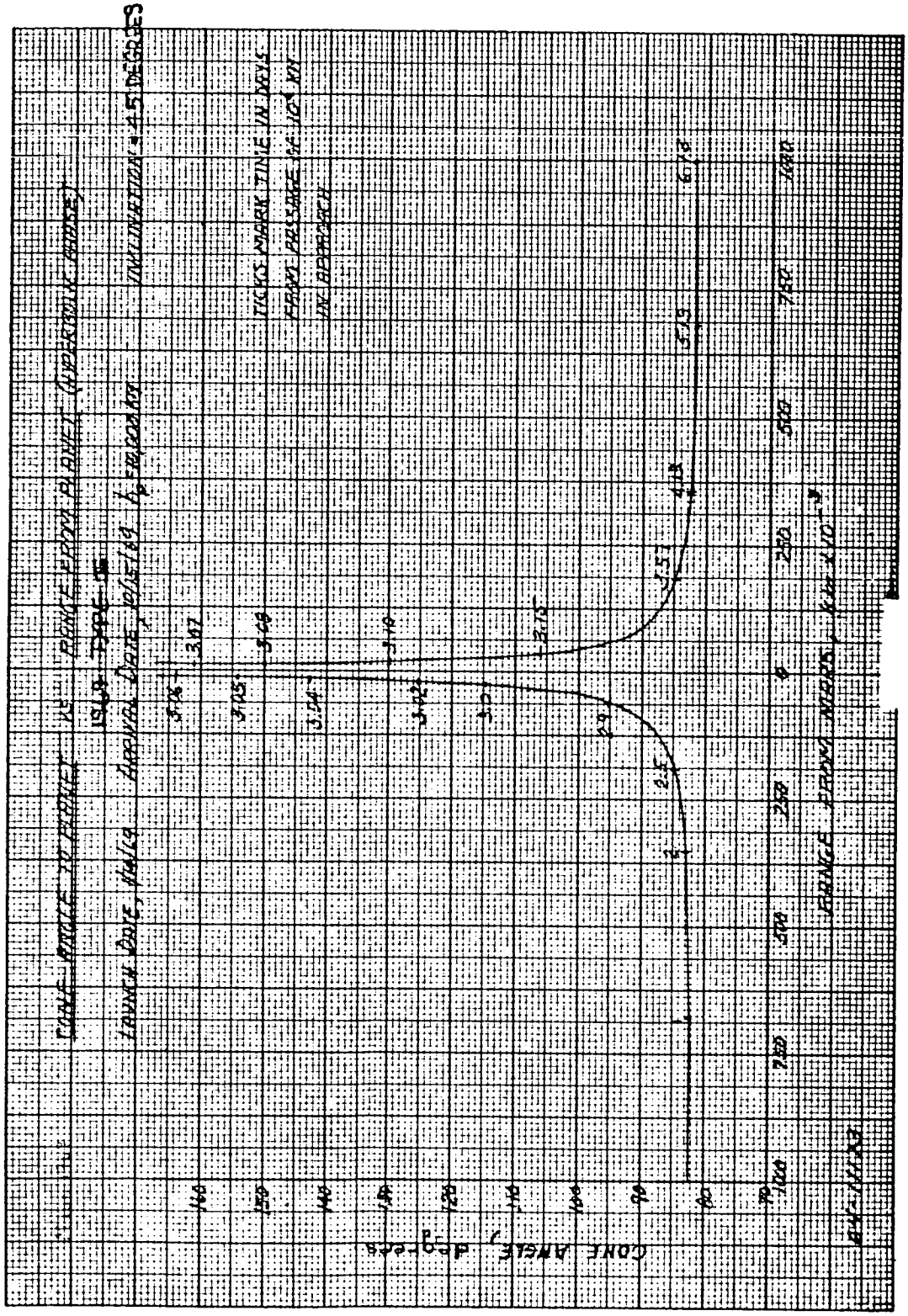

Figure 20 CONE ANGLE TO PLANET VERSUS RANGE FROM PLANET (HYPERBOLIC PHASE) 1969 TYPE II

RE-ORDER No. 64-522

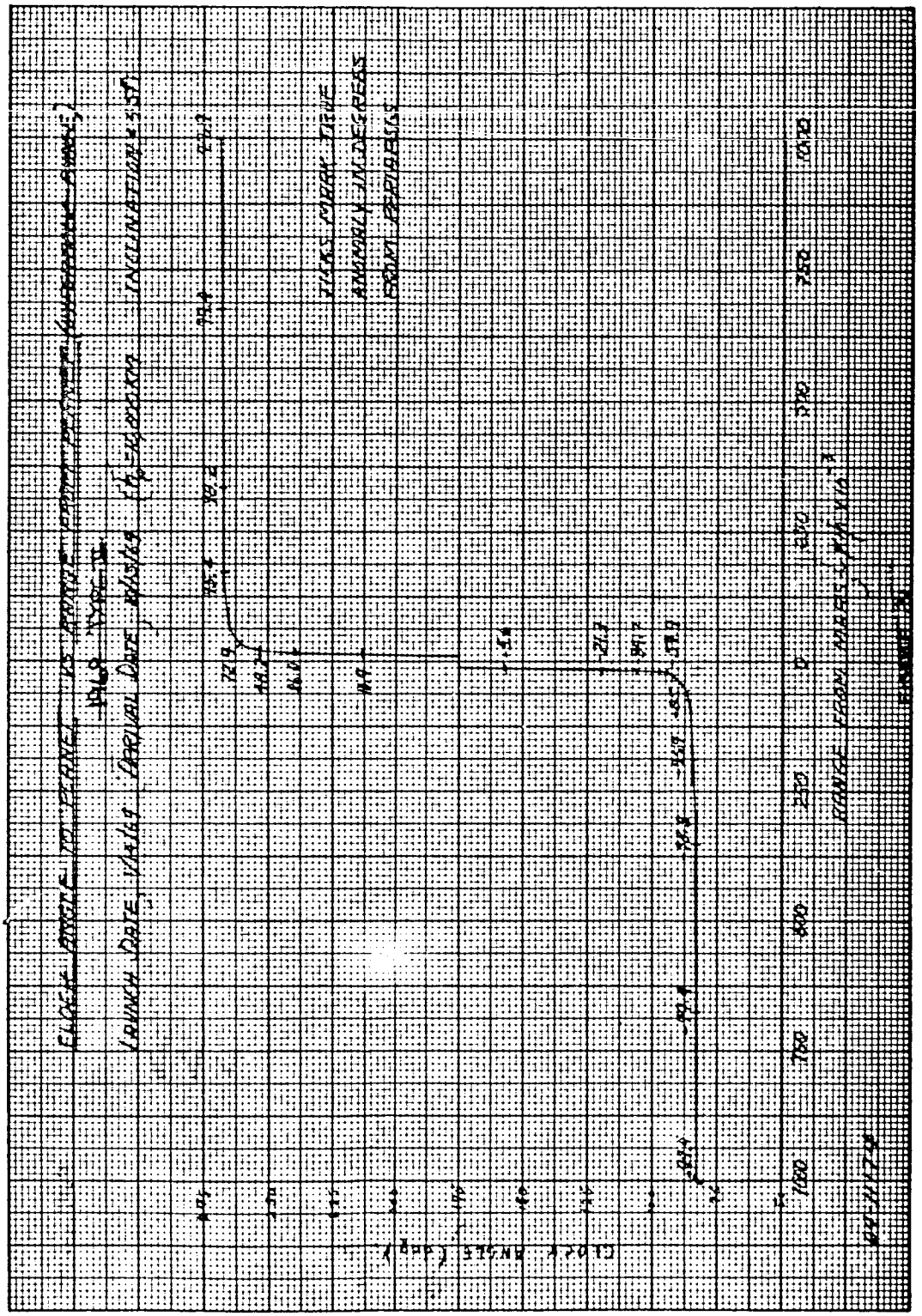

Figure 21 CONE ANGLE TO PLANET VERSUS RANGE FROM PLANET
(HYPERBOLIC PHASE) 1969 TYPE II

minimum near limb of planet-probe-target angle, is violated when, at any point on the hyperbolic trajectory, the angle to sun, Earth of Canopus falls below 5, 5, or 36 degrees, respectively. The minimum passing altitude satisfying all three constraints in association with a specific dispersion ellipse can be employed to define a nominal aim point that insures against periods of occultation. If for certain launch window selections it is impossible to avoid occultation of one or more bodies, the nominal aim point may be selected by other factors, i.e., science mission objectives, minimizing occultation periods. Also, it may be desirous to have Earth occultation to perform a bi-static radar experiment without violating the constraints of the other bodies.

To conduct this analysis, the approach hyperbola look angle program was modified to include a computation of the cone angle reduced by the apparent radius of the planet. Since the probe is being designed to pass on the sunlit side of the planet, this analysis was limited to examining favorable regions within 90 degrees of the T-axis as opposed to a 360 degree zone about the approach asymptote. For specific dates in the launch window the initial velocity vector for the hyperbolic trajectory is obtained from a 2-body interplanetary trajectory, and the occultation analysis is conducted parametrically as a function of inclination and passing altitude. For other than minimum inclinations both trajectories (more northerly passage - Case I and more southerly passage - Case II) were considered. It is obvious that the situation with respect to Canopus improves for the Case II trajectories. In this analysis only the minimum near limb of planet-probe-target angle encountered before or after periapsis passage was considered in the determination of the trajectory parameters required to avoid occultation of any or all bodies.

For the 1969 launch opportunity, the constant departure velocity launch windows selected result in approach asymptotes in the vicinity of the terminator and inclined 30-40 degrees with respect to the Martian equator. Therefore, if the probe passes on the sunlit side of the planet, as intended, it is virtually impossible to have either sun or Earth occultation regardless of the passing distance. By the same token Canopus occultation will not occur for the more southerly inclined hyperbolic trajectories. For passing altitudes between 1,000 and 10,000 km the minimum angles to the various bodies associated with the minimum inclinations are presented in figures 22-25. For a passing altitude of 1,000 km the minimum angles to Earth and Canopus are 20 and 27 degrees, respectively, and increase to 30 and 40 degrees as the passing altitude is increased to 3,000 kilometers. Therefore, between these altitudes an altitude exists such that the occultation constraints to any body are not violated for minimum inclination trajectories. These data are presented in figure 26.

For the specific launch window selected for the 1969 launch opportunity, 10 January to 12 February, a second analysis was performed to determine

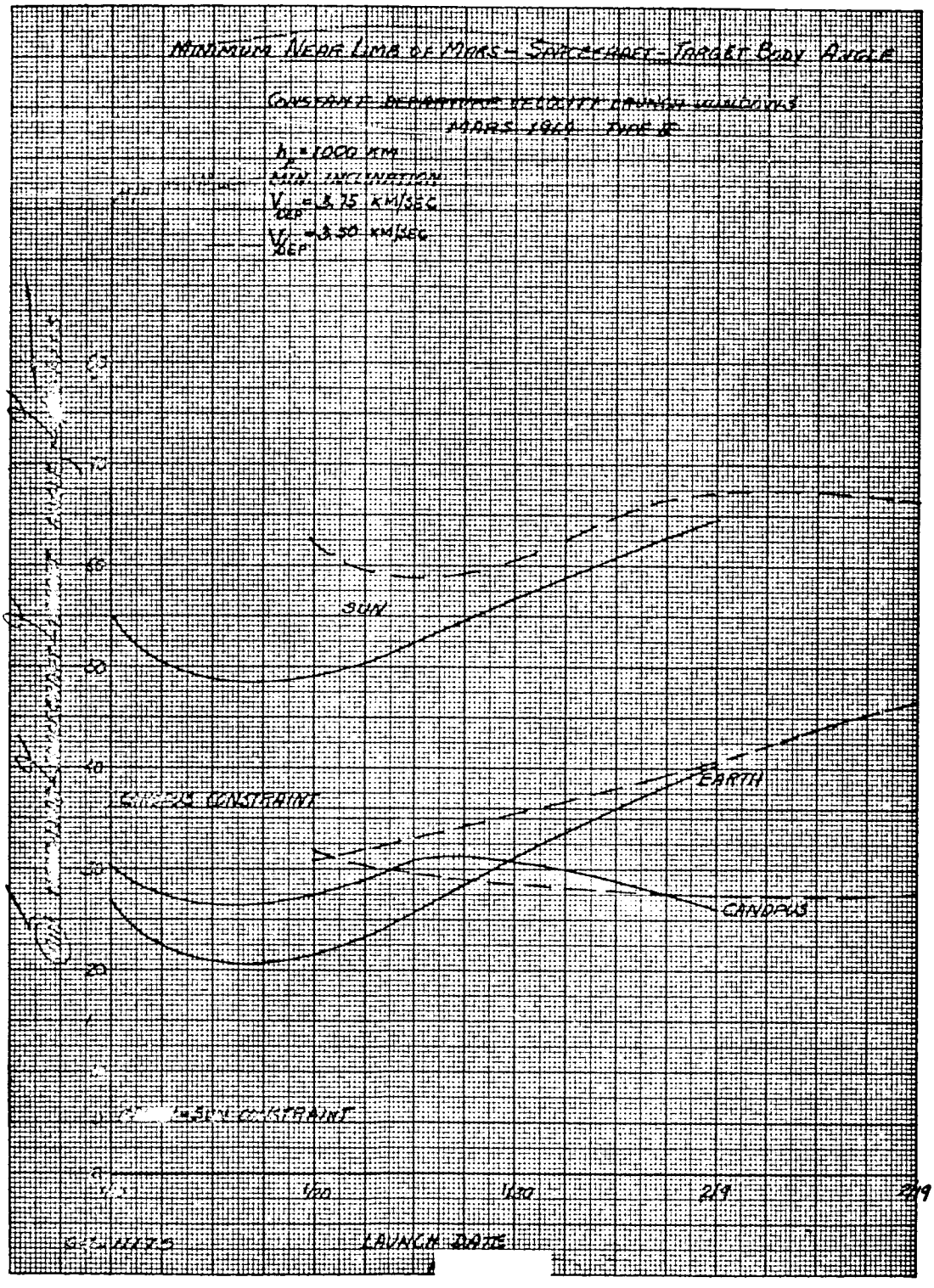

Figure 22 MINIMUM NEAR LIMB OF MARS -- SPACECRAFT -- TARGET BODY ANGLE

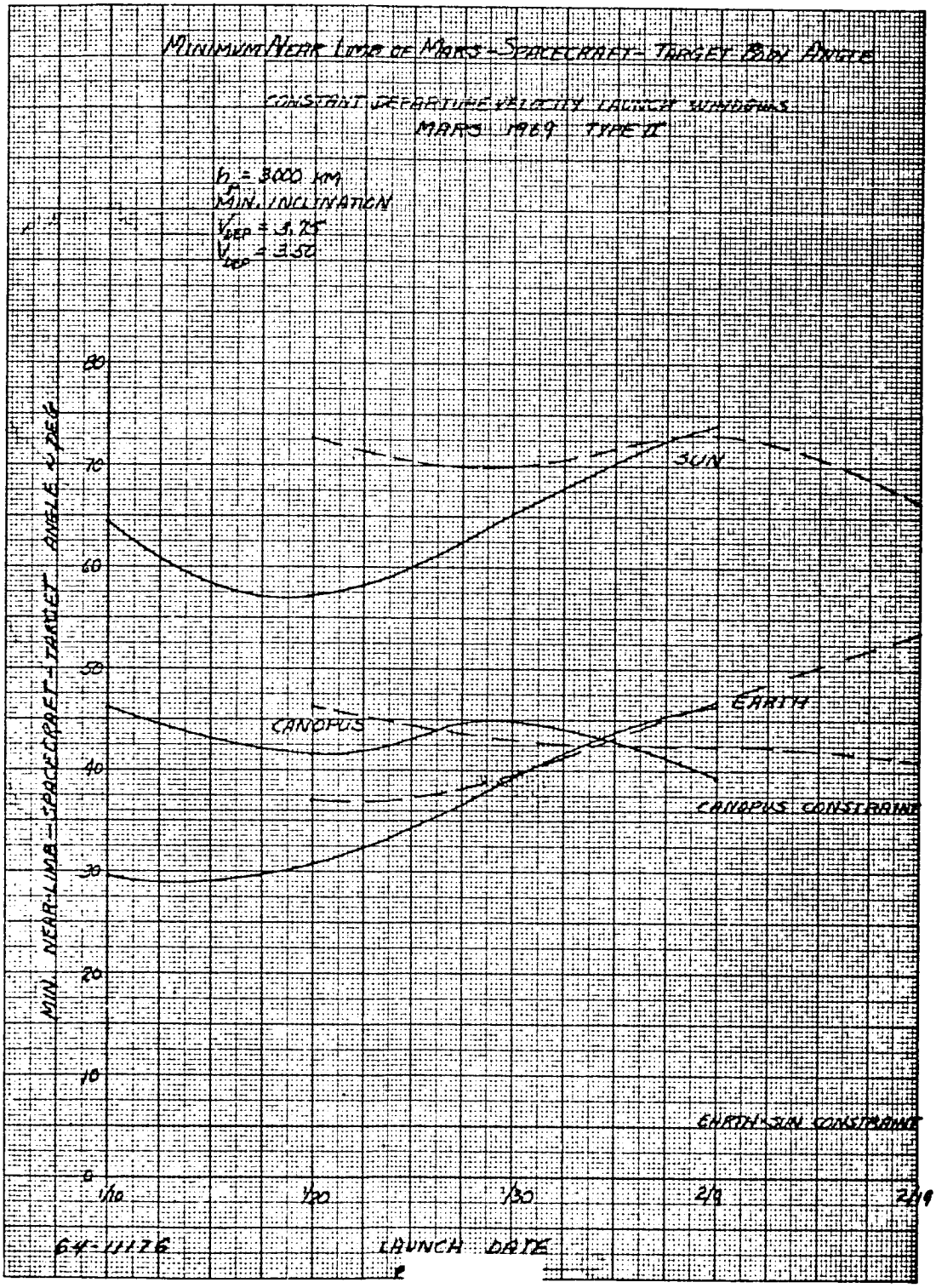

Figure 23 MINIMUM NEAR LIMB OF MARS -- SPACECRAFT -- TARGET BODY ANGLE

RE-ORDER No. 64-522

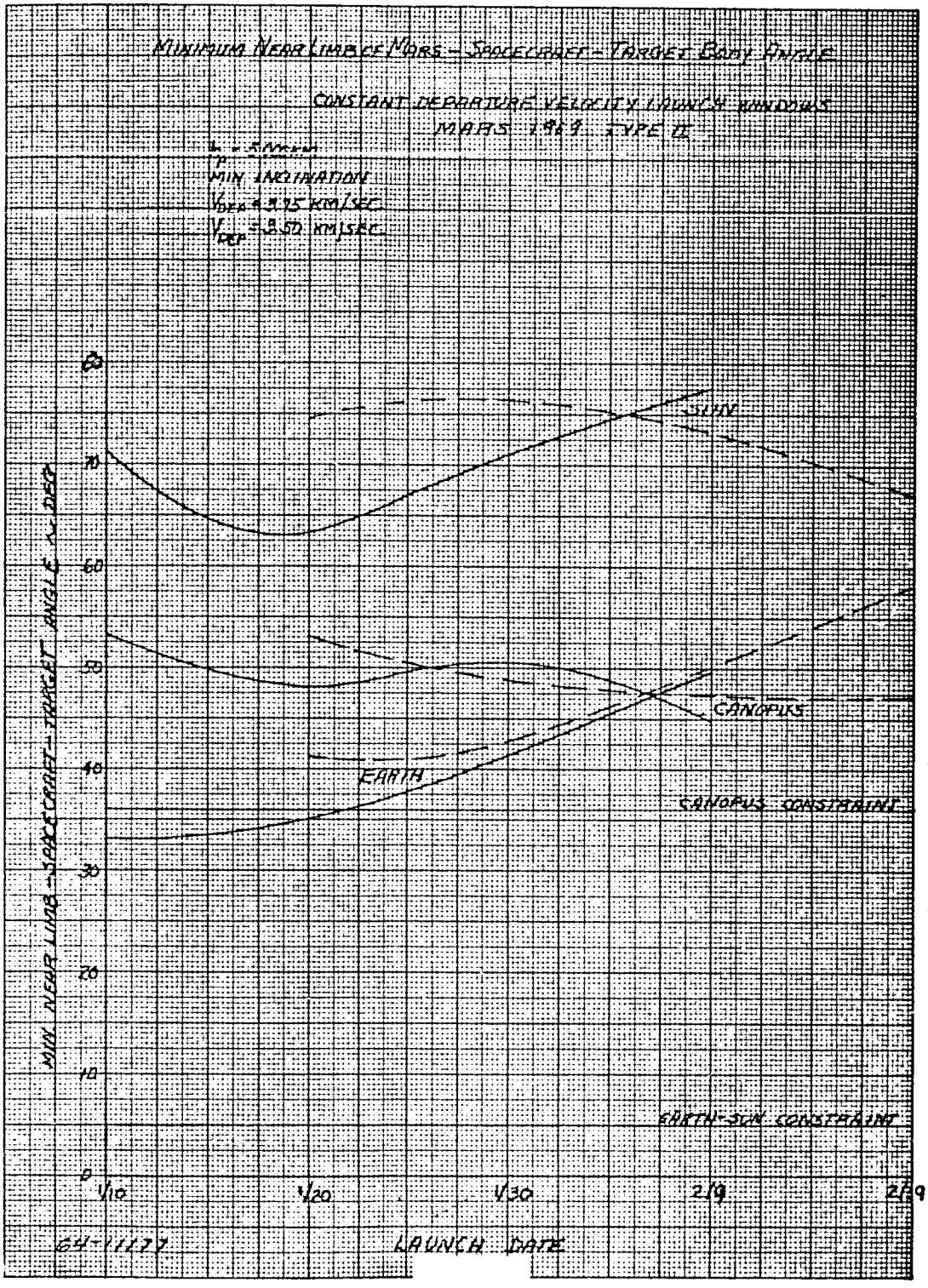

Figure 24 MINIMUM NEAR LIMB OF MARS -- SPACECRAFT -- TARGET BODY ANGLE

RE-ORDER No. 64-522

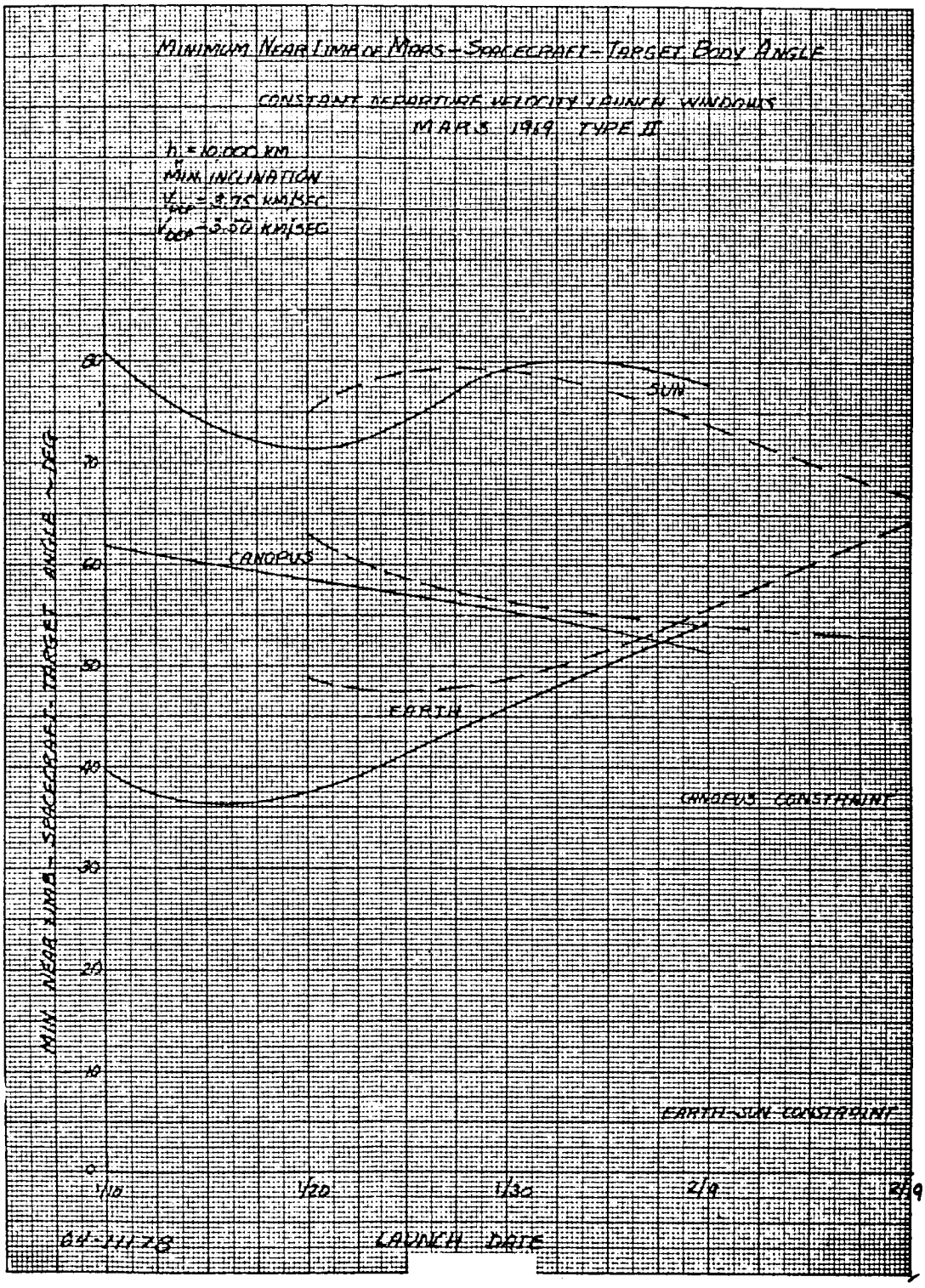

Figure 25 MINIMUM NEAR LIMB OF MARS -- SPACECRAFT -- TARGET BODY ANGLE

RE-ORDER No. 64-522

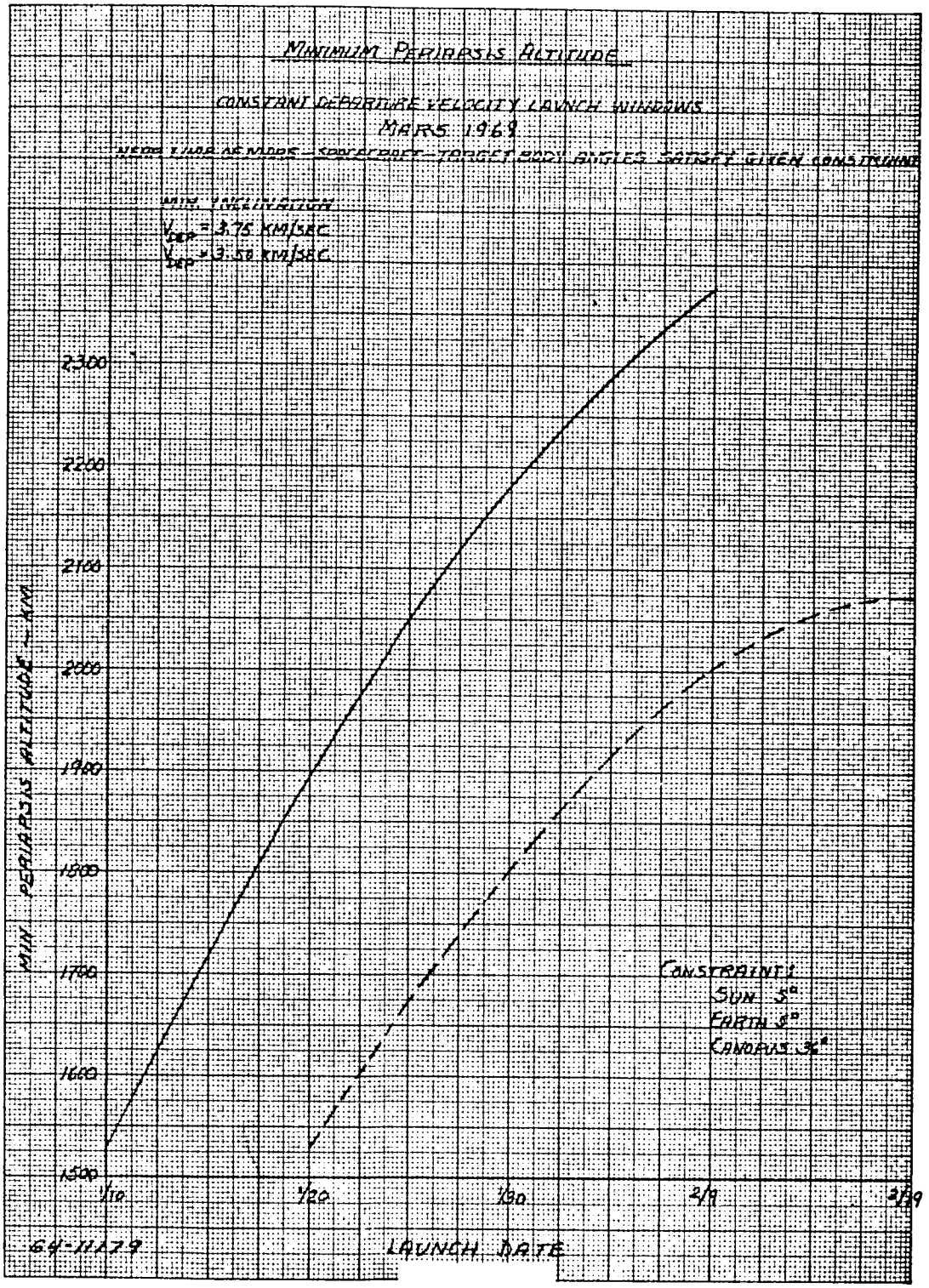

Figure 26 MINIMUM PERIAPSIS ALTITUDE

the minimum passing altitude associated with both minimum and 45 degree flyby inclinations such that the occultation constraints are not violated. For the minimum flyby inclination, 30 to 40 degrees, these results presented in figure 27 incicate that the minimum passing altitude varies between 1400 and 2000 km depending upon the specific launch date. For a 45-degree flyby inclination with a Case II trajectory (southerly passage) the minimum passing altitude is less than 1000 km and was not precisely determined since this altitude is less than the minimum altitude for sterilization requirements.

4. Lander Entry Error Analysis

With the selection of a nominal target and time of arrival, it is possible to conduct a comprehensive error analysis for the uncertainties in the lander entry parameters as a function of the flyby parameters, i.e., inclination, periapsis altitude, approach velocity, and separation range. To minimize the dispersion in the lander entry parameters, the results of the planar analysis will be utilized to the extent that the maximum entry angle is achieved with a thrust direction essentially normal to the approach velocity. Maximizing the entry angle results in minimizing the range angle which in turn implies that a lander inclination of 90 degrees should be selected unless consideration must be given to target landings at a specified time of day. For the 1969 mission, it is desirous to achieve a sunrise landing at Syrtis Major. Since the approach asymptote is essentially in the terminator plane, sunrise landings are feasible with a near polar orbit as the longitude of the impact point does not vary over the window more than 5 degrees from the longitude of the separation point.

Two specific velocity vectors are determined to perturb the lander from the flyby trajectory to the desired impact trajectory. The first velocity, ΔV, is applied in the flyby plane of motion, normal to the approach velocity, to produce a 90-degree entry condition. The magnitude of ΔV, as a function of the flyby parameters, is expressed by

$$\Delta V_1 = \frac{r_a V_{B\infty}}{r_{BS}}$$

where: r_a = aim point

V_B = asymptotic approach velocity

r_{BS} = separation range

A second velocity, ΔV_2, is applied normal to the radius vector, in a plane defined by the separation and target locations, to produce the desired entry angle. The magnitude of ΔV_2 is

$$\Delta V_2 = \left[\frac{r_{LE}^2 \cos^2 \gamma_{LE} \left(V_{BS}^2 + \Delta V_1^2 + \frac{2\mu}{r_{LE}} - \frac{2\mu}{r_{BS}} \right)}{r_{BS}^2 - r_{LE}^2 \cos^2 \gamma_{LE}} \right]^{1/2}$$

where: r_{LE} = entry range

V_{BS} = lander velocity prior to separation maneuver

γ_{LE} = desired lander entry angle

μ = gravitational parameter

The relationship between the lander range angle and entry angle is presented in figure 28.

These two velocities can now be combined to yield the lander separation velocity.

At separation, a coordinate system is established where one axis is in the direction of the approach velocity vector $\bar{V}_\infty$; a second axis in the $\bar{V}_\infty$ x R_{BS} direction; and the third axis completing the orthogonal system in the initial plane of motion normal to the approach velocity vector $\Delta\bar{V}_1$. The direction of the separation velocity can be specified by an azimuth angle, θ, measured from the approach velocity vector and an elevation angle, α, measured normal to the unperturbed flyby plane of motion.

An error analysis can now be performed to determine the effects of errors in separation position and in the magnitude and direction of the separation velocity on the entry parameters. In this analysis one-sigma errors in initial position of 150 and 350 km were considered in addition to a 1-percent error in the separation velocity, ΔV , and 1-degree errors in the direction of thrust application, θ, and α.

Since the separation maneuver is essentially an open loop guidance maneuver, variations in the vehicle altitude between separation and thrust termination cannot be accounted for and can propagate into significant perturbations on the lander entry parameters. In this analysis it was assumed that variations in the vehicle attitude produced by thrust misalignment would be the predominant error source and that the effects of tip-off rates could be neglected.

A parametric analysis was conducted to determine the spin rate requirement to maintain the vehicle attitude within prescribed limits during the thrusting phase. The variation in this altitude is a function of the thrust level, moment

arm, angle between thrust vector and vehicle axis, spin rate and vehicle moment of inertia, expressed mathematically as

$$\gamma = \frac{T l \sin \delta}{\omega^2 I_x}$$

The results of this analysis are presented in figure 29 for various values of $T l \sin \delta$ and for a vehicle moment of inertia of 20 slug ft^2 . The selected spin rate of 2 rad/sec maintains the thrust vector alignment within one degree. Since the independent error sources may be considered statistically independent total latitude and longitude variation produced by these error sources is obtained as the RSS value of the individual variations expressed by

$$\Delta \text{Lat} = \left[\sum_{i=1}^{n} \left(\frac{\partial \text{Lat}}{\partial x_n} \delta x_n \right)^2 \right]^{1/2} ,$$

and

$$\Delta \text{Long} = \left[\sum_{i=1}^{n} \left(\frac{\partial \text{Long}}{\partial x_n} \delta x_n \right)^2 \right]^{1/2}$$

Since the flyby trajectory will not be perturbed with respect to inclination changes or a slowdown maneuver until after lander separation, the flyby will be at minimum inclination at separation. As the 1969 launch window produces a variation in inclination (separation latitude) of only 10 degrees, two cases corresponding to the extremes of the window were analyzed and the results presented in table 17. This analysis indicates that the out-of-plane errors, i.e., 1-degree error in α and position error in the out of plane direction, are the major contributors to the uncertainty in entry angle and latitude, whereas, the largest contributors to longitude variations are the variation in separation velocity and the positional uncertainties in the $-\Delta V_1$ direction. These results indicate only minor dependence on variations in the initial latitude. For a positional uncertainty at separation of 150 km, the 1-sigma variation in the entry angle is approximately 3.4 degrees where the nominal entry angle varies between -66 and -74 degrees depending upon the initial latitude. The related 1-sigma uncertainties in the latitude and longitude of the entry point are 4.1 and 2.7 degrees respectively, indicating that it is entirely feasible to achieve impact at Syrtis Major.

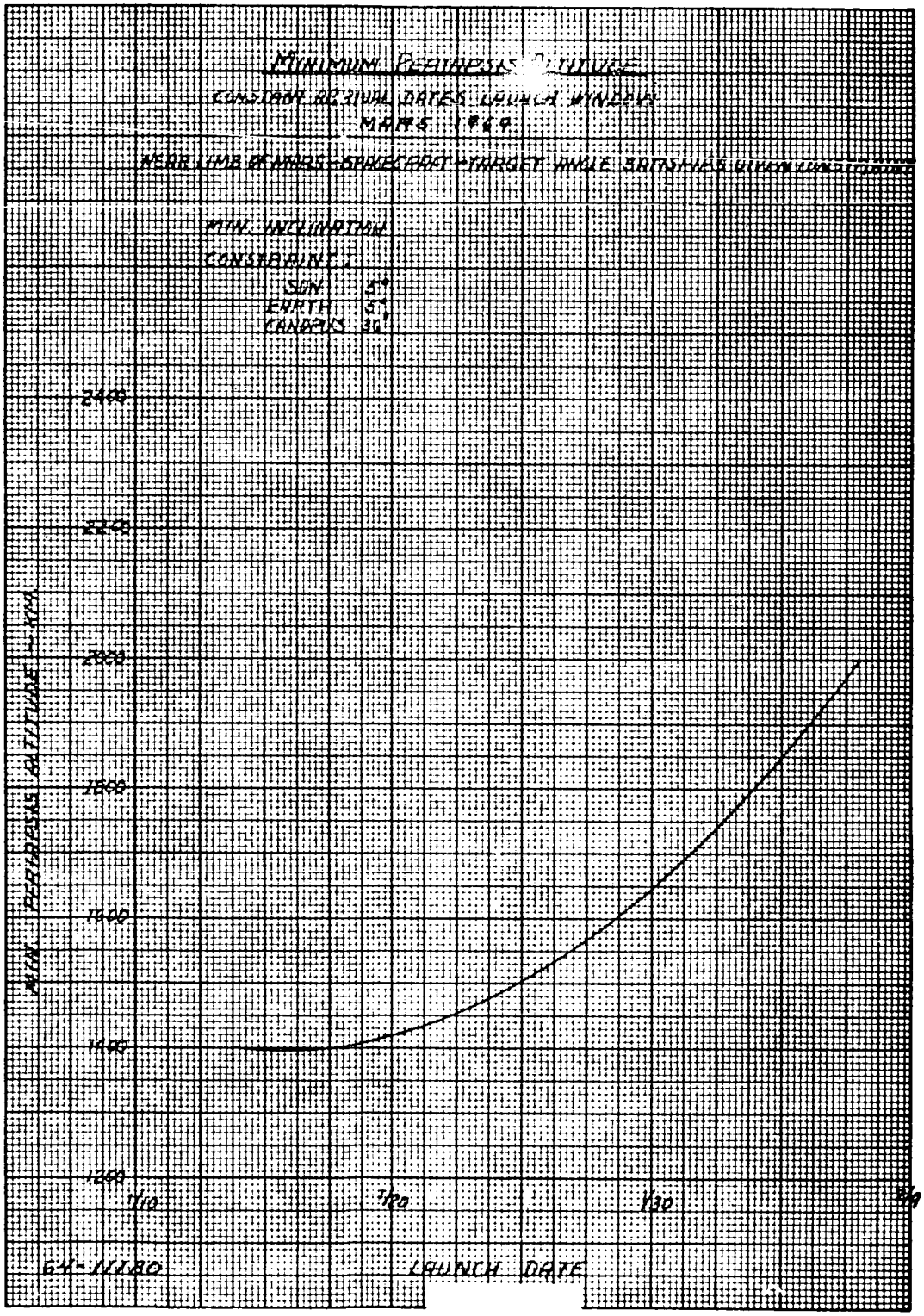

Figure 27 MINIMUM PERIAPSIS ALTITUDE

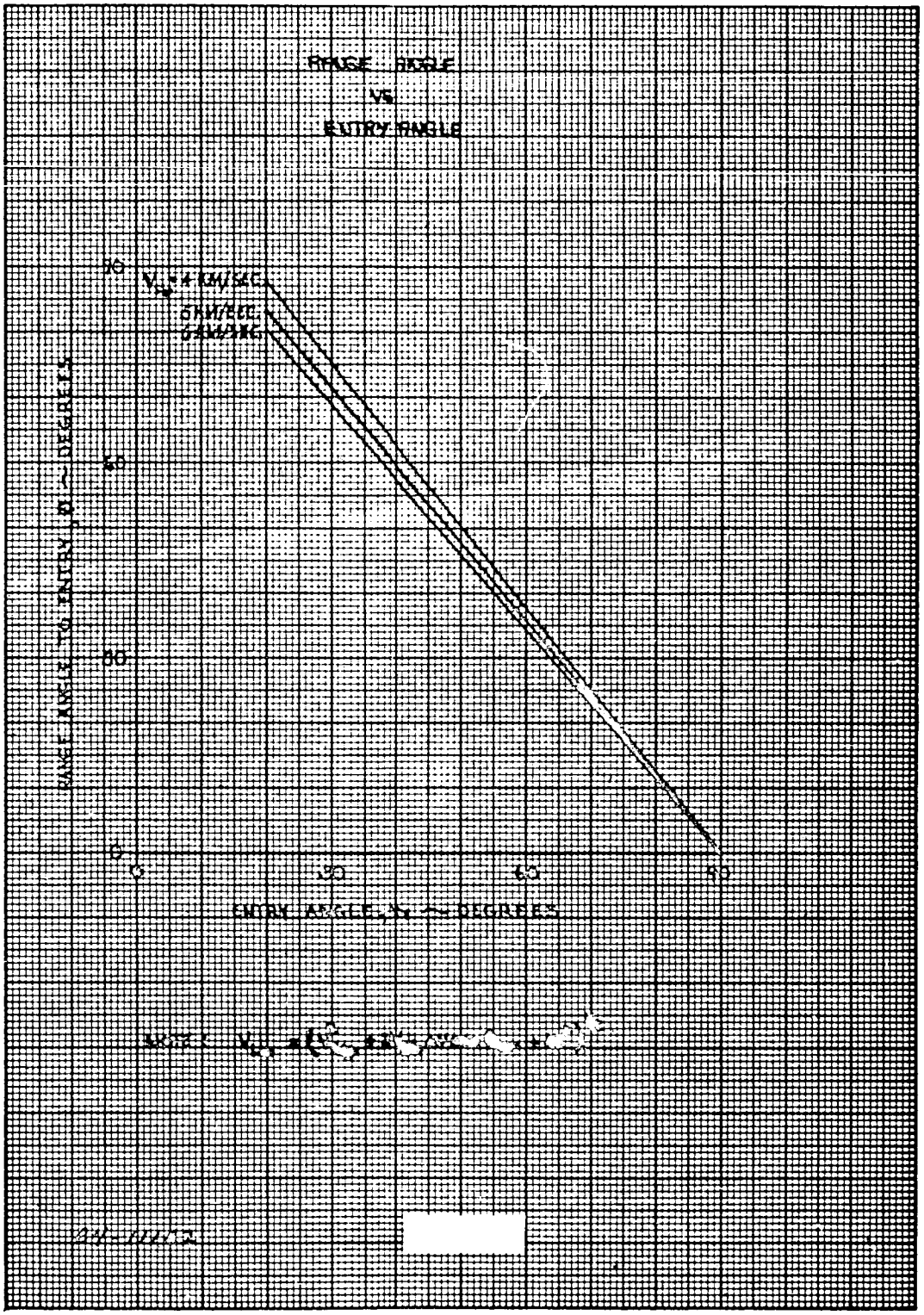

Figure 28 RANGE ANGLE VERSUS ENTRY ANGLE

RE-ORDER No. 64-522

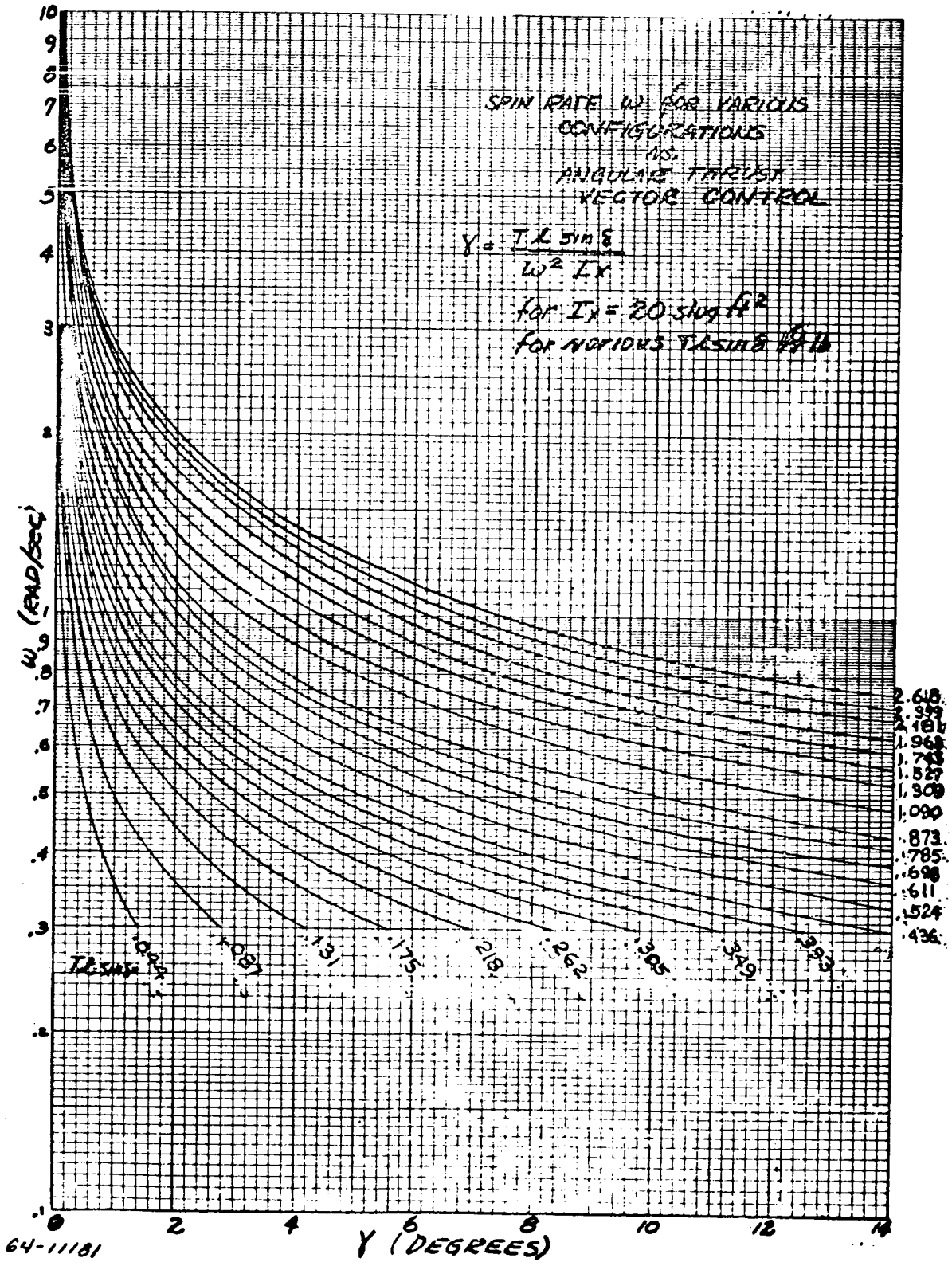

Figure 29 SPIN RATE ω FOR VARIOUS CONFIGURATIONS VERSUS ANGULAR THRUST VECTOR CONTROL

TABLE 17

THREE DIMENSIONAL ENTRY ERROR ANALYSIS

Error Source	Separation Latitude - 30°N Uncertainty in Entry Parameters			Separation Latitude - 40°N Uncertainty in Entry Parameters		
	Entry Angle (degrees)	Latitude (degrees)	Longitude (degrees)	Entry Angle (degrees)	Latitude (degrees)	Longitude (degrees)
1-percent variation in velocity	-0.08	0.18	1.96	-0.19	0.28	1.95
1-degree error in θ	-0.00	0.00	0.06	-0.00	0.00	0.06
1-degree error in α	-2.93	-3.58	0.00	-3.11	-3.82	-0.02
ΔR = 150 km along $\underline{1}\ V_\infty$	-0.00	+0.00	0.03	-0.00	0.00	0.03
ΔR = 150 km along $\underline{1} \cdot \Delta V_1$	0.07	-0.01	1.87	0.06	-0.03	1.85
ΔR = 150 km along $1_R \times V_\infty$	1.58	-1.93	0.00	1.66	-2.05	-0.01
RSS Value	3.33	4.07	2.71	3.53	4.35	2.69
ΔR = 350 km along $\underline{1}\ V_\infty$	-0.01	0.01	0.07	-0.01	0.01	0.07
ΔR = 350 km along $\underline{1} \cdot \Delta V_1$	0.40	-0.08	4.35	0.31	-0.13	4.32
ΔR = 350 km along $1_R \times V_\infty$	3.70	-4.54	0.00	3.92	-4.83	-0.02
RSS Value	4.74	5.79	4.78	5.02	6.17	4.75

RE-ORDER No. 64-522

RE-ORDER No. 64-522

For both cases the separation velocity to achieve the desired impact is about 210 ft/sec. The azimuth angle, θ, associated with the separation velocity is essentially 90 degrees, however the elevation angle, α, varies between -5.6 and -8.3 degrees as a function of separation latitude.

5. Lander-Flyby Spatial Time Relationship

In order to insure the success of a relay communication system for transmission of both pre-impact atmospheric data and post-impact biological data, two primary studies must be considered. First, the appropriate lander lead time must be developed by either a bus slowdown or a lander speed-up maneuver. Secondly, the relative inclinations of the lander and flyby trajectories must be considered since the biological experiments are conducted while the lander is on the surface and therefore rotating from the inertial landing point at the rate of 15 deg/hr. If the lander trajectory plane is coincident with the flyby plane, the flyby is either overhead at lander entry with no slowdown or over the lander entry point 5 hours later with a 5-hour slowdown maneuver. In either case after 5 hours the lander has rotated 75 degrees from the flyby plane presenting an unacceptable geometry for relay communication. Therefore a study is required to determine the appropriate inclinations and slowdown such that distance poses no problem with communication at entry and the flyby angle above the lander horizon poses no problem after the 5-hour biological mission.

To minimize the dispersion in the lander entry parameters, the optimum lander trajectory inclination to impact a specific latitude is 90 degrees. The separation latitude (latitude of the approach asymptote) is dictated by the launch trajectory parameters and is equivalent to the minimum flyby trajectory inclination. This latitude varies between 30° and 40°N for the 1969 launch window. Table 18 contains pertinent flyby trajectory parameters for various initial latitudes and inclinations consistent with the 1969 launch window parameters to illustrate the flyby inclination importance. As the flyby inclination is increased to give a more southerly passage, the longitude of the flyby as it passes over the lander latitude is diminished. This results in a decreased lead time requirement if it is desirous for the flyby to be directly over the lander as it passes over the lander latitude. With these higher inclinations the flyby is also at a correspondingly greater range angle from periapsis and therefore at considerably higher altitudes as it passes over the lander latitude. However, with larger flyby inclinations, a wider latitude excursion results. These factors are influential in selecting a nominal inclination since TV pictures are included in the flyby science mission.

To evaluate the influence of both flyby slowdown and trajectory inclination on the lander-flyby spatial-time relationship it is necessary to select the parameters yielding acceptable relay geometry for telemetry of both pre-impact atmospheric data and post impact biological data. In this analysis nominal conditions at separation were selected to be:

RE-ORDER No. 64-522

a. approach velocity of 4 km/sec

b. separation range of 10^6 km

c. passing altitude of 10^4 km.

For slowdown velocities of 700 and 900 ft/sec in combination with various flyby inclinations, the extreme separation latitudes encountered in the 1969 launch window were analyzed. The results of this analysis presented in tables 19 and 20 indicate: (1) a slowdown velocity of 700 ft/sec produces the best geometry for the first 3 hours; however, the application of a 900 ft/sec slowdown produces acceptable conditions after 5 hours with little degradation in the initial geometry; (2) improvements in the initial geometry are evident as the flyby inclination is increased, however, this improvement is more than offset by the subsequent degradation after 5 hours.

Therefore, it can be seen that both the magnitude of the slowdown velocity and the flyby trajectory inclination are functions of the desired lander mission lifetime. For a nominal mission of 5 hours duration, it is necessary to employ a 900-ft/sec slowdown in combination with a flyby inclination between 30 to 45 degrees.

6. Summary

The results of these studies indicate that the launch window selection based upon the pertinent trajectory parameters satisfies all system mission requirements. However, this window was selected with the premise that payload was not a pertinent parameter since the lander-flyby configuration fell well below the maximum floxed Atlas/Centaur capability. However, the payload penalty associated with this window may become excessive with an unfloxed Atlas/Centaur. Data have been presented to assist in the selection of a revised window where trade-off studies must be performed to assess the degradation in the various system studies introduced by the lower ZAP angles associated with more favorable payload windows. For example, a reasonable launch window exists between 26 January and 25 February where the payload is increased from 1340 pounds to 1470 pounds by allowing the minimum ZAP angle limit to be reduced from 70 degrees to 60 degrees. Another window exists between 11 February and 15 March where the payload is increased to 1560 pounds and the ZAP angle is reduced to 50 degrees.

The degradation in the direct link communication time associated with these improved payload launch windows could be minimized by landing somewhat before sunrise to reduce the penalty associated with the reduction in ZAP angle.

TABLE 18

PERTINENT LANDER/FLYBY HYPERBOLIC TRAJECTORY PARAMETERS
1969 LAUNCH OPPORTUNITY

Separation Latitude (degrees)	Flyby Inclination (degrees)	Longitude of Flyby at 10° Lat. (degrees)	Latitude of Periapsis (degrees)	Lander Time to Entry (hours)	Flyby Time to 10° Lat. (hours)	Time for Lander to rotate under flyby track (hours)	Flyby Slowdown (hours)	Flyby Altitude at 10° Latitude (km)	Δv to change flyby Inclination (km/sec)	Range Angle From 10° Latitude to Periapsis (degrees, minutes)
30	30	72	-4.3	28	68.29	4.8	4.8	11600		29° 01'
	45	25	-34.7		67.08	1.7	2.9	25000	0.038	67° 55'
	60	14	-50.8		66.50	0.9	2.7	34000	0.058	74° 0'
	75	6	-63.2		66.18	0.4	2.5	38000	0.075	77° 53'
	90	0	-68.7		66.04	0.0	2.2	40000	0.090	78° 42'
40	40	78	-5.6	68.29	68.38	5.2	5.1	11200		24° 22'
	60	23	-42.1		67.64	1.5	2.2	21500	0.053	62° 21'
	75	10	-54.1		67.11	0.7	1.9	24000	0.072	67° 20'
	90	0	-58.7		67.03	0.0	1.3	26000	0.090	68° 42'

RE-ORDER No. 64-522

107

TABLE 19

LANDER-FLYBY GEOMETRY FOR INITIAL LATITUDE OF 30°N
1969 LAUNCH OPPORTUNITY

Flyby Inclination (degrees)	Lander Inclination (degrees)	Slowdown Velocity (ft/sec)	Time*	Angle Above Lander Horizon (degrees)	Slant Range (km)
30	90	700	Entry	64.7	59770
			E+3 hours	75.1	19456
			E+5 hours	6.4	16681
45	90	700	Entry	72.7	59600
			E+3 hours	72.6	19490
			E+5 hours	<0	17070
60	90	700	Entry	77.4	59520
			E+3 hours	58.5	19790
			E+5 hours	<0	17530
30	90	900	Entry	66.4	74765
			E+3 hours	62.8	34320
			E+5 hours	87.9	11000
45	90	900	Entry	72.9	74630
			E+3 hours	62.1	34340
			E+5 hours	45.6	11770
60	90	900	Entry	76.5	74570
			E+3 hours	55.9	34510
			E+5 hours	24.4	12660

*This analysis assumes a negligible lander atmospheric flight time.

RE-ORDER No. 64-322

TABLE 20

LANDER-FLYBY GEOMETRY FOR INITIAL LATITUDE OF 40°N
1969 LAUNCH OPPORTUNITY

Flyby Inclination (degrees)	Lander Inclination (degrees)	Slowdown Velocity (ft/sec)	Time	Angle Above Lander Horizon (degrees)	Slant Range (km)
40	90	700	Entry	55.6	60050
			E+3 hours	66.9	19600
			E+5 hours	6.4	16680
60	90	700	Entry	67.1	59710
			E+3 hours	66.5	19600
			E+5 hours	< 0	17300
40	90	900	Entry	56.9	75040
			E+3 hours	57.1	34470
			E+5 hours	87.4	11000
60	90	900	Entry	66.0	74780
			E+3 hours	57.1	34480
			E+5 hours	33.6	12240

RE-ORDER No. 64-522

The payload quoted for these windows corresponds to the minimum payload at the extremes of a 30-day window. A comparison of the pertinent trajectory parameters associated with the design launch window, the minimum departure velocity window and these two new postulated windows is presented in table 21. A comparison of the trajectory parameters for the design window and the window between 26 January and 25 February indicates that except for a 10- to 15-degree variation in the longitude of the approach asymptote the variations are minor. These results are presented in figures 30-34.

Therefore, in conclusion, reasonable launch windows exist that produce improved payload capabilities without introducing a significant degradation in the remaining parameters.

7. 1971 Launch Opportunity

The Mars opposition in 1971 produces the most favorable characteristics of any opposition during the 15-year metonic cycle. This results from the fact that Mars is near perihelion at opposition and that the transfer plane is essentially coincident with the ecliptic plane, since departure and arrival can occur near the Earth-Mars nodal line. The trajectory parameters associated with a minimum departure velocity launch window centered about 24 May 1971 are presented in table 22. Although most of the parameters exhibit acceptable trends for a 30-day window, there is a 50-degree variation in the ZAP angle with a predominance of the approaches from the dark side. In addition there is a 68,000,000-kilometer variation in the communication range since the time of flight increases by 25 days producing a 55-day dispersion in the approach date. The major disadvantage of this window is the fact that the arrival dates occur 1 to 3 months after the peak wave of darkening. Therefore, the parameters associated with fixed arrival date windows were investigated for arrival dates between 15 October 1971 and 20 November 1971. Arrival dates prior to the peak wave of darkening, 15 October 1971 were not considered due to the unduly large payload penalty necessary to achieve the fast transfer trips. These data are presented in parametric form for arrival windows separated by 6-day intervals in table 23. For arrival dates during the later portion of October, the ZAP angle is in the vicinity of 140 degrees. Therefore, although the trajectory parameters, exclusive of ZAP angle, and the arrival dates are near optimum for these windows, the ramifications of this specific ZAP angle are many. The results can best be seen by analyzing the latitude and longitude of the approach asymptote for a specific window with arrival dates of 15 and 21 October. The longitude of the approach asymptote is approximately 315 degrees implying that a 45-degree longitude is required to achieve a sunrise landing at Syrtis Major. The associated latitude excursion is nearly 30 degrees thereby yielding a maximum entry angle of -45 degrees. A second extremely critical area introduced by this approach geometry is the lander-flyby geometry where both vehicles are heading to opposite sides of

TABLE 21

TRAJECTORY PARAMETER COMPARISON
1969 LAUNCH WINDOWS

Launch Date	Approach Date	Time	Payload (pounds)	Approach Velocity (km/sec)	ZAP Angle (degrees)	Communication Range (10^6 km)
17 Mar - 16 Apr	5 Jan - 10 Feb	294-300	1680	4.9-5.3	33-42	240-279
11 Feb - 15 Mar	18 Nov - 20 Dec	280	1560	4.2-4.8	50-61	192-224
26 Jan - 11 Feb	2 Nov - 18 Nov	280	1470	3.9-4.2	61-69	176-192
11 Feb - 25 Feb	10 Nov - 24 Nov	272		4.1-4.5	62-68	184-197
10 Jan - 18 Jan	15 Oct	270-278	1340	3.8	80-83	160
18 Jan - 26 Jan	21 Oct	268-276		3.8	77-80	165
26 Jan - 3 Feb	27 Oct	266-274		3.8-4.0	74-77	171
3 Feb - 11 Feb	2 Nov	264-272		4.0-4.2	72-75	176

RE-ORDER No. 64-522

TABLE 22

1971 MINIMUM DEPARTURE VELOCITY WINDOW

Launch Date	Arrival Date	Departure Velocity (km/sec)	Approach Velocity (km/sec)	Flight Time (days)	Payload (pounds)	Declination of Geo Asymptote (degrees)	ZAP Angle (degrees)	GP Angle (degrees)	Communication Range (10^6 km)	Encounter Dispersion Ellipse					
										Midcourse Correction			Tracking Error		
										Semi-Major Axis (km)	Semi-Minor Axis (km)	Orientation (degrees)	Semi-Major Axis (km)	Semi-Minor Axis (km)	Orientation (degrees)
4 May 1971	12 Nov 1971	3.137	3.170	192	1576	-32.46	113.98	3.32	118.6	981	412	171	550	21	29
8 May	18 Nov	3.027	3.042	194	1620	-31.10	109.06	1.36	125.3	1221	316	176	532	22	29
12 May	26 Nov	2.939	2.918	198	1652	-29.33	101.89	-0.74	134.5	1709	294	2	539	24	28
16 May	4 Dec	2.874	2.845	202	1678	-26.99	94.82	-3.10	143.4	2281	306	6	555	27	28
20 May	14 Dec	2.833	2.818	208	1692	-23.54	86.19	-5.86	156.1	3051	316	9	529	31	28
24 May	22 Dec	2.818	2.839	212	1700	-20.00	80.07	-8.50	166.2	3625	341	11	452	40	31
28 May	28 Dec	2.831	2.876	214	1692	-17.11	76.04	-10.63	173.8	3993	372	12	363	57	38
1 Jun	3 Jan 1972	2.871	2.927	216	1678	-14.31	72.34	-12.50	181.6	4334	399	12	261	87	49
5 Jun	9 Jan	2.938	2.990	218	1652	-11.69	68.95	-14.10	189.4	4633	422	12	180	138	65
9 Jun	15 Jan	3.028	3.061	220	1620	-9.30	65.88	-15.42	197.3	4902	443	12	242	110	151
13 Jun	21 Jan	3.141	3.138	222	1575	-7.16	63.09	-16.50	205.3	5137	459	12	352	82	163

RE-ORDER No. 64-5322

TABLE 23

COMPARISON OF PARAMETERS FOR 1971 CONSTANT ARRIVAL DATE WINDOWS

Launch Date	Arrival Date	Departure Velocity (km/sec)	Approach Velocity (km/sec)	Flight Time (days)	Payload (pounds)	Declination of Geo Asymptote (degrees)	ZAP Angle (degrees)	OP Angle (degrees)	Communication Range (10^6 km)	Encounter Dispersion Ellipse					
										Midcourse Correction			Tracking Error		
										Semi-Major Axis (km)	Semi-Minor Axis (km)	Orientation (degrees)	Semi-Major Axis (km)	Semi-Minor Axis (km)	Orientation (degrees)
16 Apr 1971	19 Oct 1971	3.862	4.172	182	1280	-35.80	133.78	9.37	90.6	1663	503	27	940	26	27
20 Apr		3.700	4.191	178	1350	-33.65	135.61	6.96		1571	445	19	876	82	25
24 Apr		3.567	4.221	174	1405	-32.07	137.21	5.06		1506	421	14	825	132	25
28 Apr		3.457	4.259	170	1450	-30.92	138.62	3.49		1451	422	9	778	178	25
2 May 1971		3.367	4.301	166	1485	-30.14	139.87	2.19		1397	439	6	735	211	27
6 May		3.296	4.346	162	1512	-29.64	140.99	1.09		1345	464	3	696	243	30
10 May		3.247	4.393	158	1534	-29.36	141.98	0.14		1295	491	0	665	268	34
14 May		3.221	4.441	154	1545	-29.25	142.86	-0.69		1228	518	179	638	285	40
18 May		3.220	4.490	150	1545	-29.26	143.61	-1.42		1180	544	177	616	297	47
24 Apr 1971	21 Oct 1971	3.519	3.918	180	1425	-33.36	131.90	5.59	96.0	1344	454	19	781	80	26
28 Apr		3.395	3.943	176	1475	-31.95	133.42	4.09		1295	420	12	738	132	26
2 May		3.294	3.974	172	1514	-30.96	134.75	2.55		1257	419	7	701	176	27
6 May		3.216	4.009	168	1545	-30.32	135.94	1.26		1219	438	4	666	213	30
10 May		3.161	4.048	164	1570	-29.93	136.98	0.16		1185	466	1	637	244	34
14 May		3.130	4.088	160	1580	-29.72	137.90	-0.78		1134	496	178	611	266	40
18 May		3.126	4.130	156	1580	-29.64	138.69	-1.60		1096	526	176	601	280	46
22 May		3.152	4.173	152	1570	-29.63	139.36	-2.33		1055	554	174	598	284	53
26 May		3.210	4.217	148	1548	-29.63	139.86	-2.99		1011	580	172	603	281	60
30 May		3.303	4.264	144	1514	-29.59	140.24	-3.58		968	604	171	615	272	65
3 Jun 1971		3.433	4.313	140	1460	-29.48	140.49	-4.12		924	624	169	629	260	69
30 Apr 1971	27 Oct 1971	3.297	3.684	180	1512	-32.36	128.59	3.86	101.9	1099	429	12	674	106	27
4 May		3.197	3.707	176	1552	-31.24	129.92	2.18		1078	409	7	646	154	29
8 May		3.123	3.735	172	1581	-30.57	131.10	0.79		1057	424	2	622	196	32
12 May		3.074	3.767	168	1600	-30.15	132.14	-0.37		745	454	1	510	192	49
16 May		3.052	3.801	164	1610	-29.92	133.03	-1.37		1007	490	176	592	248	42
20 May		3.058	3.836	160	1607	-29.79	133.78	-2.23		985	526	174	591	262	48
24 May		3.096	3.874	156	1590	-29.72	134.39	-3.00		956	559	172	597	266	55
28 May		3.168	3.913	152	1564	-29.63	134.85	-3.67		923	590	171	609	264	60
1 Jun 1971		3.277	3.955	148	1530	-29.50	135.17	-4.28		895	617	170	625	258	65

RE-ORDER No. 64-522

TABLE 23 (Concl'd)

Launch Date	Arrival Date	Departure Velocity (km/sec)	Approach Velocity (km/sec)	Flight Time (days)	Payload (pounds)	Declination of Geo Asymptote (degrees)	ZAP Angle (degrees)	GP Angle (degrees)	Communication Range (10^6 km)	Encounter Dispersion Ellipse					
										Midcourse Correction			Tracking Error		
										Semi-Major Axis (km)	Semi-Minor Axis (km)	Orientation (degrees)	Semi-Major Axis (km)	Semi-Minor Axis (km)	Orientation (degrees)
2 May 1971	4 Nov 1971	3.207	3.394	186	1550	-32.56	121.48	3.69	118.1	893	459	6	603	55	29
6 May		3.105	3.407	182	1590	-31.40	122.82	1.77		890	391	2	587	111	31
10 May		3.033	3.427	178	1618	-30.82	124.00	0.22		895	398	1	580	156	34
14 May		2.989	3.450	174	1635	-30.13	125.03	-1.06		882	439	179	578	189	38
18 May		2.975	3.476	170	1640	-29.82	125.91	-2.14		880	489	177	582	214	43
22 May		2.991	3.505	166	1635	-29.62	126.64	-3.07		872	537	176	592	230	49
26 May		3.041	3.537	162	1615	-29.45	127.20	-3.88		865	580	176	607	239	54
30 May		3.126	3.571	158	1580	-29.28	127.62	-4.59		855	618	177	625	243	58
3 Jun 1971		3.249	3.608	154	1533	-29.05	127.88	-5.22		848	649	179	645	244	62
2 May 1971	12 Nov 1971	3.202	3.171	194	1550	-33.36	113.24	4.62	118.6	1010	482	165	552	52	28
6 May		3.082	3.171	190	1600	-31.73	114.67	2.18		958	368	175	547	36	30
10 May		2.996	3.180	186	1630	-30.63	115.91	0.27		942	355	180	552	90	33
14 May		2.942	3.195	182	1652	-29.91	117.00	-1.26		917	403	3	557	132	37
18 May		2.920	3.213	178	1661	-29.44	117.94	-2.53		928	465	5	579	165	40
22 May		2.930	3.235	174	1657	-29.13	118.71	-3.59		928	524	9	598	189	45
26 May		2.974	3.260	170	1640	-28.88	119.32	-4.49		935	572	10	619	207	49
30 May		3.053	3.289	166	1610	-28.65	119.76	-5.27		943	610	13	641	220	53
3 Jun 1971		3.170	3.321	162	1564	-28.39	120.05	-5.95		955	638	16	662	229	56
4 May 1971	20 Nov 1971	3.151	3.013	200	1572	-32.96	105.56	4.18	127.6	1456	362	166	524	108	24
8 May		3.027	3.006	196	1620	-31.07	106.94	1.44		1347	304	175	528	70	28
12 May		2.944	3.008	192	1650	-29.83	108.15	-0.64		1293	329	2	546	49	31
16 May		2.895	3.017	188	1670	-29.01	109.21	-2.28		1253	388	7	565	92	35
20 May		2.880	3.031	184	1675	-28.47	110.11	-3.60		1241	451	11	592	129	39
24 May		2.899	3.048	180	1668	-28.11	110.84	-4.69		1232	505	14	619	158	42
28 May		2.953	3.070	176	1648	-27.83	111.41	-5.61		1234	549	16	647	182	46
1 Jun		3.044	3.096	172	1612	-27.56	111.82	-6.38		1242	583	18	672	202	49
5 Jun 1971		3.173	3.126	168	1562	-27.28	112.07	-7.04		1251	610	19	695	219	51

RE-ORDER No. 64-522

114

RE-ORDER No. 64-522

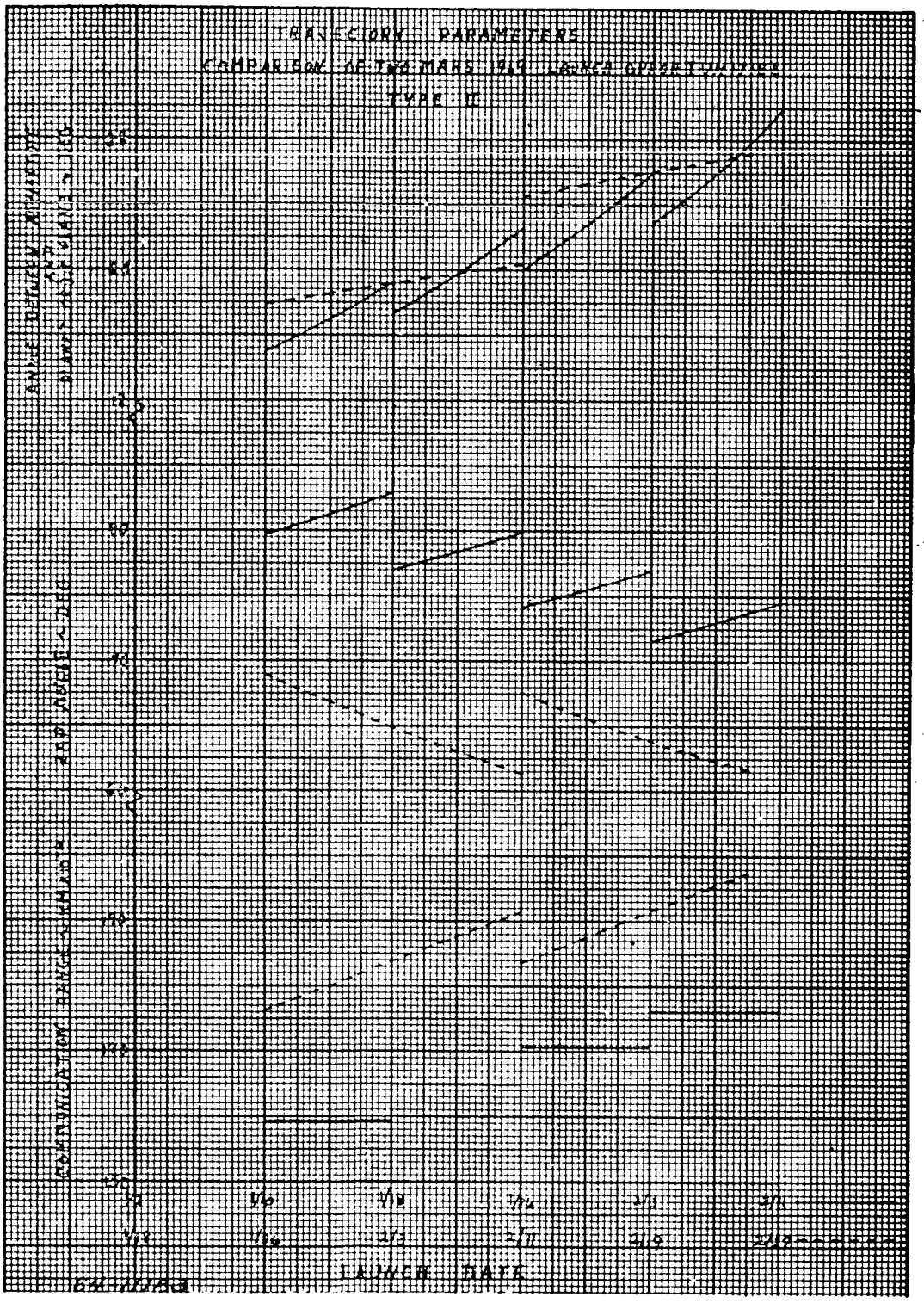

Figure 30 TRAJECTORY PARAMETERS COMPARISON OF TWO MARS 1969 LAUNCH OPPORTUNITIES TYPE II

RE-ORDER No. 64-522

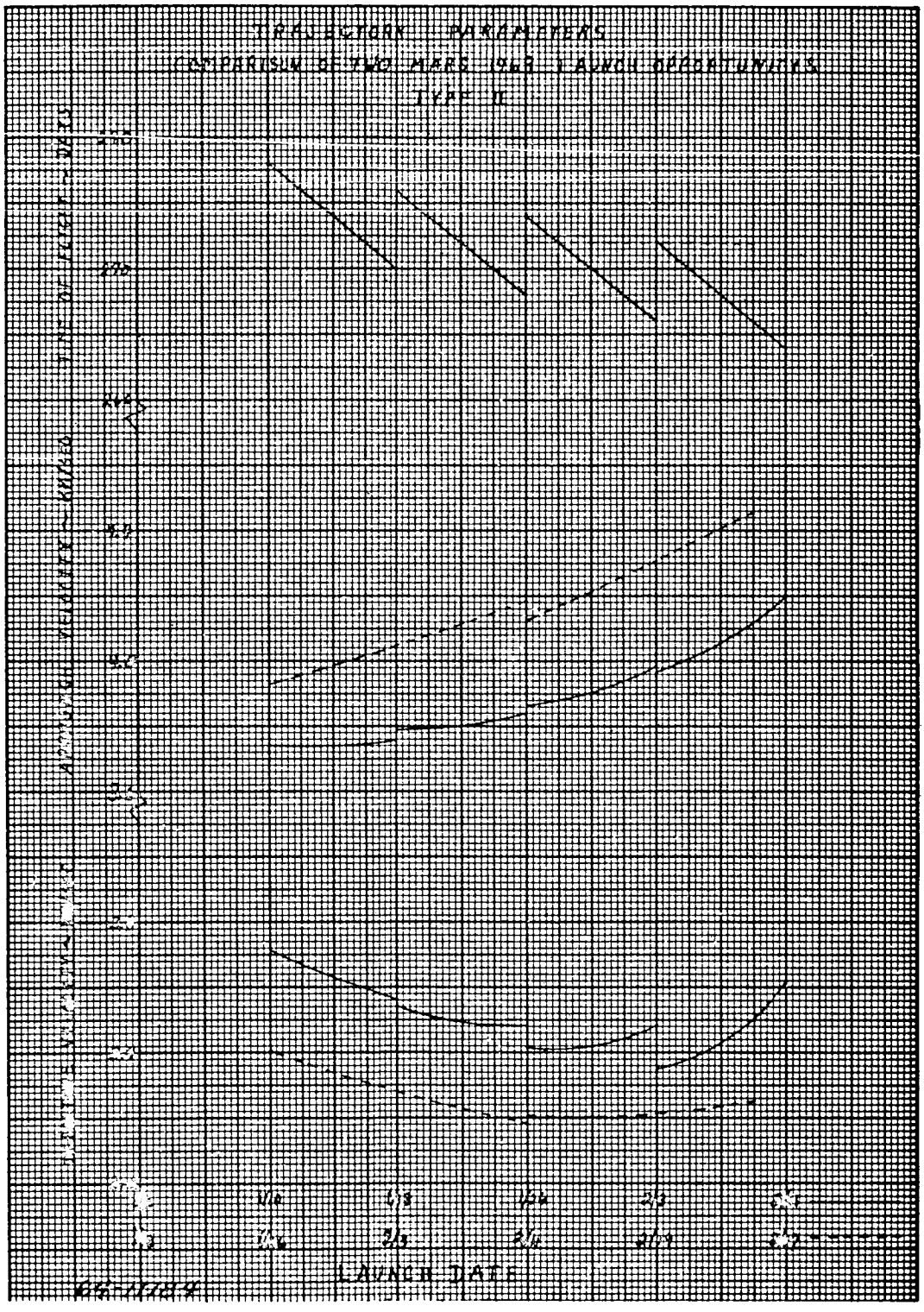

Figure 31 TRAJECTORY PARAMETERS COMPARISON OF TWO MARS 1969 LAUNCH OPPORTUNITIES TYPE II

RE-ORDER No. 64-522

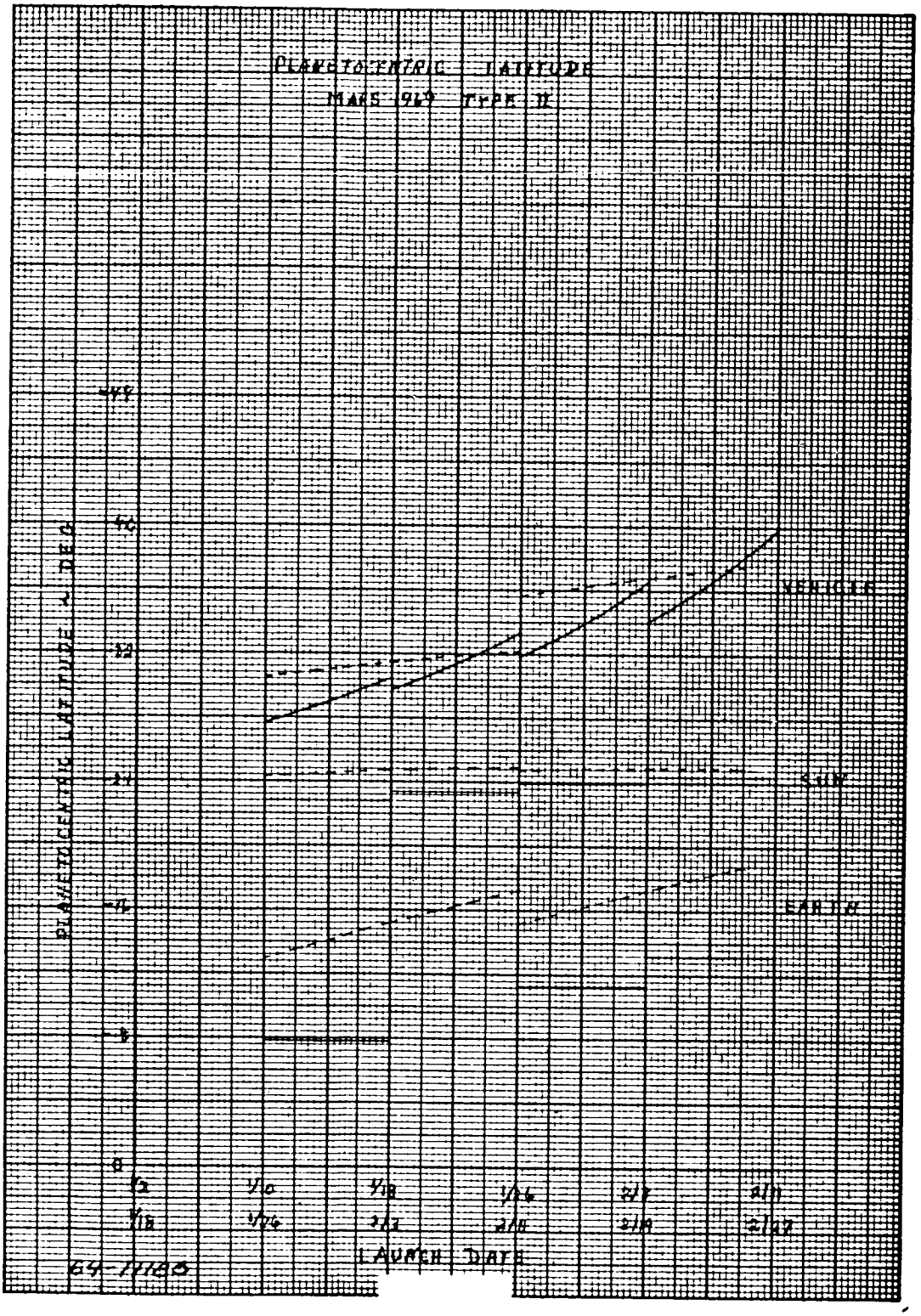

Figure 32 PLANETOCENTRIC LATITUDE MARS 1969 TYPE II

RE-ORDER No. 64-522

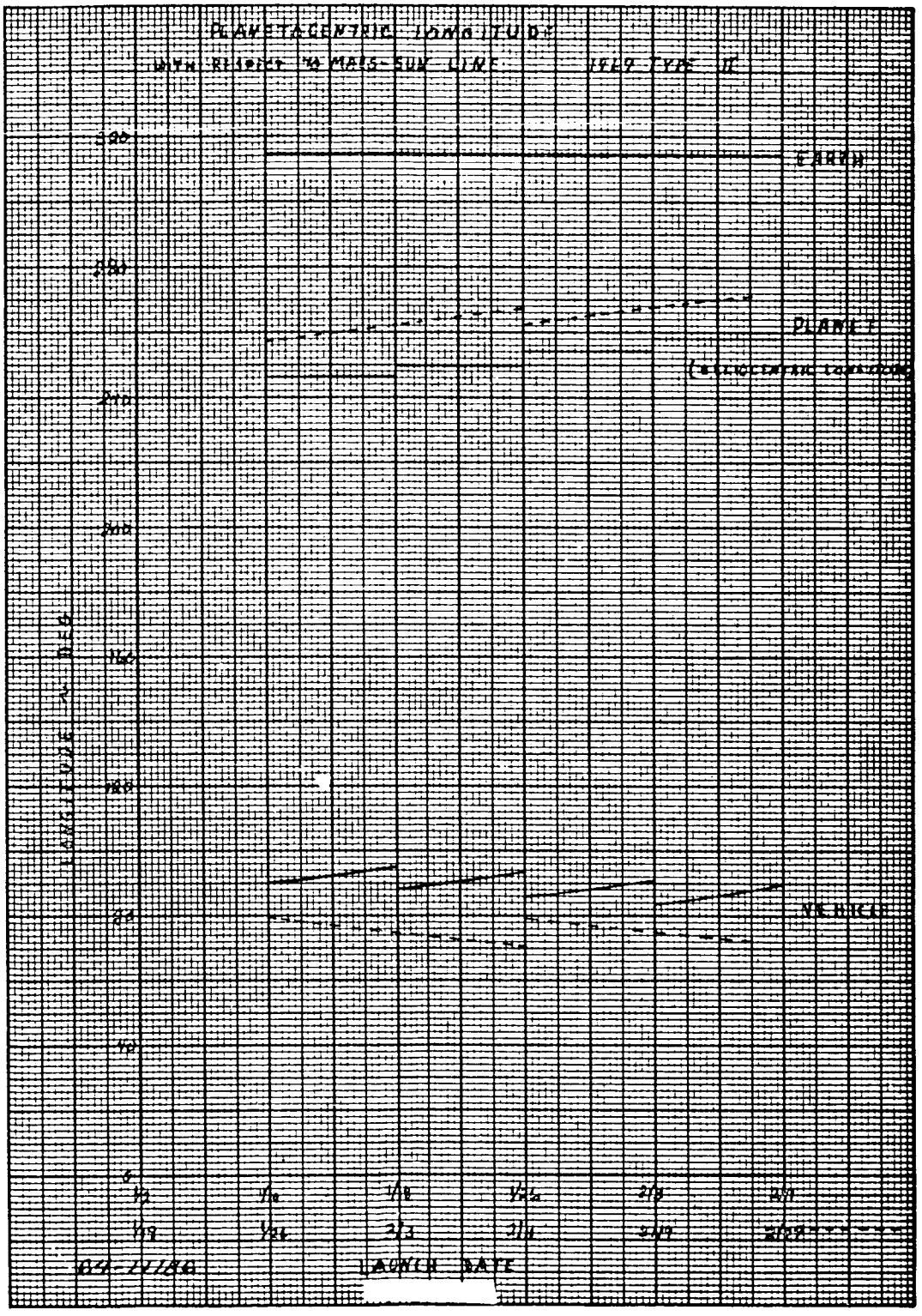

Figure 33 PLANETOCENTRIC LONGITUDE

RE-ORDER No. 64-522

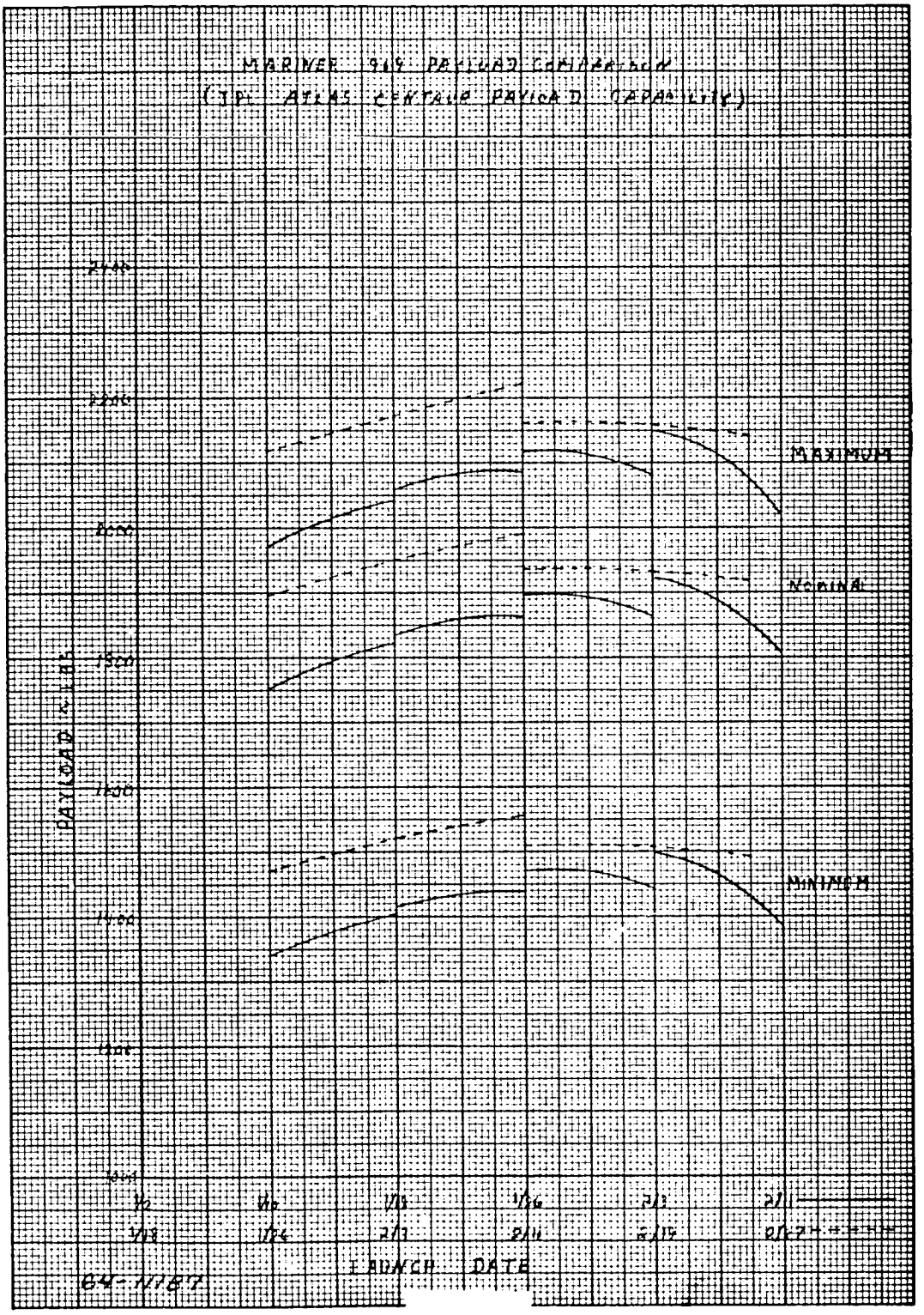

Figure 34 MARINER 1969 PAYLOAD COMPARISON

the planet. This motion complicates the problem of obtaining pre-impact atmospheric and post-impact biological data via the relay communication link. A third major problem is introduced since the approach asymptote is within several degrees, in both latitude and longitude, of the Mars-Earth line implying that is is virtually impossible to avoid Earth occultation during the encounter phase and maintain a flyby on the sunlit side of the planet. The pertinent trajectory parameters for a typical October arrival window are presented in figures 35-38.

If the arrival date is shifted back into November these problem areas can be alleviated. For example, the ZAP angle associated with a 12 November arrival date is about 115 degrees. This reduction in ZAP angle decreases the longitude excursion to achieve a sunrise landing at Syrtis Major, eliminates Earth occultation and reduces the problems associated with the relay communication link. Specifically, the longitude excursion is now reduced to between 17 and 27 degrees which, when coupled with a latitude excursion of between 31 and 23 degrees, produces a maximum entry angle of -62 degrees. This increase of 17 degrees in the maximum entry angle will propagate into a significant reduction in the impact dispersion ellipse.

Based upon this cursory analysis of the trajectory parameters, the constant arrival date window for 12 November was selected as the tentative 1971 launch window. The parameters associated with this window are presented in table 24. This window also produces significant reductions in the time of flight and communication range over the corresponding values associated with the minimum departure velocity window, whereas the departure and approach velocities are unchanged. The dispersion ellipses associated with 1 and 2 midcourse maneuvers are presented where it was assumed that the first maneuver occurs one day after injection and has spherically distributed velocity uncertainties of 0.1 m/sec. It was assumed that sufficient time elapses between maneuvers so that the major axis of the tracking error is reduced by a factor of 10 basically, since the primary function of the second maneuver is to remove velocity errors developed during the first maneuver.

The trajectory parameters associated with this window are presented in figures 39 to 43. If after the completion of various pertinent system studies, additional iterations are required to obtain the optimum window, the parametric information in table 23 can be employed to aid in the selection of a more refined window.

8. Look Angles

The Earth cone-clock angles for the launch window selected are presented in table 25 for 5 representative dates in the window. The cone angle variation associated with this window indicates that over the first portion of this

TABLE 24

TRAJECTORY PARAMETERS
1971 LAUNCH OPPORTUNITY

Launch Date	Arrival Date	Departure Velocity (km/sec)	Approach Velocity (km/sec)	Flight Time (days)	Payload (pounds)	Declination of Launch Asymptote (degrees)	ZAP Angle (degrees)	Minimum Flyby Inclination (degrees)	Communication Range (10^6 km)	Encounter Dispersion Ellipse					
										1 Midcourse Correction			2 Midcourse Corrections		
										Semi-Major Axis (km)	Semi-Minor Axis (km)	Orientation (degrees)	Semi-Major Axis (km)	Semi-Minor Axis (km)	Orientation (degrees)
2 May 1971	12 Nov 1971	3.202	3.171	194	1550	-33.36	113.24	21.40	118.6	1100	590	176	507	92	28
6 May		3.082	3.171	190	1600	-31.73	114.67			1068	462	4	507	80	29
10 May		2.996	3.180	186	1630	-30.63	115.91	18.08		1060	450	8	507	77	32
14 May		2.942	3.195	182	1652	-29.91	117.00			1040	499	12	506	79	36
18 May		2.920	3.213	178	1661	-29.44	117.94	16.02		1059	565	16	506	82	40
22 May		2.930	3.235	174	1657	-29.13	118.71			1065	627	20	506	86	44
26 May		2.974	3.260	170	1640	-28.88	119.32	14.55		1079	680	24	507	89	48
30 May		3.053	3.289	166	1610	-28.65	119.76			1096	721	29	507	91	52
3 Jun 1971		3.170	3.321	162	1564	-28.39	120.05	13.37		1116	751	33	507	93	56

RE-ORDER No. 64-522

TABLE 25

INTERPLANETARY EARTH CONE-CLOCK ANGLES
MARS 1971 TYPE I
ARRIVAL DATE: 12 NOVEMBER

	Launch Date: 2 May		Launch Date: 10 May		Launch Date: 18 May		Launch Date: 26 May		Launch Date: 3 June	
Time (days)	Cone Angle (degrees)	Clock Angle (degrees)	Cone Angle (degrees)	Clock Angle (degrees)	Cone Angle (degrees)	Clock Angle (degrees)	Cone Angle (degrees)	Clock Angle (degrees)	Cone Angle (degrees)	Clock Angle (degrees)
1	108.9	103.9	99.5	99.2	88.3	97.0	75.3	96.3	62.5	96.5
5	105.1	103.8	95.7	99.6	84.2	97.9	71.2	97.5	58.5	97.9
10	100.4	104.0	90.8	100.4	79.0	99.1	66.0	99.0	53.3	99.9
20	91.2	105.2	80.8	102.6	68.5	102.0	55.4	102.8	42.5	104.7
40	72.1	110.2	60.0	109,3	46.3	110.9	32.7	114.7	20.6	122.6
60	51.0	119.2	36.9	121.6	23,3	129.7	12.5	152.4	8.8	208.5
80	28.2	138.0	15.9	157.3	10.9	206.6	14.8	246.8	20.5	262.4
100	14.3	199.8	16.1	241.7	21.7	260.7	26.8	269.2	30.9	273.8
120	22.6	256.4	27.6	267.8	31.8	273.4	35.0	276.6	37.5	278.7
140	32.4	272.1	35.7	276.3	38.1	278.7	39.9	280.2	41.2	281.2
160	38.6	278.4	40.4	280.3	41.6	281.4	42.4	282.1	42.9	282.5
162	39.0	278.8	40.7	280.6	41.9	281.7	42.5	282.2	42.9	282.6
170	40.5	280.2	41.7	281.5	42.5	282.2	42.9	282.6		
178	41.7	281.3	42.4	282.2	42.9	282.6				
180	41.9	281.5	42.6	282.3						
186	42.4	282.0	42.9	282.6						
194	42.9	282.6								

RE-ORDER No. 64-532

RE-ORDER No. 64-522

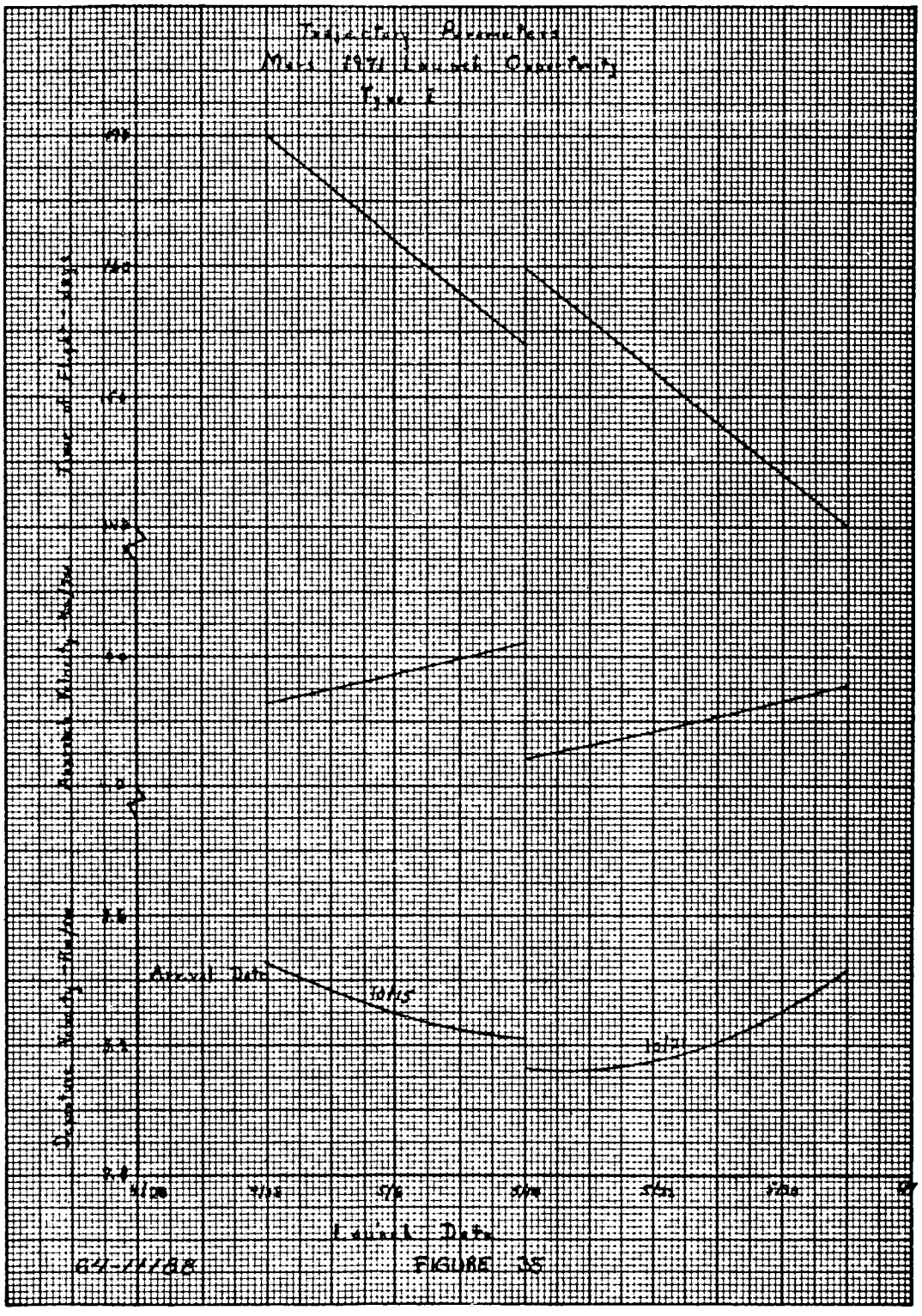

Figure 35 TRAJECTORY PARAMETERS MARS 1971 LAUNCH OPPORTUNITY TYPE I

RE-ORDER No. 64-522

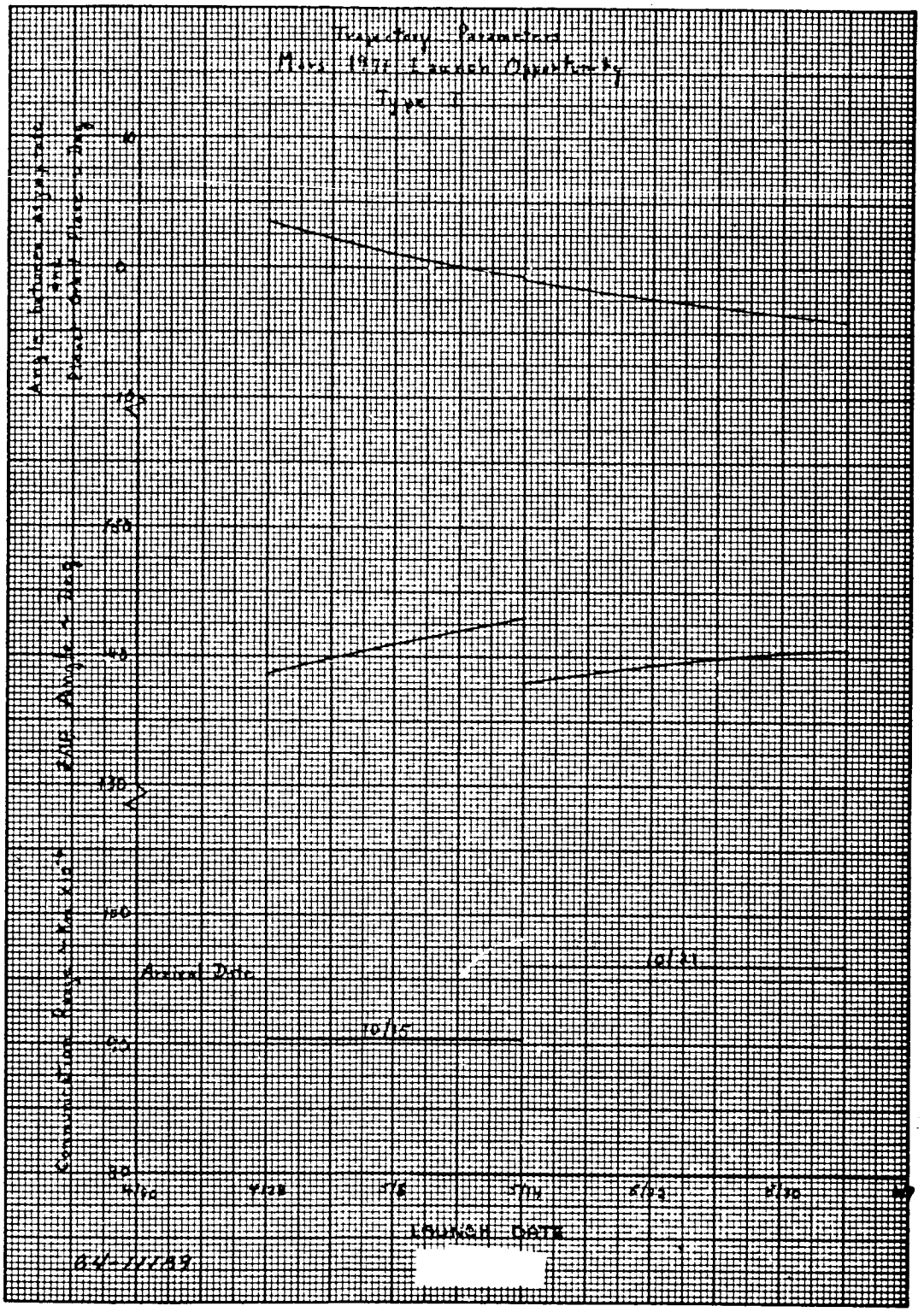

Figure 36 TRAJECTORY PARAMETERS MARS 1971 LAUNCH OPPORTUNITY TYPE I

RE-ORDER No. 64-522

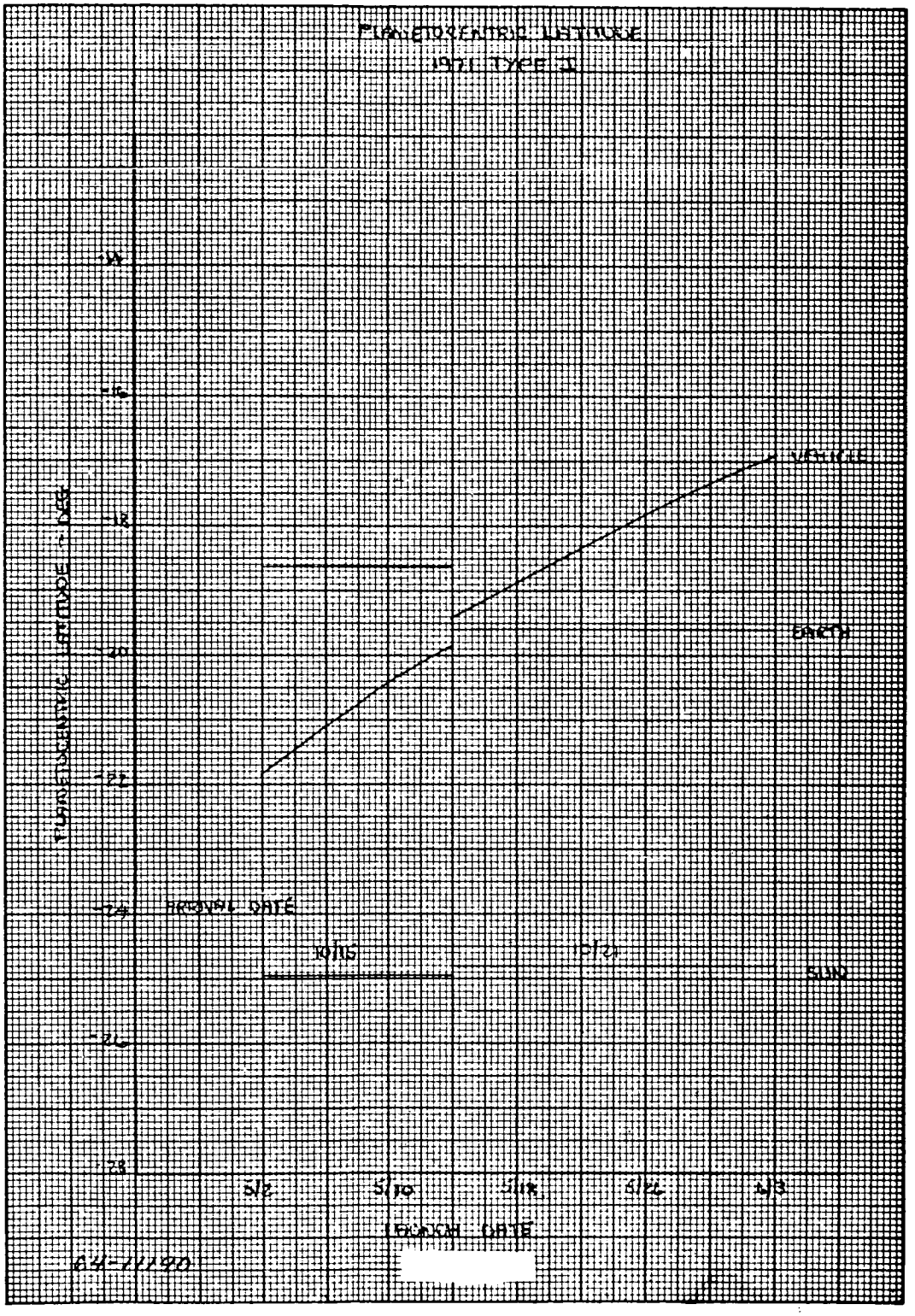

Figure 37 PLANETOCENTRIC LATITUDE 1971 TYPE I

RE-ORDER No. 64-522

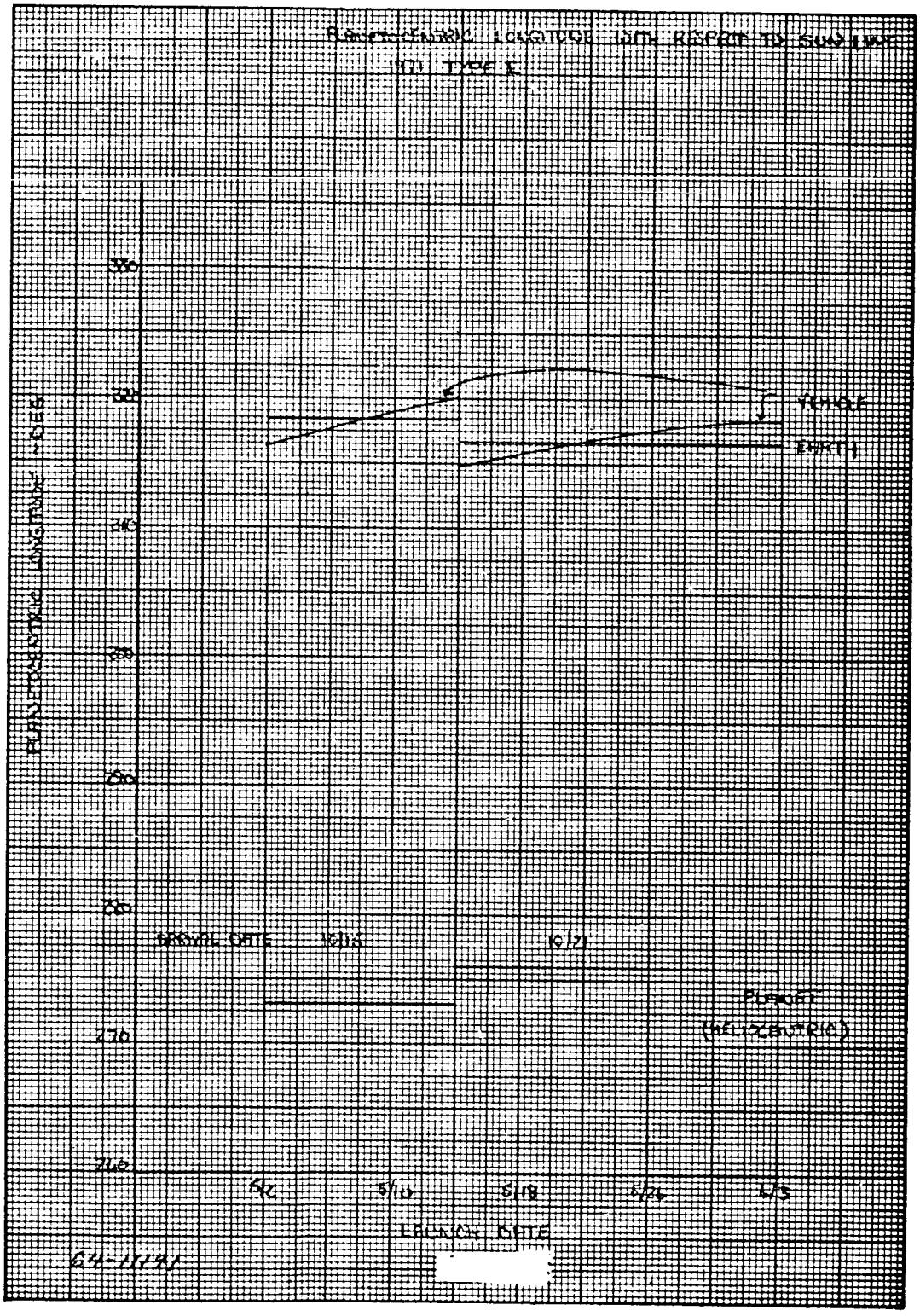

Figure 38 PLANETOCENTRIC LONGITUDE WITH RESPECT TO SUN LINE 1971 TYPE I

RE-ORDER No. 64-522

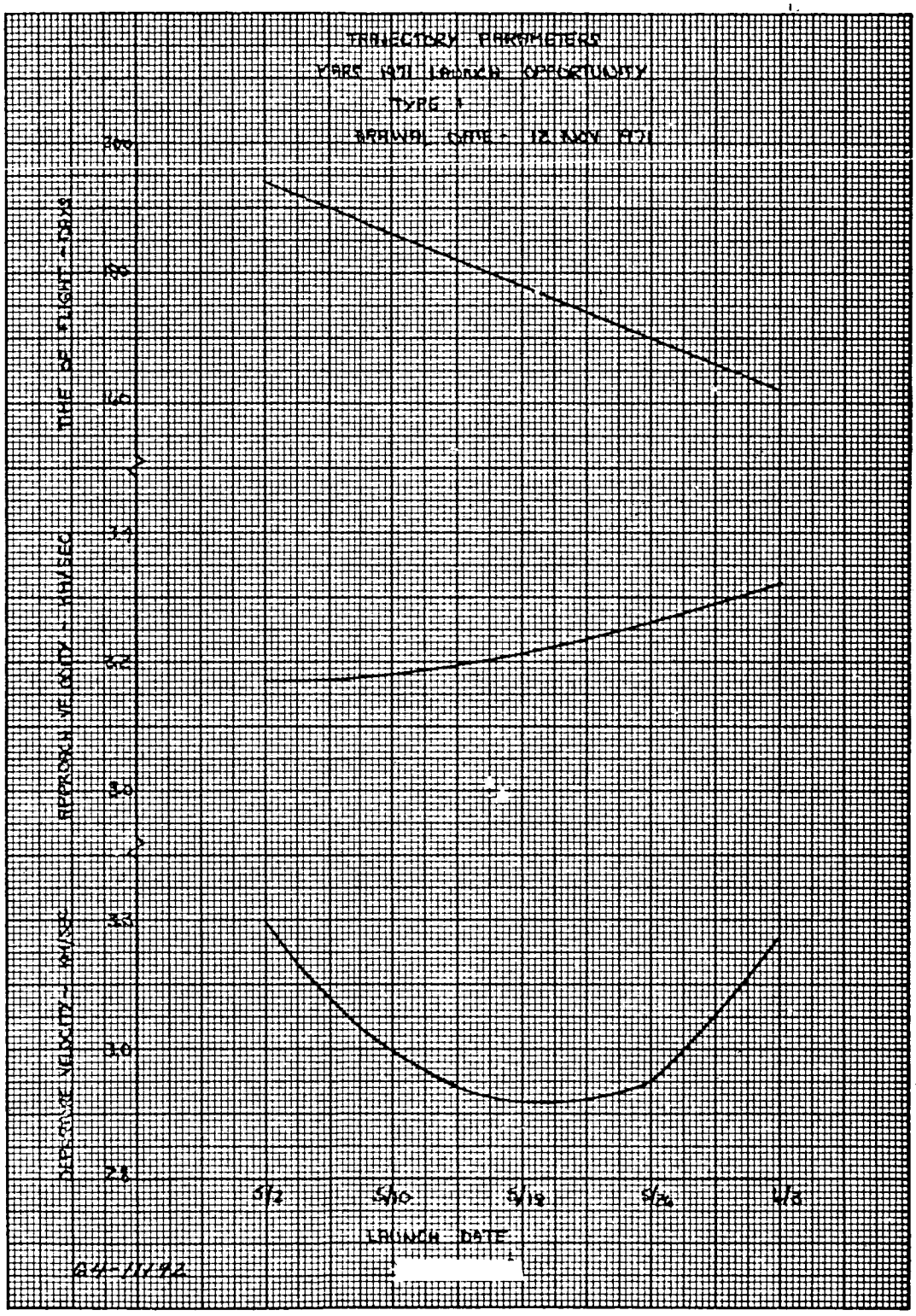

Figure 39 TRAJECTORY PARAMETERS MARS 1971 LAUNCH OPPORTUNITY TYPE I

RE-ORDER No. 64-522

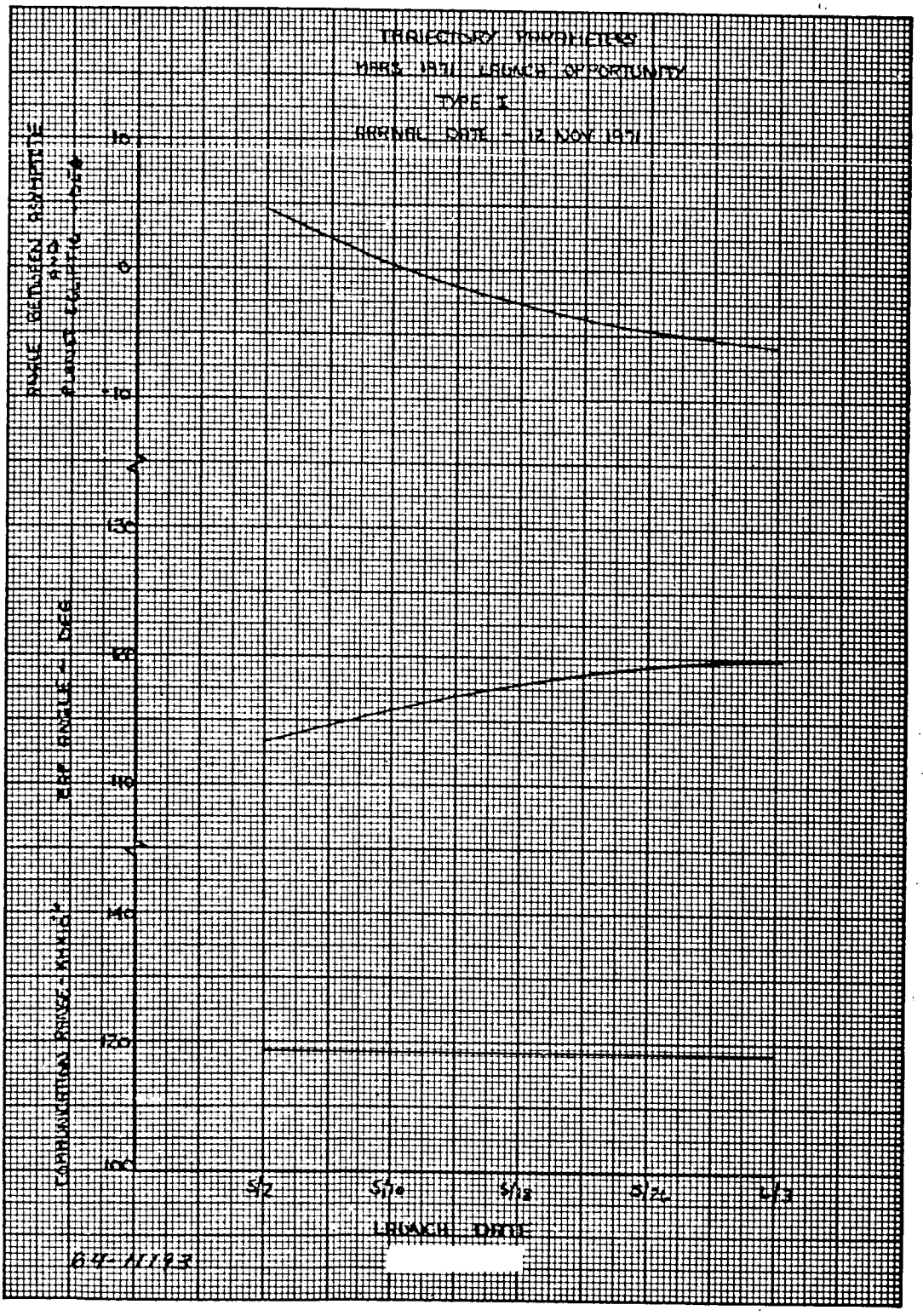

Figure 40 TRAJECTORY PARAMETERS MARS 1971 LAUNCH OPPORTUNITY TYPE I

RE-ORDER No. 64-522

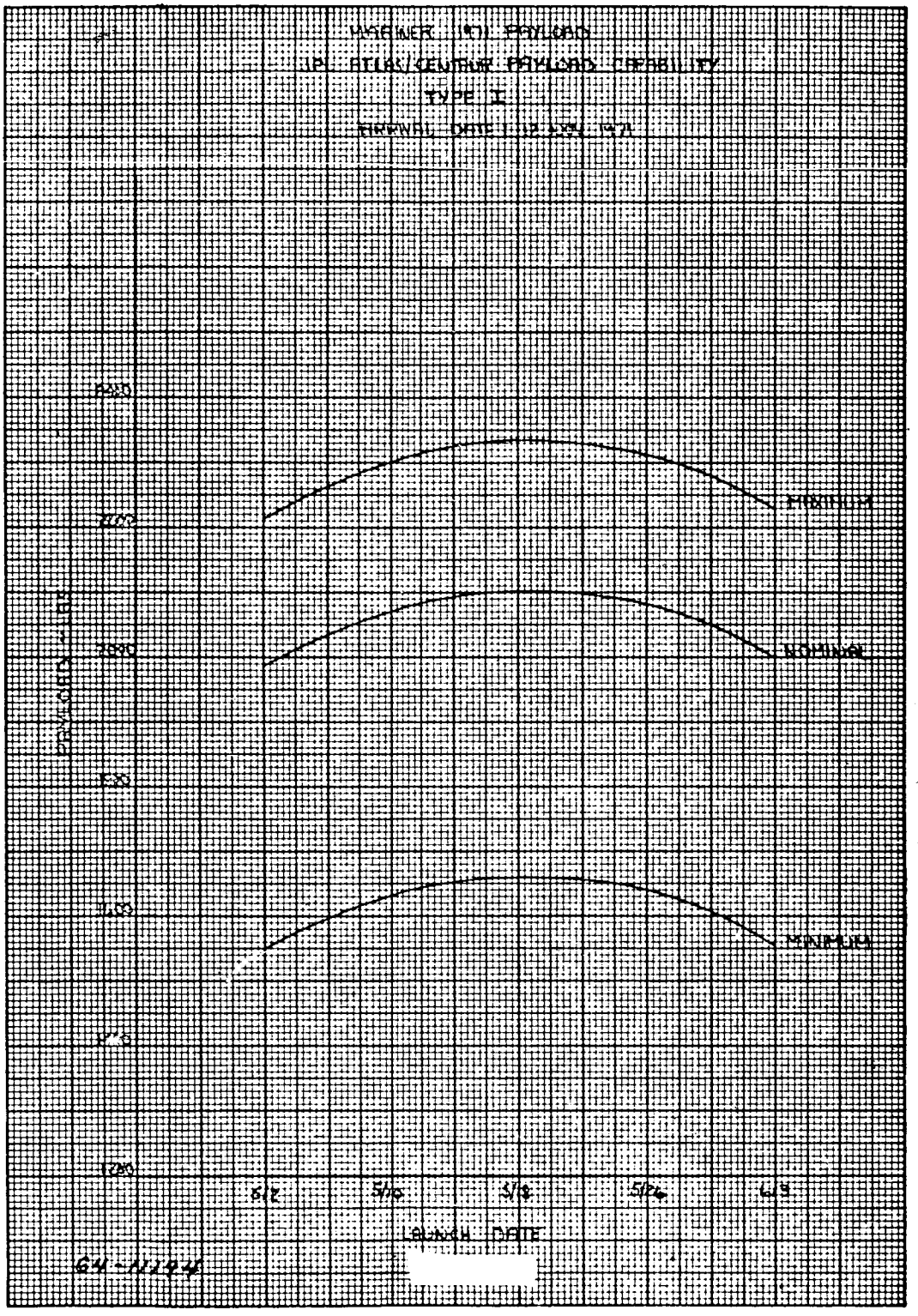

Figure 41 MARINER 1971 PAYLOAD JPL ATLAS/CENTAUR PAYLOAD CAPABILITY TYPE I

RE-ORDER No. 64-522

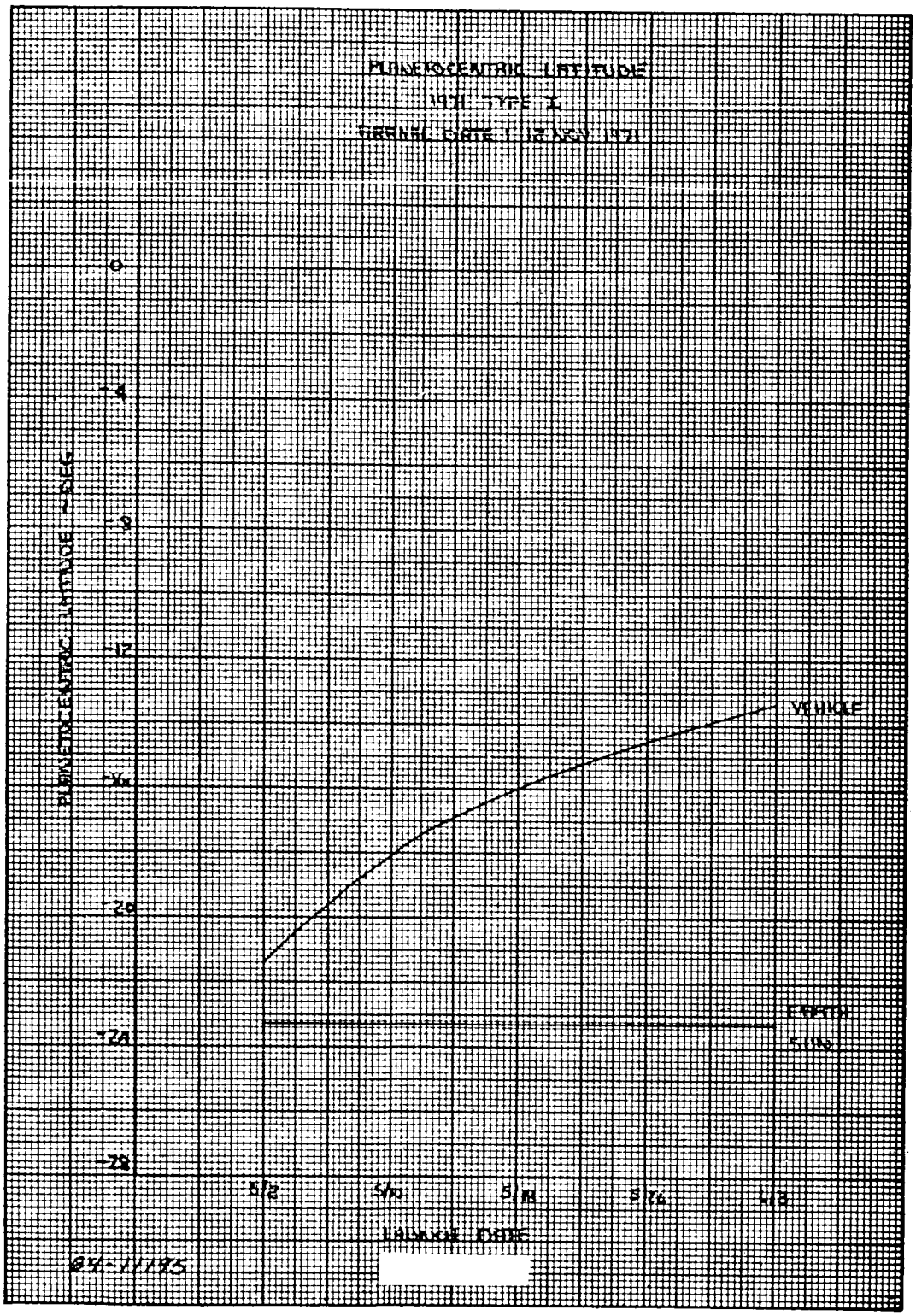

Figure 42 PLANETOCENTRIC LATITUDE 1971 TYPE I

130

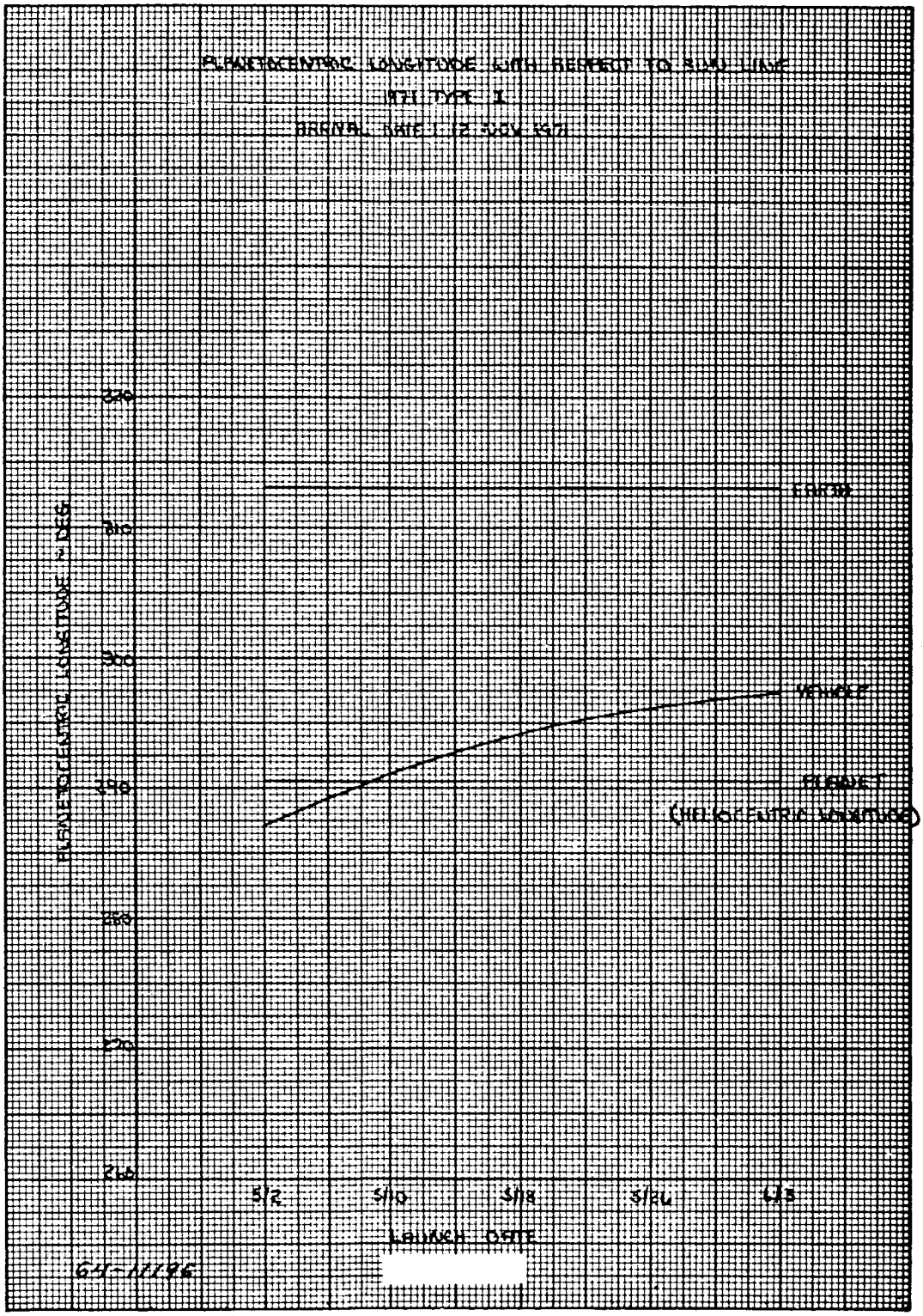

Figure 43 PLANETOCENTRIC LONGITUDE WITH RESPECT TO SUN LINE 1971 TYPE I

RE-ORDER No. 64-522

window the probe is launched prior to perihelion and initially passes inside the Earth's orbit for a period of 10 to 20 days. The probe initially moves ahead of the Earth and remains there for approximately 60 days or until the probe-Earth distance is about 20×10^6 km. At this point the cone angle is minimized and the clock angle switches from the second to the third quadrant indicating that the probe now lags behind the Earth. Shortly after this time both angles achieve steady-state conditions. For one representative date in the launch window the cone and clock angles are presented as a function of distance from Earth in figures 44 and 45.

The variation in the Canopus cone angle shows a significant reduction over the excursion encountered during the 1969 launch window. Since Canopus is not at the ecliptic south pole the variation experienced in this angle is a function of the launch date and heliocentric angle traversed prior to the Martian encounter. If the Canopus tracker was located with a nominal 84-degree cone angle the gimbal motion could be reduced to about ±7 degrees. These data are presented in table 26.

During the encounter phase,this analysis was conducted for a nominal passing altitude of 10,000 kilometers. Two specific flyby trajectory inclinations were considered: the minimum inclination and a constant inclination of 45 degrees. As expected, there is a marked similarity between the planet cone angle and the ZAP angle at encounter, whereas at departure, the cone angle is essentially the supplement of the ZAP angle decreased by approximately 19 degrees to account for the trajectory bending produced by the planet's gravitational attraction during the encounter phase. The clock angle variation indicates that just prior to periapsis passage the vehicle passes from the southern to the northern hemisphere as the clock angle proceeds from the second to the fourth quadrant. For 30 days after encounter, the Earth cone-clock angles and the Canopus cone angle remain essentially invariant.

For an intermediate date in this launch window the cone-clock angles to the various bodies are presented in table 27 to illustrate the variation in these angles over the encounter phase. In addition, this information is presented in graphical form as a function of distance from the center of the planet in figures 46 and 47. The discontinuity in the figures is due to the fact that the probe never passes within 10,000 kilometers of the planet.

There is relatively no change in the data as the inclination is increased to 45 degrees except that the maximum cone angle is reduced by 35 degrees from 163 to 128 degrees. The maximum cone angle occurs near the point where the Sun, probe, Canopus, and Mars are in the same plane, and is 180 degrees only when at this time the probe is on the planet-Sun line. As the probe inclination increases the angle between the probe-Sun line and the planet-sun line increases thereby decreasing the maximum cone angle. The

TABLE 26

1971 INTERPLANETARY TRAJECTORIES
CANOPUS CONE ANGLE

Arrival Date: 12 Nov. 1971

Time (days)	Launch Date				
	2 May	10 May	18 May	26 May	3 June
	Cone Angle (degrees)	Cone Angle (degrees)	Cone Angle (degrees)	Cone Angle (degrees)	Cone Angle (degrees)
0	83.8	82.2	80.7	79.3	78.2
5	82.9	81.3	79.9	78.6	77.6
10	82.0	80.5	79.2	78.1	77.2
20	80.5	79.1	78.0	77.2	76.6
40	78.5	77.6	77.0	76.7	76.7
60	78.0	77.5	77.4	77.6	78.1
80	78.7	78.6	79.0	79.5	80.3
100	80.3	80.6	81.2	81.9	82.9
120	82.4	82.9	83.7	84.6	85.6
140	84.8	85.5	86.4	87.3	88.3
160	87.2	88.0	89.0	90.0	91.0
162				90.2	91.2
170	88.4	89.3	90.2	91.2	
178			91.2		
180	89.6	90.5			
186	90.3	91.2			
190	90.8				
194	91.2				

RE-ORDER No. 64-522

RE-ORDER No. 64-522

TABLE 27

ADVANCED MARINER 1971
HYPERBOLIC LOOK ANGLES

Launch Date 5/18/71, t_f = 178 days, R_p = 13400 km, i = 16.0 degrees

Time (days)	Planet		Earth		Canopus Cone (degrees)	Range from Planet (km x 10^{-3})
	Cone (degrees)	Clock (degrees)	Cone (degrees)	Clock (degrees)		
0	118.6	99.4	43.0	282.6	91.3	1000
1.0	118.4	99.3	43.1	282.7	91.4	725
2.0	118.7	99.0			91.5	444
2.5	119.4	98.6			91.6	305
3.0	121.7	97.6				164
3.2	124.6	96.3				107
3.4	134.2	91.4		282.8	91.7	50
3.5	156.5	65.6				21
3.51	160.6	51.6				20
3.52	163.5	26.5				17
3.53	161.9	351.8				15
3.54	154.2	325.1				14
3.55	142.2	310.0				14
3.60	86.8	286.9				20
3.66	64.0	279.7				36
3.76	52.6	274.9				63
3.96	46.2	271.5				122
4.56	42.2	268.8			91.8	291
5.61	41.3	267.9			92.0	585
6.61	41.3	267.7			92.1	864
12.11	43.5	268.1	42.9	282.9	92.8	2400
22.11	48.1	269.0	42.5	282.9	94.1	
32.11	52.5	269.6	41.9	282.7	95.3	

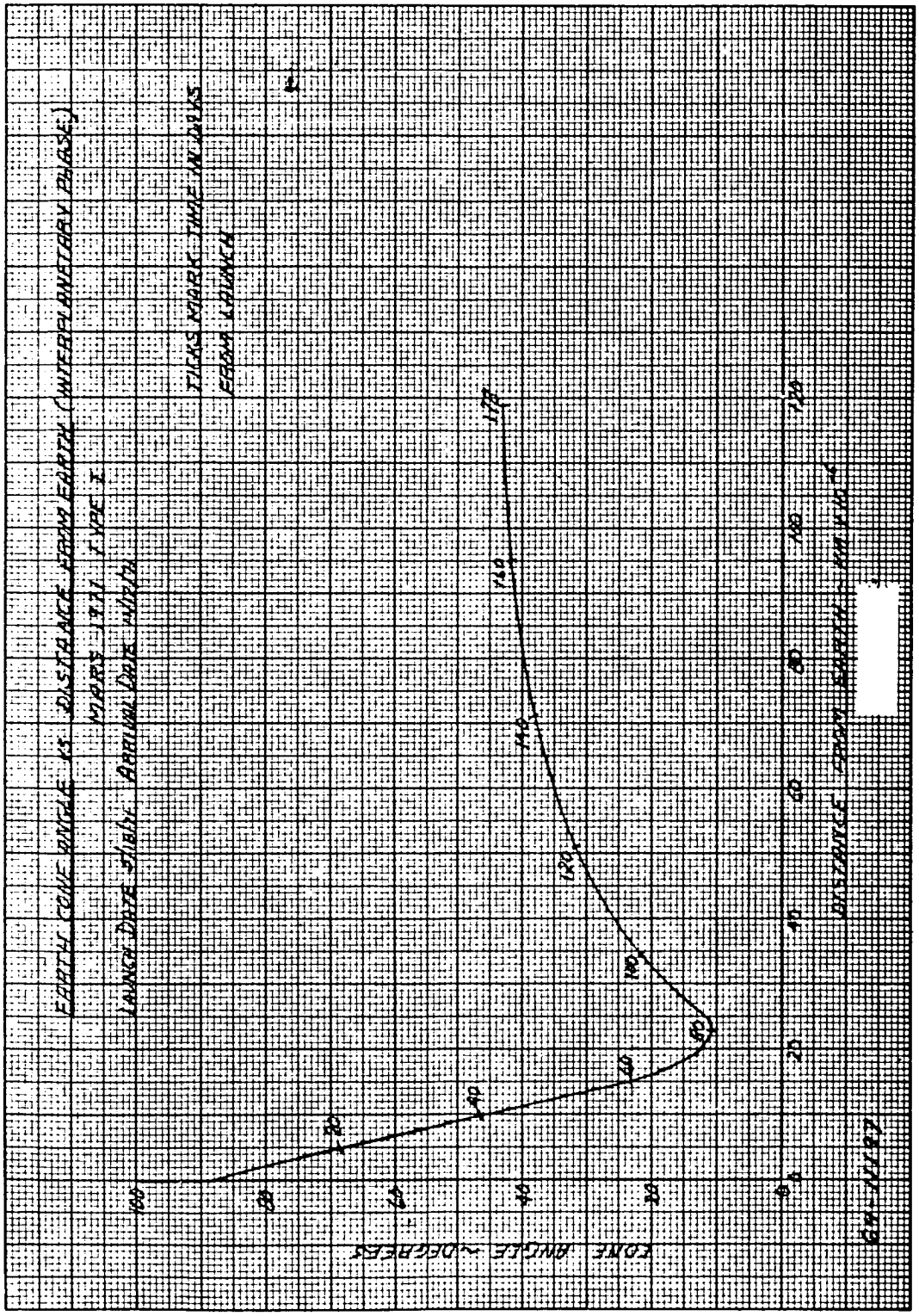

Figure 44 EARTH CONE ANGLE VERSUS DISTANCE FROM EARTH (INTERPLANETARY PHASE)

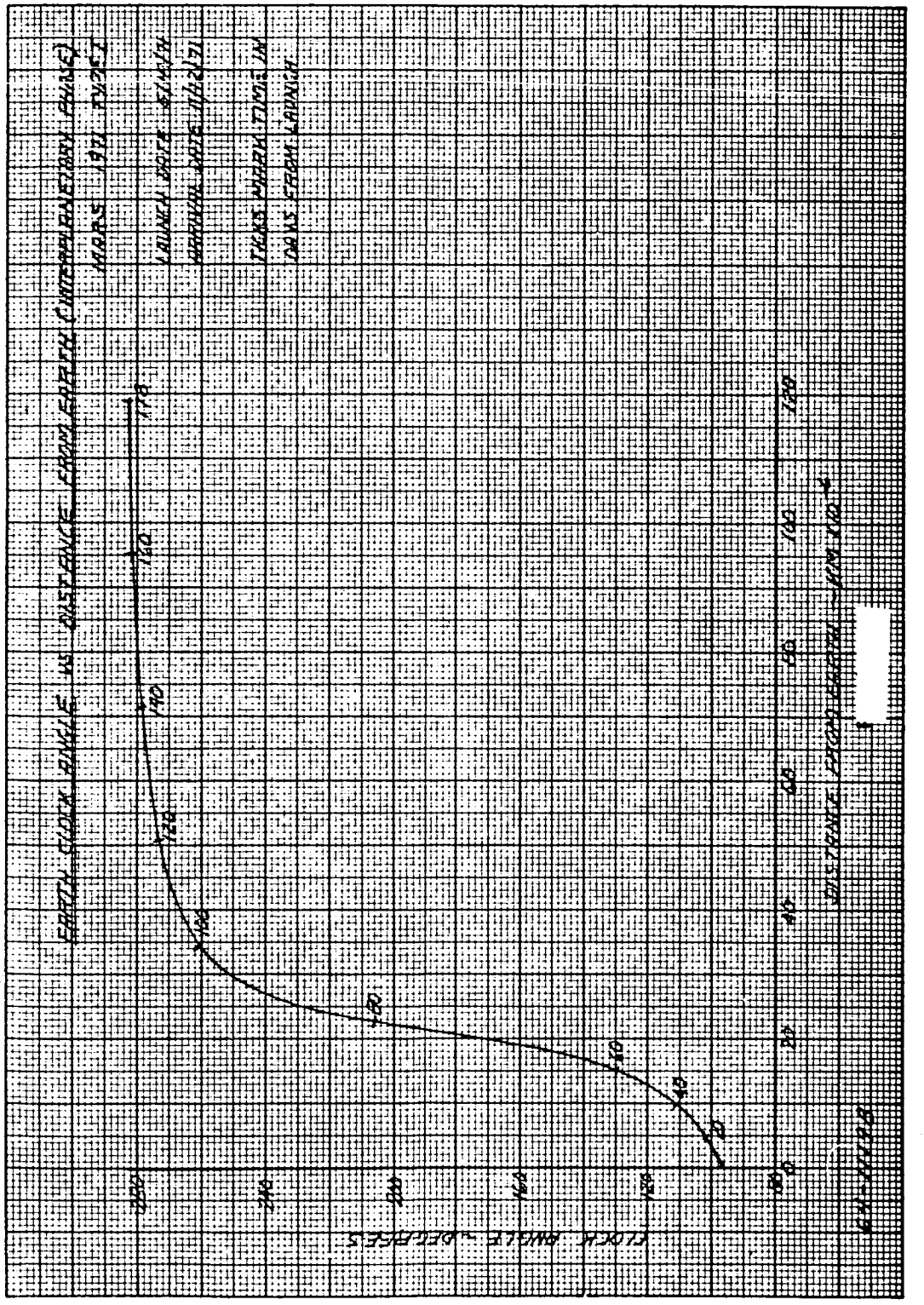

Figure 45 EARTH CLOCK ANGLE VERSUS DISTANCE FROM EARTH (INTER-PLANETARY PHASE)

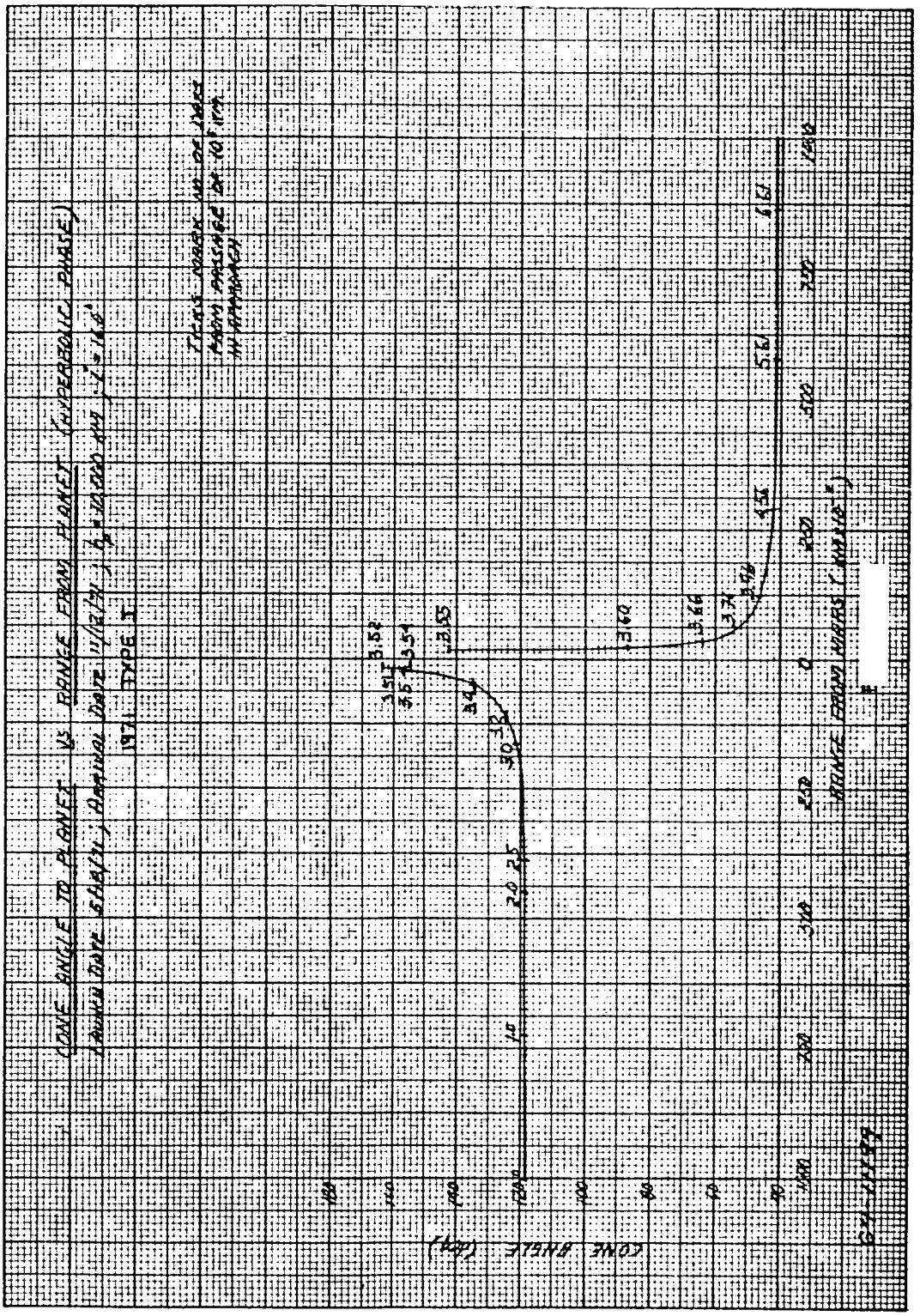

Figure 46 CONE ANGLE TO PLANET VERSUS RANGE FROM PLANET (HYPERBOLIC PHASE)

RE-ORDER No. 64-522

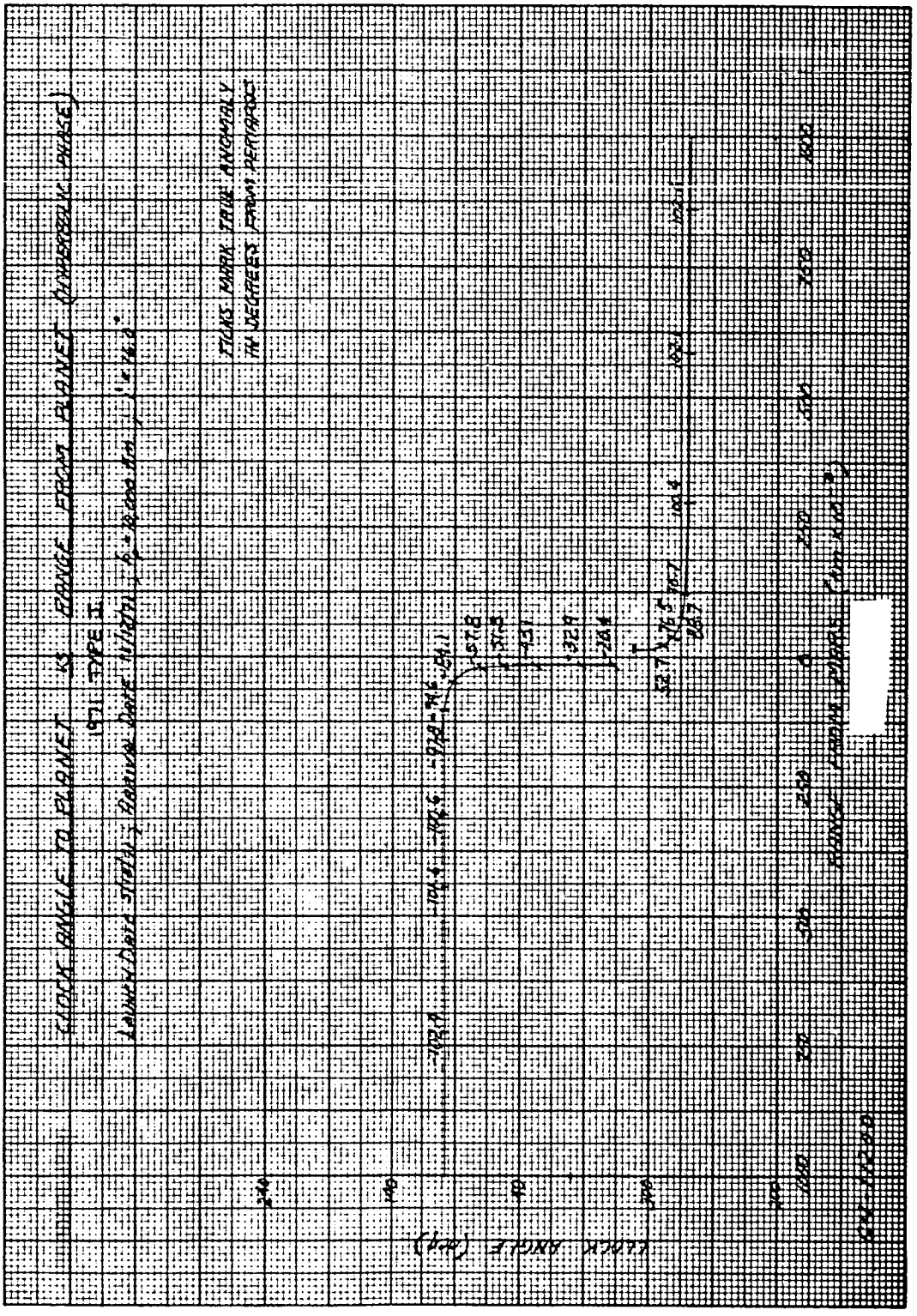

Figure 47 CLOCK ANGLE TO PLANET VERSUS RANGE FROM PLANET (HYPERBOLIC PHASE)

RE-ORDER No. 64-522

data for a 45 degree flyby trajectory inclination is summarized in table 28 and figures 48 and 49.

9. Lander-Flyby Spatial Time Relationship

For the 1971 launch opportunity the lander-flyby spatial time relationship poses a more serious problem for the relay communication link if the mission objectives of a sunrise landing at Syrtis Major are maintained. The difficulty arises due to the sunlit approaches which characterize Type 1 Martian trajectories and require the lander be placed in a retrograde orbit with an inclination that is a function of the ZAP angle. For the optimum arrival date window, 15 to 21 October, a ZAP angle of 140 degrees produces a lander trajectory inclination requirement of 150 degrees, whereas, the flyby trajectory is nominally inclined about 15 degrees with periapsis on the sunlit side of the planet near the terminator. Therefore, the vehicles are heading toward opposite poles and relay communication will only be feasible if a sufficiently large slowdown velocity is applied to the flyby to allow completion of the communication phase while the flyby is still approaching the planet along the approach asymptote. Communications under these conditions would at best be marginal since there is a 55 degree central angle between the asymptote and the lander impact position.

For a slowdown velocity of 2,000 ft/sec the flyby-lander slant ranges at entry, E + 3, and E + 5 hours are 158,000, 120,000 and 95,000 kilometers, respectively. The corresponding angles above the lander horizon to the flyby are 28, 58, and 54 degrees. The improvement in the angle with time arises from the fact that the lander is rotating at a rate of 15 deg/hr whereas the flyby is sufficiently far from the planet to be experiencing little latitude or longitude excursion.

For the tentative launch window selected for this launch opportunity, 2 May to 3 June with an arrival date of 12 November, the communication problem is greatly alleviated by the fact that the ZAP angle is reduced to 115 degrees. The lander inclination is 135 degrees and the central angle between separation and the nominal lander impact position is reduced to 35 degrees. For a flyby trajectory inclination of 15 degrees, the lander-flyby spatial time relationship was analyzed for slowdown velocities of 750, 1,000, and 1,250 ft/sec. For this specific inclination, a slowdown velocity of 1,000 ft/sec produces near optimum communication conditions in that the lander and flyby vehicles are at coincident longitudes at both 3 and 5 hours after impact. Therefore, the angle above the lander horizon to the flyby is only a function of the latitude difference and the flyby altitude.

For a 1,000 fps slowdown the geometry improves as the inclination of the flyby trajectory is increased to 45 degrees thereby rotating the flyby trajectory in the direction of the impact point. The angle from the lander

RE-ORDER No. 64-522

TABLE 28

ADVANCED MARINER 1971
HYPERBOLIC LOOK ANGLES

Launch Date 5/18/71, t_f = 178 days, R_p = 13400 km, i = 45 degrees

Time (days)	Planet		Earth		Canopus Cone (degrees)	Range from Planet (km x 10^{-3})
	Cone (degrees)	Clock (degrees)	Cone (degrees)	Clock (degrees)		
0	118.1	98.8	43.0	282.6	91.3	1000
1.0	117.8	98.4	43.1	282.7	91.4	725
2.0	117.6	97.6			91.5	444
2.5	117.9	96.6			91.6	305
3.0	118.8	93.8				164
3.2	120.1	90.6				107
3.4	123.9	79.1		282.8	91.7	50
3.5	128.2	46.9				21
3.51	127.8	38.6				20
3.52	126.6	28.4				17
3.53	123.9	16.3				15
3.54	119.1	2.7				14
3.55	112.1	348.8				14
3.60	77.1	300.7				20
3.66	64.2	279.5				36
3.76	58.8	267.1				63
3.96	56.4	259.3			91.8	122
4.56	55.3	254.0				291
5.61	55.3	252.3		282.7	92.0	585
6.61	55.6	251.8			92.2	864
12.11	57.9	252.0			93.0	2392
22.11	62.0	253.1	42.8	282.5	94.4	
32.11	65.9	253.9	42.3	282.2	95.8	

RE-ORDER No. 64-522

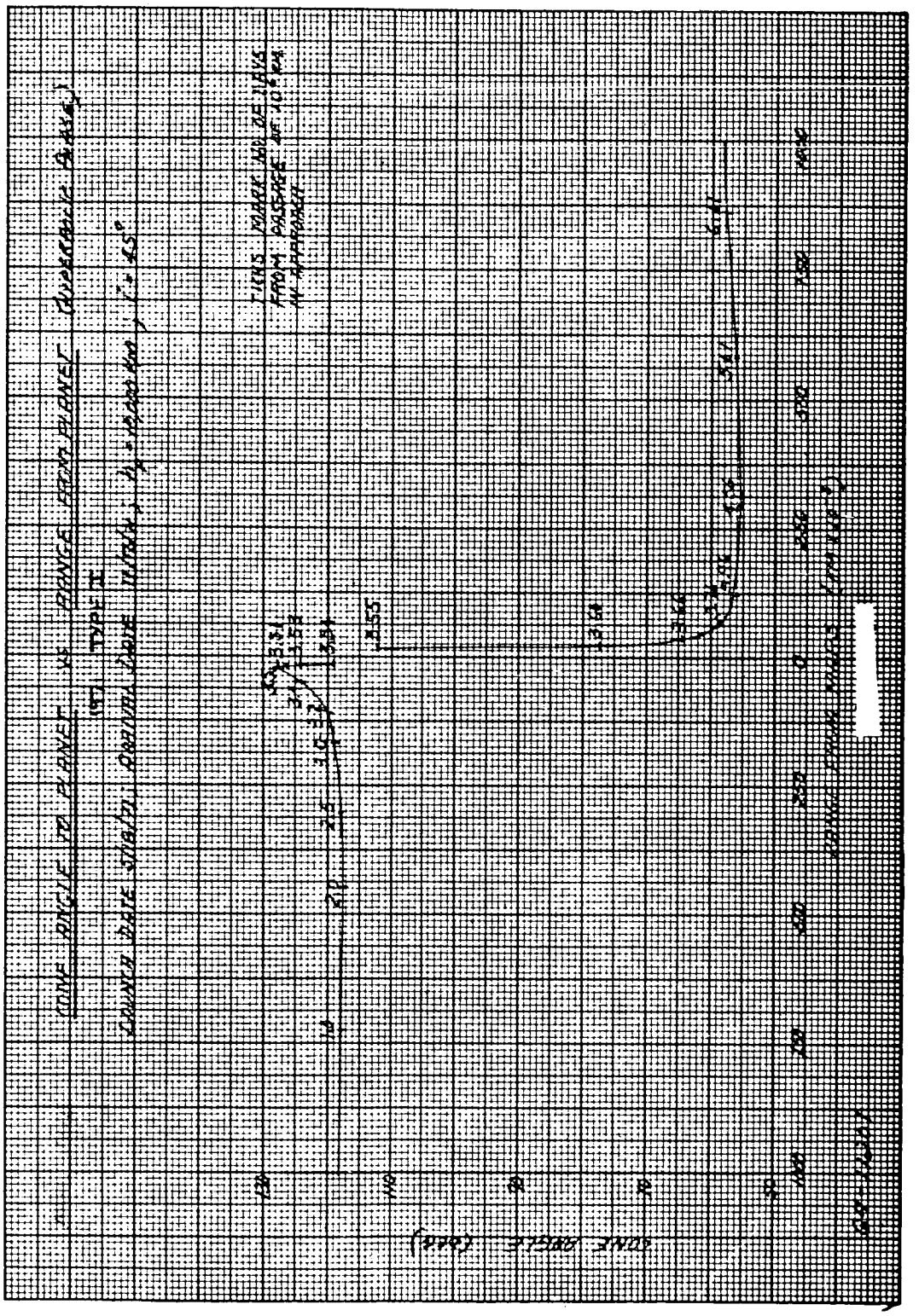

Figure 48 CONE ANGLE TO PLANET VERSUS RANGE FROM PLANET (HYPERBOLIC PHASE)

RE-ORDER No. 64-522

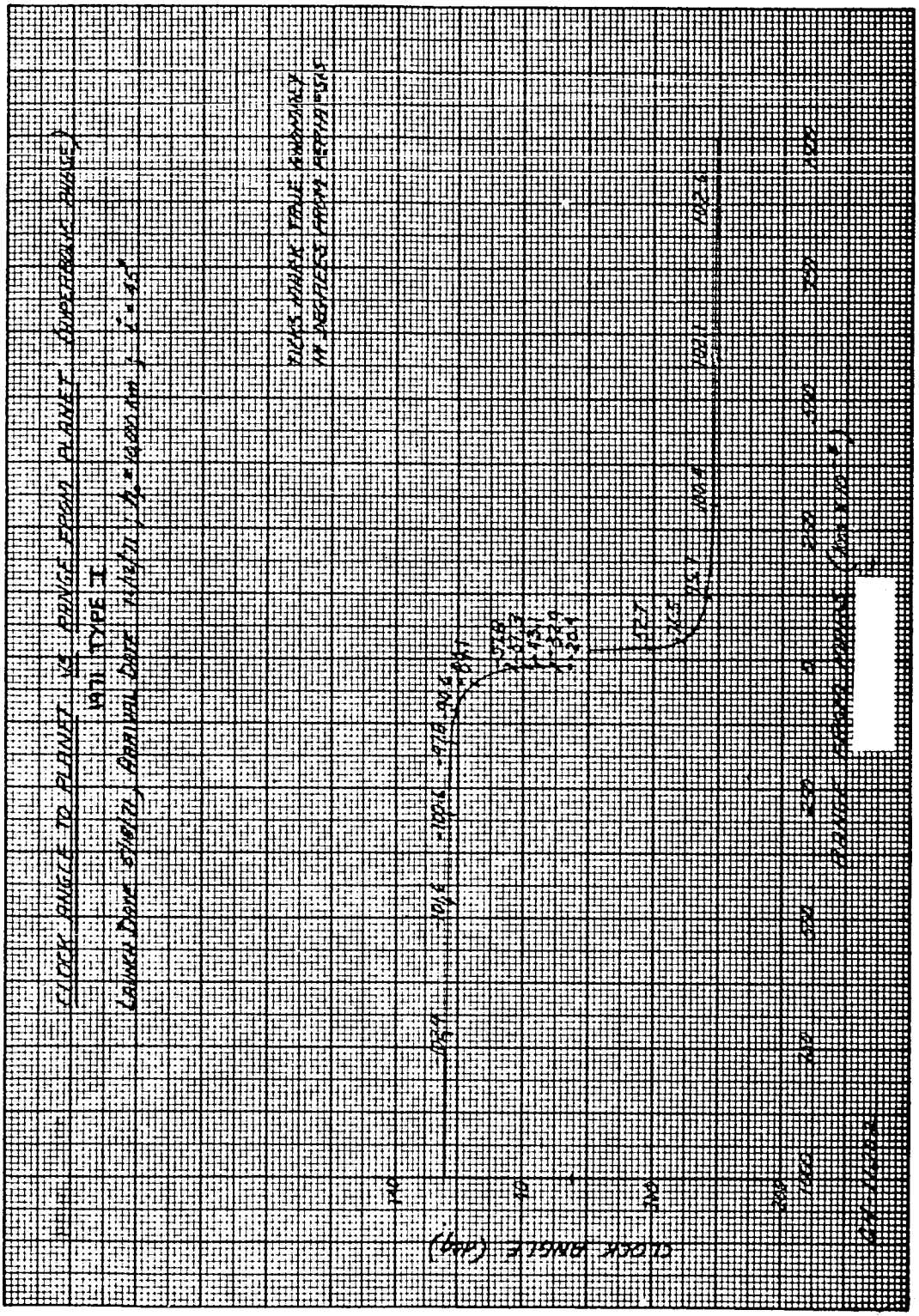

Figure 49 CLOCK ANGLE TO PLANET VERSUS RANGE FROM PLANET (HYPERBOLIC PHASE)

RE-ORDER No. 64-522

horizon to the flyby is increased by 5 to 10 degrees while the slant range remains constant. The results of this analysis are presented in table 29.

10. Lander Entry Error Analysis

The same procedure previously described was employed to determine the uncertainty in the entry parameters for one representative date in the launch window, 18 May 1971. For this date a longitude excursion of 25 degrees and a latitude excursion of 26 degrees are required from lander separation to entry to achieve a sunrise landing at Syrtis Major. The resultant range angle excursion of 35 degrees with an approach velocity of 3.2 km/sec produces a nominal entry angle of -61 degrees. The maximum possible entry angle on this date to impact Syrtis Major is around -70 degrees; however, to achieve this angle it is necessary to arrive at the target several hours after sunrise at which point earth communication via a direct link system is possible for a period of 4 hours after impact. An approach velocity of 3.2 km/sec coupled with an unperturbed flyby periapsis altitude of 10,000 km yield requirements for a separation velocity of 206 ft/sec. The azimuth angle, θ, of the separation is essentially 90 degrees and the elevation angle, α, is 6.5 degrees to achieve the desired impact location.

The error sources employed in this analysis are identical with those previously stated, i.e., positional errors of 150 and 350 kilometers, a 1-percent variation in the separation velocity and a 1-degree uncertainty in the thrust application angles. The results of this analysis, presented in table 30, indicate that the 1-sigma variation in entry angle is 3.30 degrees and the corresponding uncertainties in latitude and longitude are 4.51 and 3.06 degrees respectively, for a positional uncertainty of 150 kilometers. The major error source contributing to the uncertainty in the entry angle and latitude is the error in the out-of-plane pointing accuracy associated with the separation velocity. These errors would be reduced by approximately 35 percent if this error source were reduced by 50 percent. There are two predominant error sources that account for the majority of the longitude variation; the first is the perturbation in the separation velocity and the second is a positional error producing a translation of the approach asymptote in the initial plane of motion.

The uncertainties in the lander entry parameters associated with this window are almost identical with those developed for the 1969 launch opportunity and again indicate the feasibility of a Syrtis Major impact.

11. Occultation - Minimum Passing Altitude Analysis

For the 1971 launch opportunity, the approach geometry associated with the launch window yielding the optimum arrival date presents an entirely

TABLE 29

LANDER-FLYBY GEOMETRY FOR INITIAL LATITUDE OF 15°S
1971 LAUNCH OPPORTUNITY - ARRIVAL DATE: 12 NOVEMBER 1971

Flyby Inclination (degrees)	Lander Inclination (degrees)	Slowdown Velocity (ft/sec)	Time	Angle Above Lander Horizon (degrees)	Slant Range (km)
15	134	750	Entry	42.5	63330
			E+3 hours	58.6	22380
			E+5 hours	-4.6	15340
15	134	1000	Entry	45.6	82030
			E+3 hours	63.9	41000
			E+5 hours	66.1	15730
15	134	1250	Entry	47.5	100820
			E+3 hours	63.2	60610
			E+5 hours	51.6	34540
45	134	1000	Entry	51.6	81790
			E+3 hours	76.0	40810
			E+5 hours	70.1	15660

RE-ORDER No. 64-5222

RE-ORDER No. 64-522

TABLE 30

THREE DIMENSIONAL ENTRY ERROR ANALYSIS

Separation Latitude -15°S

Error Source	1 Sigma Uncertainty in Entry Parameters		
	Entry Angle (degrees)	Latitude (degrees)	Longitude (degrees)
1-percent variation in velocity	1.57	0.48	-2.41
1-degree error in θ	0.04	0.01	-0.08
1-degree error in a	2.47	4.10	-0.40
ΔR= 150 km along $\underline{1}_{V_{\infty 1}}$	0.02	0.01	-0.04
ΔR= 150 km along $\underline{1}_{-\Delta V}$	1.10	0.19	-1.85
ΔR= 150 km along $\underline{1}_{R \times V_\infty}$	1.06	1.80	-0.16
RSS Value[1]	3.30	4.51	3.06
ΔR= 350 km along $\underline{1}_{V_\infty}$	0.05	0.02	-0.08
ΔR= 350 km along $\underline{1}_{-\Delta V_1}$	2.64	0.46	-4.35
ΔR= 350 km along $\underline{1}_{R \times V_\infty}$	2.54	4.23	-0.42
RSS Value	4.69	5.93	5.00

different problem than the 1969 opportunity, in that Earth occultation cannot be easily avoided due to the fact that the approach asymptote is essentially along the Earth-Mars line. Therefore, regardless of which side of the planet the probe passes, the trajectory, after periapsis passage, will bend behind the planet and a period of earth occultation will occur except possibly for passing altitudes in excess of 100,000 km. It is interesting to note in this situation that the period of occultation decreases as the passing altitude is reduced. This situation arises due to the increased gravitational attraction and subsequent trajectory bending as the passing altitude is reduced thereby producing a departure asymptote that is sufficiently removed from the Earth-Mars line to eliminate occultation sooner.

A significant improvement in this problem is realized for the 1971 launch window selected for analysis. The ZAP angle associated with this window is about 115 degrees, and therefore the approach asymptote is sufficiently removed from the planet-Earth line such that occultation may not result except for extremely small passing distances. Since there is now approximately 25 degrees between the Mars-Earth line and the approach asymptote, occultation will not occur unless a passing altitude small enough to introduce a 25-degree bending of the trajectory is employed.

For minimum inclination trajectories this altitude varies between 6,000 and 11,000 kilometers depending upon the specific launch date. This dependence on launch date is introduced due to variation in ZAP angle with launch date. As the inclination is increased to 45 degrees both Case I (northerly passage) and Case II (southerly passage) trajectories were considered. The minimum passing altitude with no Earth occultation is about 4,000 kilometers occuring with a Case I trajectory as opposed to an altitude between 4,000 and 16,000 kilometers for the corresponding Case II trajectory. These data are presented in figure 50.

Therefore, the Case I trajectory which produces the best lander-flyby geometry also results in the minimum passing altitude without violation of the Earth occultation constraint.

For these Case I trajectories, even though the occultation constraint, minimum near limb of planet-probe-Earth angle less than 5 degrees, is violated below altitudes of 4,000 kilometers, a passing altitude of 1,000 kilometers would be required for the probe to pass behind the planet if it was desirous to conduct a bi-static radar experiment.

There is no Canopus occultation present with either the minimum inclination trajectories or Case II trajectories associated with larger inclinations since Canopus is in the southern hemisphere.

However, for the corresponding Case I trajectories, relatively short periods of occultation exist. For a passing altitude of 10,000 kilometers, the

RE-ORDER No 64-522

occultation period is about 1.5 hours and decreases to 1 hour for the minimum passing altitude satisfying the earth occultation constraint. These results are presented in figure 51.

12. Summary

The results of these studies indicate that the constant arrival date launch window, 2 May through 3 June with an arrival date of 12 November 1971, satisfies the mission objectives. This window results in a more favorable payload and ZAP angle than the optimum arrival date window. The payload is increased from 1450 to 1560 pounds, whereas the ZAP angle is reduced from 140 to 115 degrees. Additional improvements in these parameters could be realized by further shifts in the arrival date window; however, each shift decreases the possibility of determining the existence of life on the planet.

It is interesting to note that although the 1971 launch opportunity is the best during the 15-year cycle, it is feasible to develop a vehicle configuration satisfying both the 1969 and 1971 launch opportunities. A launch window exists in 1969 between 11 February and 15 March that has a payload capability of 1560 pounds. The arrival date for this window is likewise several weeks after the peak wave of darkening; however, the remaining trajectory parameters are clearly more favorable for the 1971 launch opportunity.

RE-ORDER No. 64-522

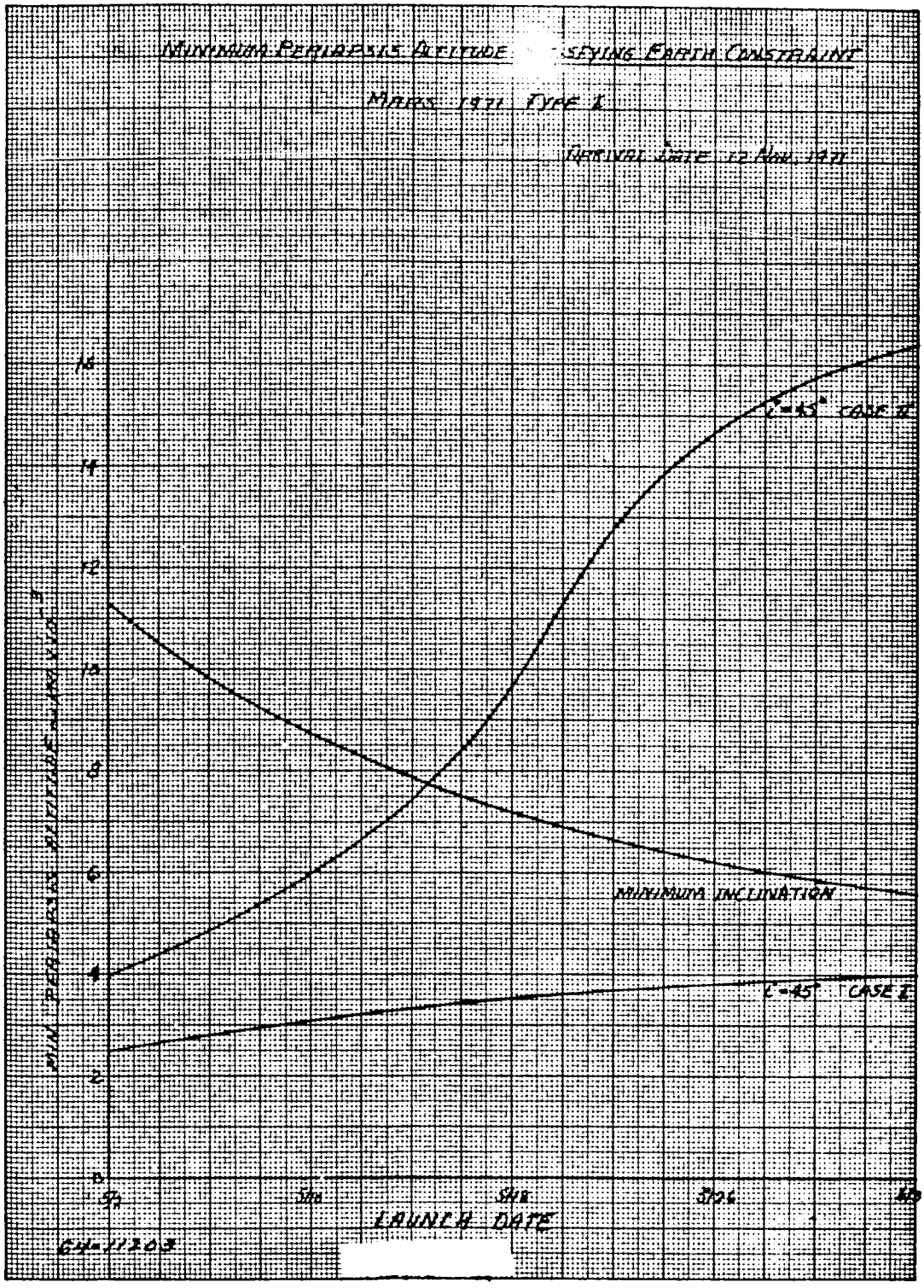

Figure 50 MINIMUM PERIAPSIS ALTITUDE SATISFYING EARTH CONSTRAINT

142

RE-ORDER No. 64-522

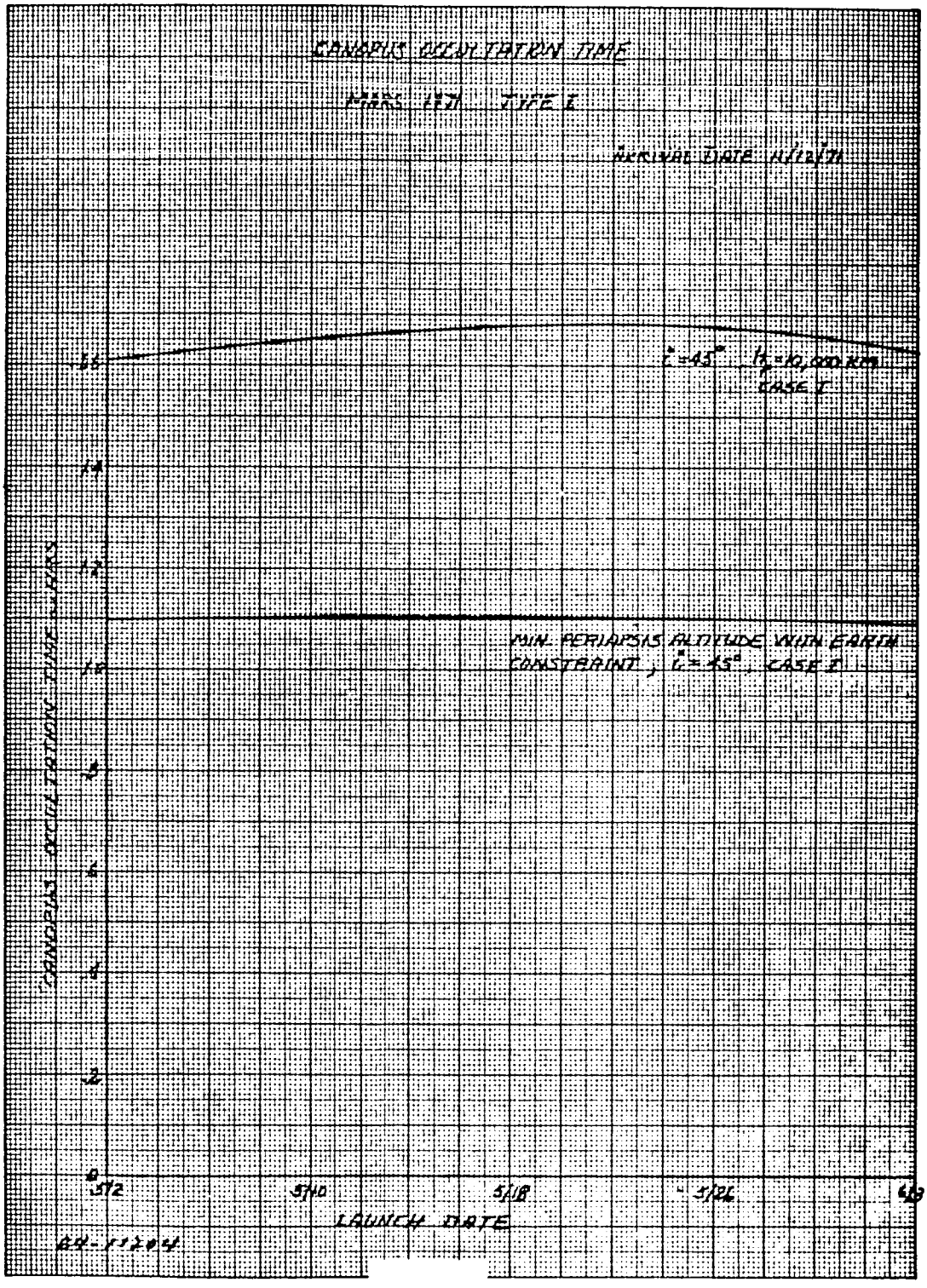

Figure 51 CANOPUS OCCULTATION TIME

RE-ORDER No. 64-522

3.2 LANDER SEPARATION ANALYSIS

Separation of the lander from the flyby bus to accomplish atmospheric entry may be done in several ways. During this maneuver, however, every effort must be made to protect the sterility of the planet mass from contamination by the unsterilized flyby bus. The probability of planet contamination can be considerably lessened if the flyby bus is maintained on a transfer trajectory which is raised away from the planet sufficiently to accomodate approximately a 4 sigma error in aiming point; the lander separation analysis assumes this biased flyby bus trajectory.

For a split, lander-flyby, mission, a number of trade-off areas require analysis before the selection of a nominal set of separation parameters, i.e., separation velocity, thrust application angle, separation range and aiming point, can be accomplished. With known system errors in these parameters, it remains to select the specific parameters in order to achieve minimum dispersion in the lander entry conditions. To perform this analysis, a digital computer program was developed at Avco and is completely described in Reference 1. This program assumes that Keplerian equations are adequate to completely describe the vehicle motion in the vicinity of the target planet. In reference 2 an analysis was performed for one specific trajectory indicating that the differences between hyperbolic and n-body influence coefficients are negligible for separation ranges up to several million kilometers and decrease as the planet is approached.

The digital computer simulation is based upon the parametric evaluation of analytically derived partial derivatives of a sequence of equations used to describe the hyperbolic orbit and the separation maneuver. For the present analysis the perturbation in the lander entry angle, γ_e (angle between lander velocity vector and the local horizontal at 800,000 feet) and the lander range angle, ϕ_e, (angle between the planetary radius vectors at lander separation and entry) were examined for disturbances in:

1. magnitude of separation velocity, δV ;
2. direction of applied velocity, $\delta \theta$; and
3. flight path angle at separation, $\delta \gamma_s$.

An assumption was made that nominal errors in the in-track vehicle position and velocity prior to separation would produce negligible error contributions in the entry and range angle when compared with the contributions form the above mentioned sources.

Since the pertinent error sources are statistically independent, the variation in the entry angle can be expressed by

$$\Delta\gamma_e = \left[\left(\frac{\partial\gamma_e}{\partial\theta}\ \delta\theta\right)^2 + \left(\frac{\partial\gamma_e}{\partial\Delta V}\ \delta\Delta V\right)^2 + \left(\frac{\partial\gamma_e}{\partial\gamma_s}\ \delta\gamma_s\right)^2\right]^{1/2},$$

and the variation in the range angle by

$$\Delta\phi_e = \left[\left(\frac{\partial\phi_e}{\partial\theta}\ \delta\theta\right)^2 + \left(\frac{\partial\gamma_e}{\partial\Delta V}\ \delta\Delta V\right)^2 + \left(\frac{\partial\phi_e}{\partial\gamma_s}\ \delta\gamma_s\right)^2\right]^{1/2}.$$

A secondary output of this analysis is the separation velocity - thrust application angle combinations to realize a specific entry angle for a given separation range, approach velocity and periapsis altitude. For example, figures 52 to 66 present the variation in the entry angle caused by perturbations in the thrust application angle, $\partial\gamma_e/\partial\theta$, as a function of entry angle for various values of approach velocity and periapsis altitude. Contours of constant thrust application angles and separation velocities provide a means for determining various velocity-angle combinations to achieve a specific entry condition. Separation range is introduced as a parameter for constant application angles and is seen to be a negligible factor in influencing the magnitude of the influence coefficient although the effect becomes more pronounced as the passing altitude is increased. The constant separation velocity contours apply for only a separation range of 1,000,000 kilometers and the velocity for any other range, R, is

$$\Delta V_R = \Delta V_{R=10^6}\left(\frac{10^6}{R}\right).$$

The results of this analysis dramatically indicate the advisability of applying the separation velocity normal to the hyperbolic approach velocity. The influence coefficient is essentially zero for this application as opposed to approximately 5 deg/deg for a thrust application angle of 20 degrees. The results also indicate that:

1. The separation velocity increases by a factor of between 3.5 and 5, depending upon the entry angle, as the periapsis altitude is increased from 5,000 to 30,000 km; and

2. the separation velocity increases by approximately 50 percent as the approach velocity is increased from 4 to 6 km/sec.

For a specific separation velocity and entry angle the variation in the entry angle introduced by disturbances in the separation velocity, $\partial\gamma_e/\partial\Delta V$, is presented in figures 67 to 81 for various approach velocities and periapsis altitudes. The separation velocities presented in these figures depict the actual separation range-velocity conditions as opposed to the previous set of figures where the separation velocity was for a specific separation range of 1,000,000 kilometers.

RE-ORDER No. 64-522

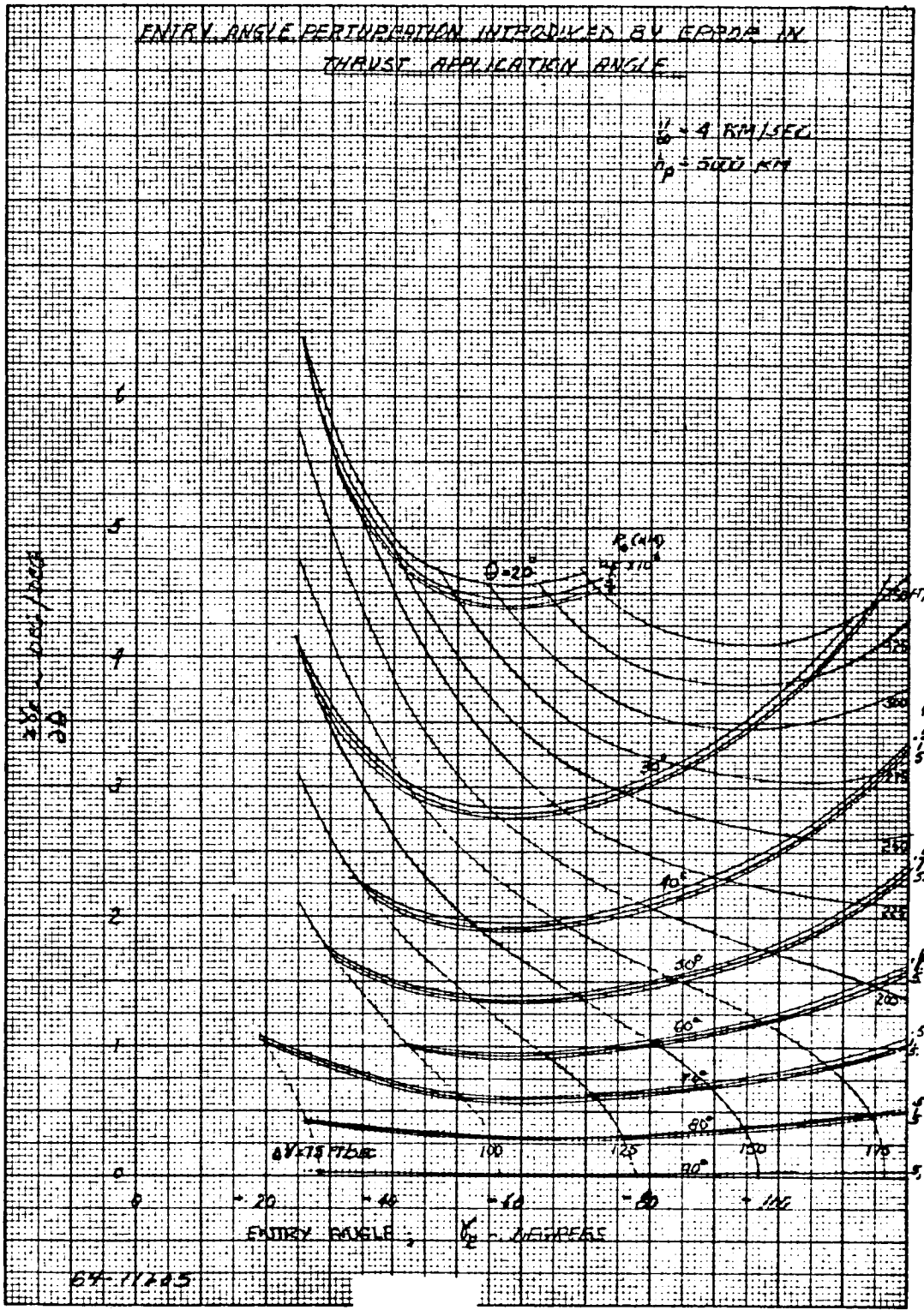

Figure 52 ENTRY ANGLE PERTURBATION INTRODUCED BY ERROR IN THRUST APPLICATION ANGLE

RE-ORDER No. 64-522

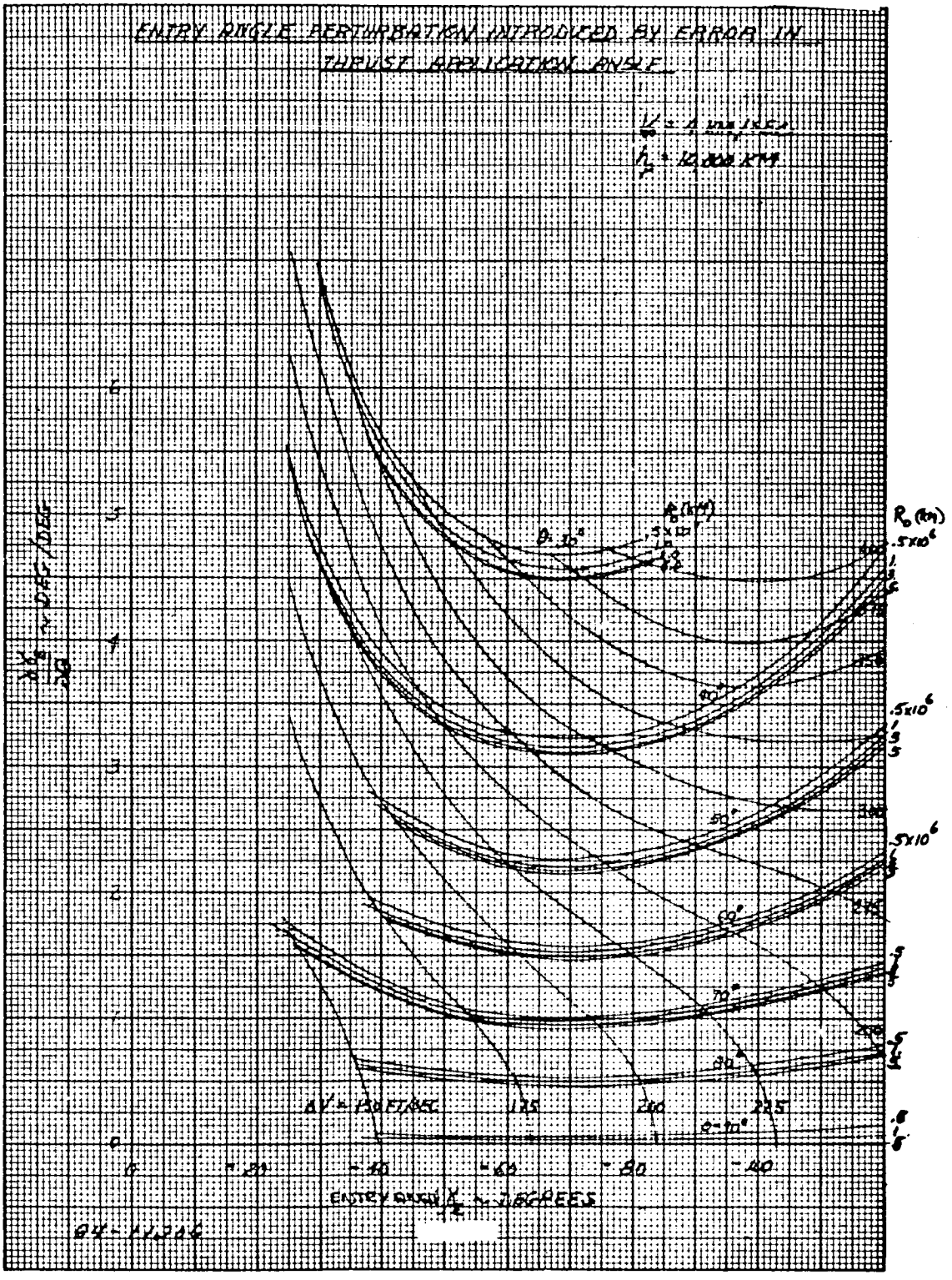

Figure 53 ENTRY ANGLE PERTURBATION INTRODUCED BY ERROR IN THRUST APPLICATION ANGLE

RE-ORDER No. 64-522

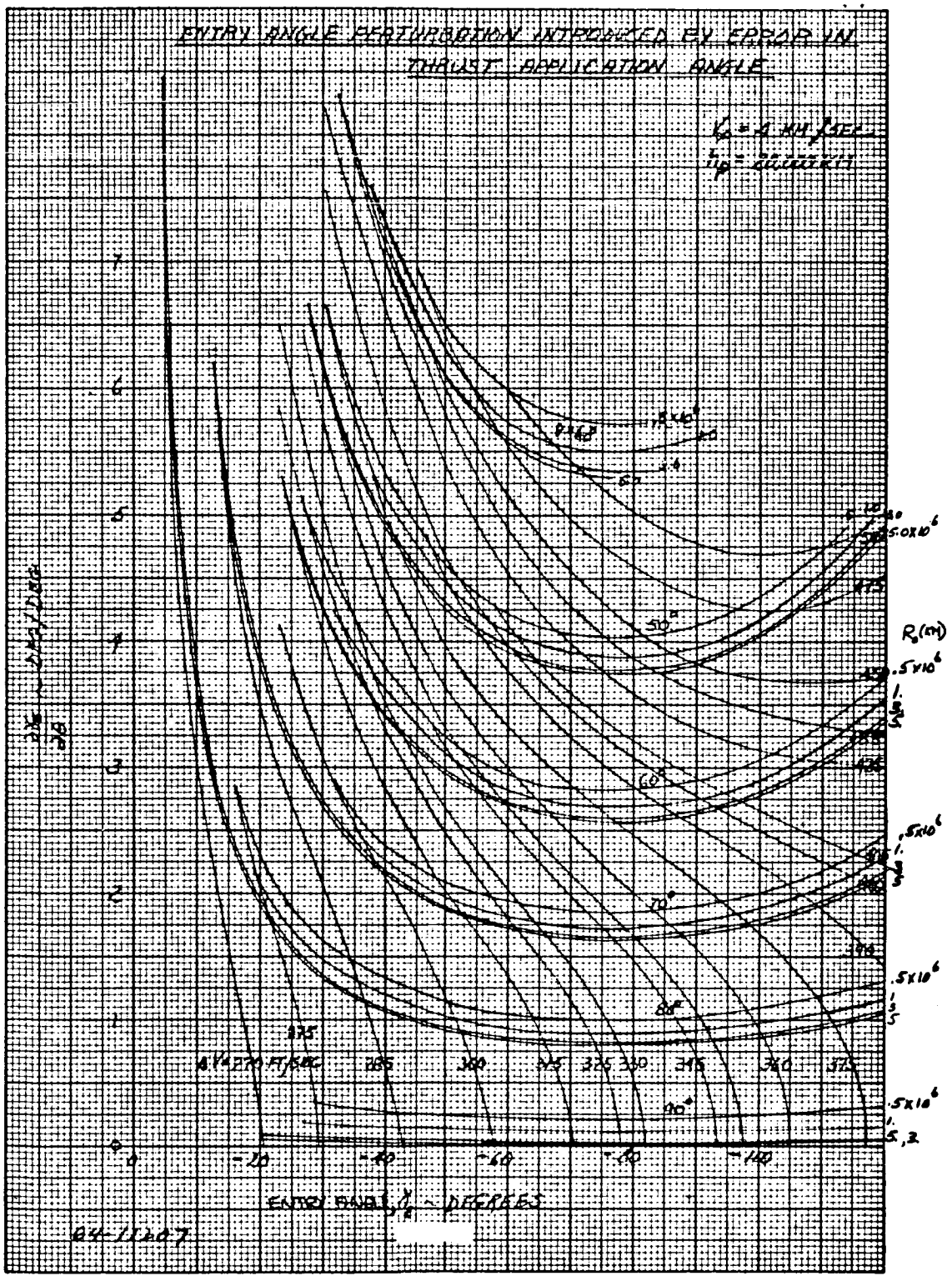

Figure 54 ENTRY ANGLE PERTURBATION INTRODUCED BY ERROR IN THRUST APPLICATION ANGLE

RE-ORDER No. 64-522

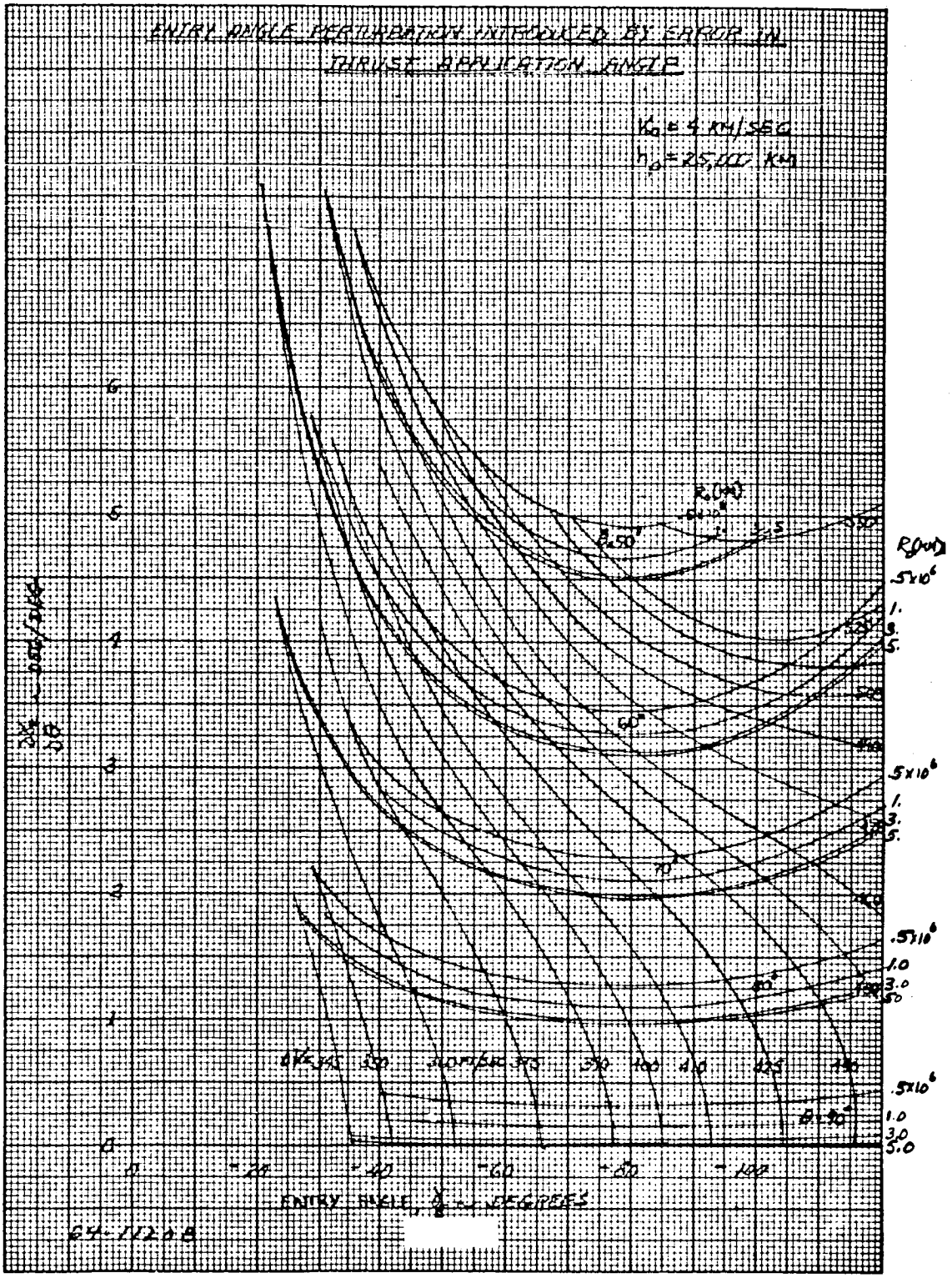

Figure 55 ENTRY ANGLE PERTURBATION INTRODUCED BY ERROR IN THRUST APPLICATION ANGLE

RE-ORDER No. 64-522

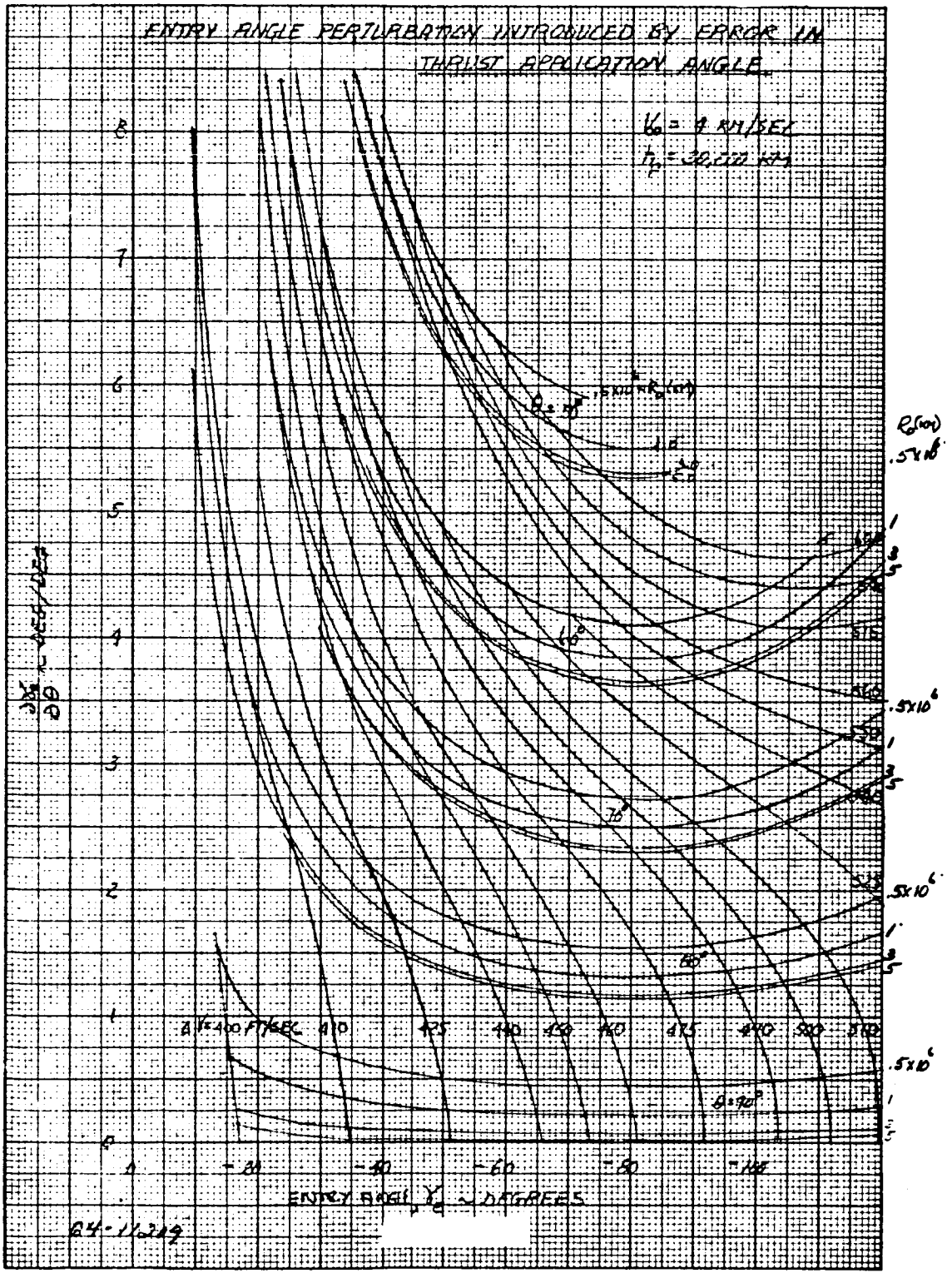

Figure 56 ENTRY ANGLE PERTURBATION INTRODUCED BY ERROR IN THRUST APPLICATION ANGLE

RE-ORDER No. 64-522

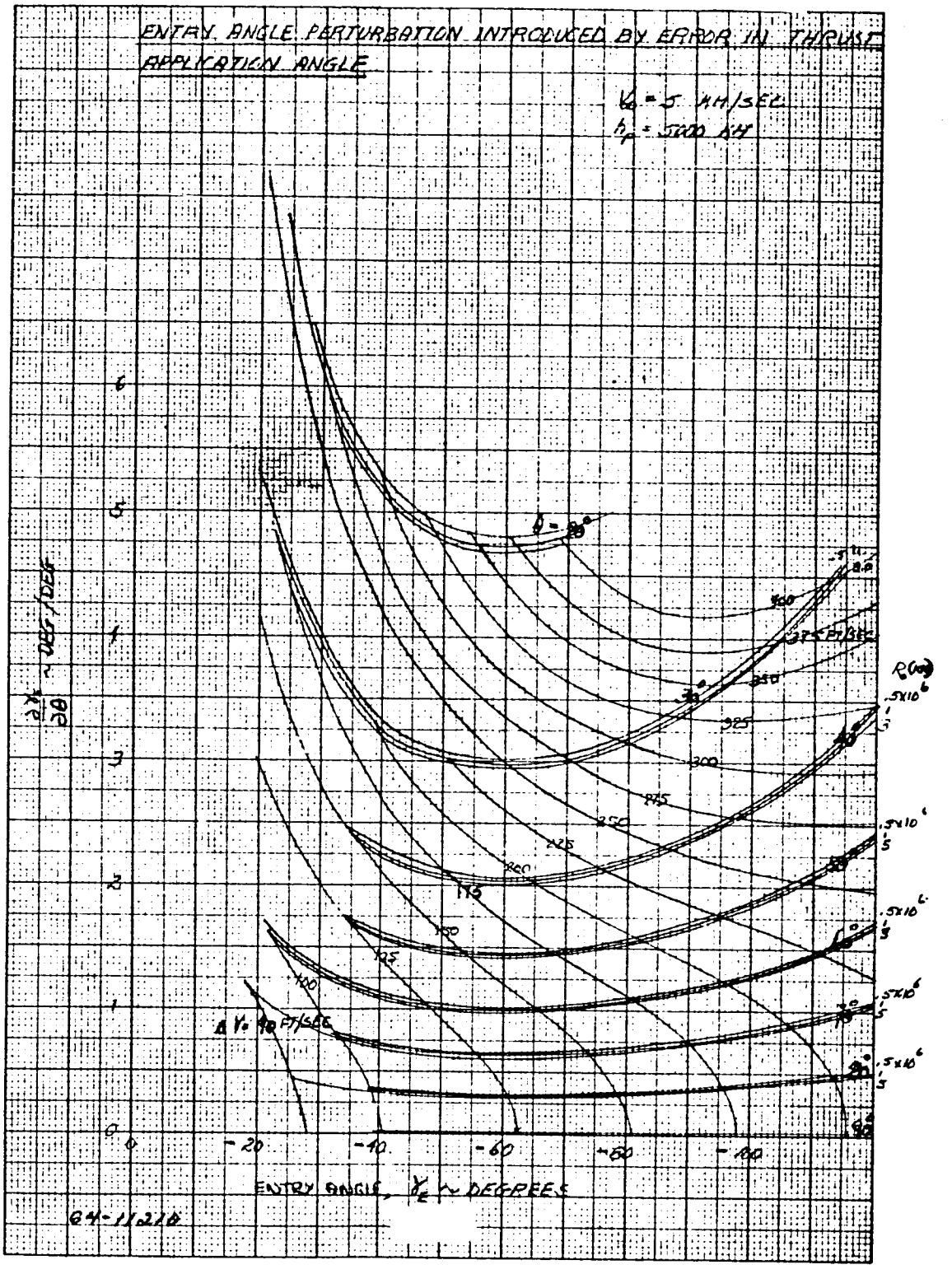

Figure 57 ENTRY ANGLE PERTURBATION INTRODUCED BY ERROR IN THRUST APPLICATION ANGLE

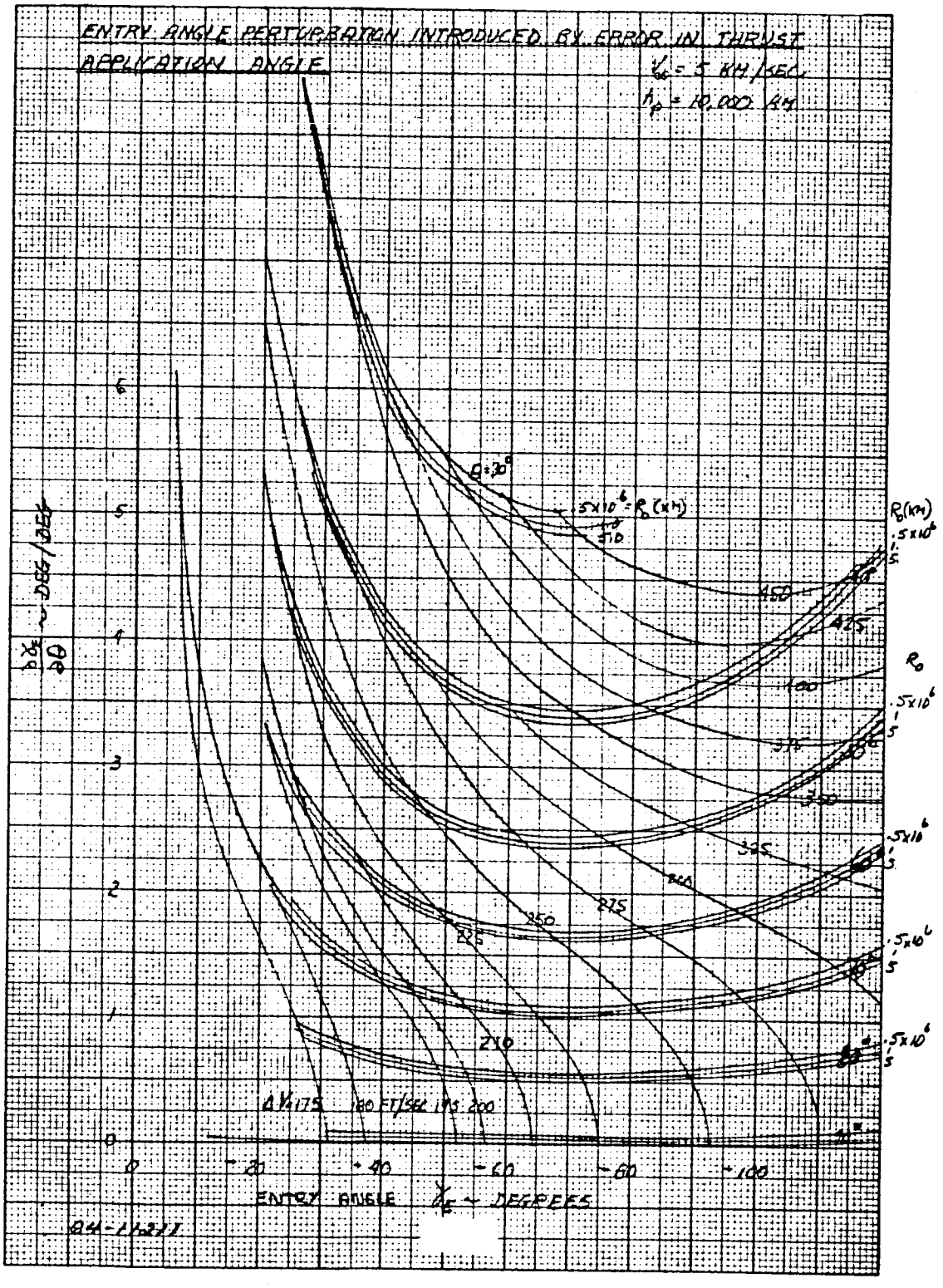

Figure 58 ENTRY ANGLE PERTURBATION INTRODUCED BY ERROR IN THRUST APPLICATION ANGLE

RE-ORDER No. 64-522

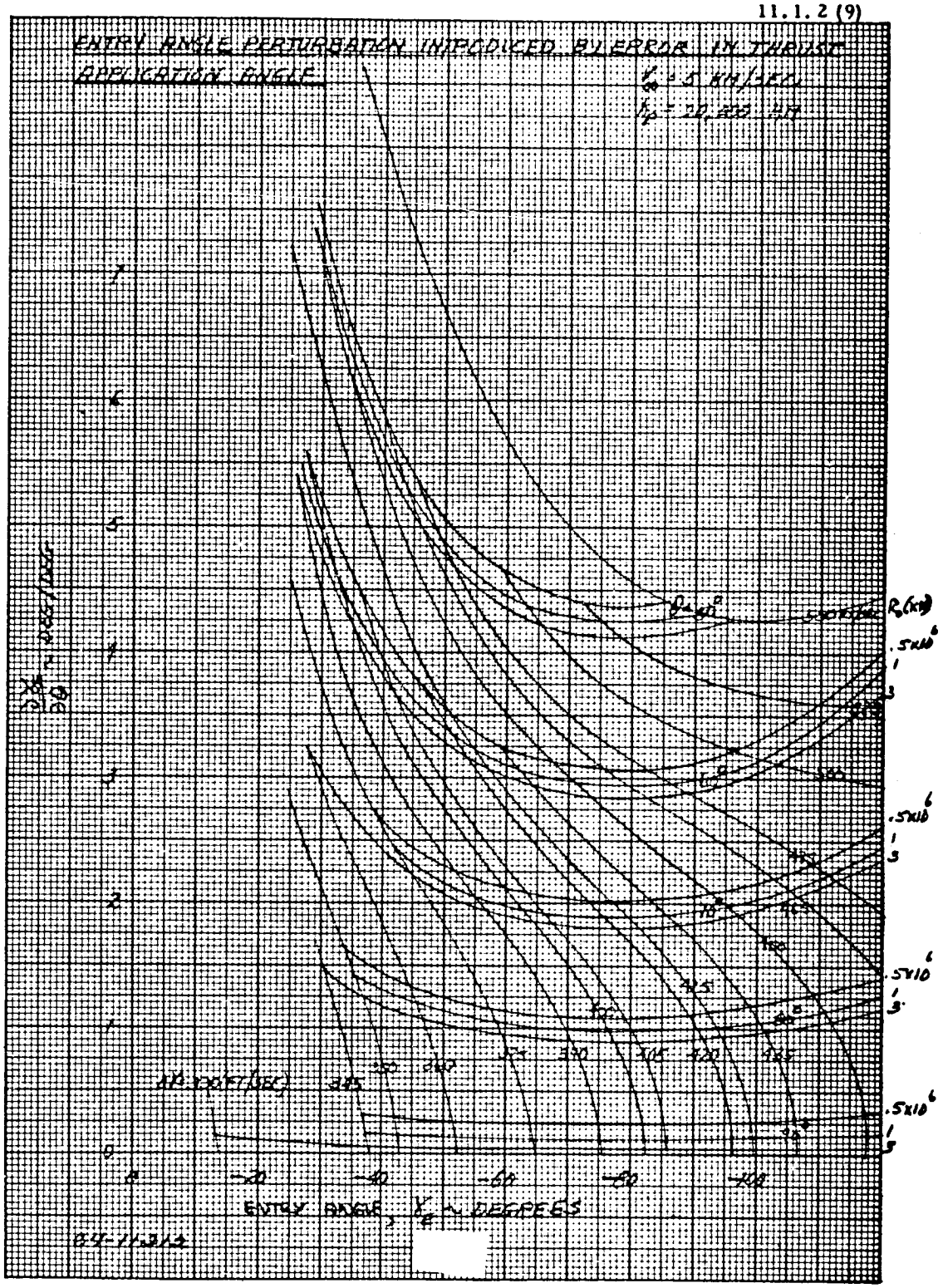

Figure 59 ENTRY ANGLE PERTURBATION INTRODUCED BY ERROR IN THRUST APPLICATION ANGLE

RE-ORDER No. 64-522

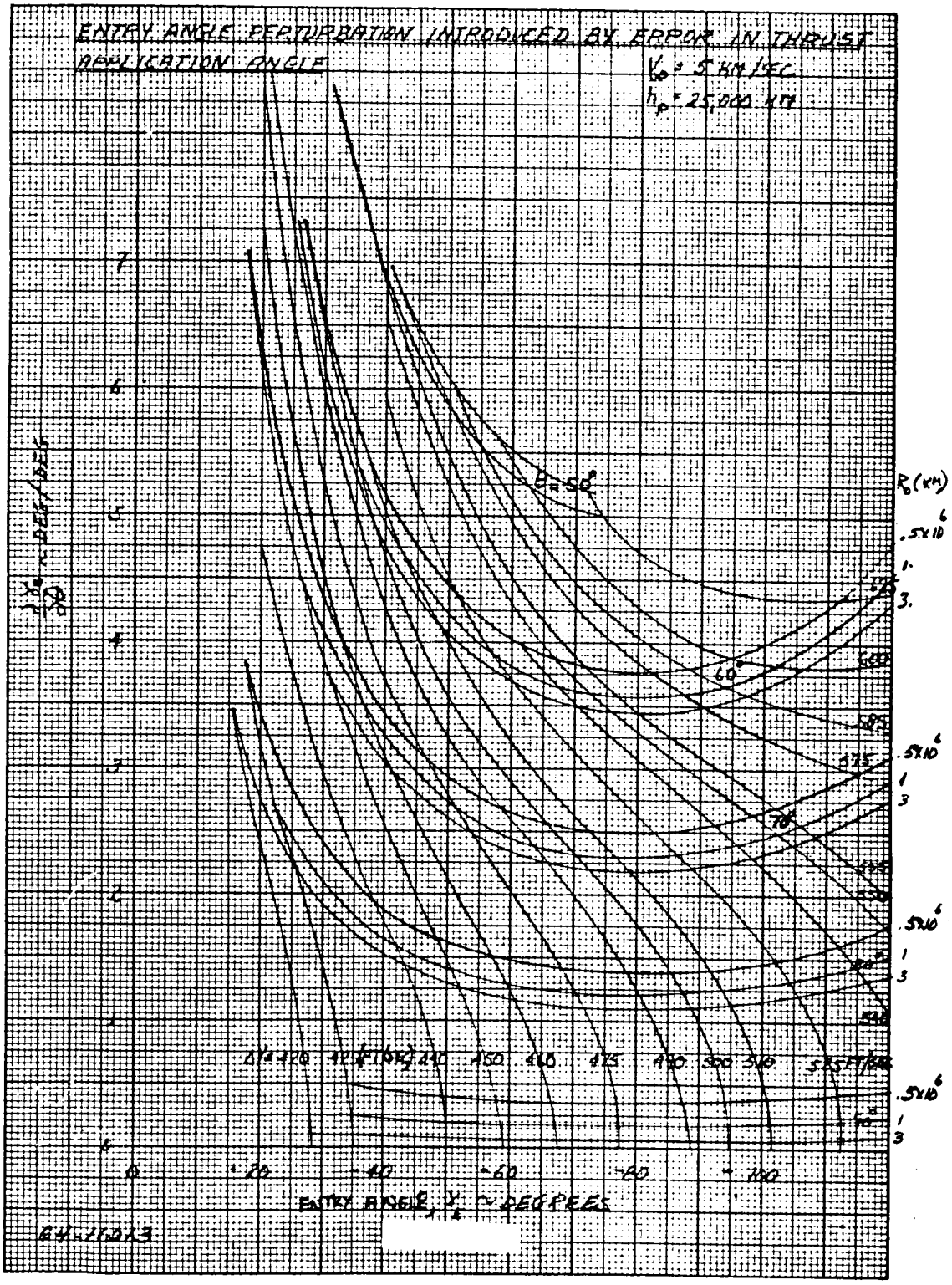

Figure 60 ENTRY ANGLE PERTURBATION INTRODUCED BY ERROR IN THRUST APPLICATION ANGLE

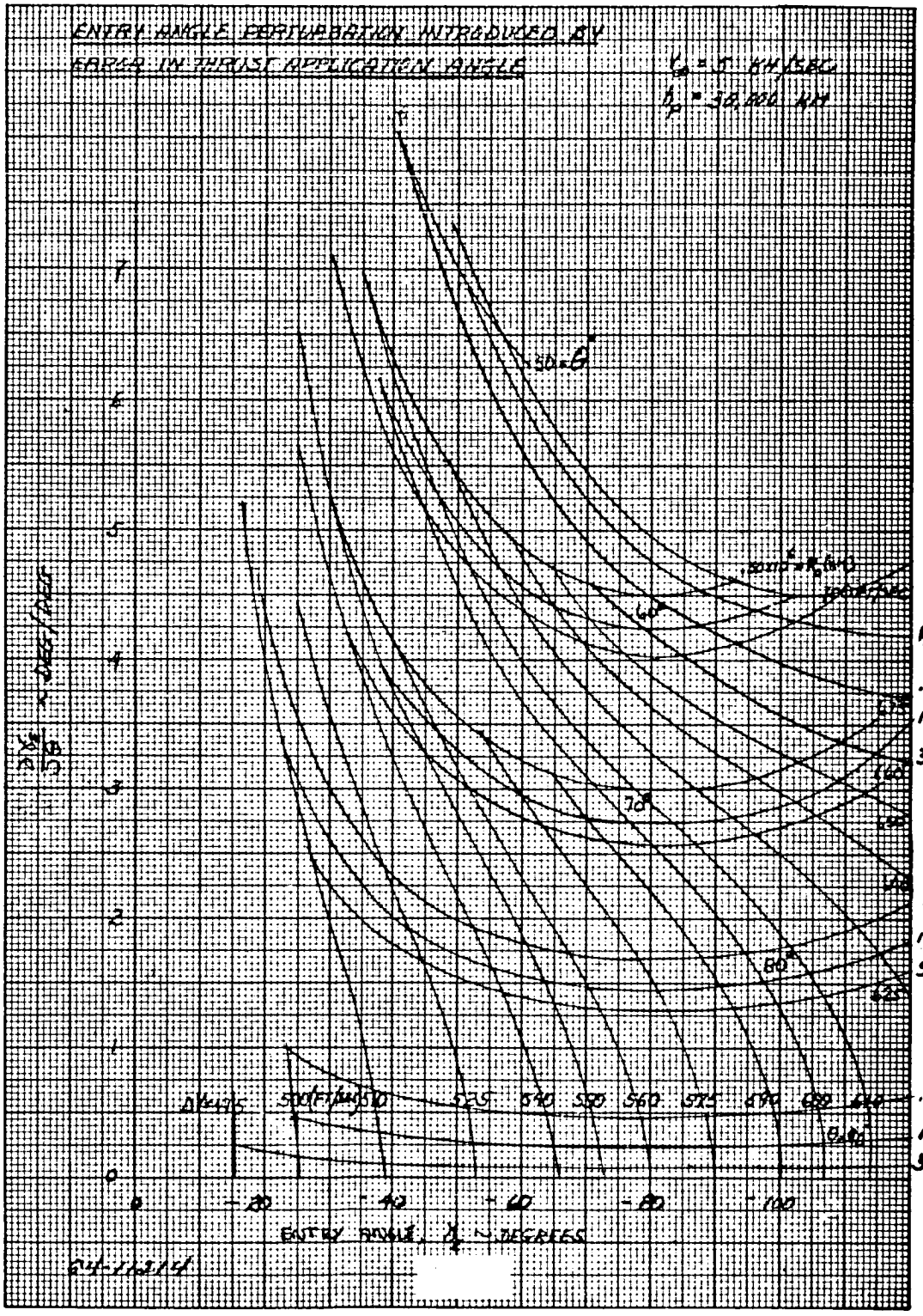

Figure 61 ENTRY ANGLE PERTURBATION INTRODUCED BY ERROR IN THRUST APPLICATION ANGLE

RE-ORDER No. 64-522

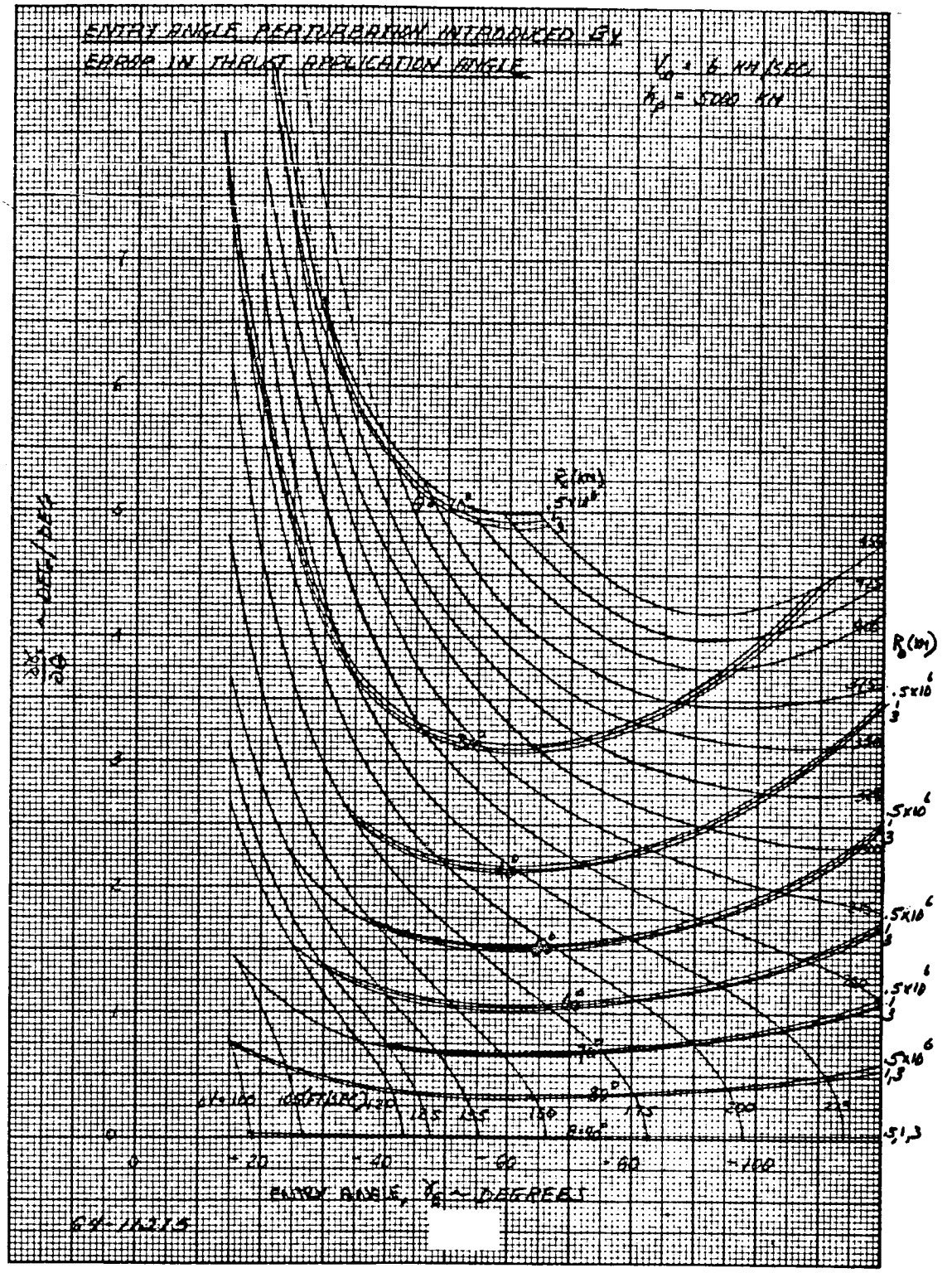

Figure 62 ENTRY ANGLE PERTURBATION INTRODUCED BY ERROR IN THRUST APPLICATION ANGLE

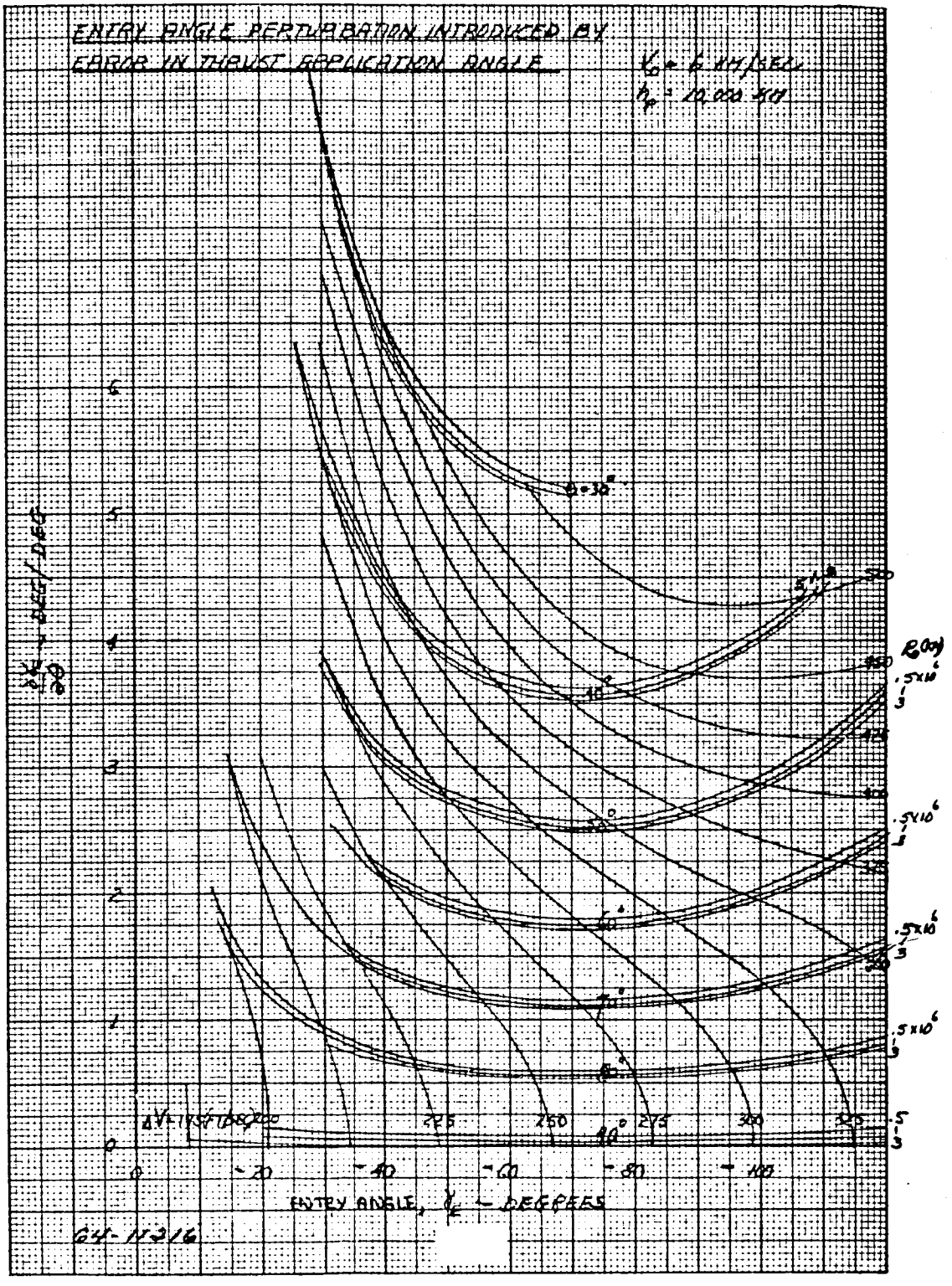

Figure 63 ENTRY ANGLE PERTURBATION INTRODUCED BY ERROR IN THRUST APPLICATION ANGLE

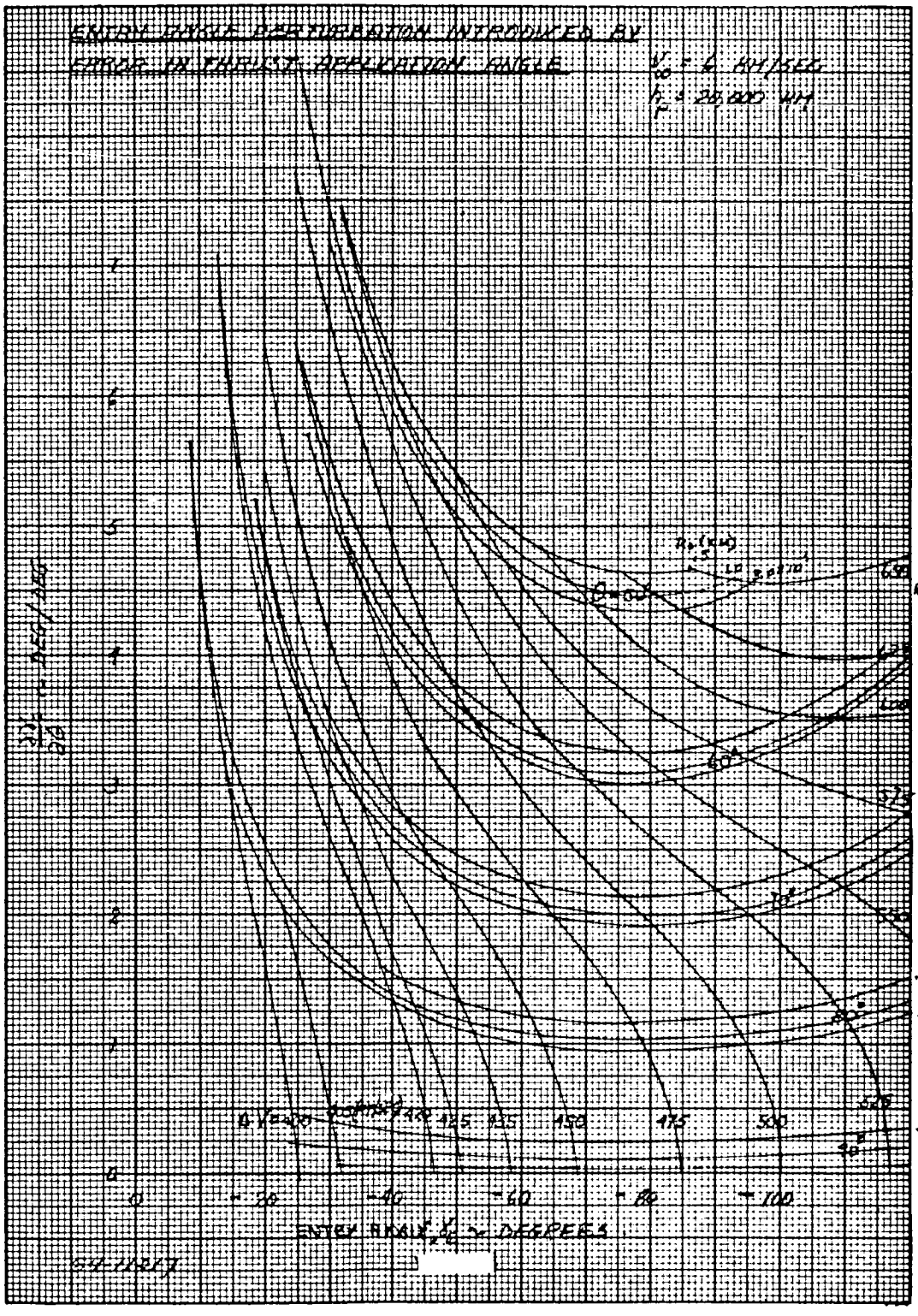

Figure 64 ENTRY ANGLE PERTURBATION INTRODUCED BY ERROR IN THRUST APPLICATION ANGLE

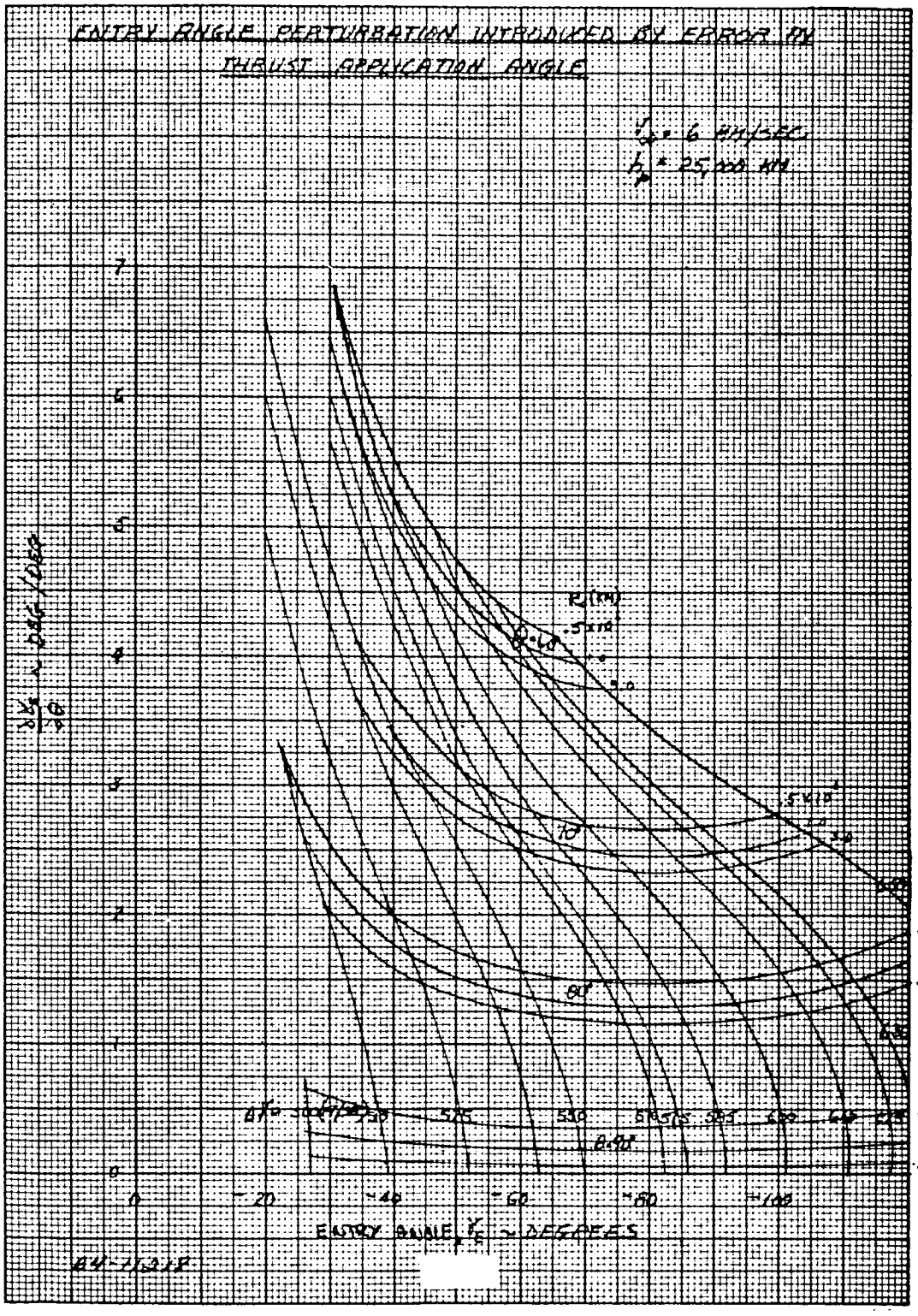

Figure 65 ENTRY ANGLE PERTURBATION INTRODUCED BY ERROR IN THRUST APPLICATION ANGLE

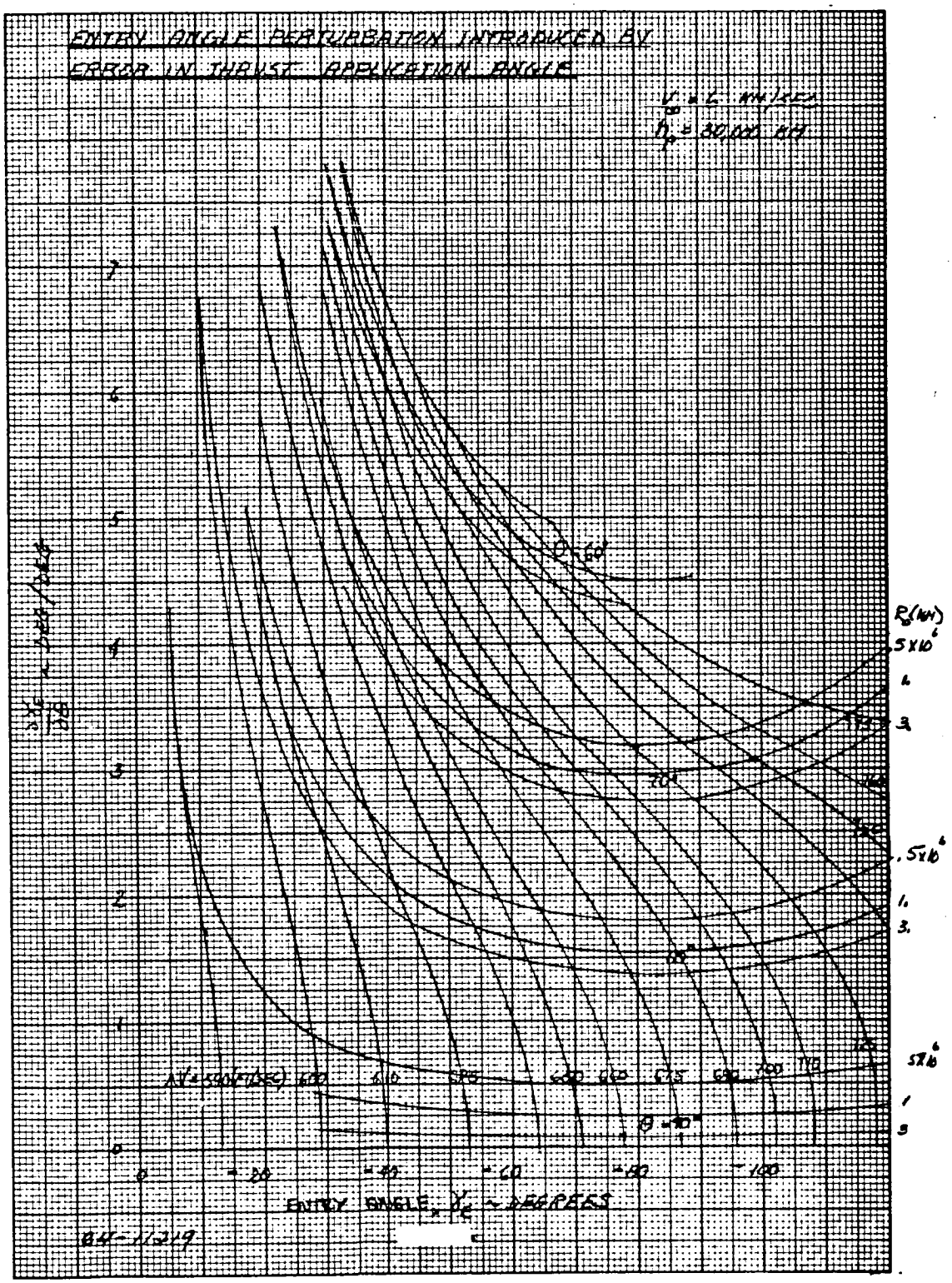

Figure 66 ENTRY ANGLE PERTURBATION INTRODUCED BY ERROR IN THRUST APPLICATION ANGLE

RE-ORDER No. 64-522

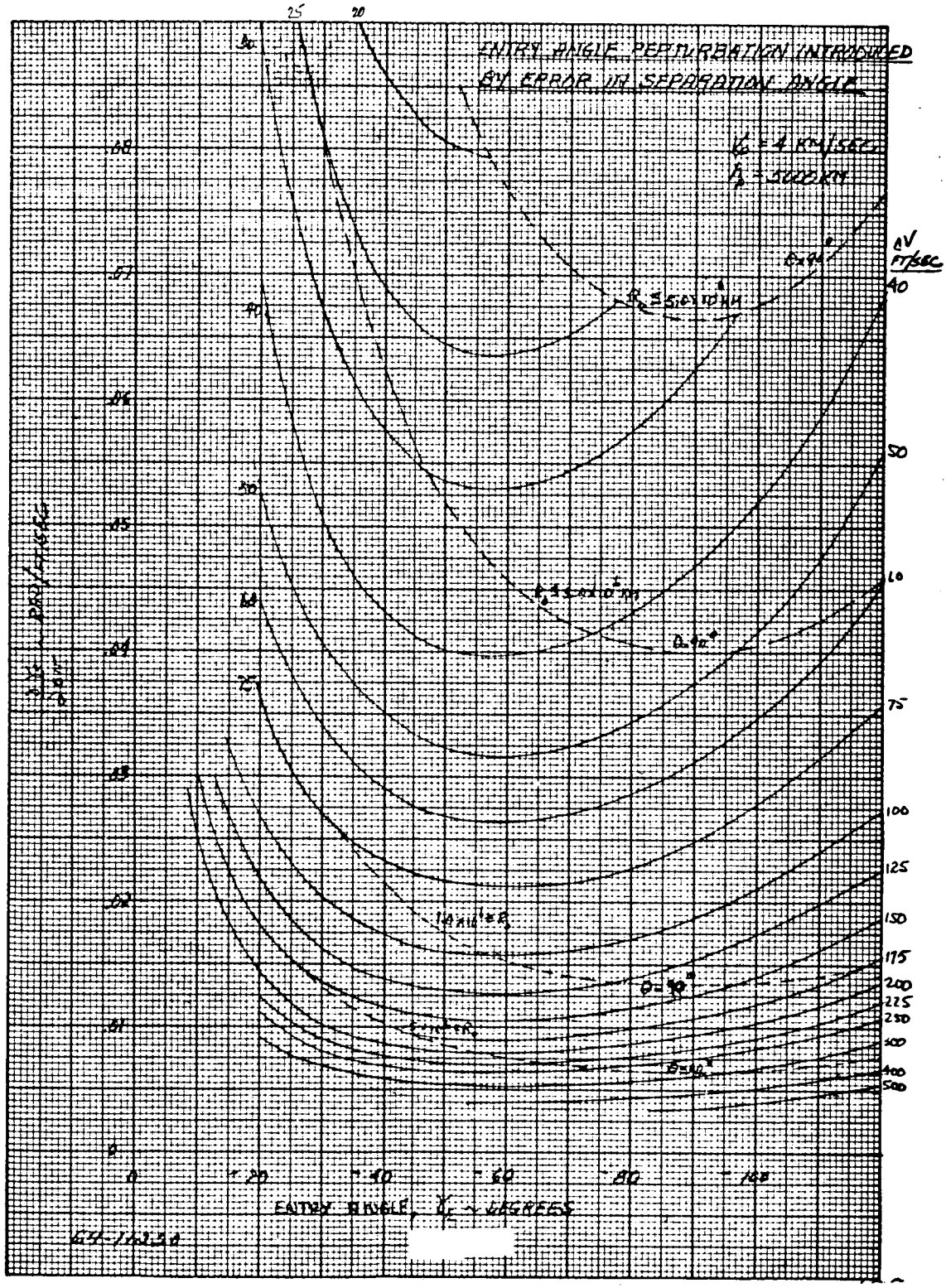

Figure 67 ENTRY ANGLE PERTURBATION INTRODUCED BY ERROR IN SEPARATION ANGLE

RE-ORDER No. 64-522

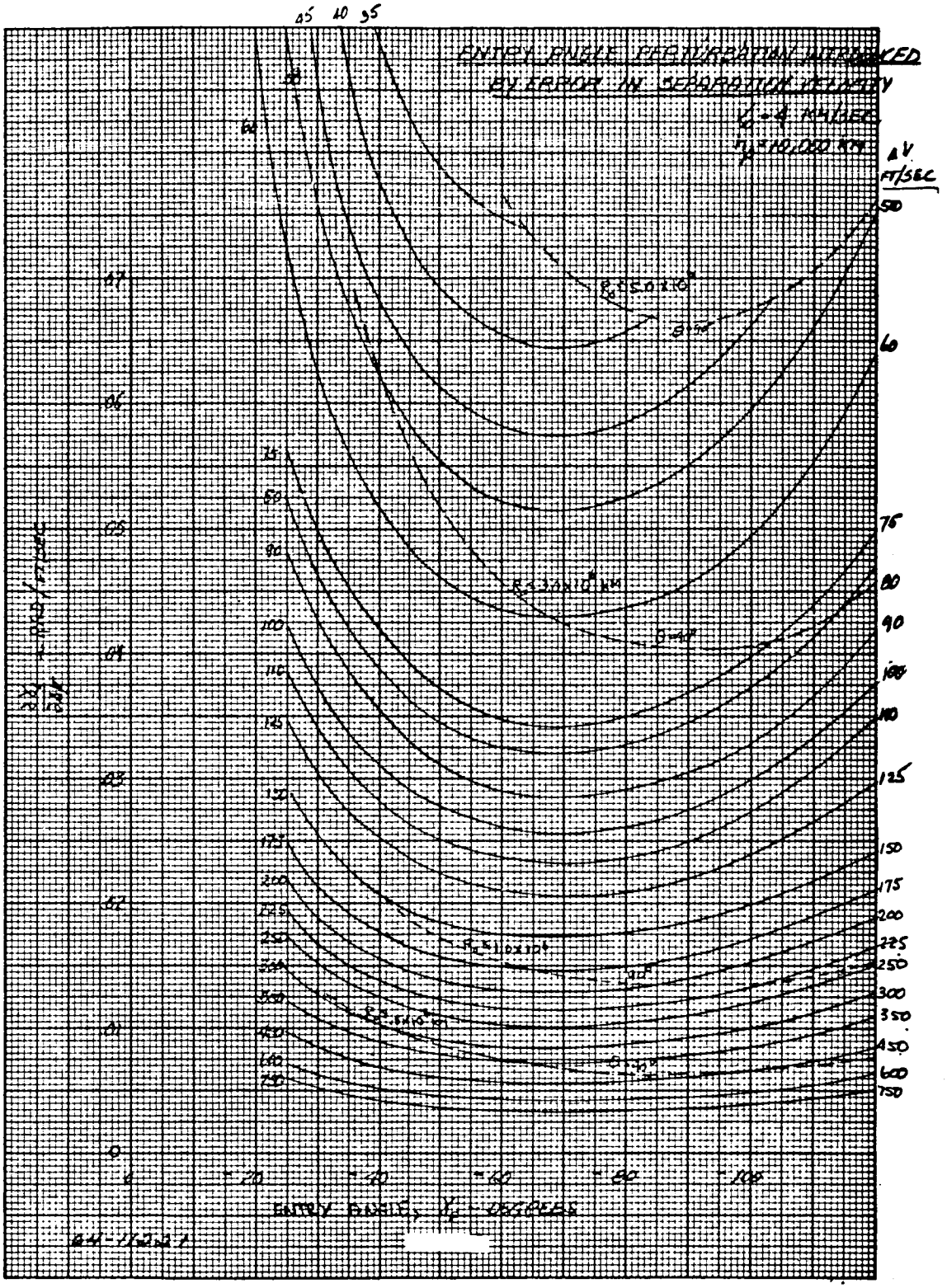

Figure 68 ENTRY ANGLE PERTURBATION INTRODUCED BY ERROR IN SEPARATION VELOCITY

RE-ORDER No. 64-522

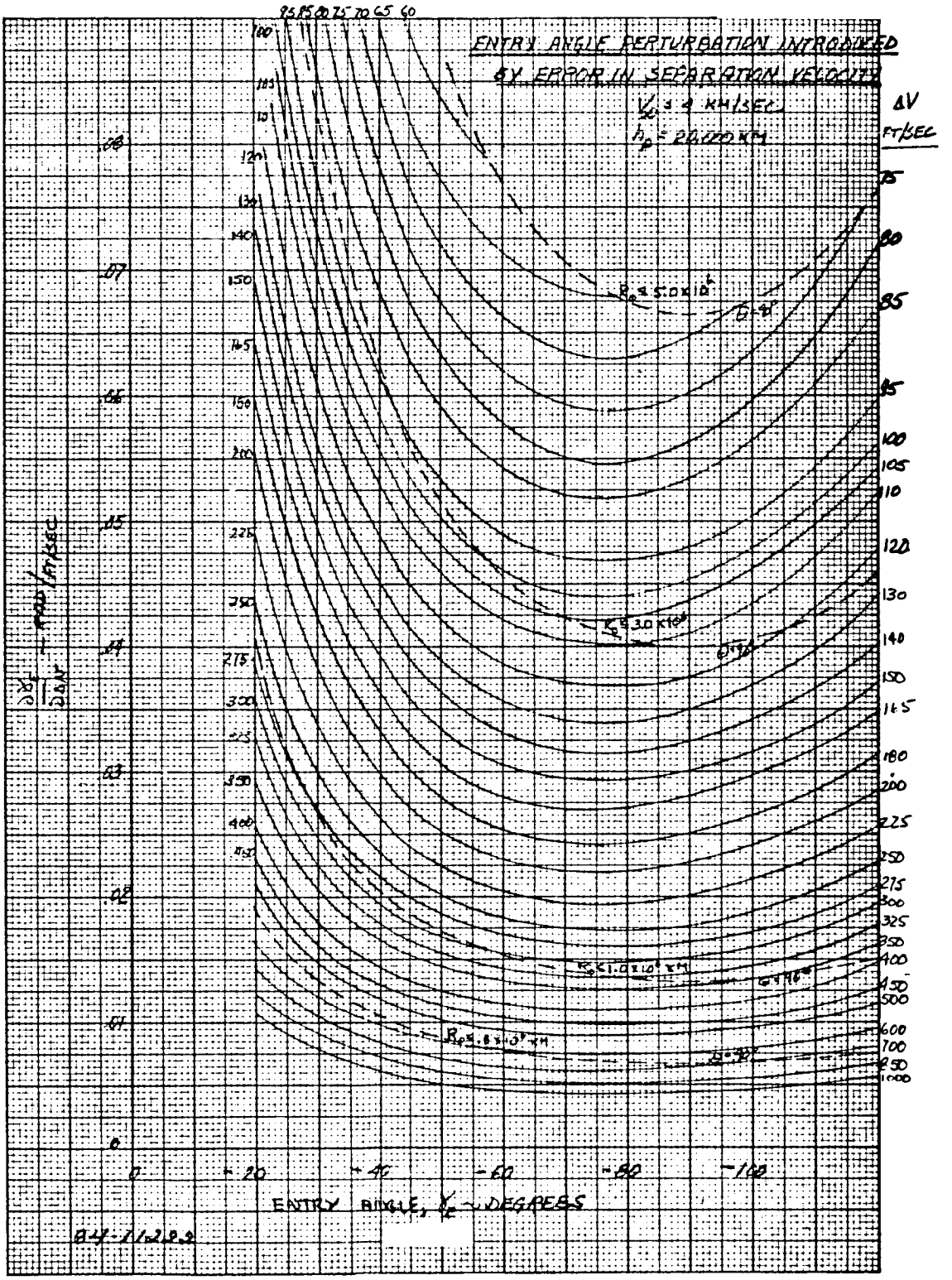

Figure 69 ENTRY ANGLE PERTURBATION INTRODUCED BY ERROR IN SEPARATION VELOCITY

RE-ORDER No. 64-522

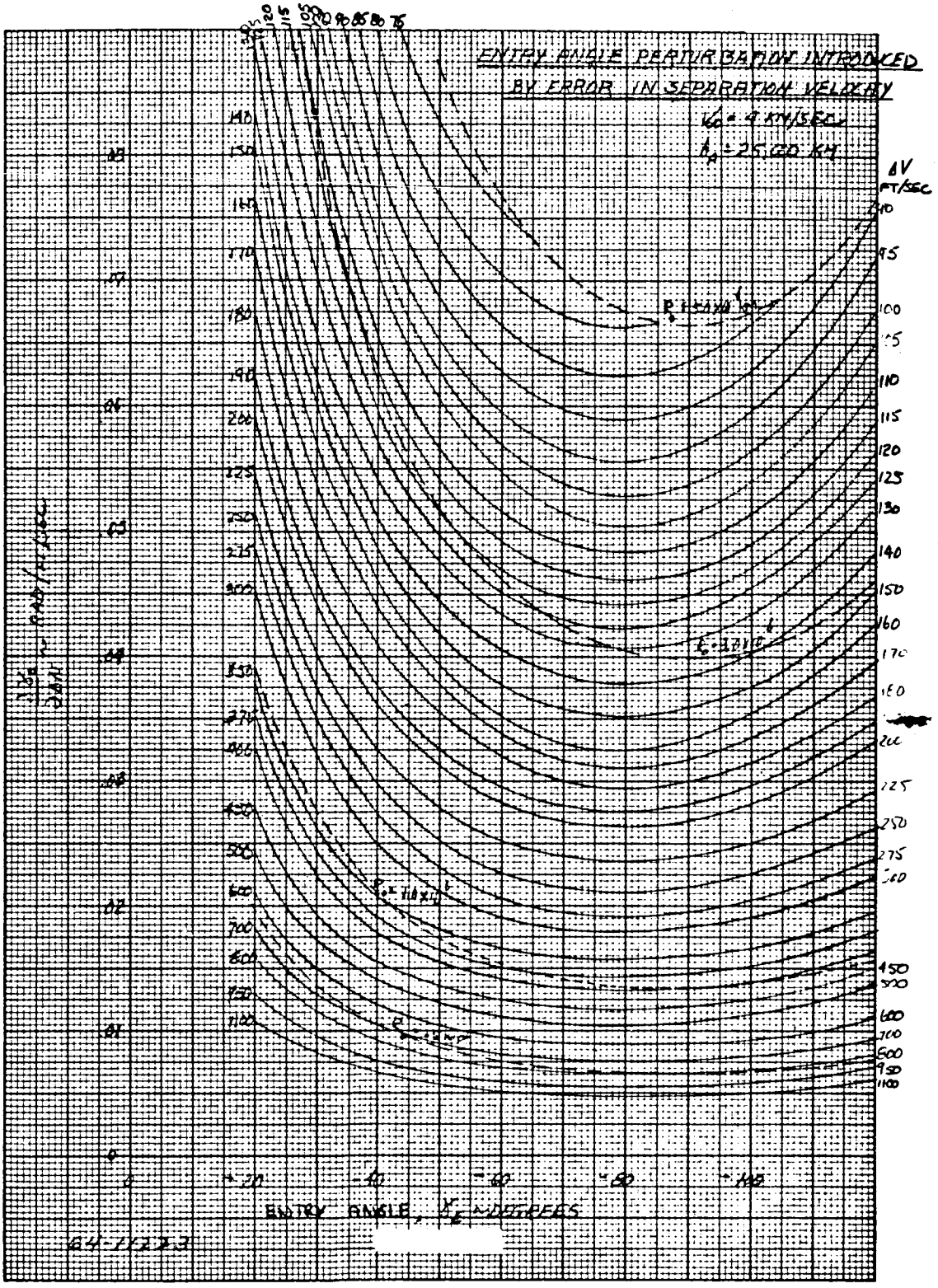

Figure 70 ENTRY ANGLE PERTURBATION INTRODUCED BY ERROR IN SEPARATION VELOCITY

RE-ORDER No. 64-522

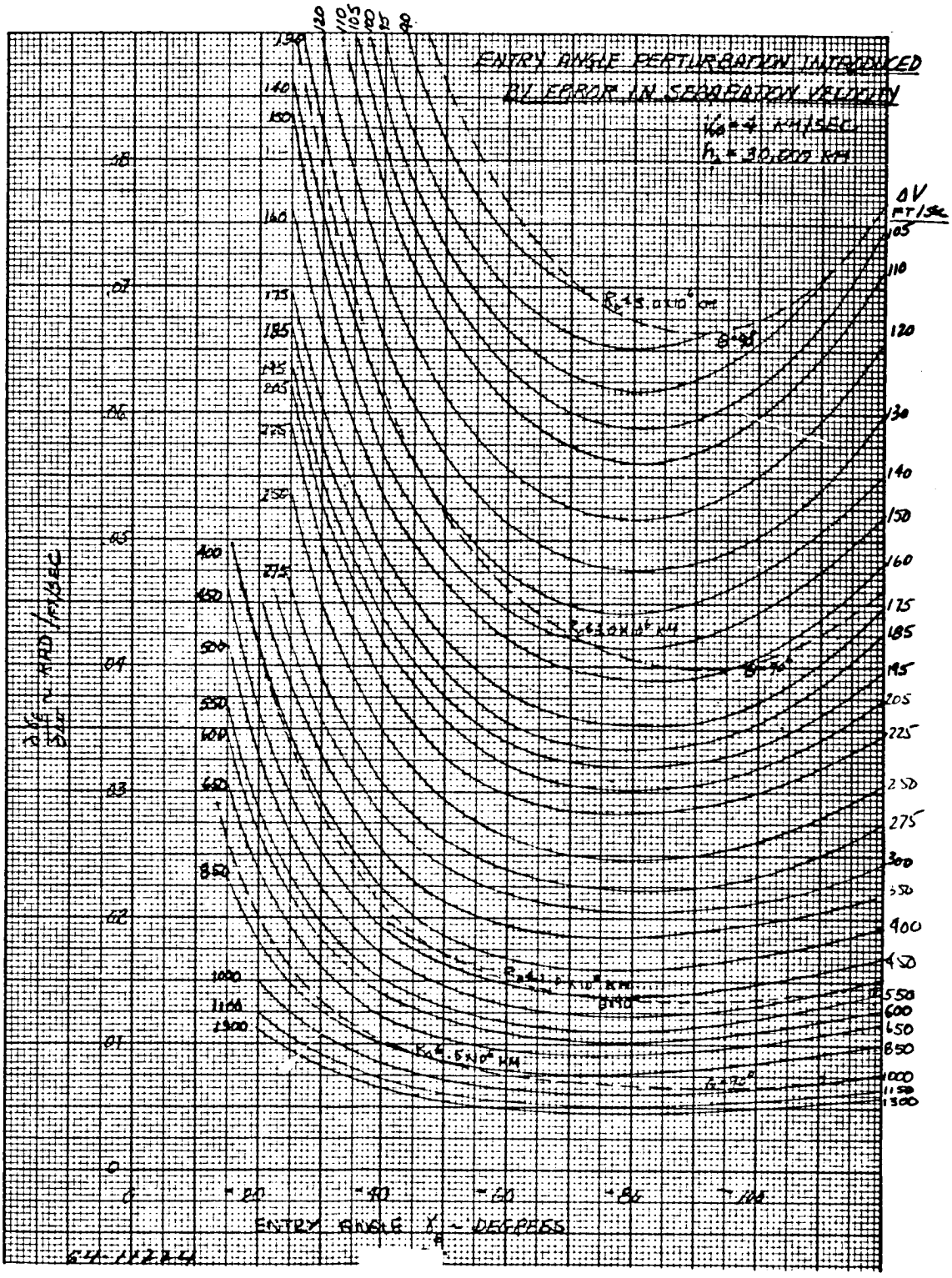

Figure 71 ENTRY ANGLE PERTURBATION INTRODUCED BY ERROR IN SEPARATION VELOCITY

RE-ORDER No. 64-522

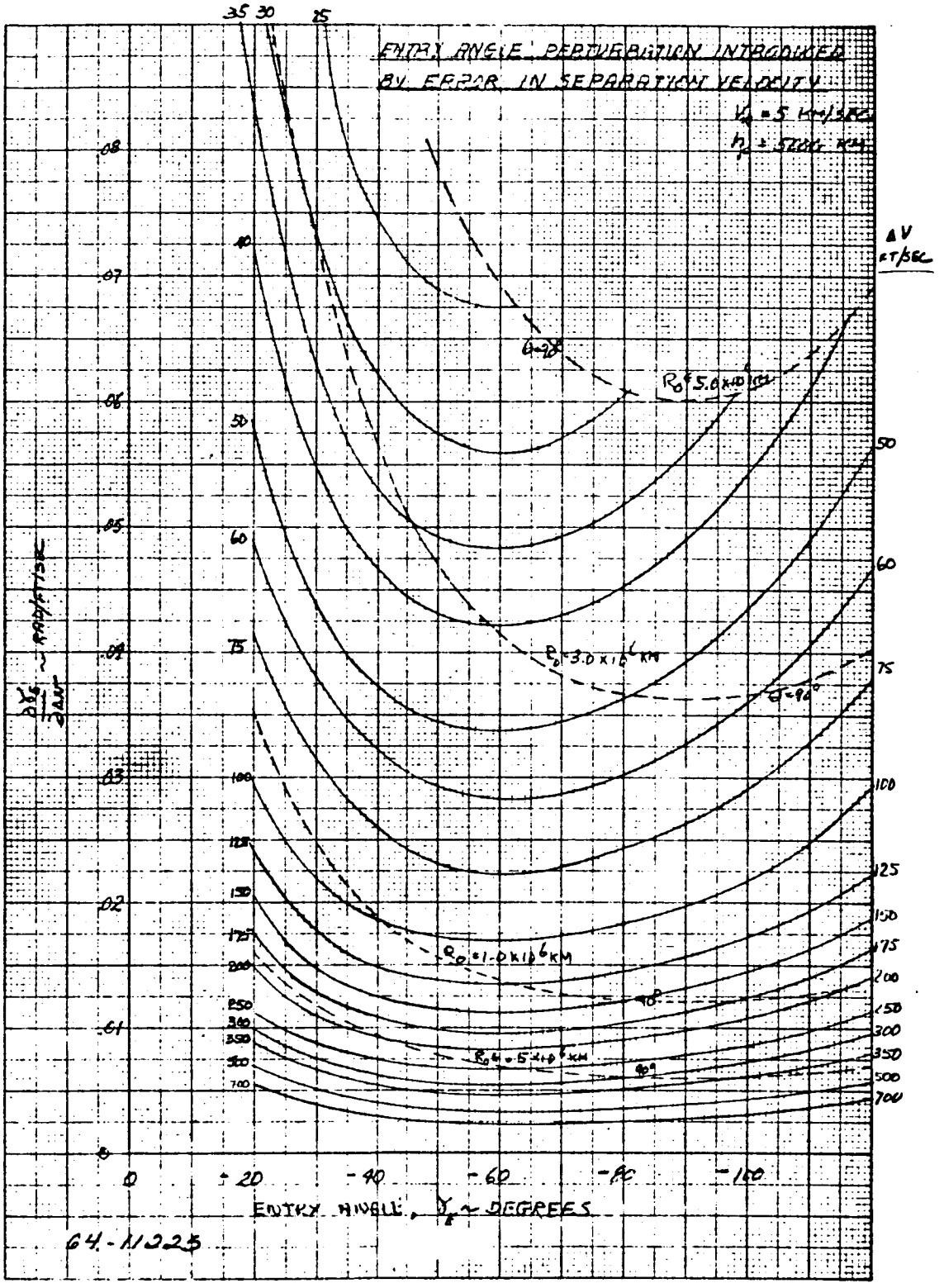

Figure 72 ENTRY ANGLE PERTURBATION INTRODUCED BY ERROR IN SEPARATION VELOCITY

RE-ORDER No. 64-522

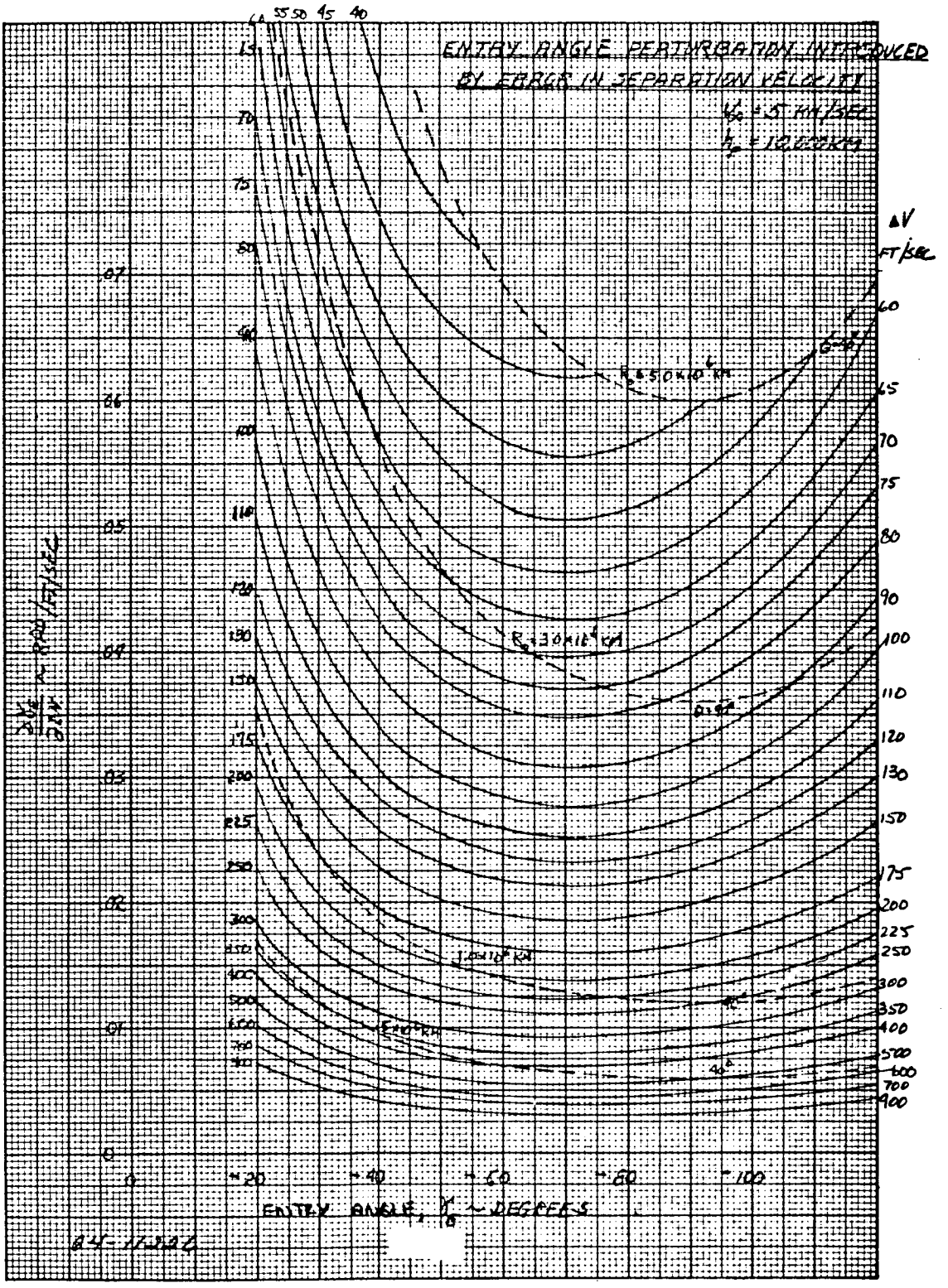

Figure 73 ENTRY ANGLE PERTURBATION INTRODUCED BY ERROR IN SEPARATION VELOCITY

RE-ORDER No. 64-522

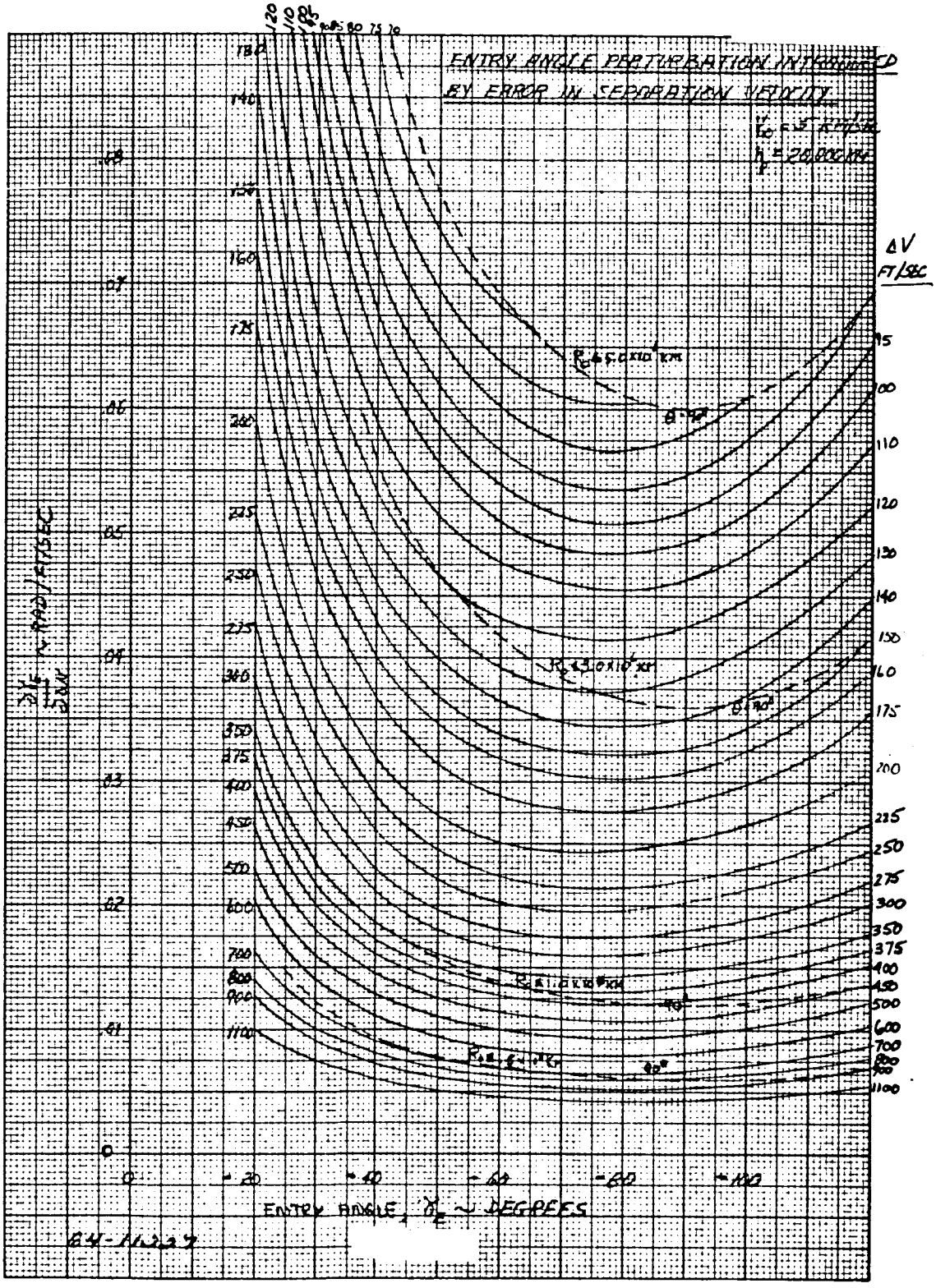

Figure 74 ENTRY ANGLE PERTURBATION INTRODUCED BY ERROR IN SEPARATION VELOCITY

17

RE-ORDER No. 64-522

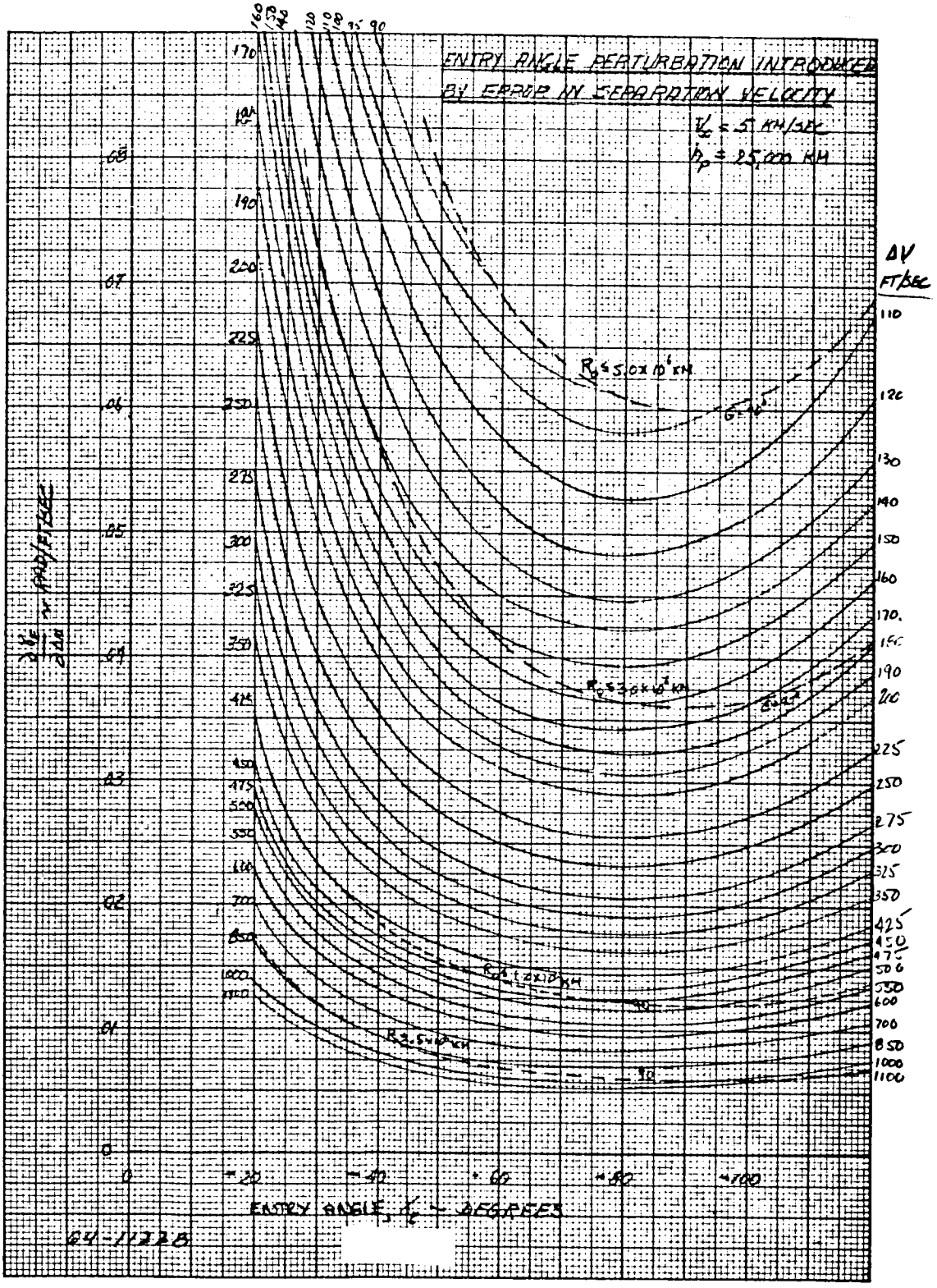

Figure 75 ENTRY ANGLE PERTURBATION INTRODUCED BY ERROR IN SEPARATION VELOCITY

RE-ORDER No. 64-522

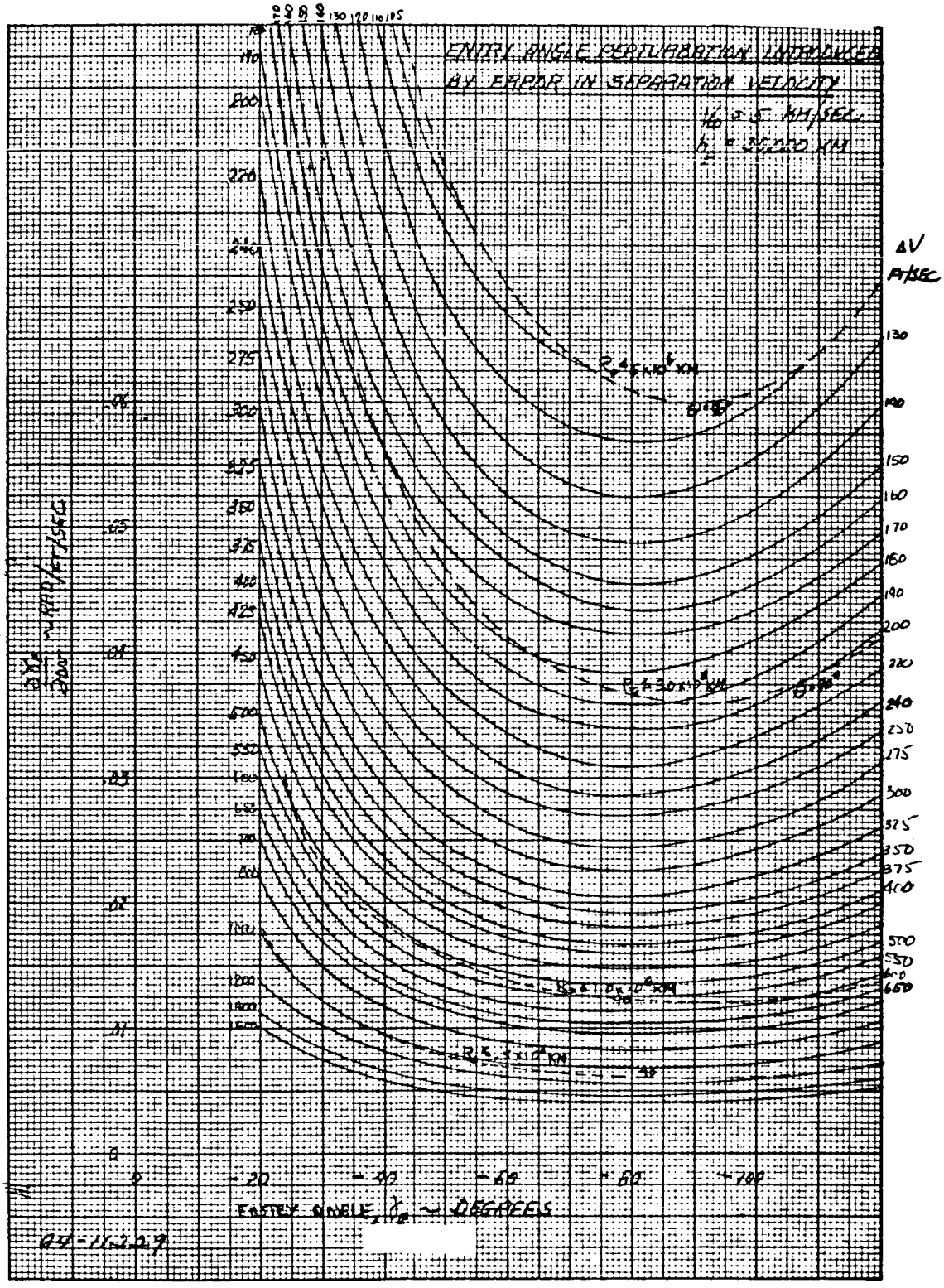

Figure 76 ENTRY ANGLE PERTURBATION INTRODUCED BY ERROR IN SEPARATION VELOCITY

RE-ORDER No. 64-522

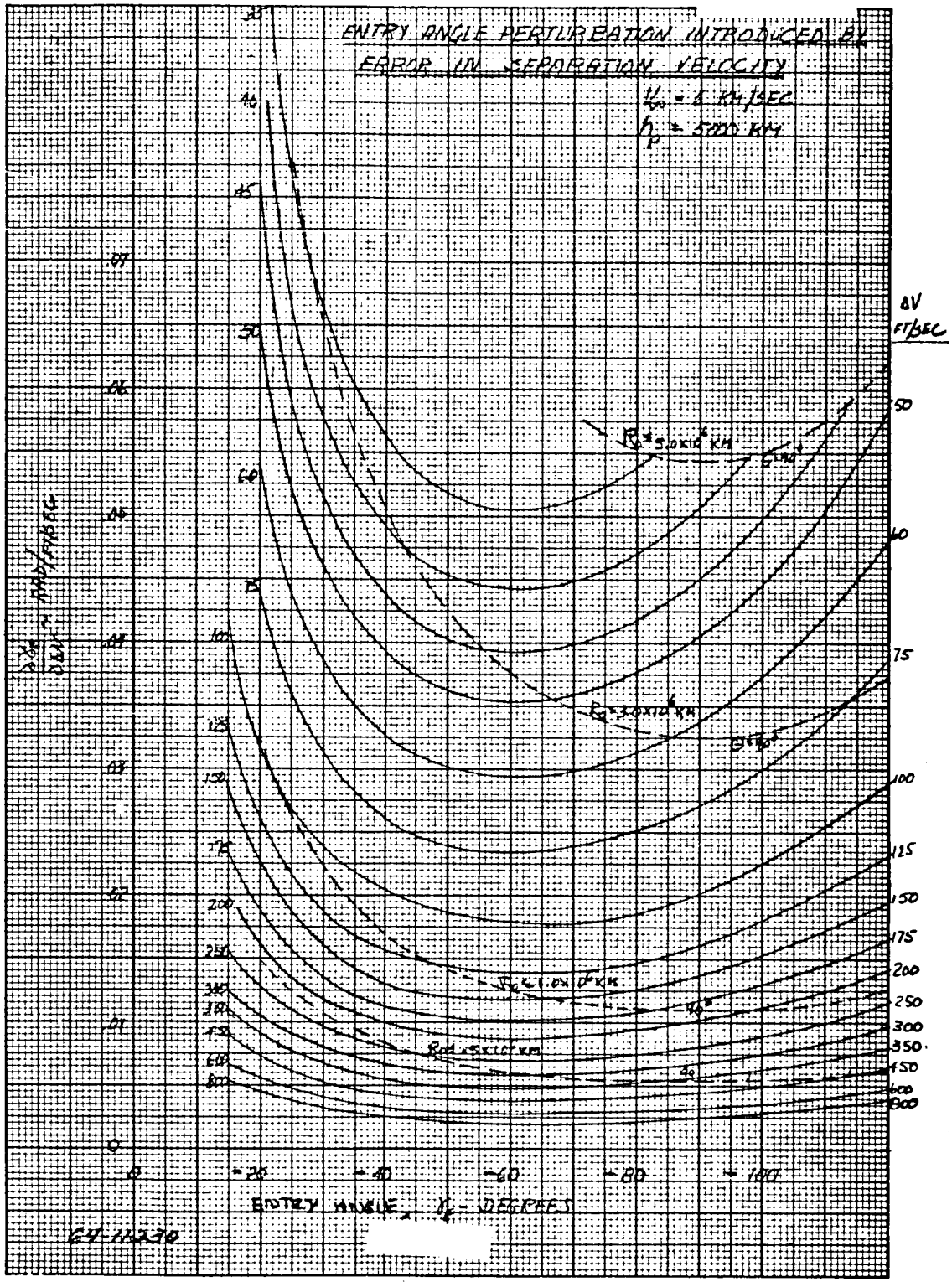

Figure 77 ENTRY ANGLE PERTURBATION INTRODUCED BY ERROR IN SEPARATION VELOCITY

RE-ORDER No. 64-522

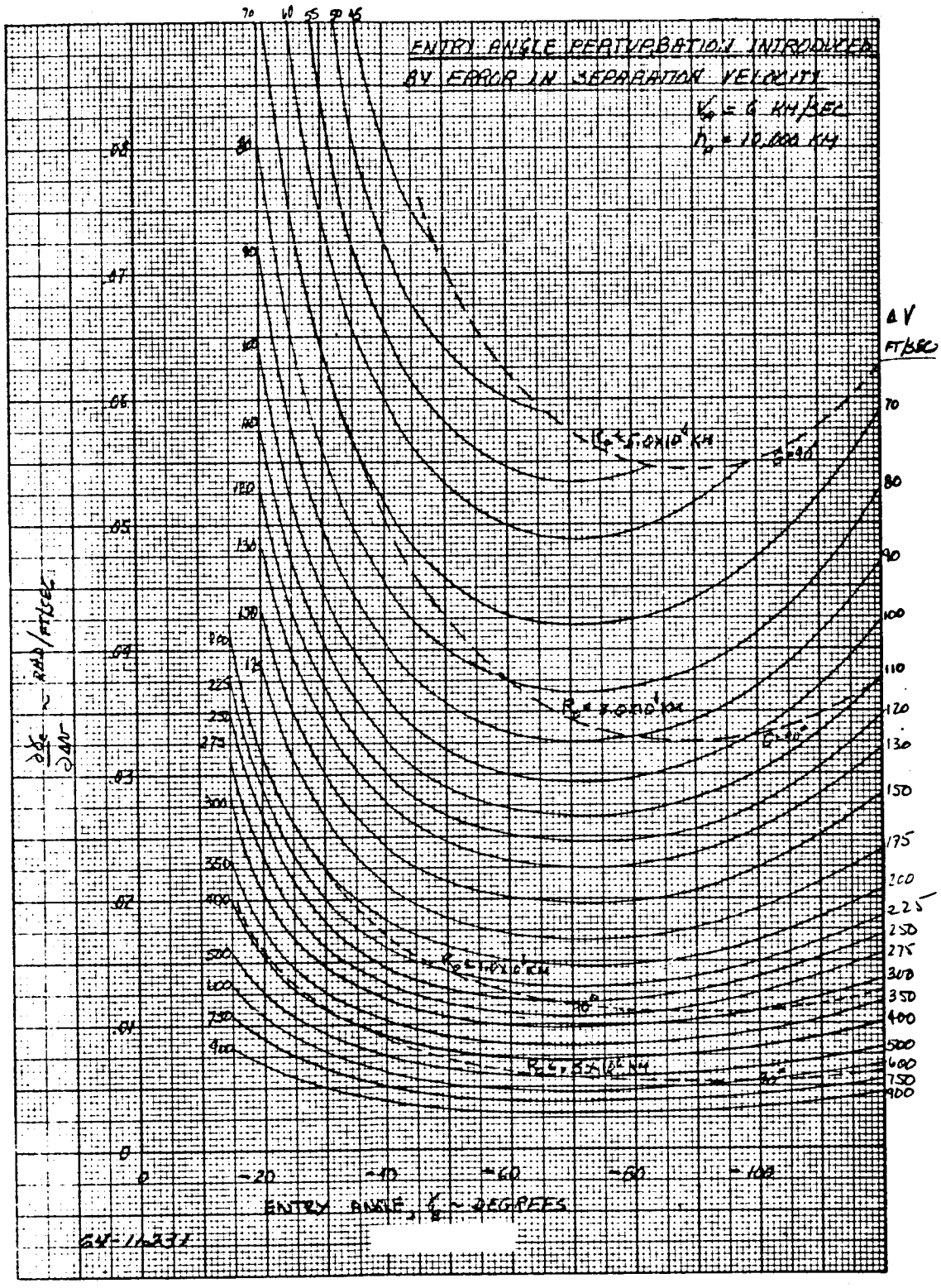

Figure 78 ENTRY ANGLE PERTURBATION INTRODUCED BY ERROR IN SEPARATION VELOCITY

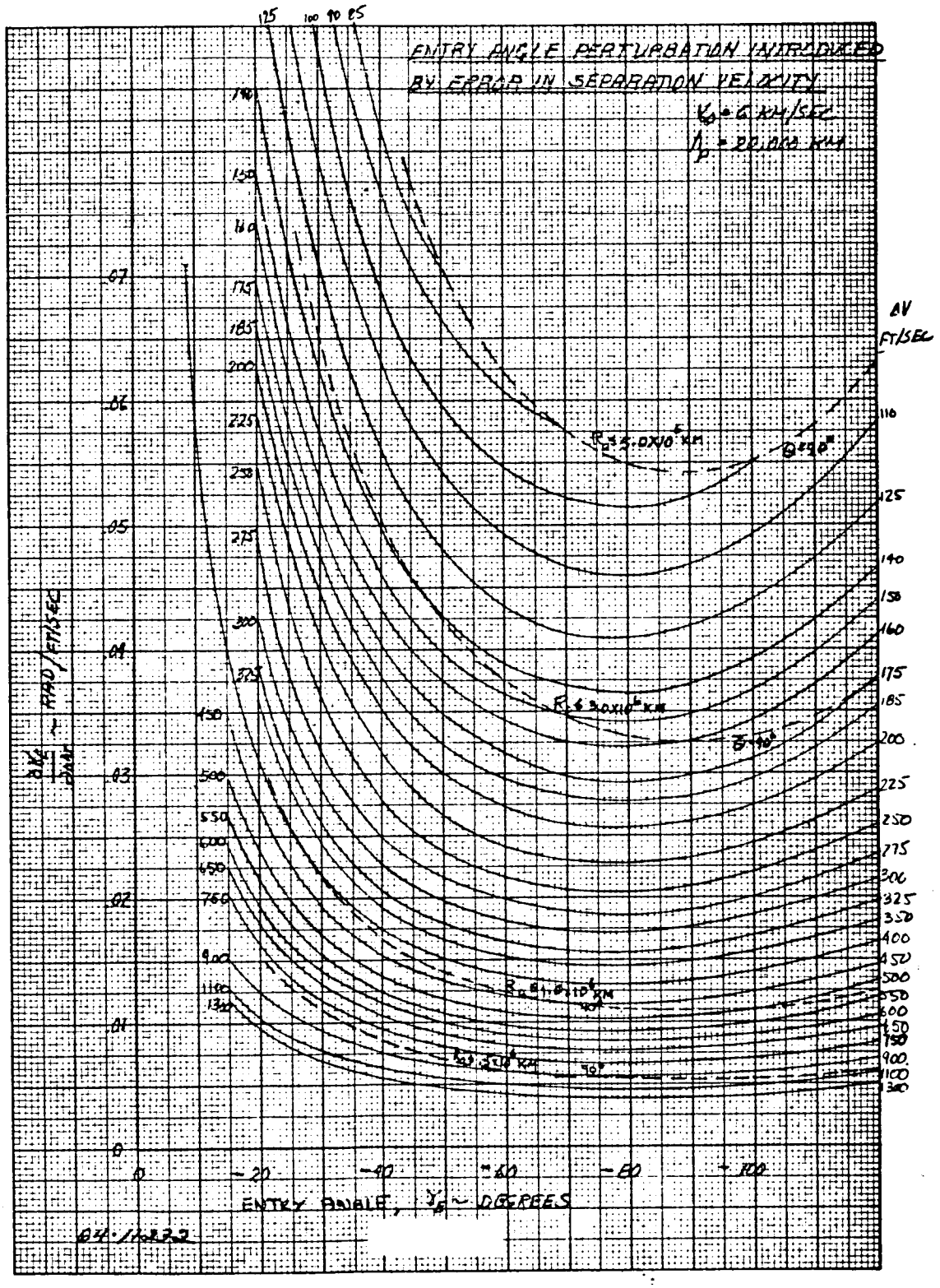

Figure 79 ENTRY ANGLE PERTURBATION INTRODUCED BY ERROR IN SEPARATION VELOCITY

RE-ORDER No. 64-522

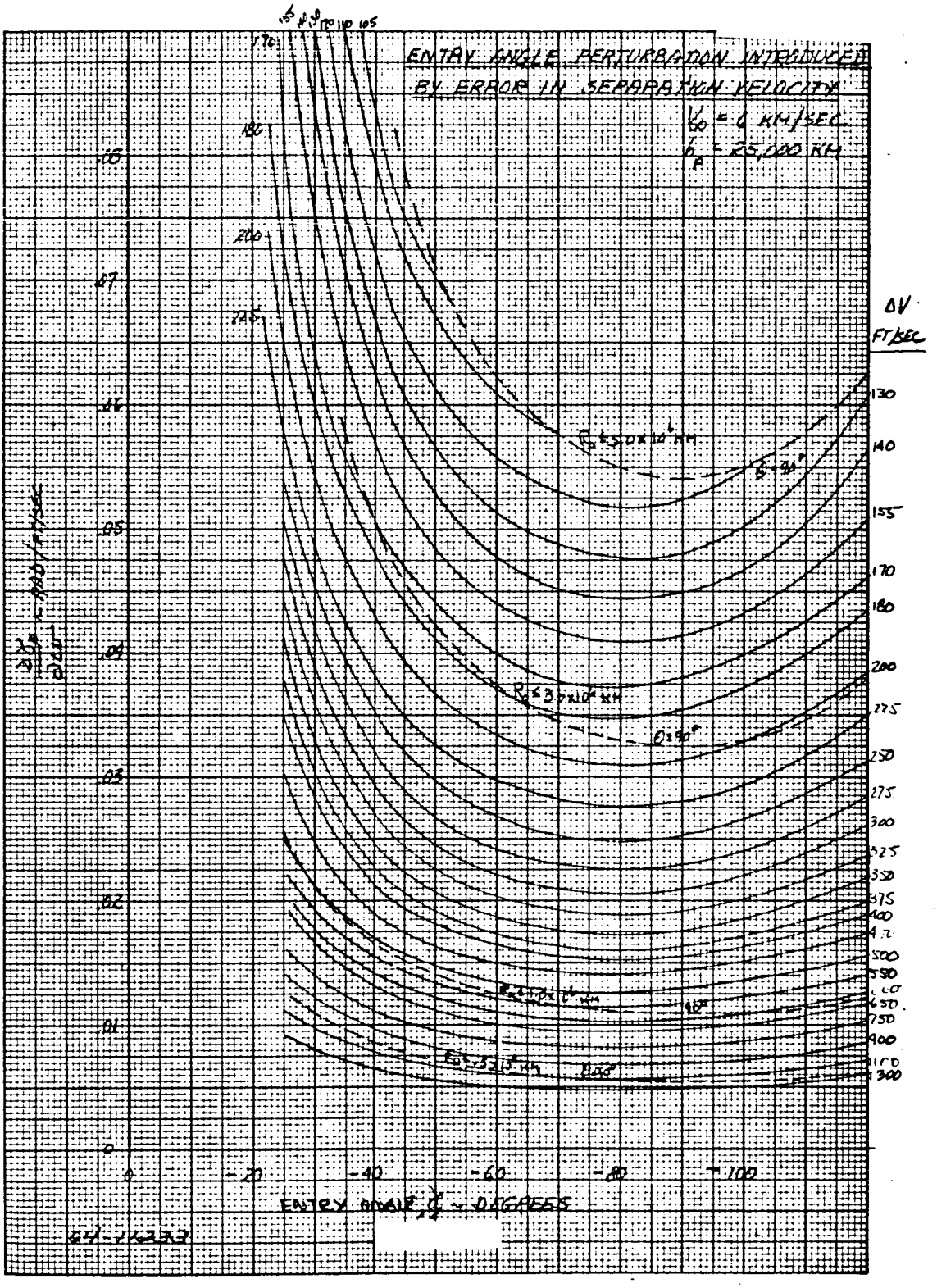

Figure 80 ENTRY ANGLE PERTURBATION INTRODUCED BY ERROR IN SEPARATION VELOCITY

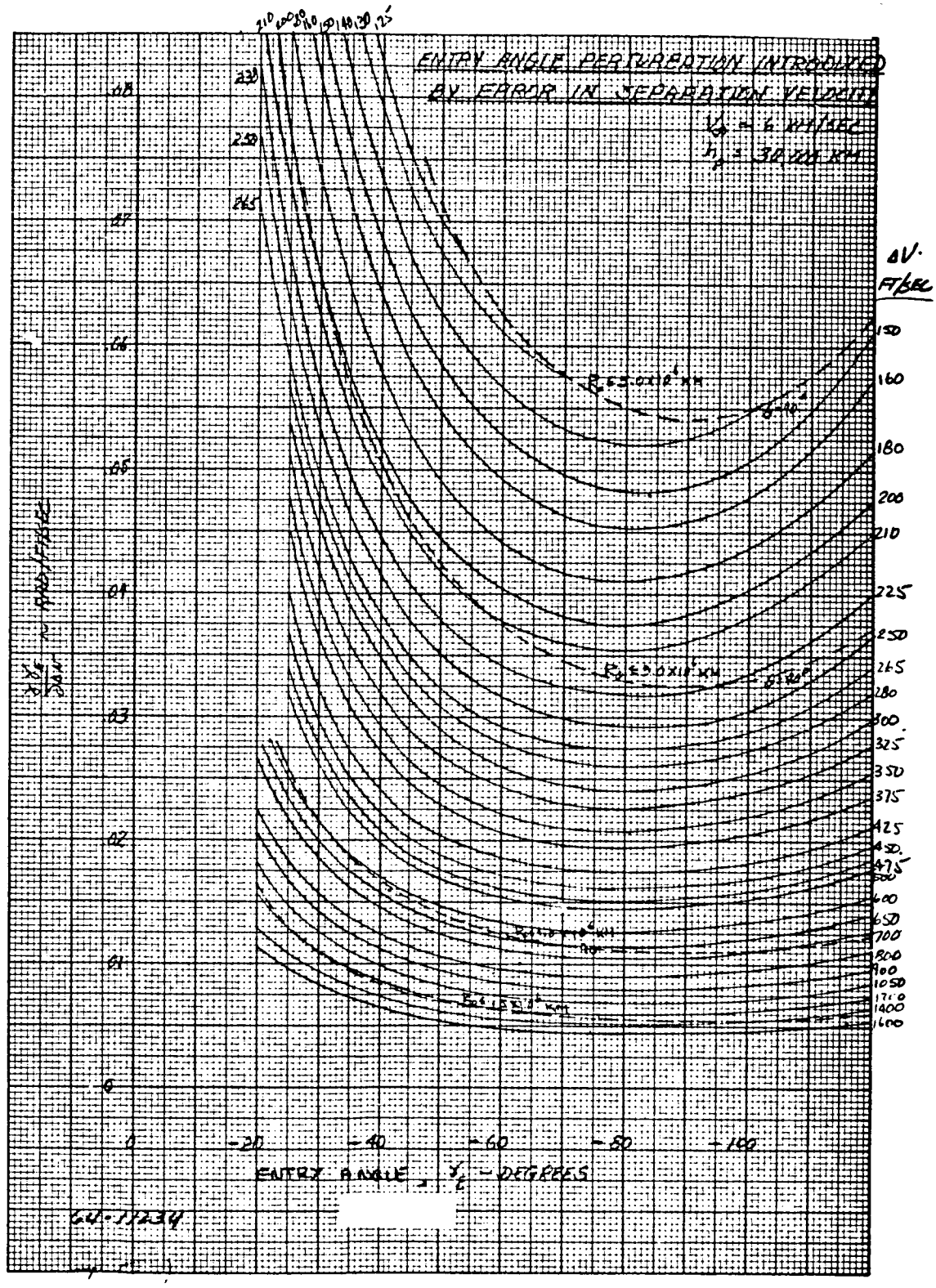

Figure 81 ENTRY ANGLE PERTURBATION INTRODUCED BY ERROR IN SEPARATION VELOCITY

RE-ORDER No. 64-522

The constant 90 degree thrust application angle contours indicate regimes where smaller separation velocities can no longer be applied to achieve a specific entry angle for that separation range.

These results indicate that, whereas the magnitude of the separation velocity, and hence the error source, is a function of the approach velocity and periapsis altitude, the influence coefficient is essentially independent of these parameters. Therefore, that portion of the uncertainty in entry angle due to separation velocity perturbation will be minimized by employing the smallest separation velocity to achieve the desired entry angle. Since this velocity is realized with a thrust application angle of 90 degrees these results are compatible with those previously discussed in that the dispersions are minimized for velocity applications normal to the approach velocity.

The uncertainty in the vehicle flight path angle prior to the separation maneuver can be related to an in-plane positional error (translation of the approach asymptote) by

$$\delta \gamma_s = \frac{\Delta R_a}{R_s}$$

where:

ΔR_a - position error of approach asymptote

R_s - separation range

The influence coefficient relating variations in the entry angle to disturbances in the flight path angle at separation, $\partial \gamma_e / \partial \gamma_s$, exhibits no dependence on periapsis altitude and only weak dependence on the approach velocity. The results presented in figure 82 indicate that the contribution to the entry angle uncertainty produced by variations in the initial flight path angle are mimimized by employing entry angles near 90 degrees.

To summarize the results of this analysis, it has been demonstrated that the dispersion in the entry angle due to errors in separation velocity, thrust application angle and initial flight path angle will be minimized when the separation parameters are selected such that a steep entry angle consistent with mission objectives is achieved by employing a thrust application angle essentially normal to the approach velocity vector.

The analysis to determine the perturbations in the lander range angle produced by disturbances in the separation parameters is identical in nature and results in identical conclusions to the previous analysis, i. e., range angle dispersions are minimized by utilizing a steep entry angle and a thrust application angle normal to the approach velocity. The influence coefficients relating perturbations in range angle to disturbances in thrust application angle, $\partial \phi_e / \partial \theta$, are

RE-ORDER No. 64-522

presented in figures 83-94; the influence coefficients relating perturbations in the range angle to disturbances in separation velocity, $\partial \phi_e / \partial \Delta V$, in figures 95-106 with the influence coefficients relating perturbations in the range angle to disturbances in initial flight path angle, $\partial \phi_e / \partial \gamma_s$, in figure 107.

A separate analysis was performed to determine the effects on entry angle and range angle of inadvertent thrust application angle errors in a plane normal to the plane of motion. Since the direction of the applied velocity is controlled by the ACS system, it is as feasible to assume the existence of an out-of-plane error source as the previously employed in-plane error source. The resulting out-of-plane velocity error is

$$\Delta V_{\text{out-of-plane}} = \Delta V \sin \alpha$$

For out-of-plane angles, α, of 1 and 3 degrees, the resulting cross-range error is presented in figures 108 and 109 for an approach velocity of 4 km/sec and periapsis altitudes of 5,000 and 10,000 km. For the range of parameters selected these results indicate that the cross-range angle varies linearly with the periapsis altitude and α. Similar results for the variation in entry angle are presented in figures 110 and 111.

RE-ORDER No. 64-522

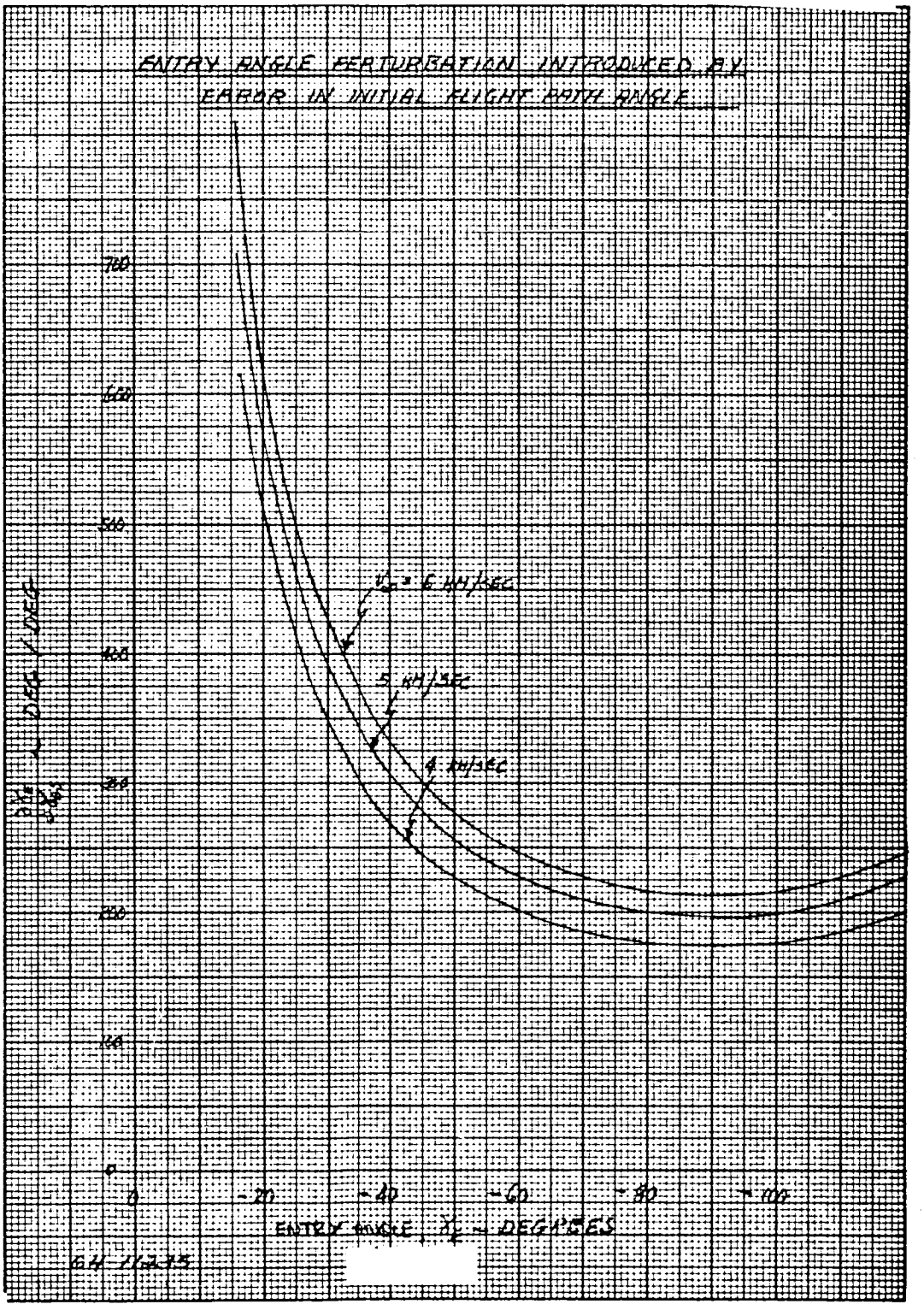

Figure 82 ENTRY ANGLE PERTURBATION INTRODUCED BY ERROR IN INITIAL FLIGHT PATH ANGLE

RE-ORDER No. 64-522

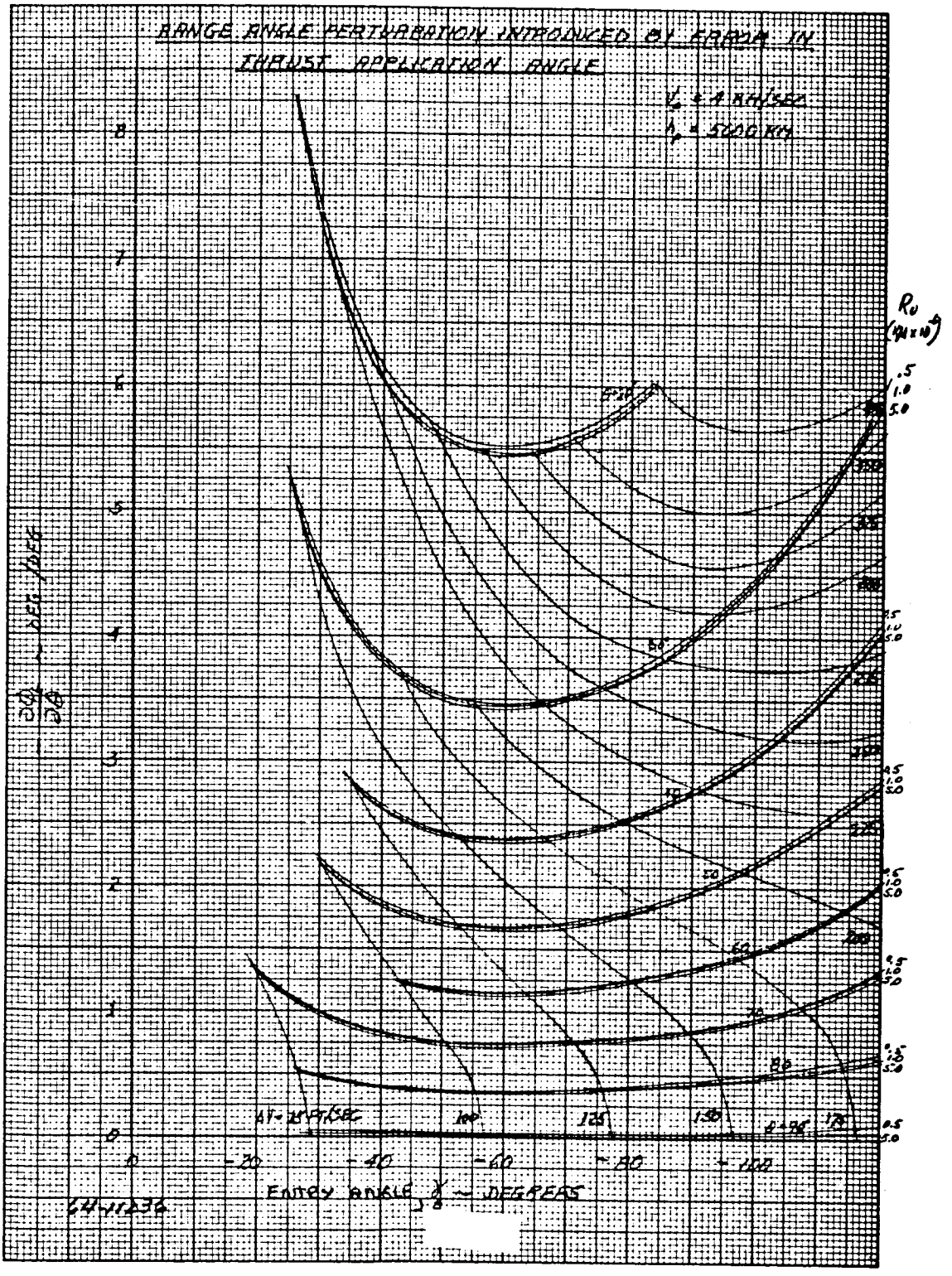

Figure 83 RANGE ANGLE PERTURBATION INTRODUCED BY ERROR IN THRUST APPLICATION ANGLE

RE-ORDER No. 64-522

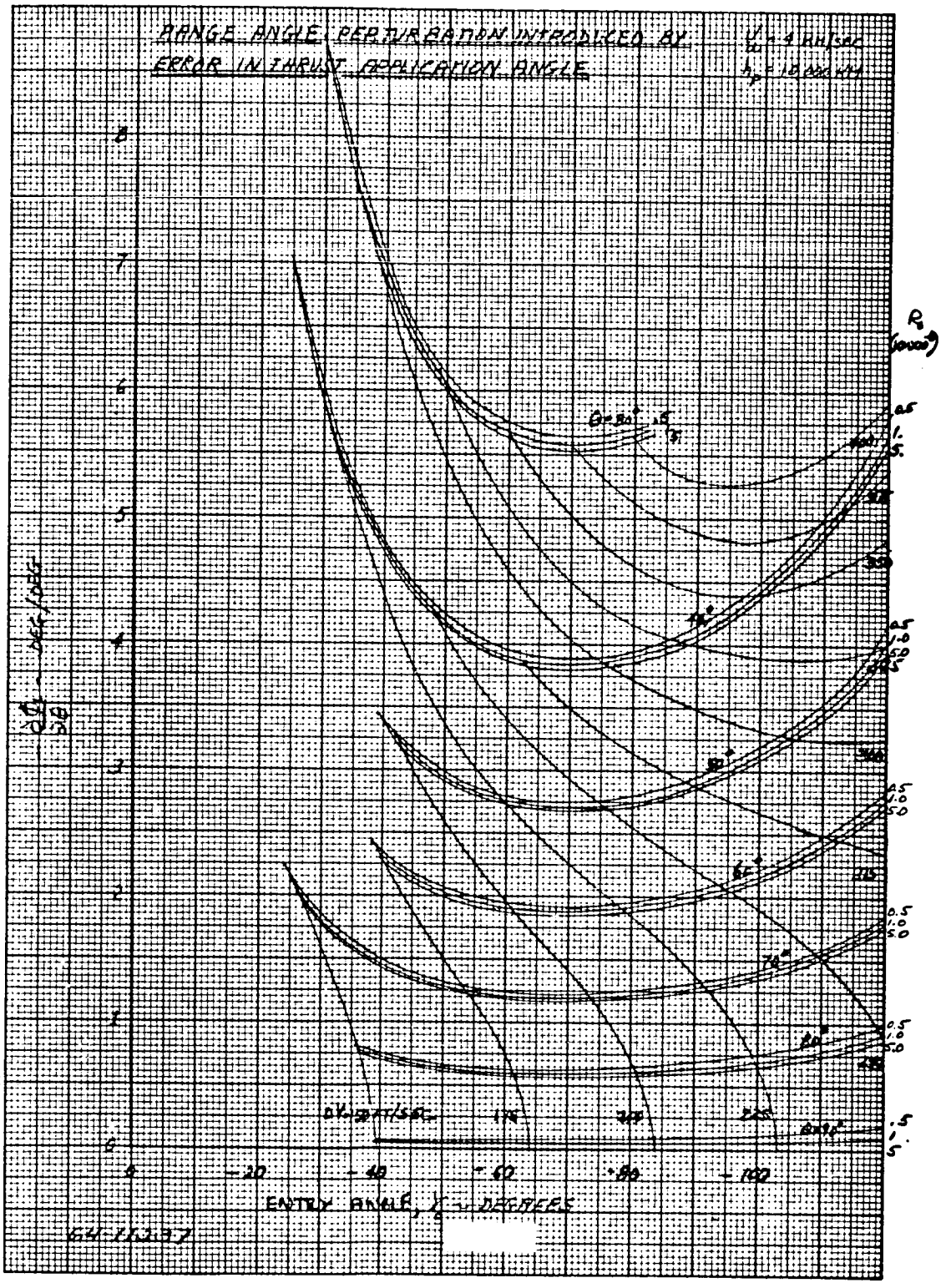

Figure 84 RANGE ANGLE PERTURBATION INTRODUCED BY ERROR IN THRUST APPLICATION ANGLE

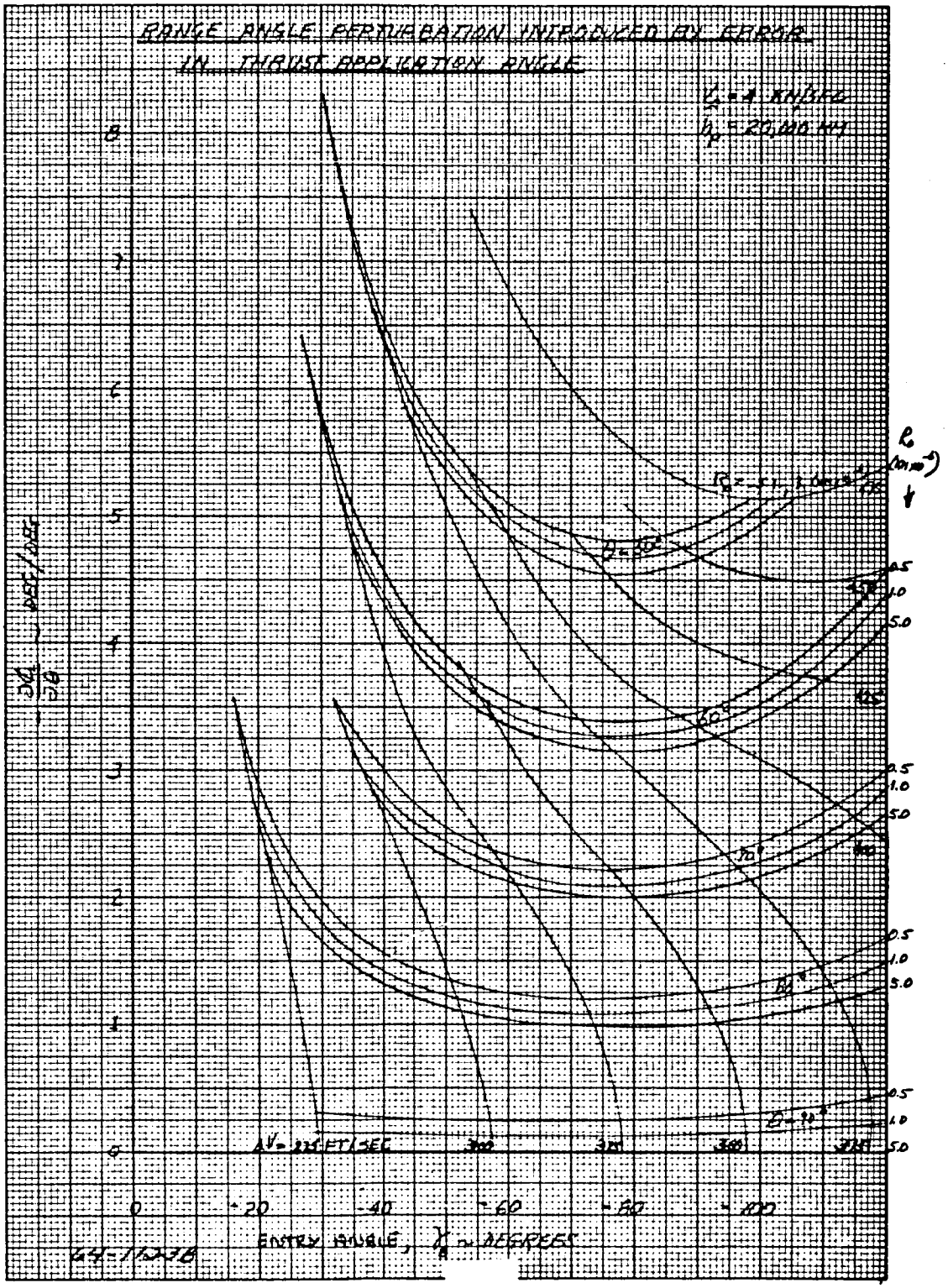

Figure 85 RANGE ANGLE PERTURBATION INTRODUCED BY ERROR IN THRUST APPLICATION ANGLE

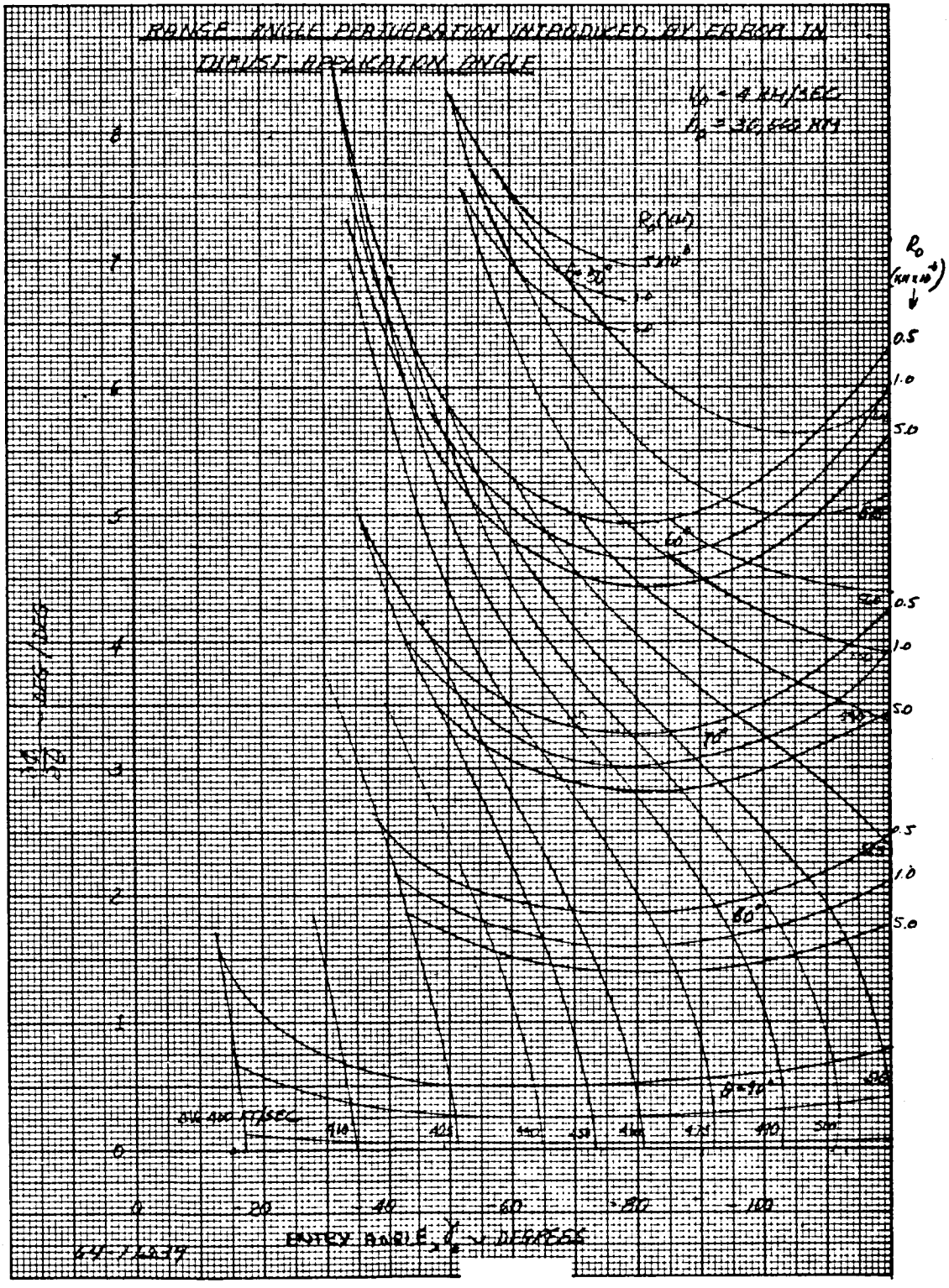

Figure 86 RANGE ANGLE PERTURBATION INTRODUCED BY ERROR IN THRUST APPLICATION ANGLE

RE-ORDER No. 64-522

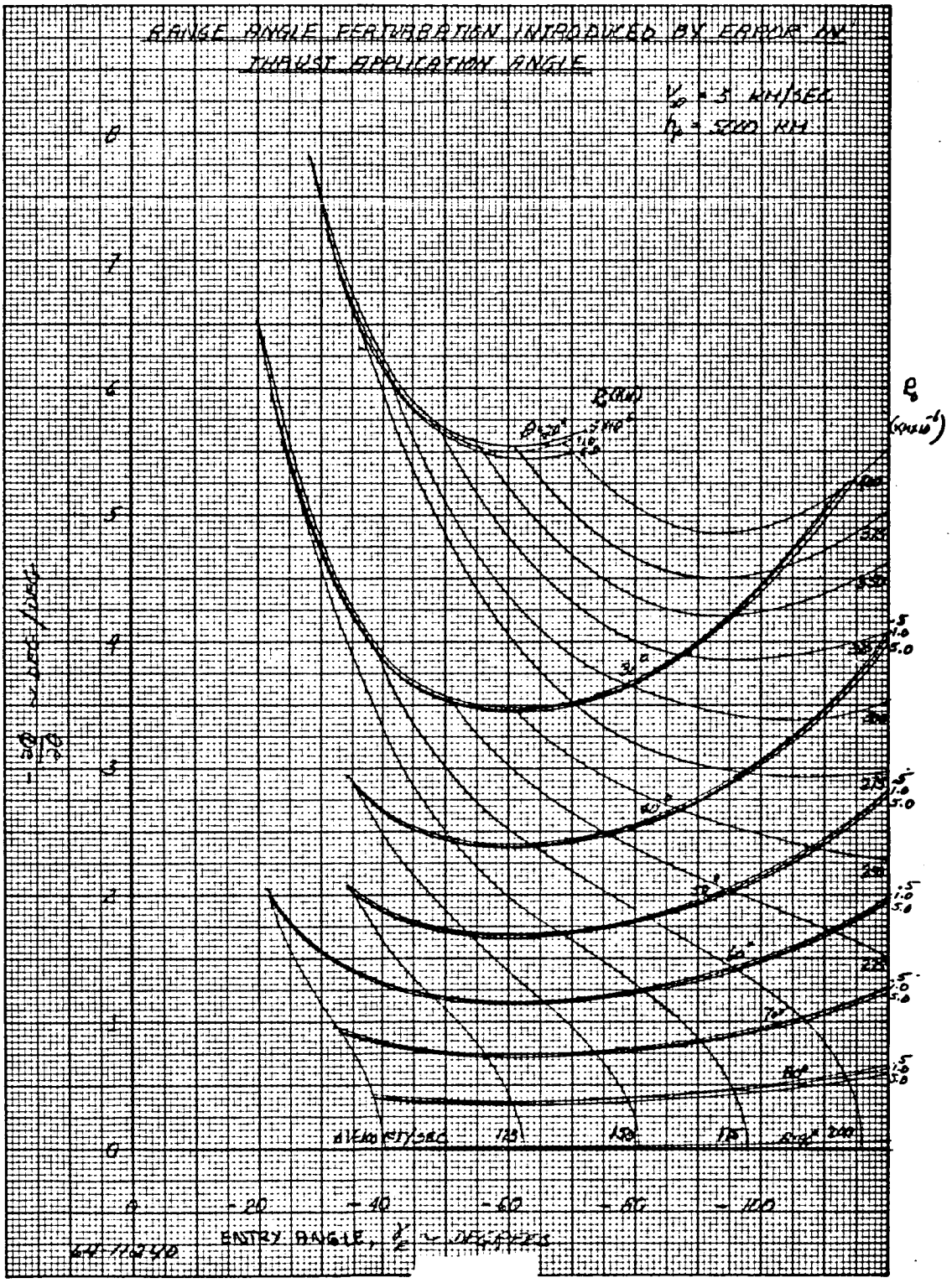

Figure 87 RANGE ANGLE PERTURBATION INTRODUCED BY ERROR IN THRUST APPLICATION ANGLE

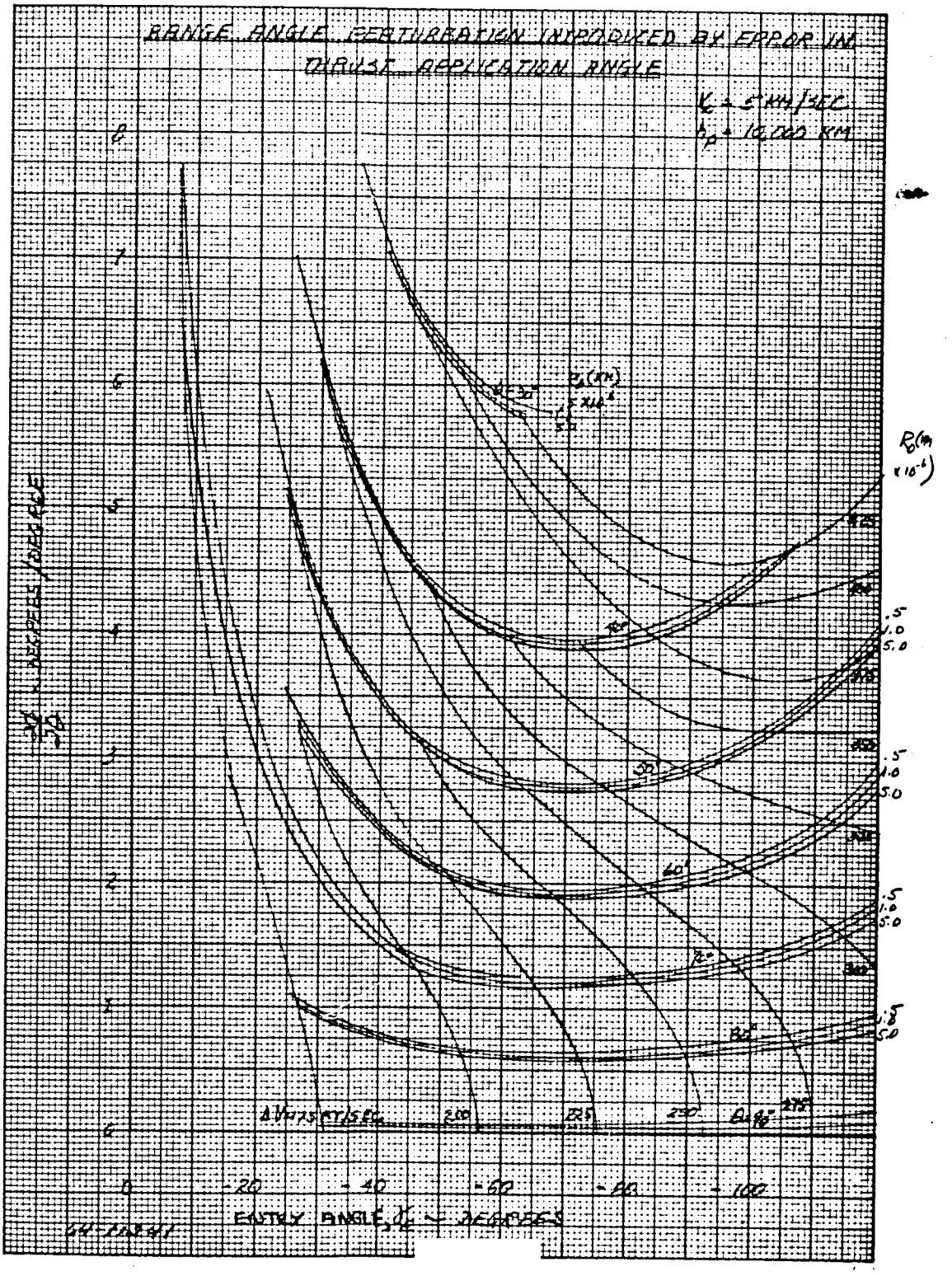

Figure 88 RANGE ANGLE PERTURBATION INTRODUCED BY ERROR IN THRUST APPLICATION ANGLE

RE-ORDER No. 64-522

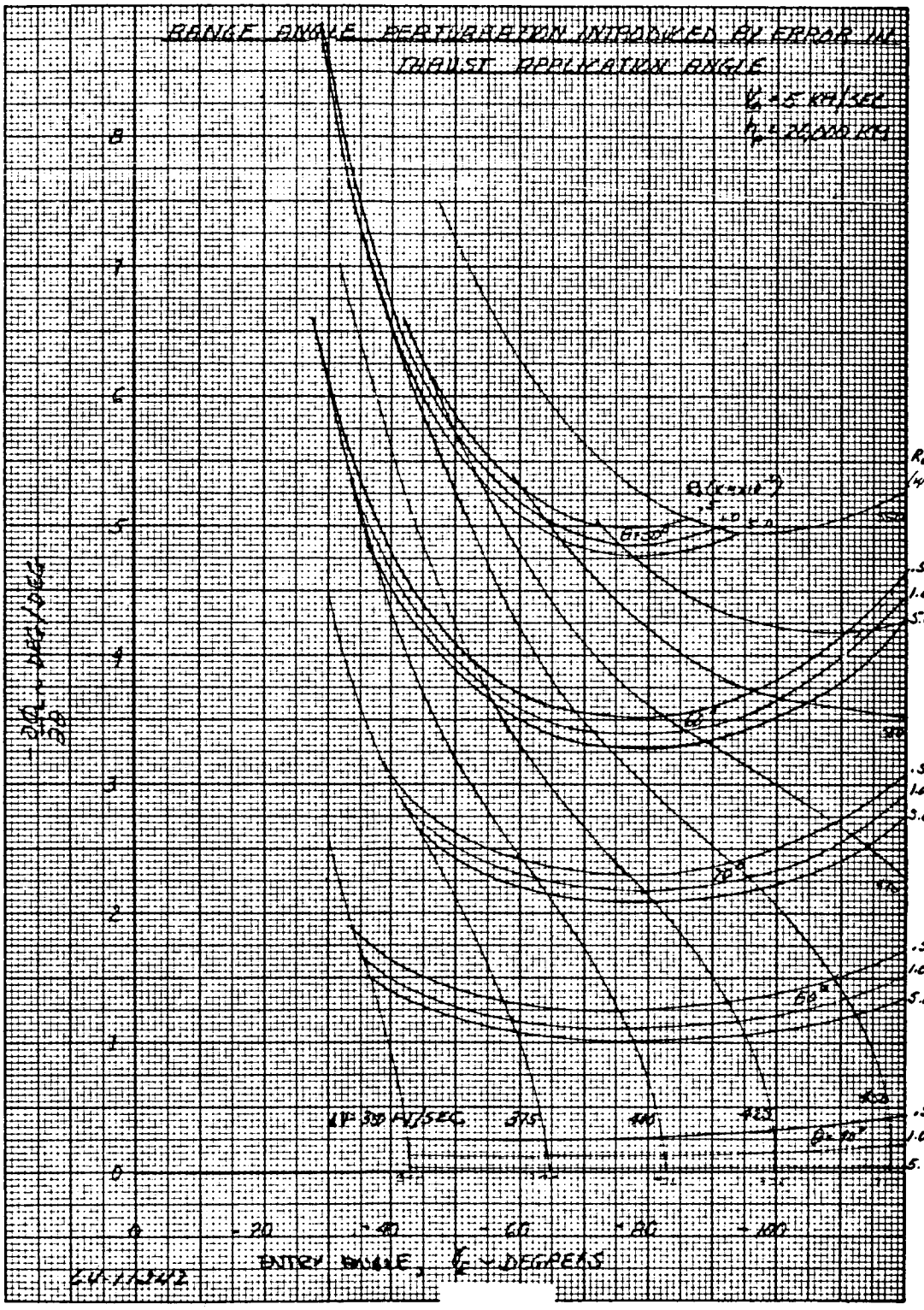

Figure 89 RANGE ANGLE PERTURBATION INTRODUCED BY ERROR IN THRUST APPLICATION ANGLE

RE-ORDER No. 64-522

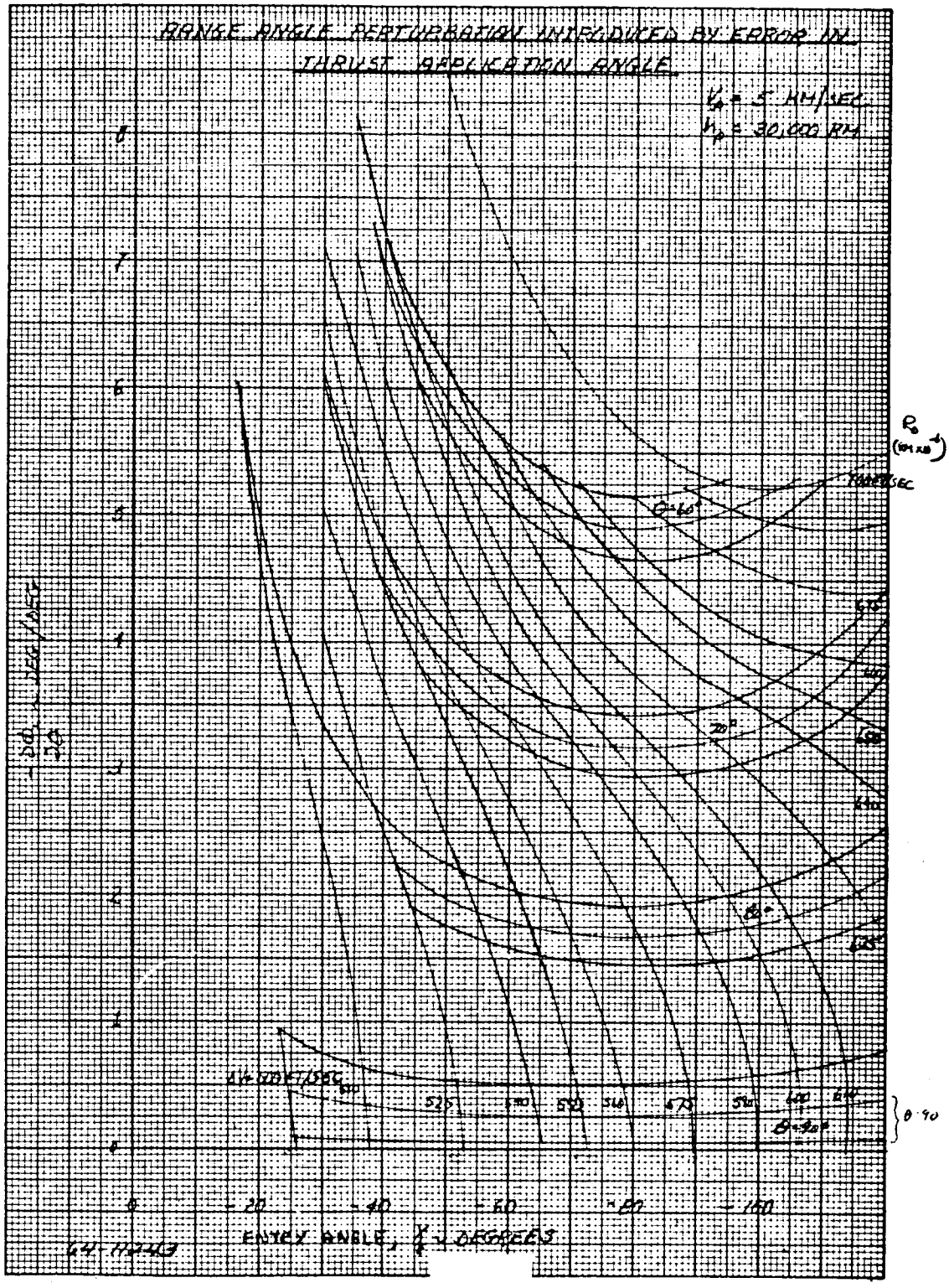

Figure 90 RANGE ANGLE PERTURBATION INTRODUCED BY ERROR IN THRUST APPLICATION ANGLE

RE-ORDER No. 64-522

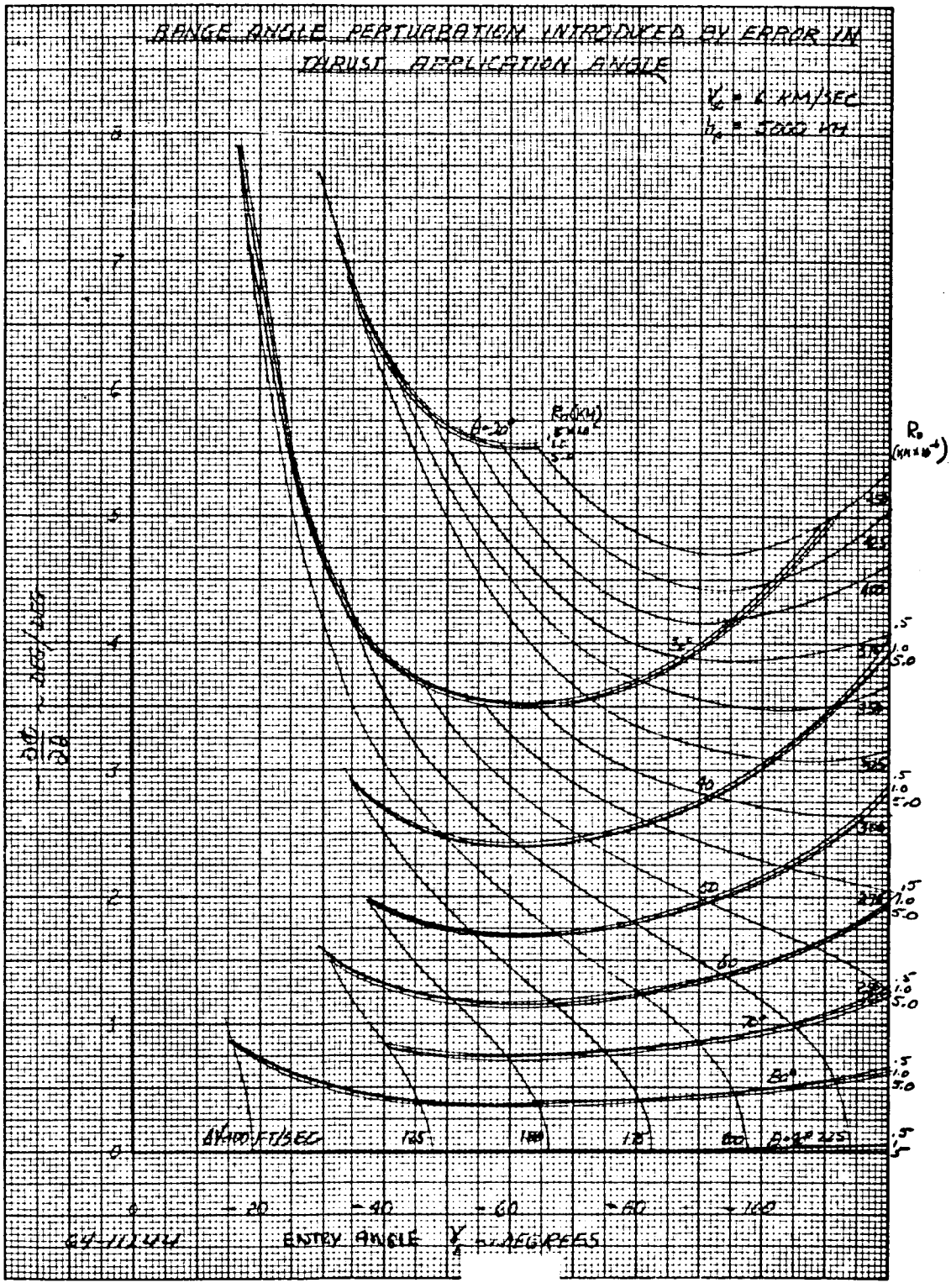

Figure 91 RANGE ANGLE PERTURBATION INTRODUCED BY ERROR IN THRUST APPLICATION ANGLE

RE-ORDER No. 64-522

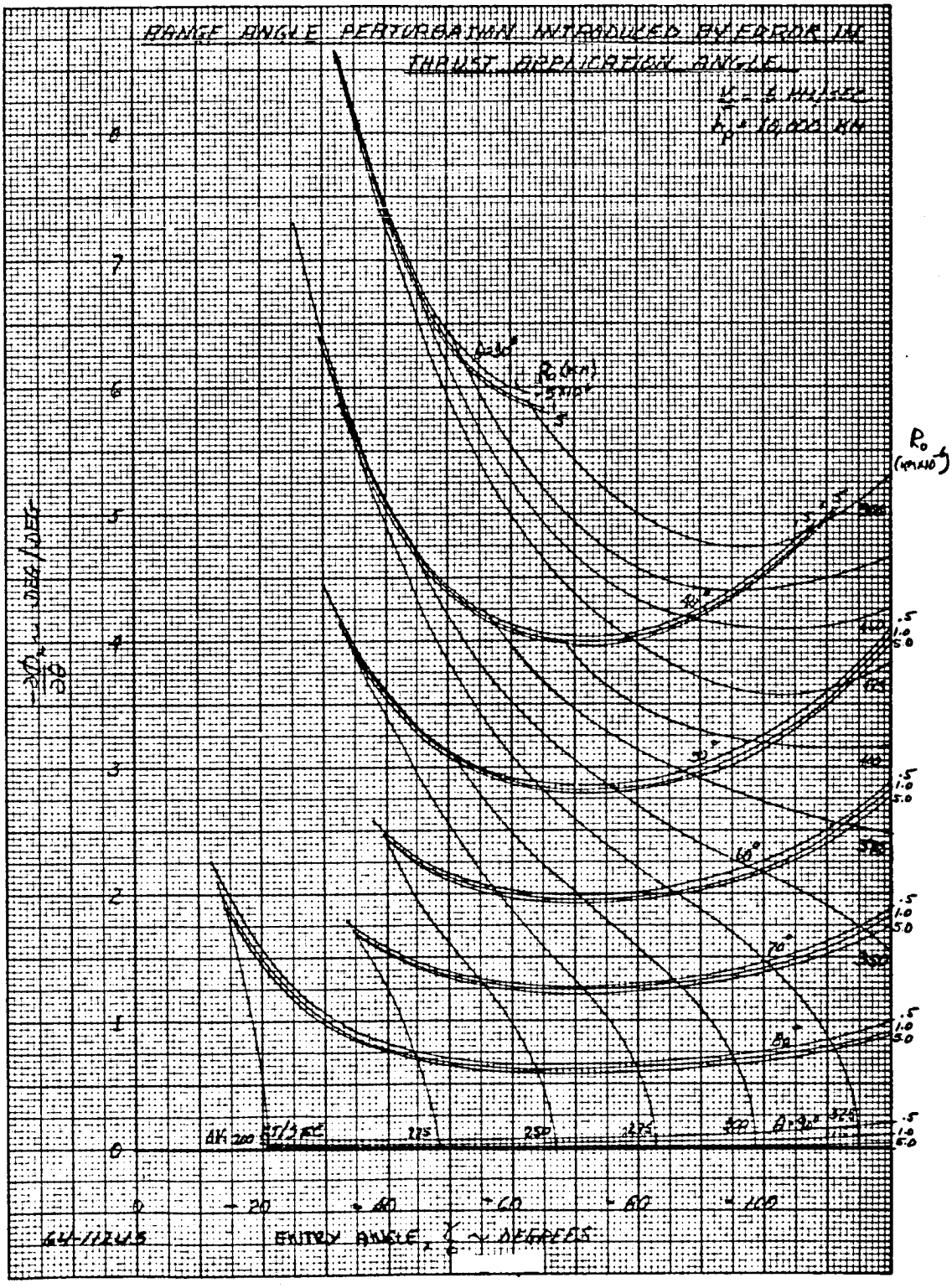

Figure 92 RANGE ANGLE PERTURBATION INTRODUCED BY ERROR IN THRUST APPLICATION ANGLE

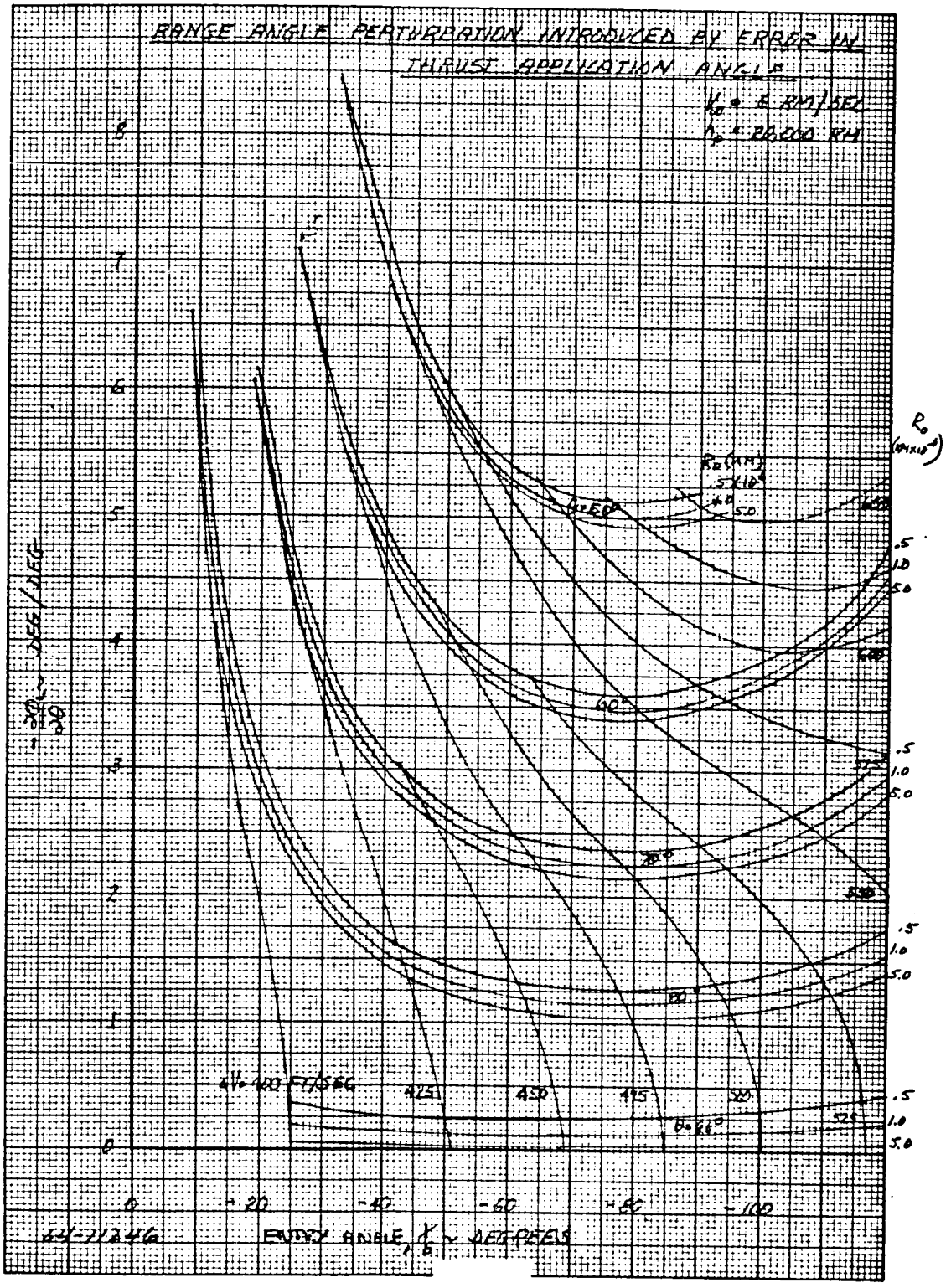

Figure 93 RANGE ANGLE PERTURBATION INTRODUCED BY ERROR IN THRUST APPLICATION ANGLE

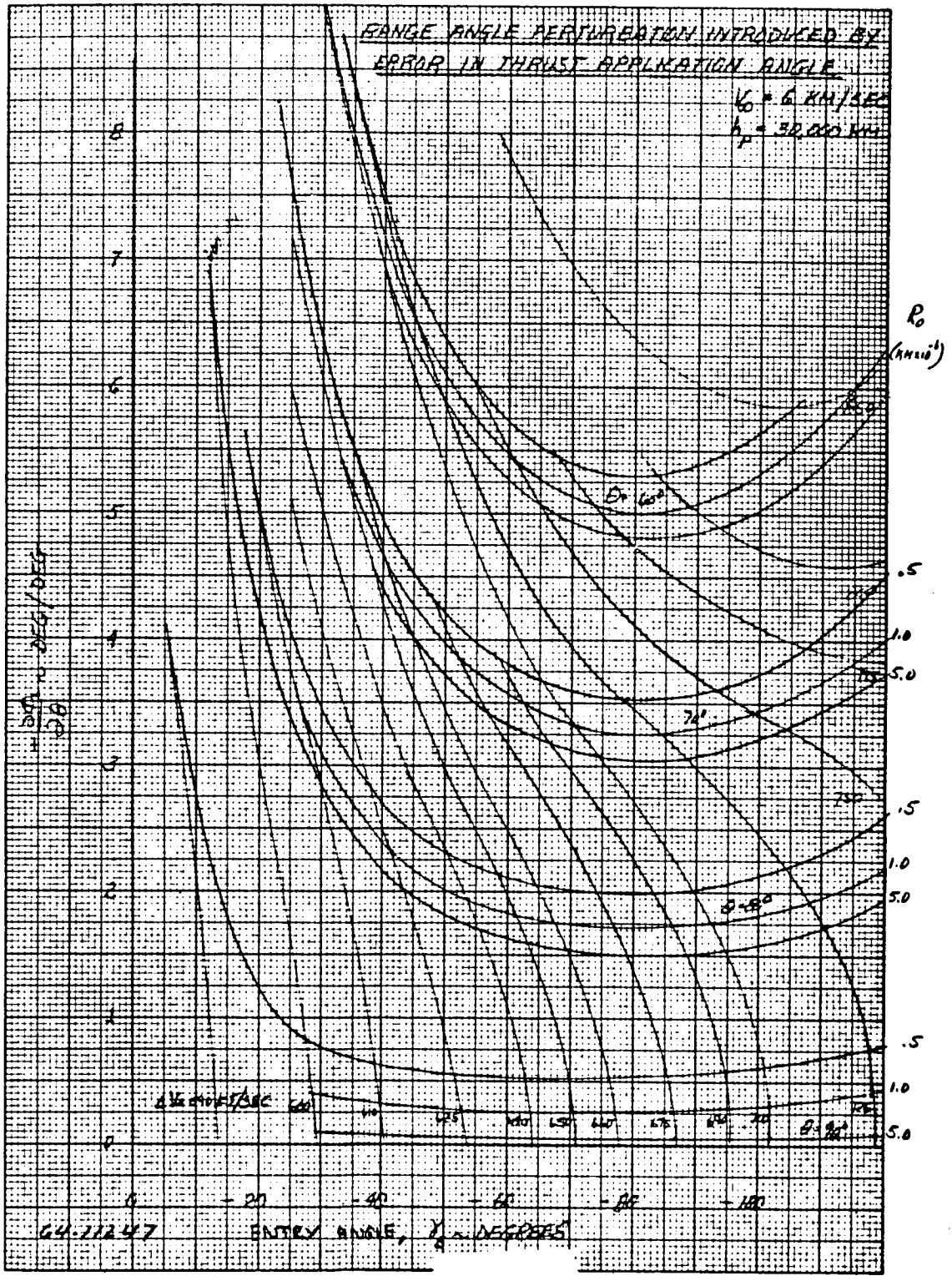

Figure 94 RANGE ANGLE PERTURBATION INTRODUCED BY ERROR IN THRUST APPLICATION ANGLE

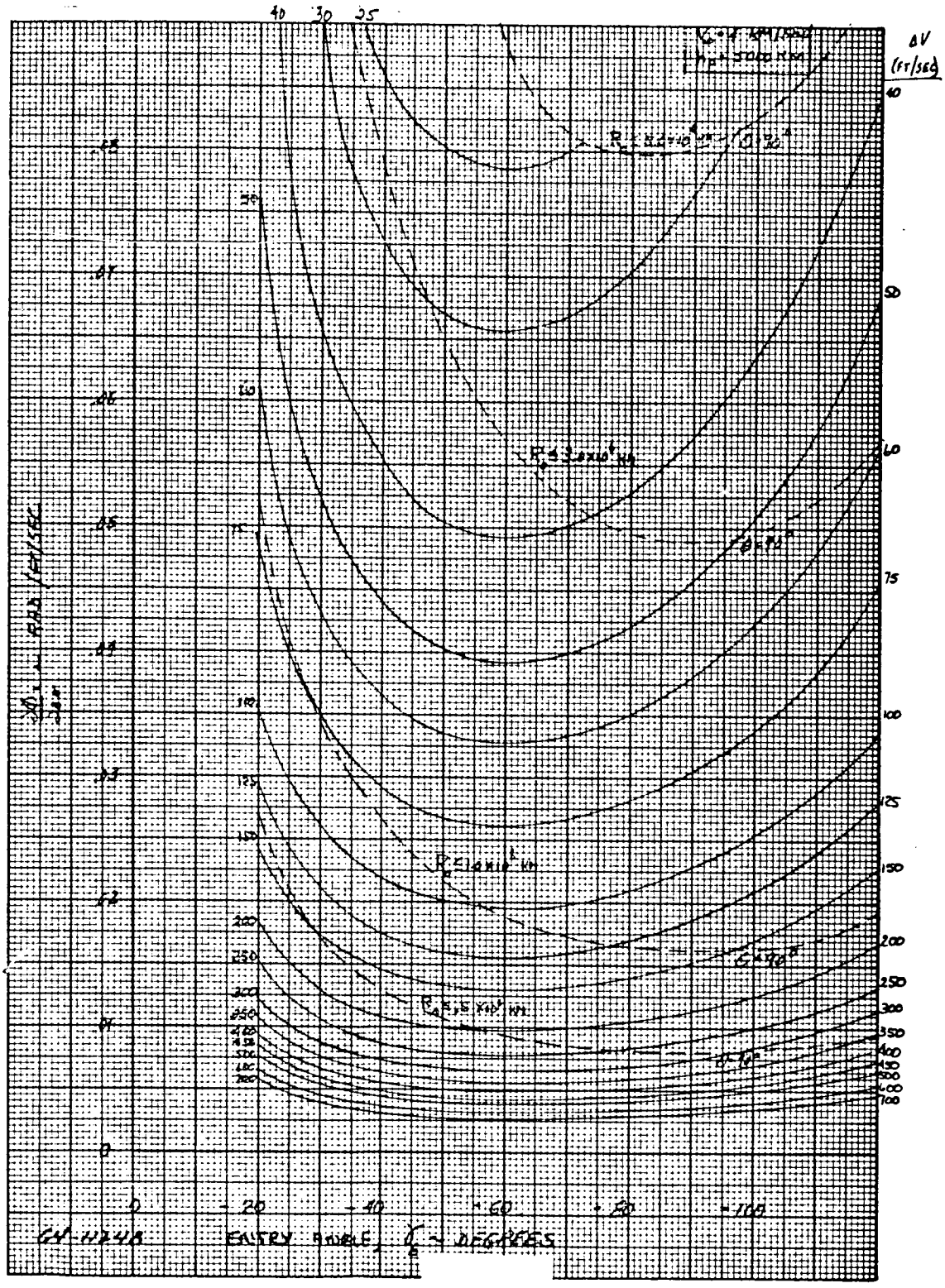

Figure 95 RANGE ANGLE PERTURBATION INTRODUCED BY ERROR IN SEPARATION VELOCITY

RE-ORDER No. 64-522

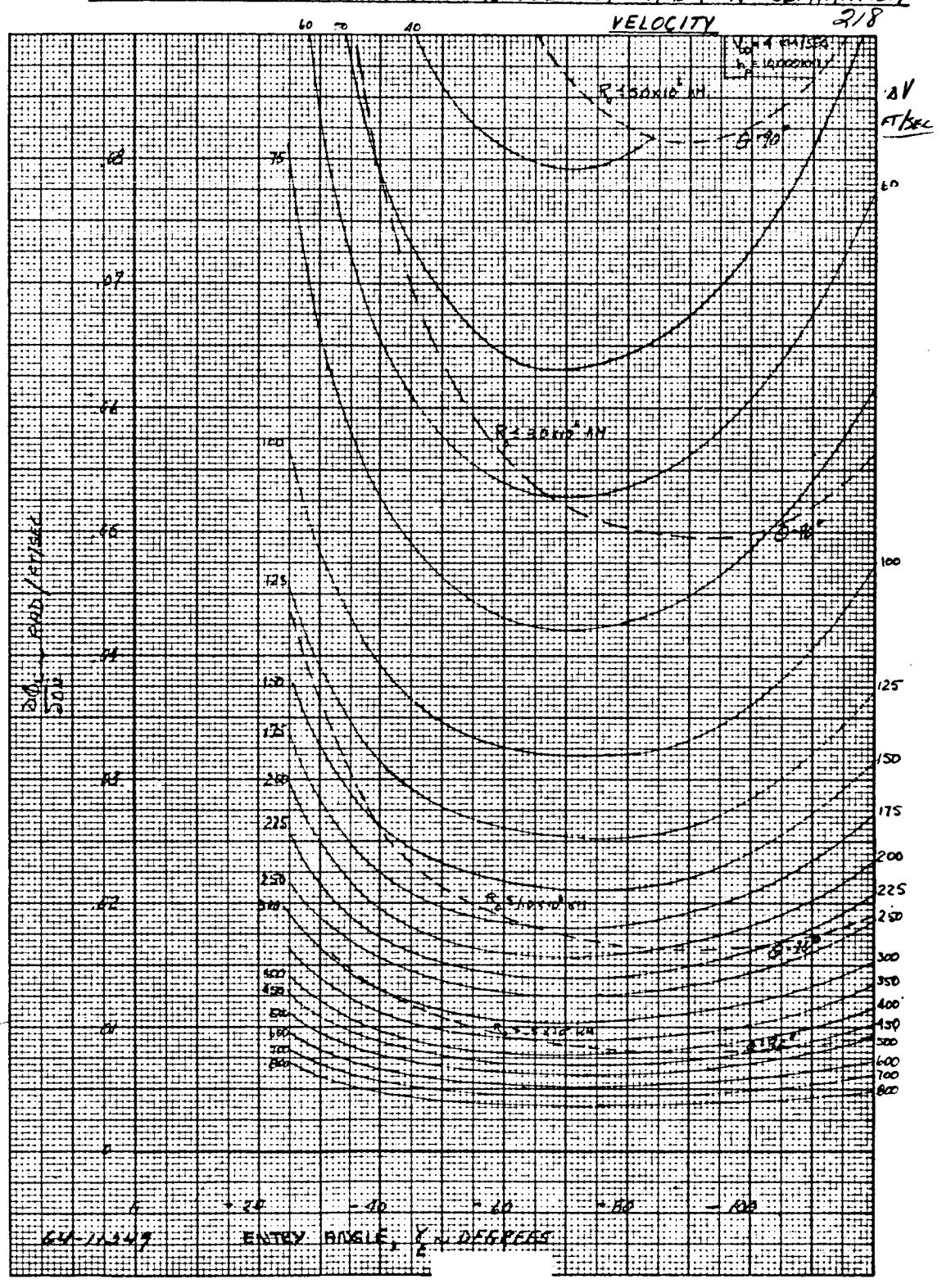

Figure 96 RANGE ANGLE PERTURBATION INTRODUCED BY ERROR IN SEPARATION VELOCITY

RE-ORDER No. 64-522

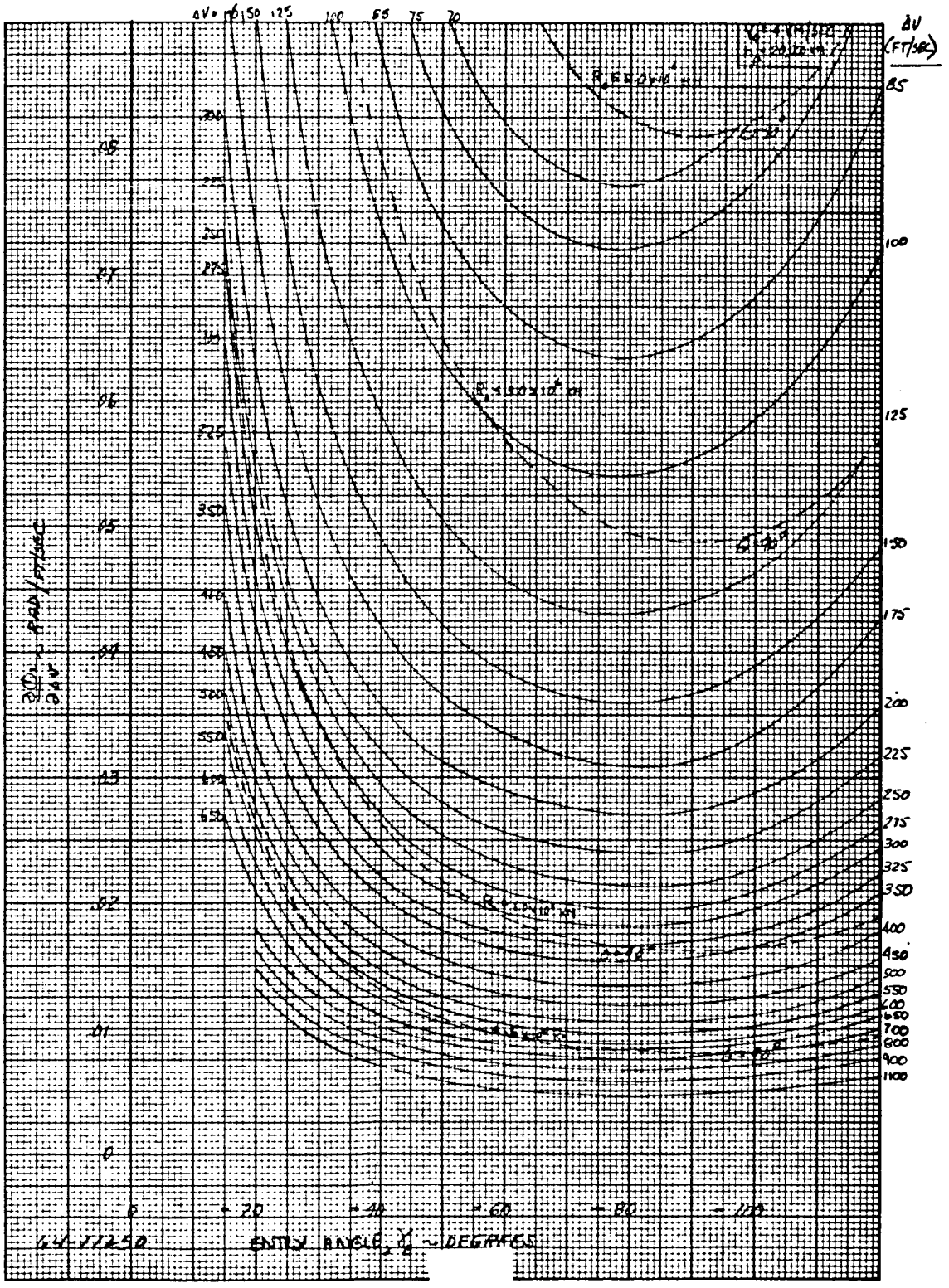

Figure 97 RANGE ANGLE PERTURBATION INTRODUCED BY ERROR IN SEPARATION VELOCITY

RE-ORDER No. 64-522

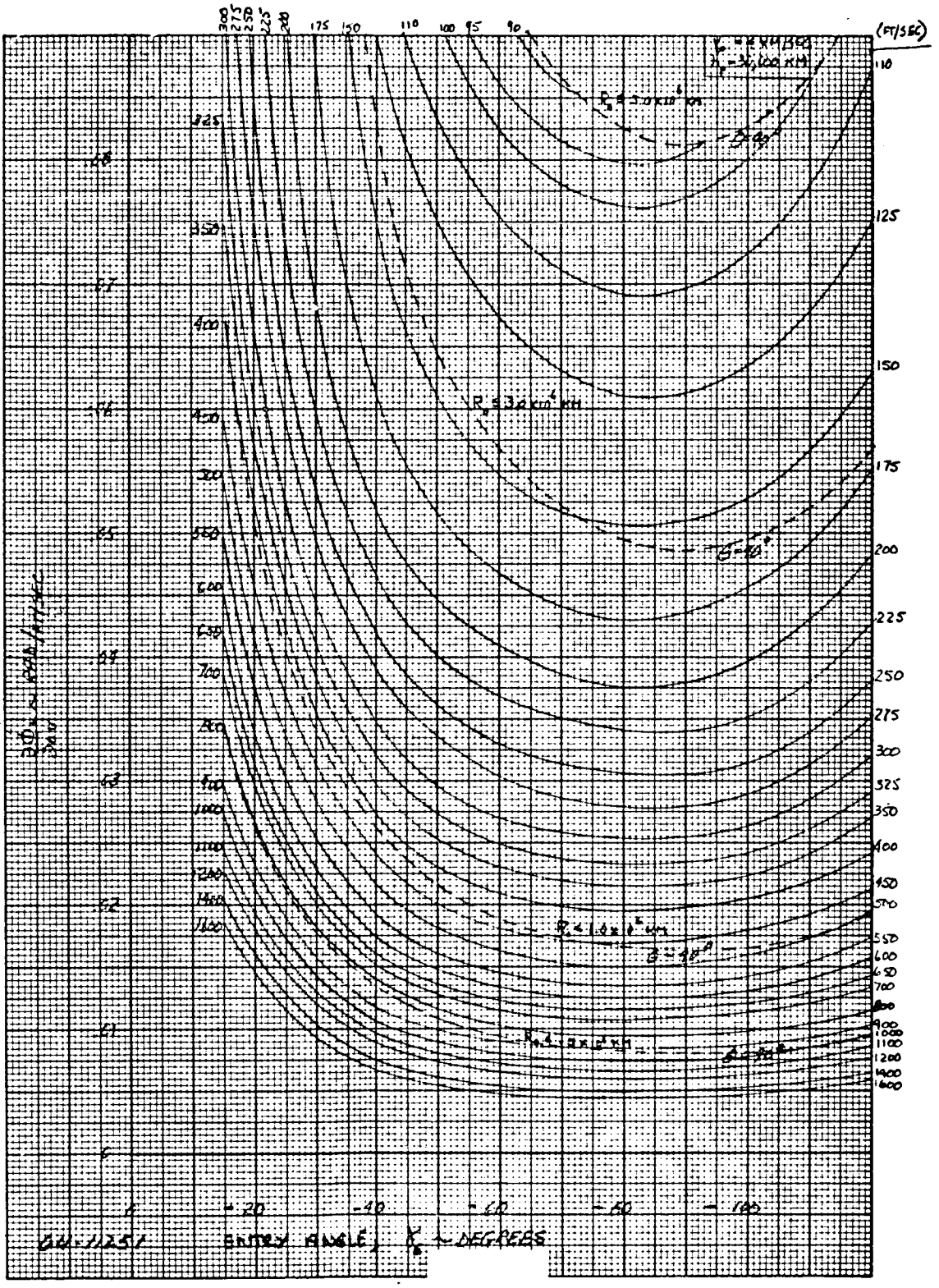

Figure 98 RANGE ANGLE PERTURBATION INTRODUCED BY ERROR IN SEPARATION VELOCITY

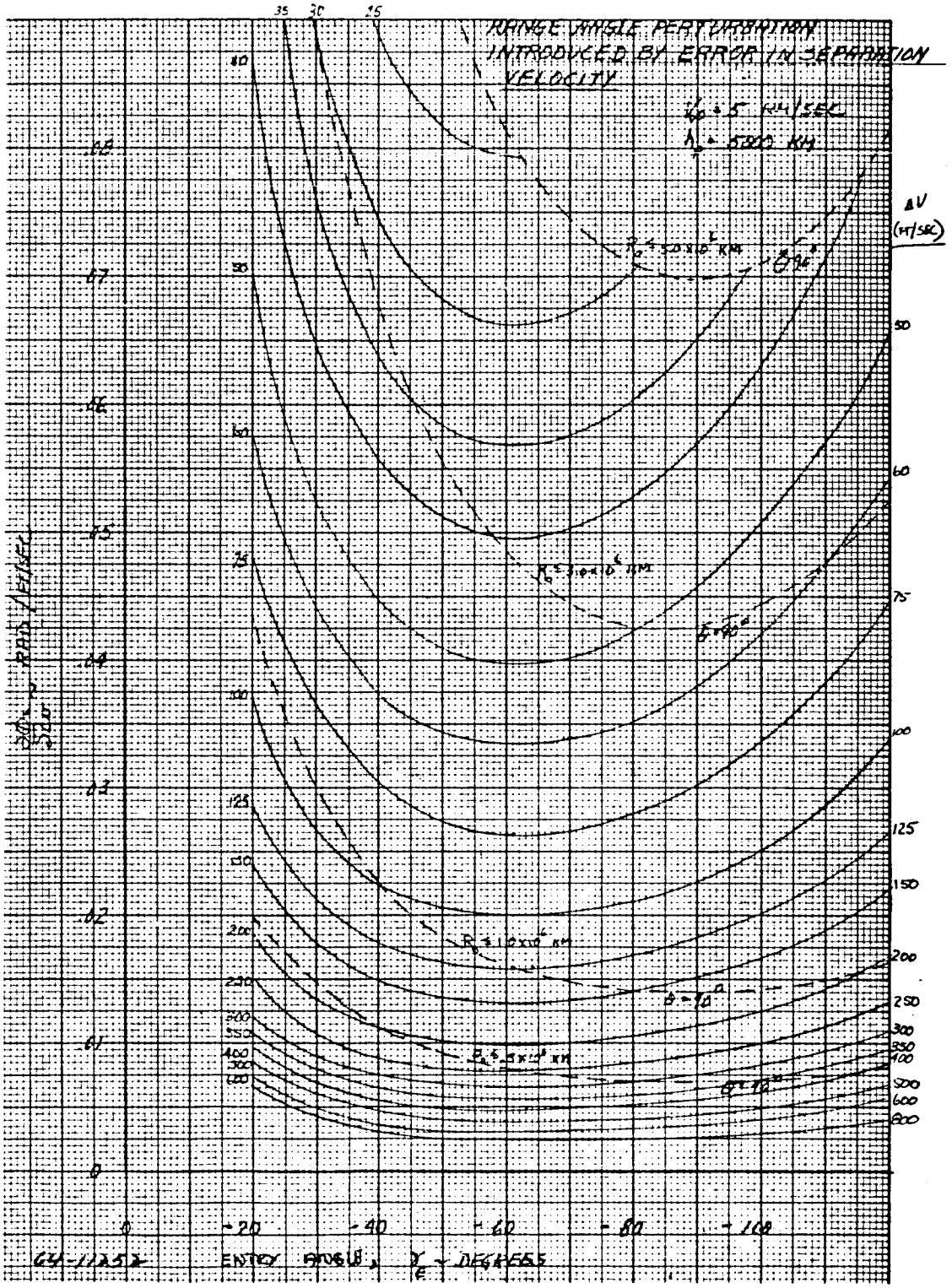

Figure 99 RANGE ANGLE PERTURBATION INTRODUCED BY ERROR IN SEPARATION VELOCITY

RE-ORDER No. 64-522

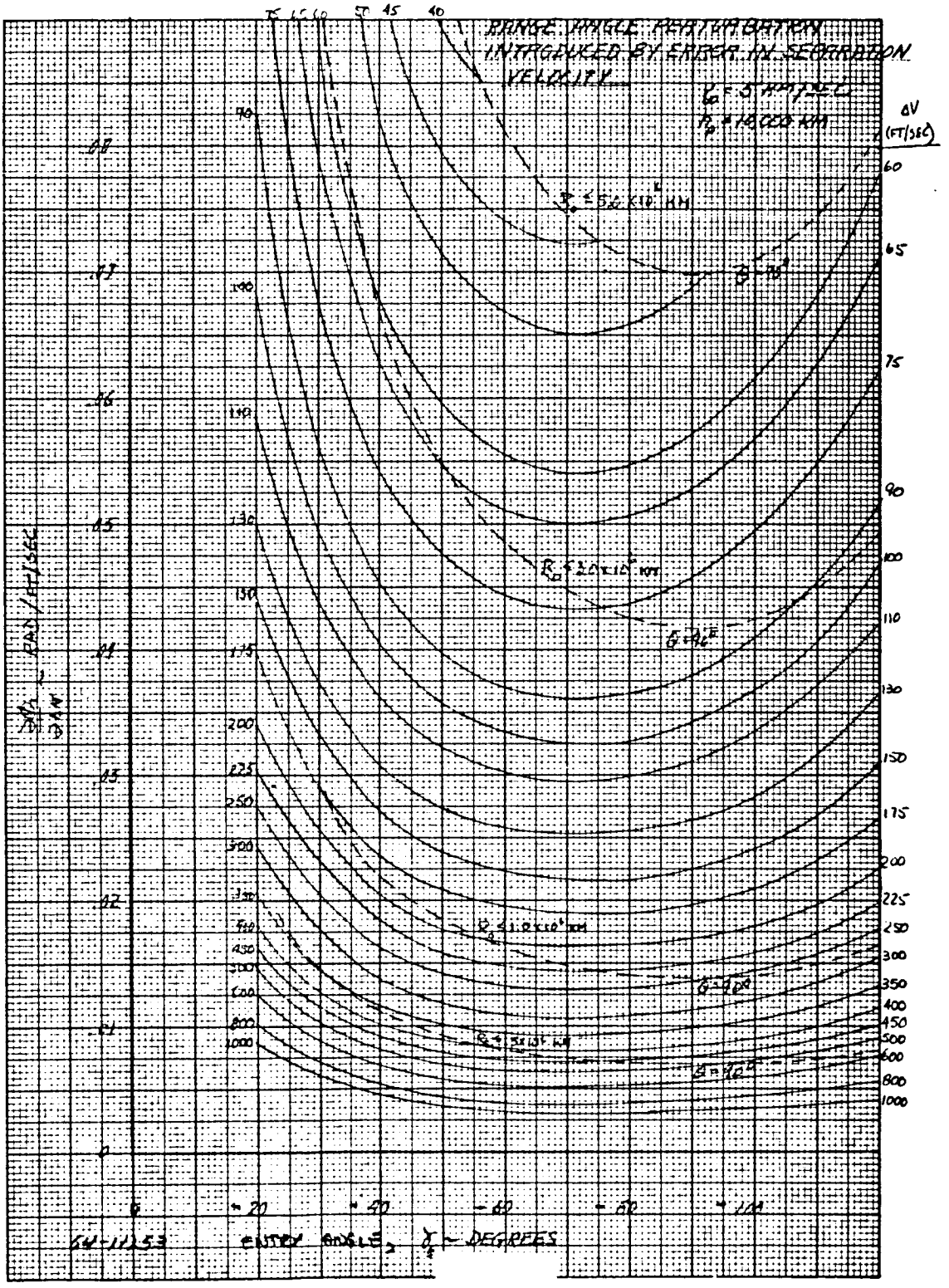

Figure 100 RANGE ANGLE PERTURBATION INTRODUCED BY ERROR IN SEPARATION VELOCITY

RE-ORDER No. 64-522

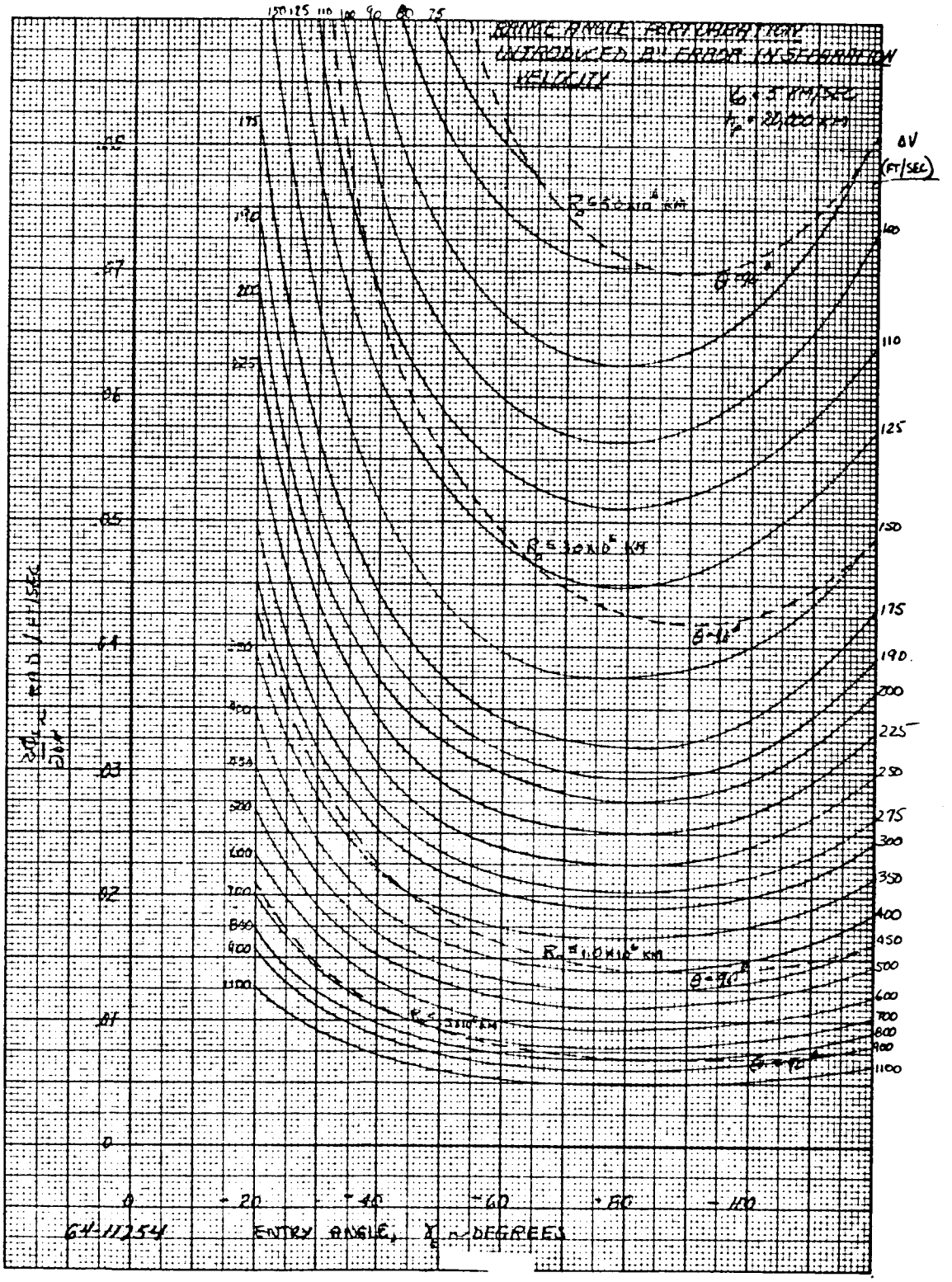

Figure 101 RANGE ANGLE PERTURBATION INTRODUCED BY ERROR IN SEPARATION VELOCITY

RE-ORDER No. 64-522

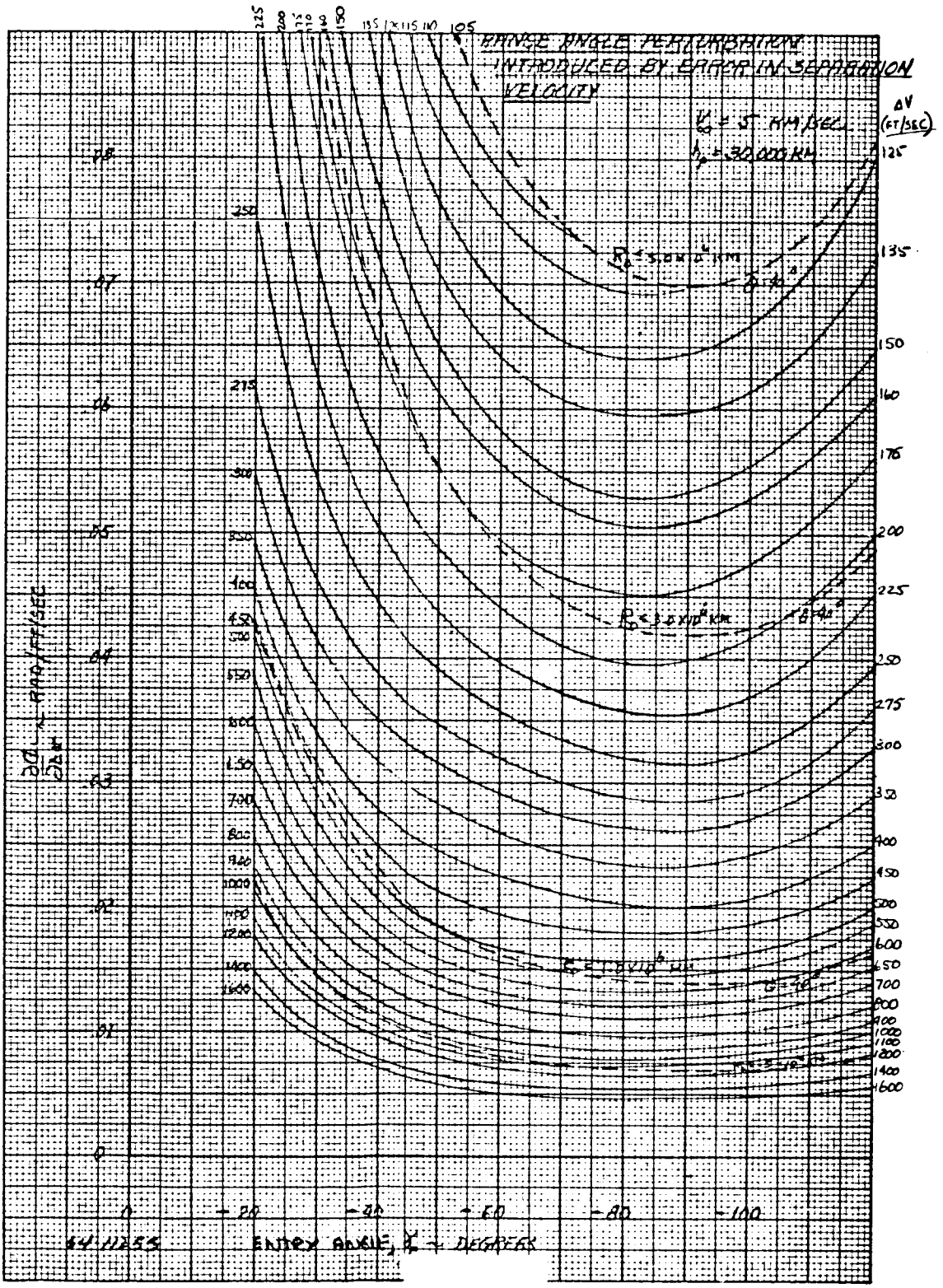

Figure 102 RANGE ANGLE PERTURBATION INTRODUCED BY ERROR IN SEPARATION VELOCITY

RE-ORDER No. 64-522

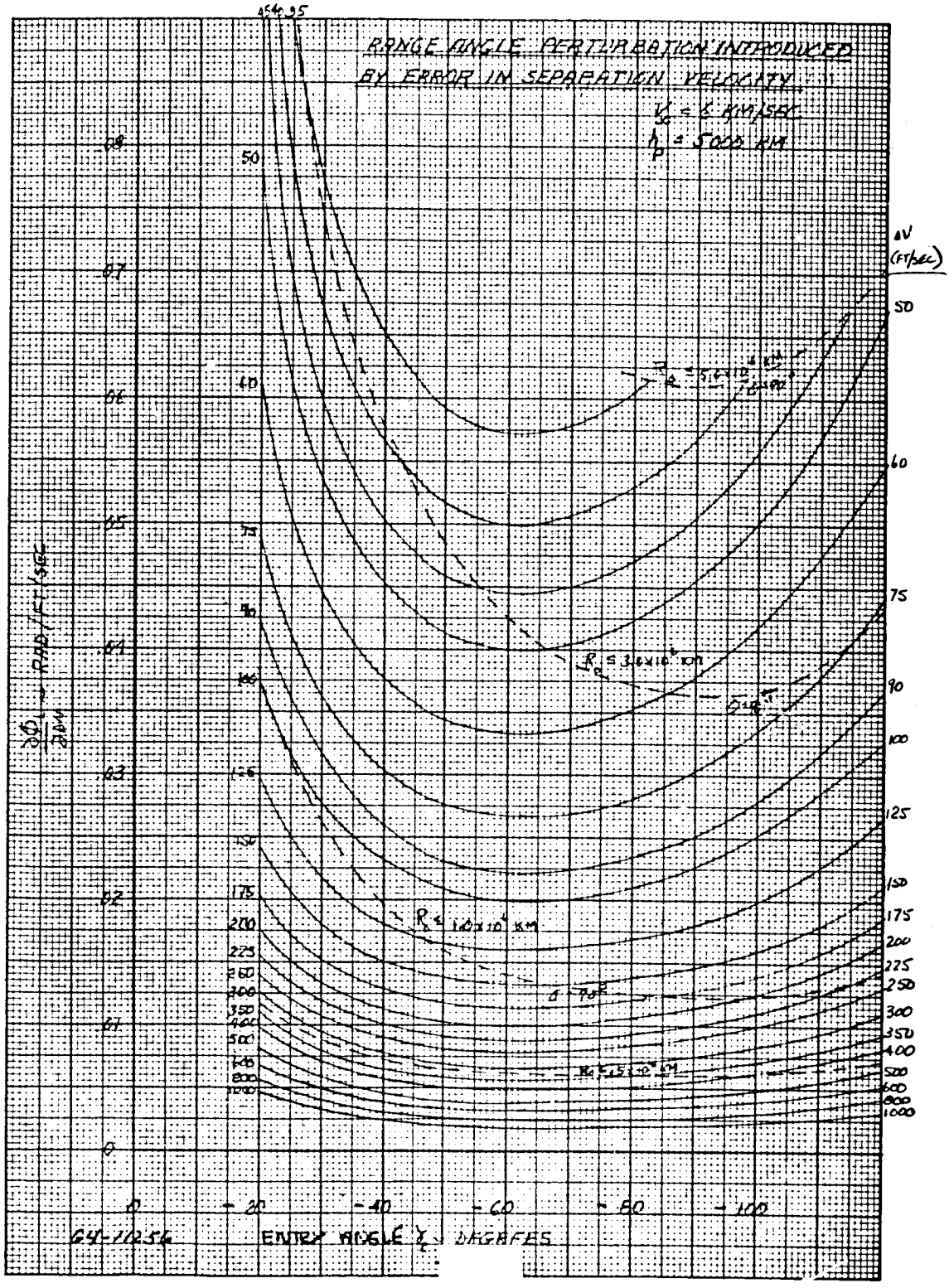

Figure 103 RANGE ANGLE PERTURBATION INTRODUCED BY ERROR IN SEPARATION VELOCITY

RE-ORDER No. 64-522

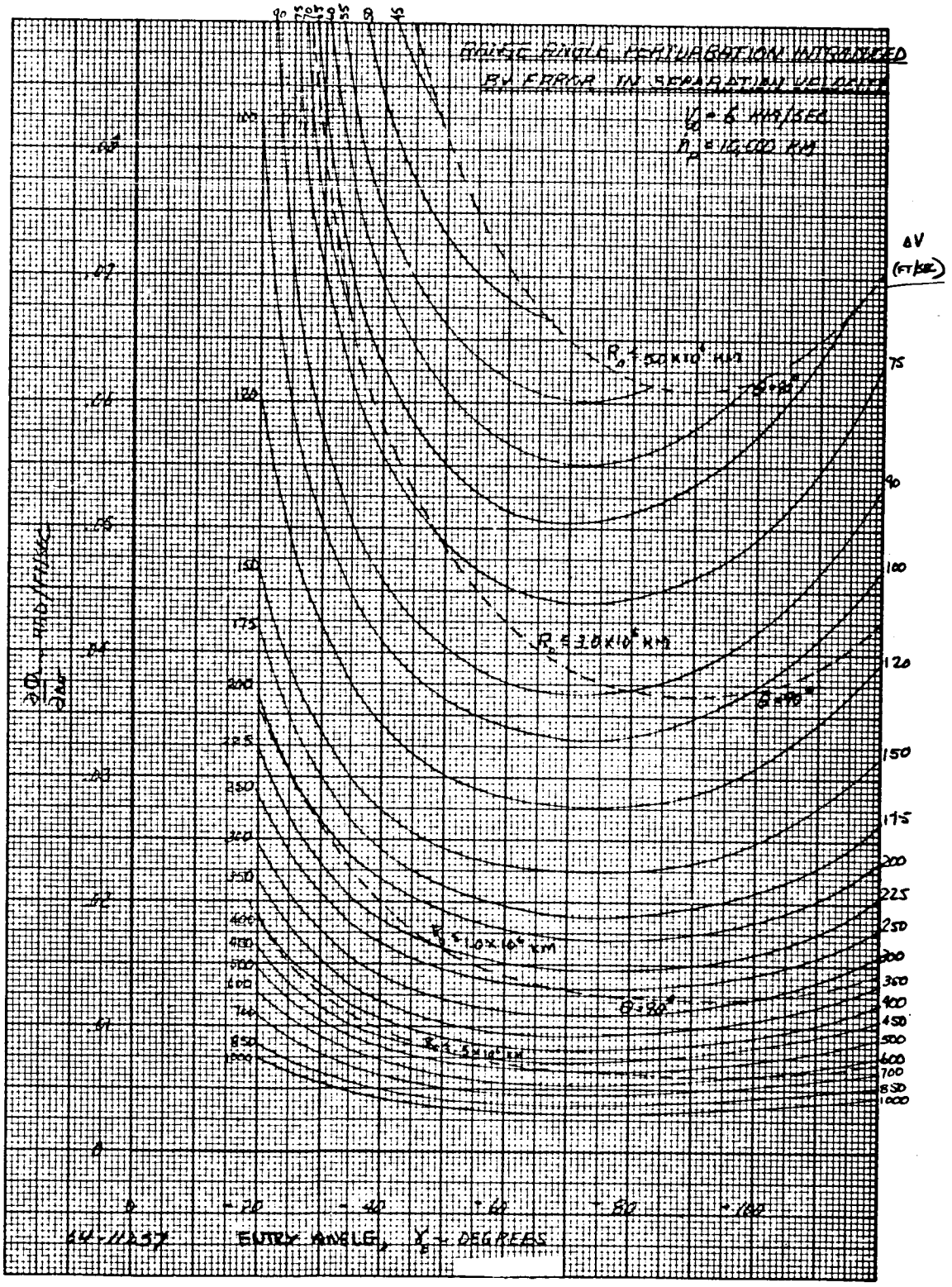

Figure 104 RANGE ANGLE PERTURBATION INTRODUCED BY ERROR IN SEPARATION VELOCITY

RE-ORDER No. 64-522

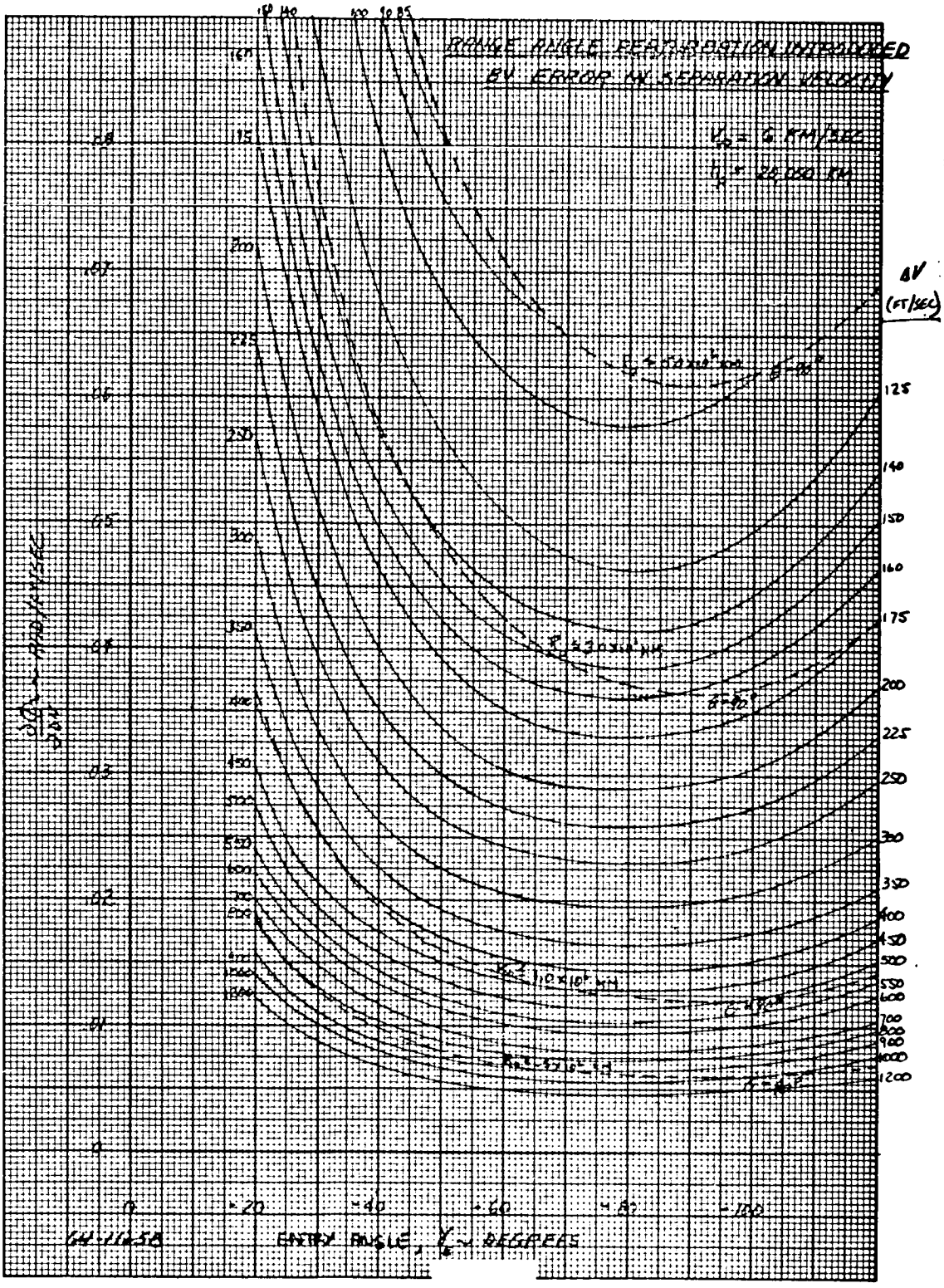

Figure 105 RANGE ANGLE PERTURBATION INTRODUCED BY ERROR IN SEPARATION VELOCITY

207

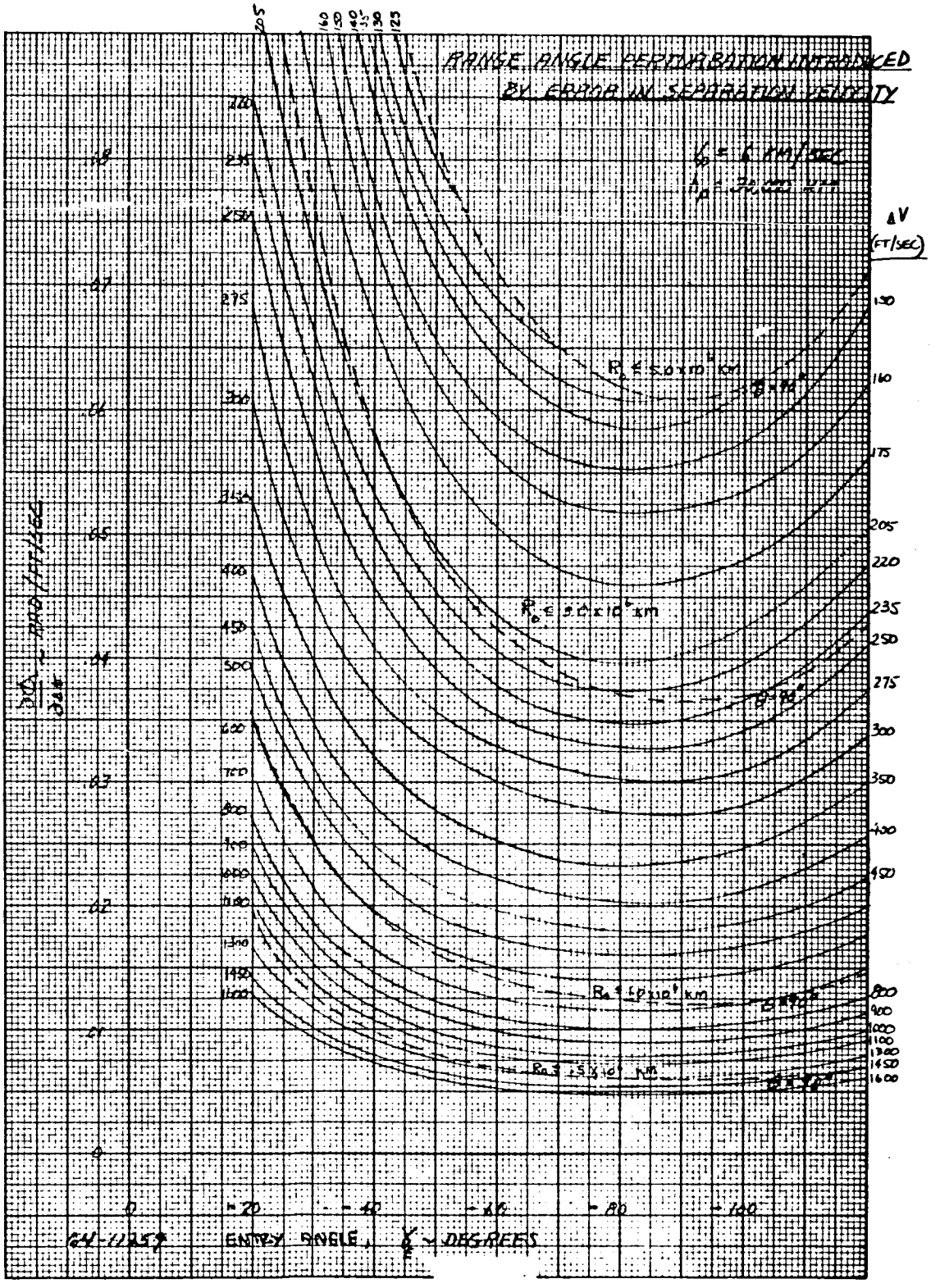

Figure 106 RANGE ANGLE PERTURBATION INTRODUCED BY ERROR IN SEPARATION VELOCITY

RE-ORDER No. 64-522

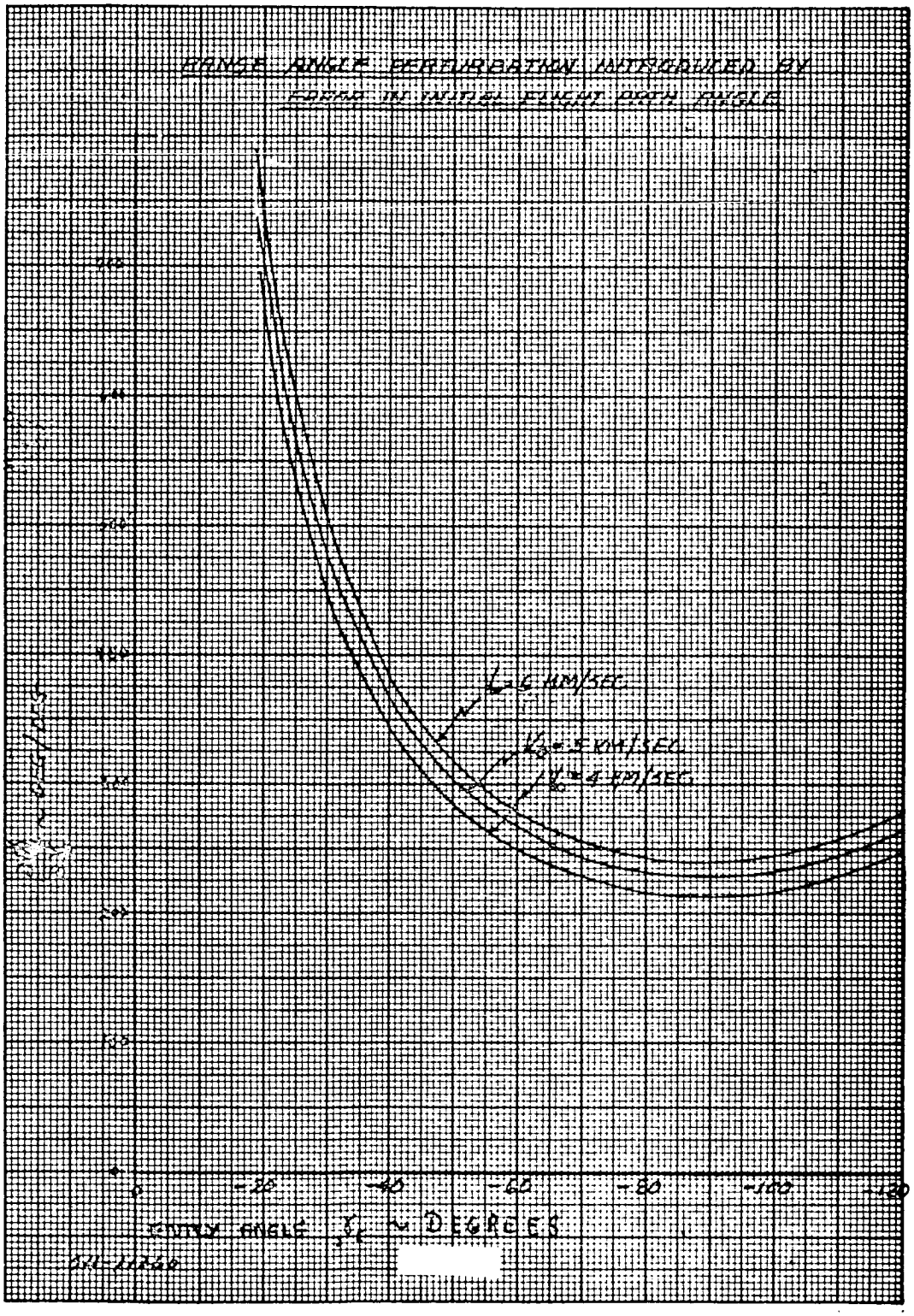

Figure 107 RANGE ANGLE PERTURBATION INTRODUCED BY ERROR IN INITIAL FLIGHT PATH ANGLE

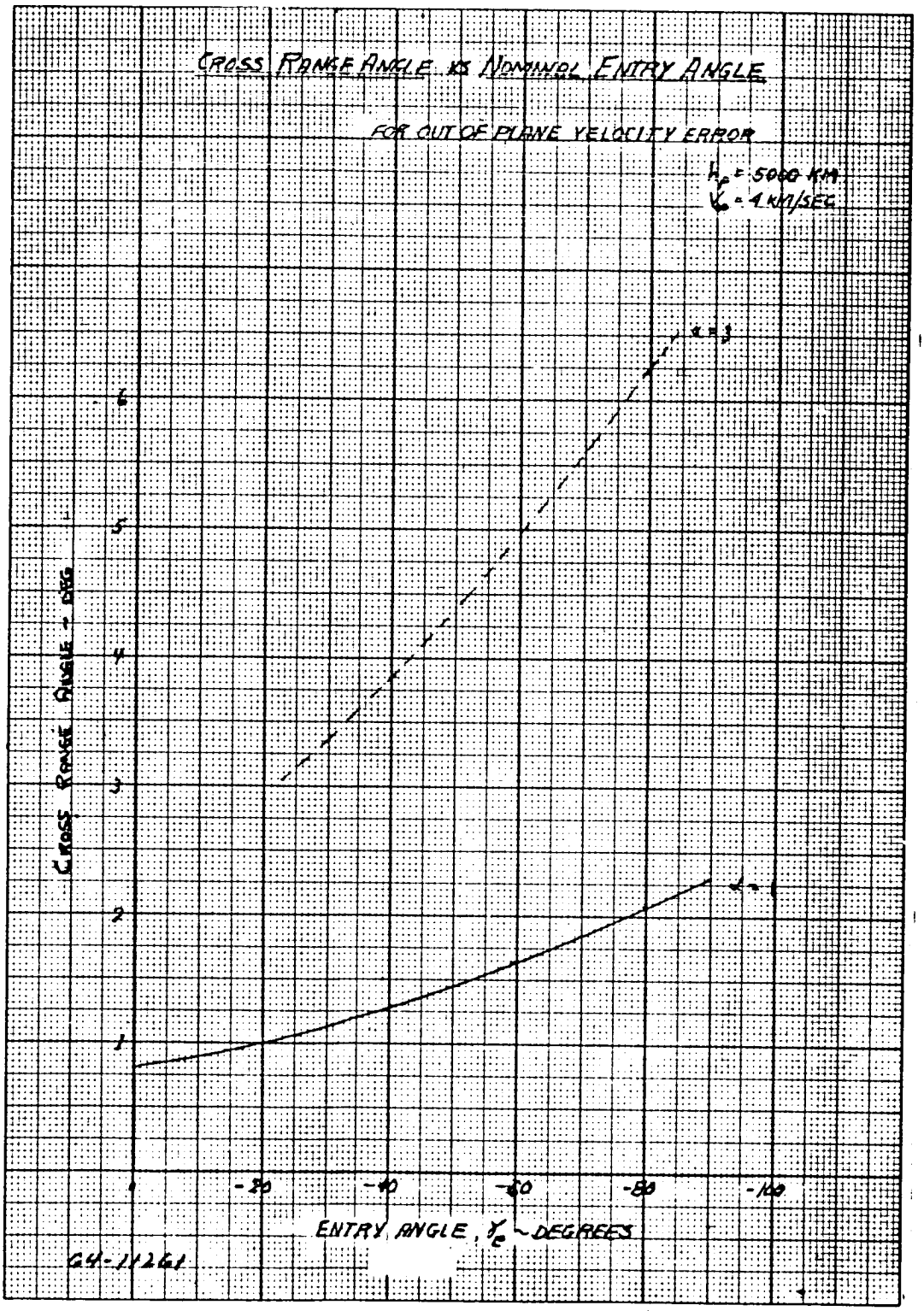

Figure 108 CROSS RANGE ANGLE VERSUS NOMINAL ENTRY ANGLE

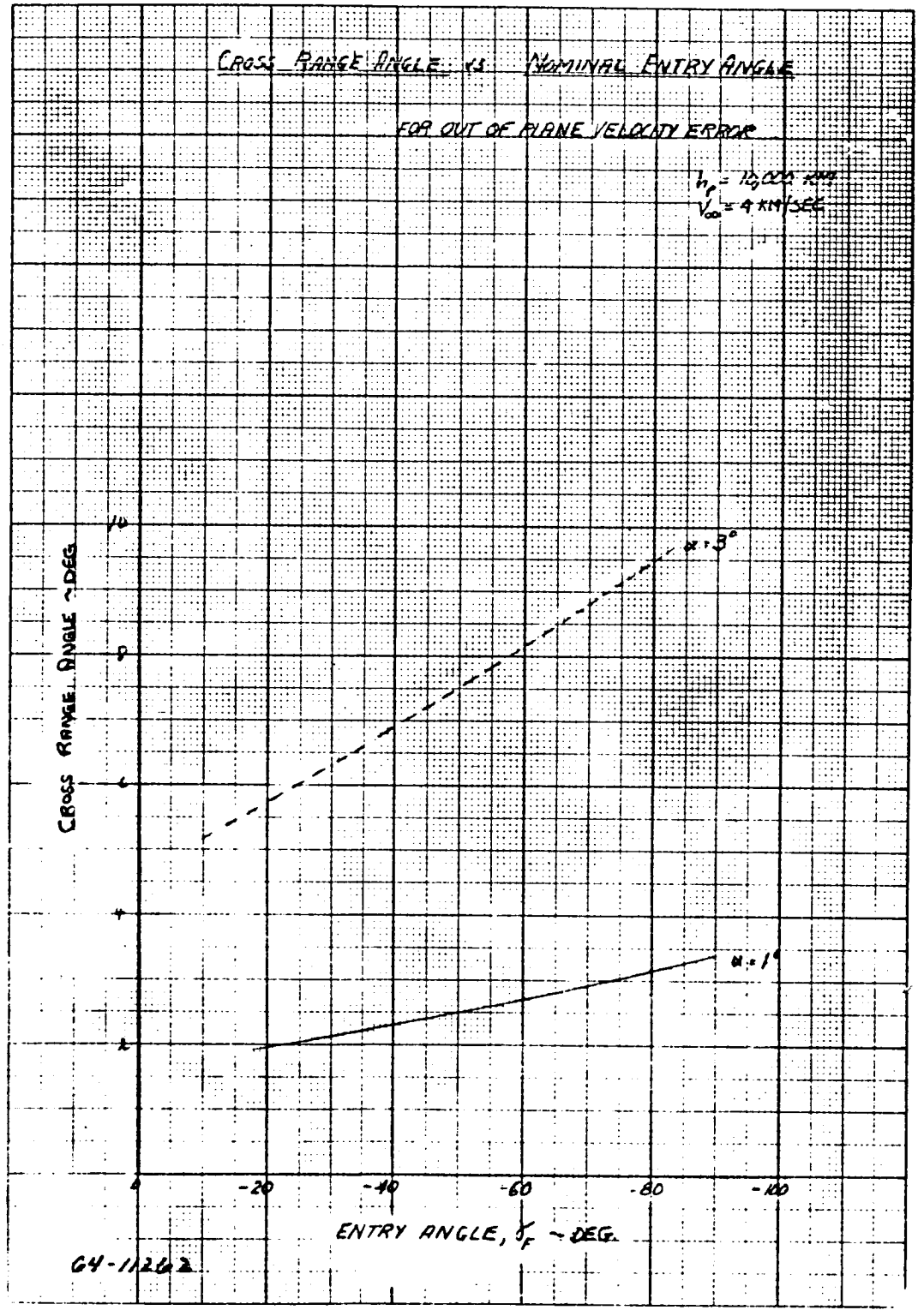

Figure 109 CROSS RANGE ANGLE VERSUS NOMINAL ENTRY ANGLE

RE-ORDER No. 64-522

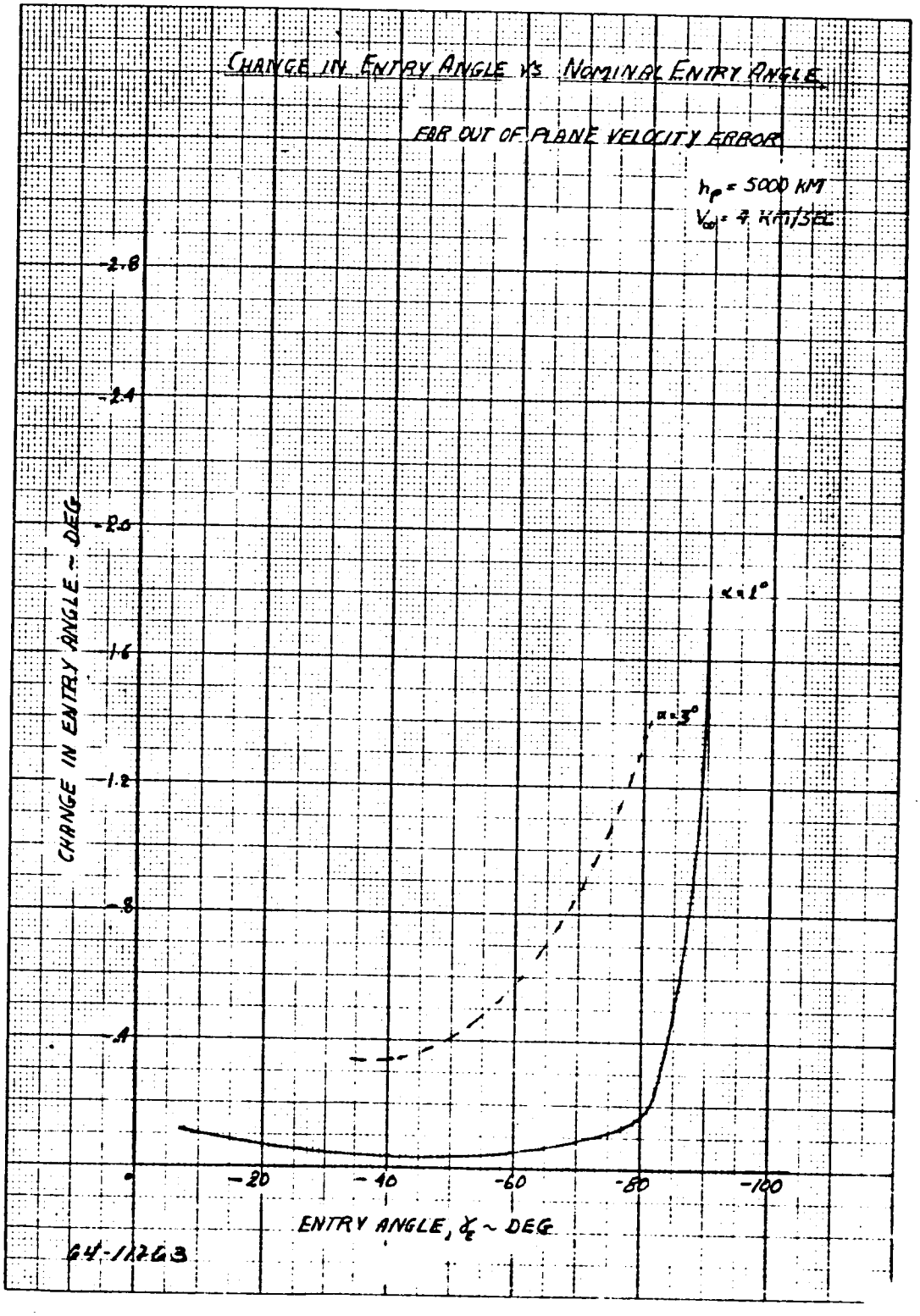

Figure 110 CHANGE IN ENTRY ANGLE VERSUS NOMINAL ENTRY ANGLE

RE-ORDER No. 64-522

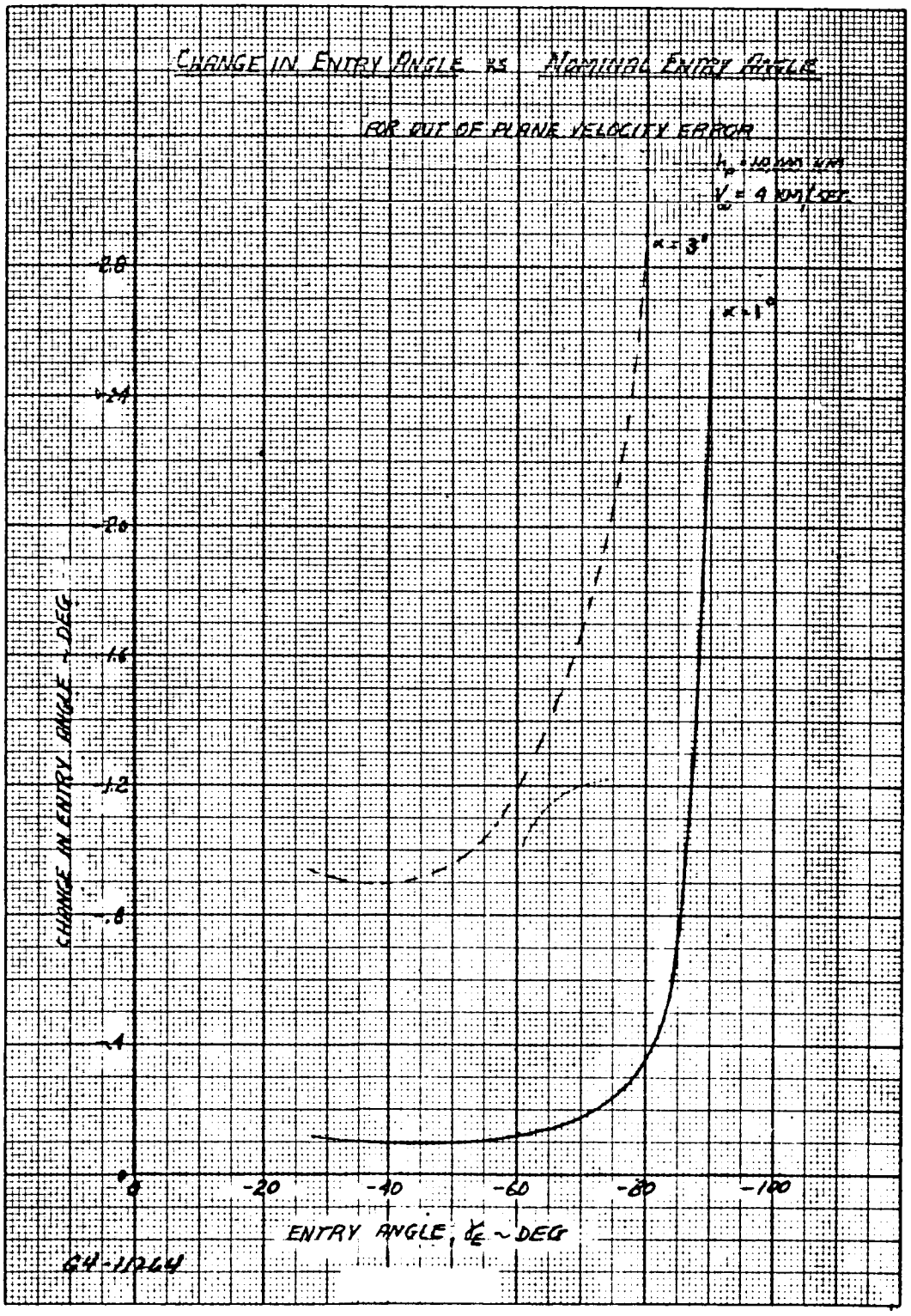

Figure 111 CHANGE IN ENTRY ANGLE VERSUS NOMINAL ENTRY ANGLE

RE-ORDER No. 64-522

3.3 MINIMUM ENTRY ANGLE DETERMINATION

For the minimum postulated Martian atmosphere, atmosphere G, an analysis was conducted to determine the minimum entry angle, for a direct, nonskip, ballistic entry trajectory as a function of m/C_DA. This analysis was conducted using a modular reentry trajectory program where the vehicle is simulated by a point mass. The importance of this analysis stems from the relationship between the lander entry angle and range angle,

$$|\gamma_e| + |\phi_e| \approx 90°;$$

which determines the maximum planetocentric angle of lander impact site from the approach velocity asymptote.

For thrust application angles of 90 degrees the relationship between the hyperbolic approach velocity and the entry velocity presented in figure 112 is seen to be independent of entry angle, periapsis altitude and separation range. The skip-out angle is presented in figure 113 as a function of entry velocity and m/C_DA. For a nominal approach velocity of 4 km/sec and a vehicle m/C_DA of 0.35 slugs/ft^2 the skip-out angle is -15.8 degrees. Due to the extreme sensitivity of skip-out angles at hyperbolic velocities this analysis assumed that the vehicle would skip-out of the atmosphere if the flight path angle became positive. For the maximum postulated atmosphere, atmosphere K, the skip-out angle is approximately 2.5 degrees less for an m/C_DA of 0.35 slugs/ft.^{2}

In the event the vehicle developed and maintained a positive lift with an L/D ratio of 0.5 the vehicle would skip above an altitude of 500,000 feet, with an entry velocity corresponding to an approach velocity of 4 km/sec for entry angles less than -20 degrees. These data are presented parametrically in figure 114 as a function of entry velocity for an m/CDA of 0.35 slugs/ft^2.

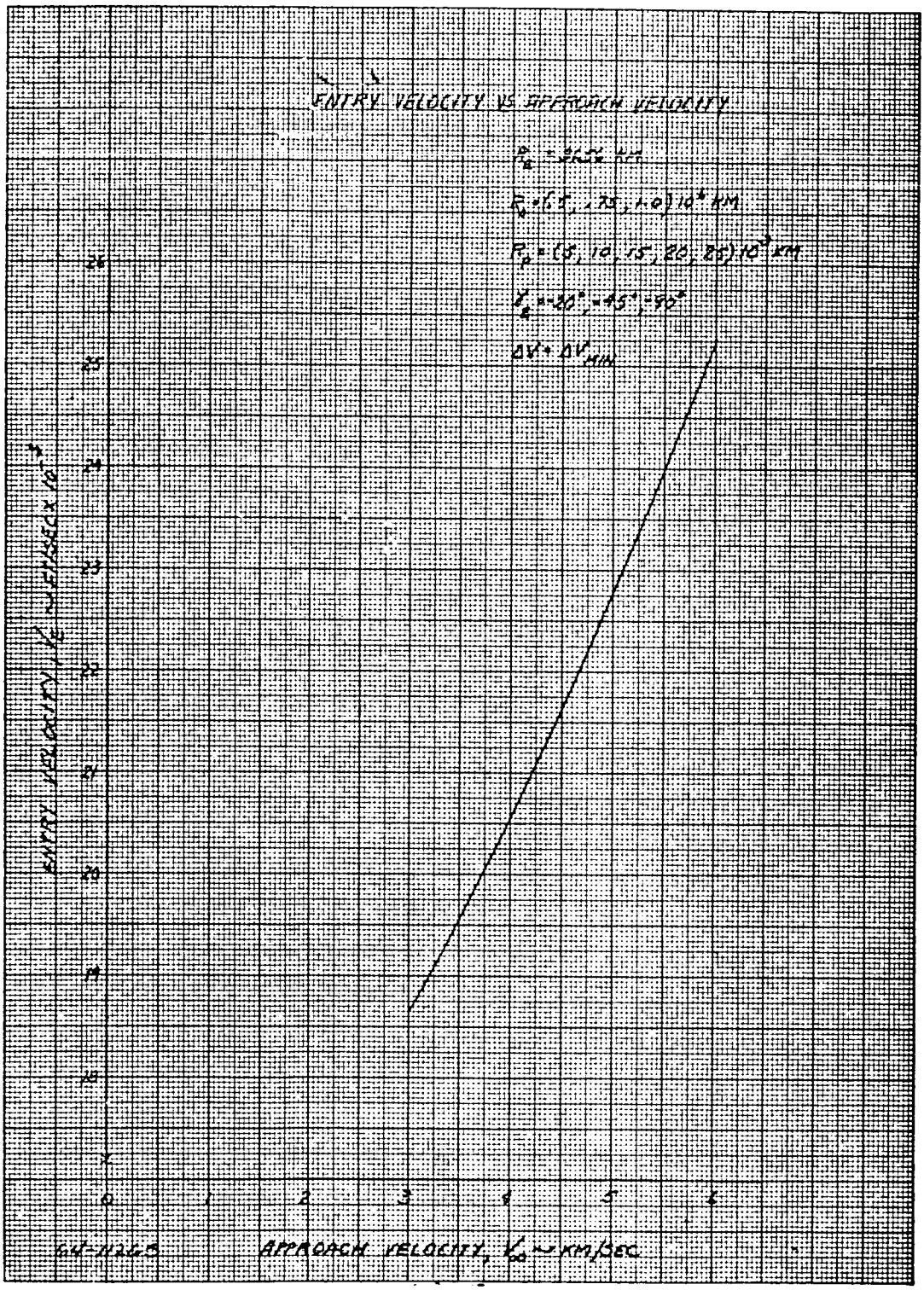

Figure 112 ENTRY VELOCITY VERSUS APPROACH VELOCITY

RE-ORDER No. 64-522

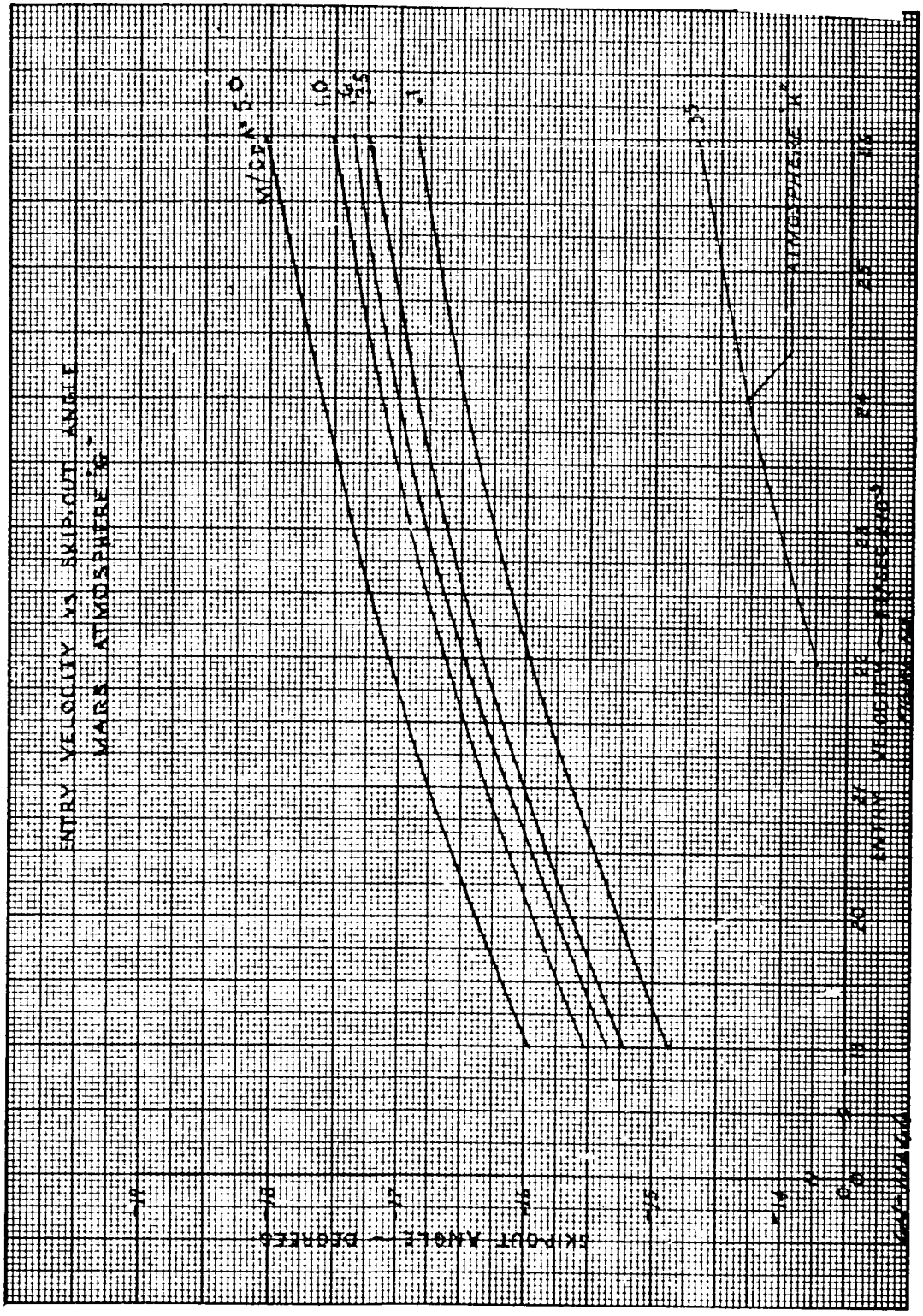

Figure 113 ENTRY VELOCITY VERSUS SKIP-OUT ANGLE

RE-ORDER No. 64-522

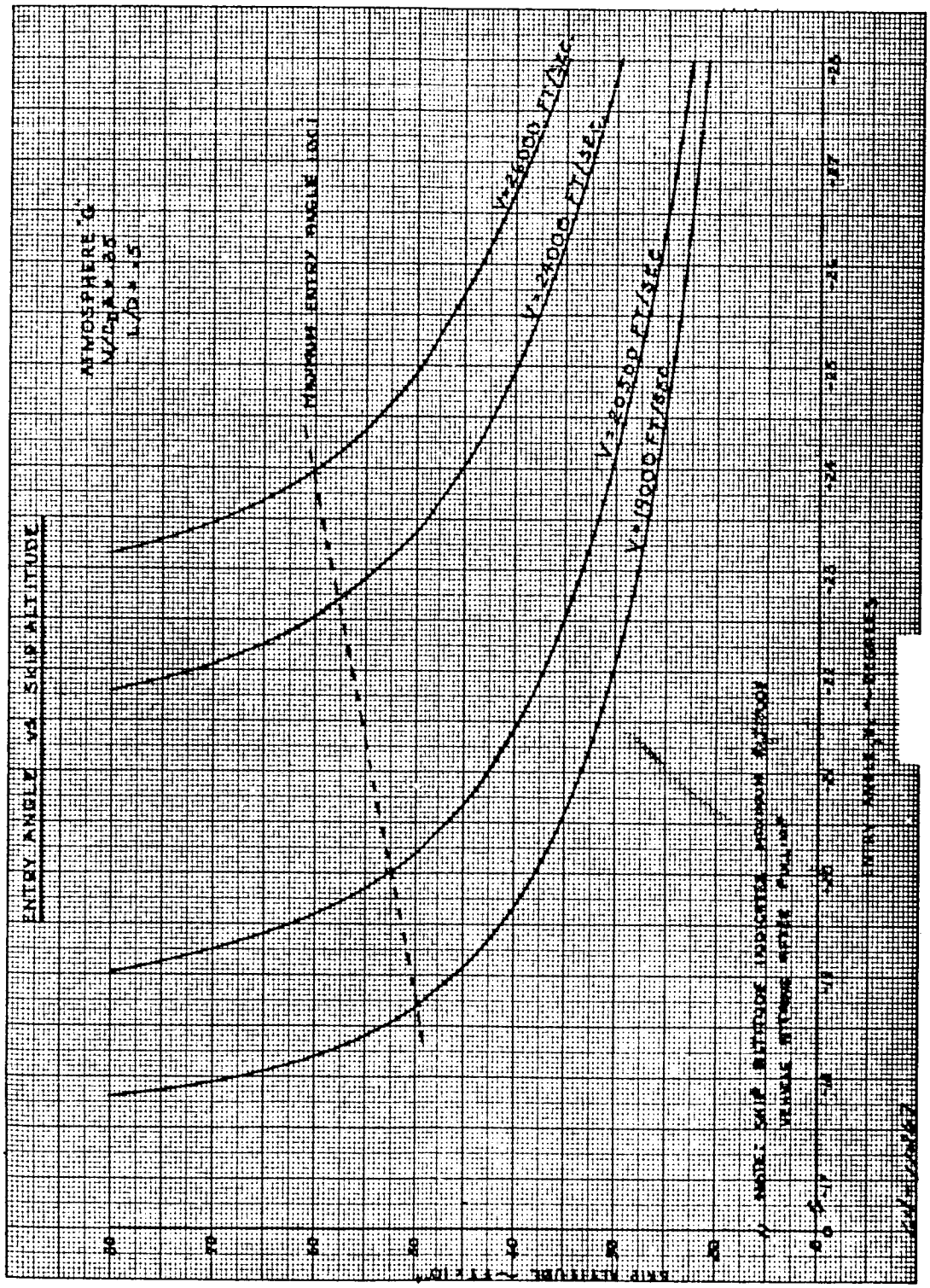

Figure 114 ENTRY ANGLE VERSUS SKIP ALTITUDE

RE-ORDER No. 64-522

3.4 LANDER-FLYBY COMMUNICATION

There are two distinct critical problem areas which must be analyzed to insure an adequate lander -flyby communication relay link for transmission of both pre-impact telemetry data and post-impact science data. The first factor which must be considered is the development of the appropriate lander lead time such that the flyby is in range for both periods of communication; the second requires a sufficient variation between the respective orbit inclinations so that the lander will not rotate out of view of the flyby as it approaches the lander latitude.

The lead time requirement can be achieved by either of two separate maneuvers: lander speedup or bus slowdown. However, the lander separation analysis indicated that due to the rapid increase in the uncertainty of the entry parameters as the thrust application angle is reduced from 90 degrees, bus slowdown is the better solution provided the bus engine has the restart capability to perform the slowdown maneuver.

This present parametric analysis was conducted to show the time gain associated with a bus slowdown maneuver with the resultant periapsis perturculation as a function of separation ramp, approach velocity and nominal passing altitude.

This maneuver must be analyzed not only in connection with lead time requirement but also with respect to perturbations in the flyby periapsis altitude introduced by the application of a significant velocity decrement. The time from separation to nominal flyby periapsis, t_{BSP}, is shown in figure 115 as a function of separation range and approach velocity. This time is essentially independent of the periapsis radius for radii between 5,000 and 25,000 km. The lead time, defined as the difference in times between flyby separation to periapsis, t_{BSP}, and lander separation to entry, t_{LSE}, associated with the unperturbed flyby trajectory is presented in figure 116. Although the lead times associated with this maneuver are less than 0.5 hours, the lead time appears to be a function of passing altitude in addition to entry angle. Since the time from lander separation to entry is constant for a given entry angle, the dependence of the curve on passing altitude indicates the variation in the flyby time from separation to periapsis. The lead time is a function of passing altitude in addition to entry angle; but, since the lead times associated with this maneuver are less than 0.5 hours, t_{BSP} is indeed essentially independent of passing altitude. With the introduction of a bus slowdown maneuver there will be a definite separation range dependence associated with the lead time.

To determine the range of reasonable separation velocities, the time gain, time from separation to perturbed periapsis, t_{BSPP}, minus time from separation to nominal periapsis, t_{BSP}, was analyzed for separation ranges up to 5×10^6 km and slowdown velocities to 6,000 fps for an approach velocity of 4 km/sec and a nominal periapsis altitude of 10,000 km. These data presented in figure 117 indicate that the time gain varies nearly linearly with both seperation range and separation velocity. For a separation velocity of 1,000 ft/sec at a range of

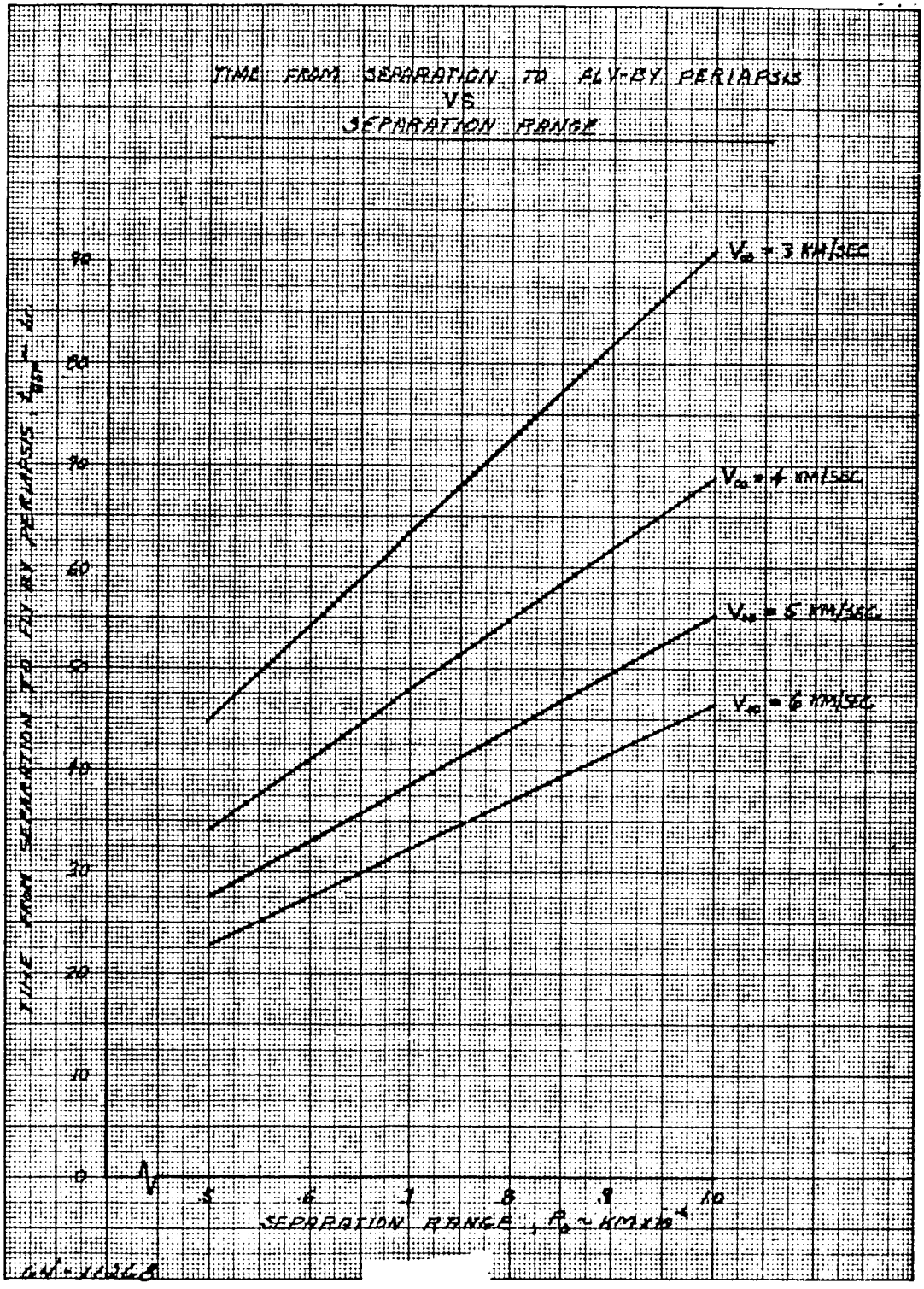

Figure 115 TIME FROM SEPARATION TO FLYBY PERIAPSIS VERSUS SEPARATION RANGE

RE-ORDER No. 64-522

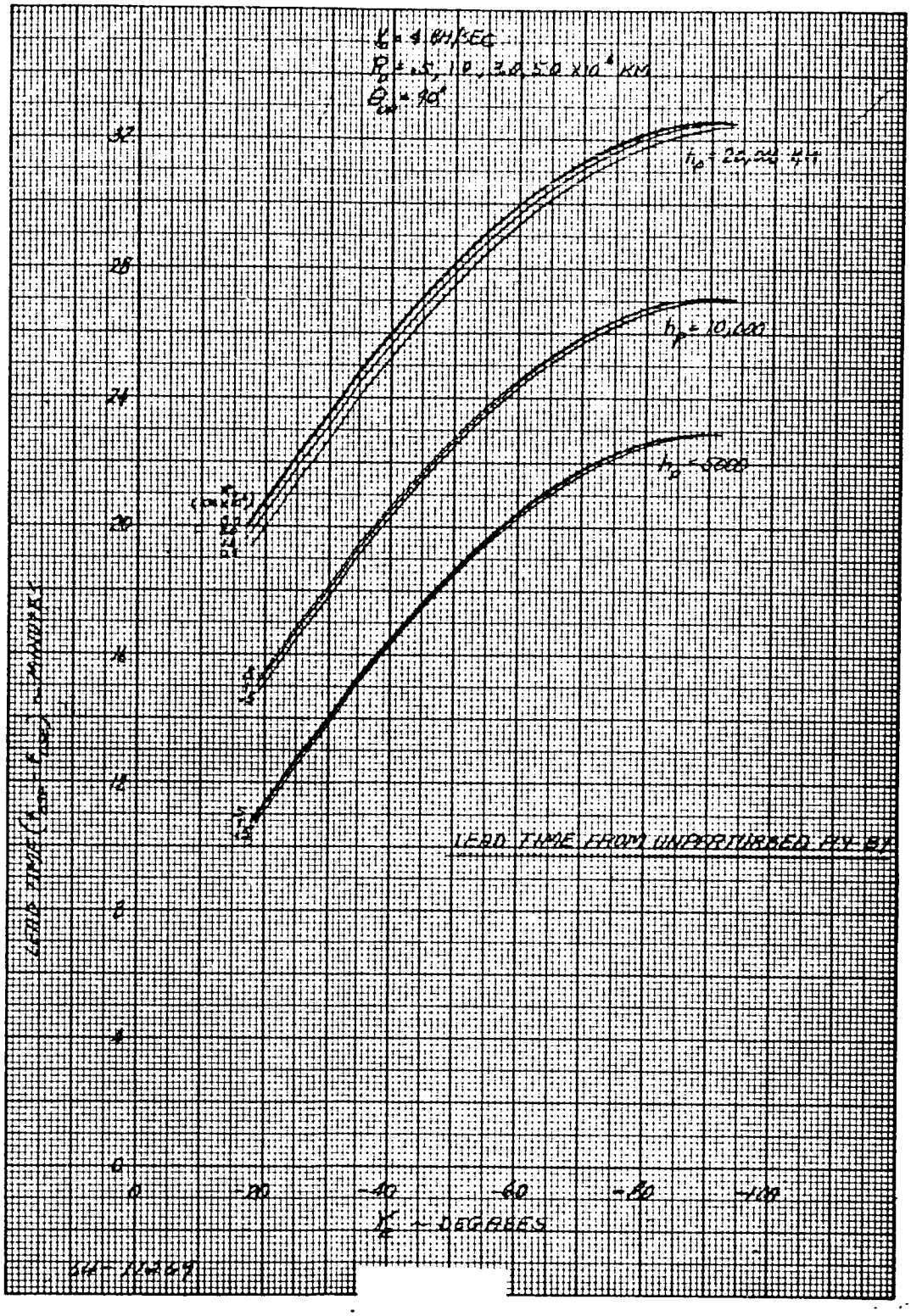

Figure 116 LEAD TIME FROM UNPERTURBED FLYBY

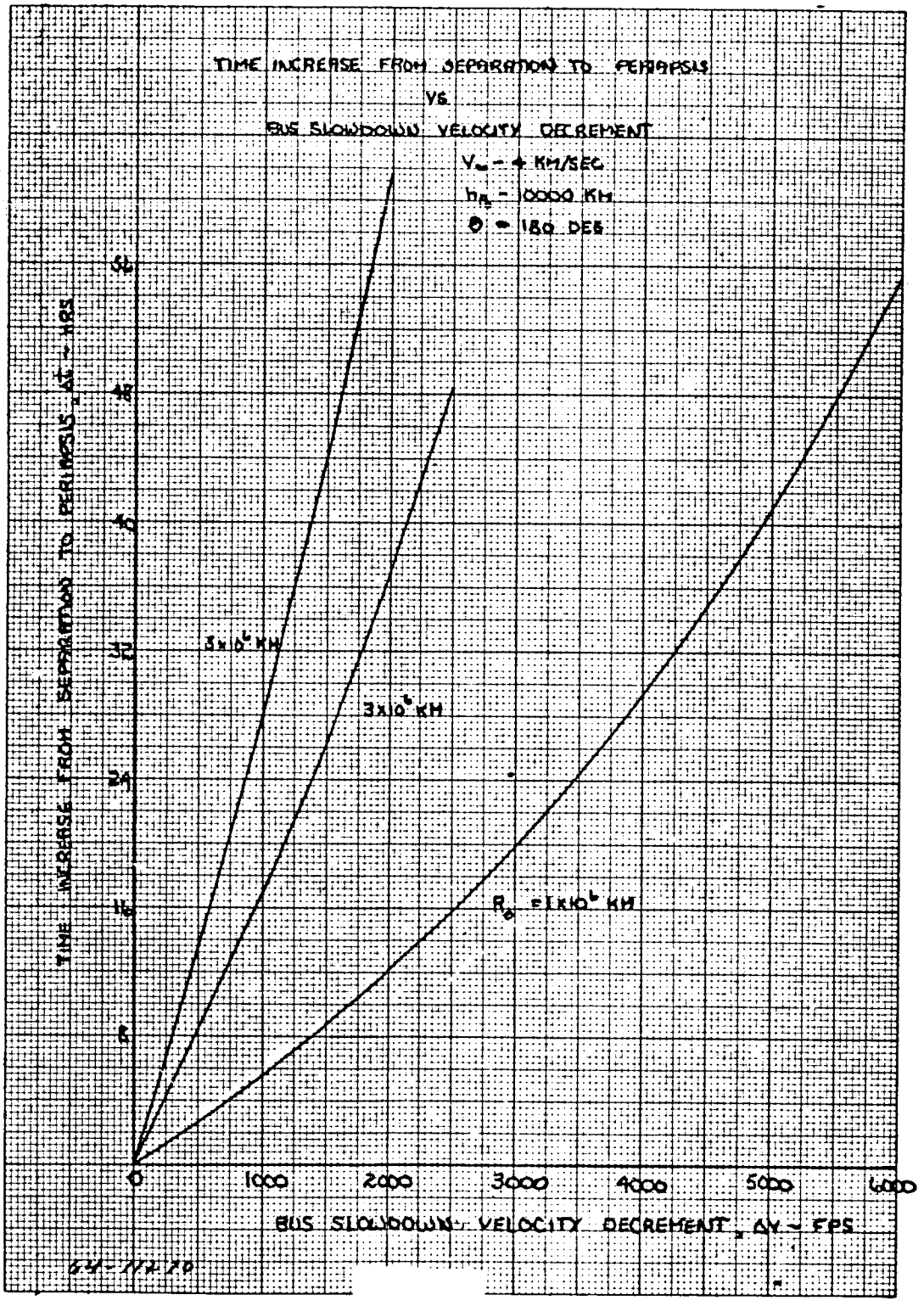

Figure 117 TIME INCREASED FROM SEPARATION TO PERIAPSIS VERSUS BUS SLOWDOWN VELOCITY DECREMENT

10^6 km the time gain is 5.5 hours. Since the desired nominal life of the landed science package is approximately 5 hours, a more comprehensive analysis was conducted parametrically for separation velocities up to 1,000 ft/sec. In this analysis presented in figure 118, the following range of parameters was investigated:

1. nominal periapsis altitude, 5,000-30,000 km
2. approach velocity, 3-5 km/sec
3. separation range, 10^6 - 5 x 10^6 km

This analysis shows not only the time gain but also the variation in the periapsis altitude associated with thrust application angles of 180 degrees, i.e., slowdown velocity applied to change magnitude of the approach velocity but not the direction. These results again indicate that there is essentially no dependence of either time gain or the decrease in periapsis altitude with periapsis altitude. For these slowdown velocities, the time gain is linear with respect to velocity with the slope increasing as the approach velocity is reduced for a constant separation range and also as the separation range is increased for a constant approach velocity. For an approach velocity of 4 km sec a time gain of 5 hours is achieved from separation ranges of 10^6 kms and 5 x 10^6 km for slowdown velocities of 900 and 190 ft/sec, respectively. For nominal passing altitudes between 5,000 and 30,000 km the decrease in periapsis altitude is linear with respect to separation velocity and is about 350 km for an approach velocity of 4 km/sec. in combination with a slowdown of 1,000 ft/sec.

Uncertainties in the periapsis altitude and lead time will be introduced through perturbations in the thrust application angle and slowdown velocity. The thrust application angle selected to produce the maximum lead time with the minimum velocity requirement produces the maximum perturbation in periapsis altitude for disturbances in the slowdown parameters. The variation in the periapsis altitude introduced by perturbations in the thrust application angle, $\partial r_{pp}/\partial \theta$, is presented parametrically in figure 119 for the spectrum of separation parameters and separation velocities. These data indicate a relatively strong dependence on approach velocity while again there is essentially no dependence on periapsis altitude and seperation range for a particular lead time. For an approach velocity of 4 km/sec there is a variation of 1,330 km in the periapsis altitude associated with a 1 degree uncertainty in the thrust application angle for a 5-hour slowdown maneuver (900 ft/sec at 10^6 km and 190 ft/sec at 5 x 10^6 km).

The variation in the periapsis altitude due to perturbations in the slowdown velocity, $\partial r_{pp}/\partial \Delta V$, is presented in figure 120. These data exhibit only mild dependence on separation range and a dependence on periapsis altitude that becomes stronger as the approach velocity decreases indicating that the contribution to uncertainty in periapsis by perturbations in the separation velocity will be minimized by employing the minimum separation velocity to achieve a specific time

RE-ORDER No. 64-522

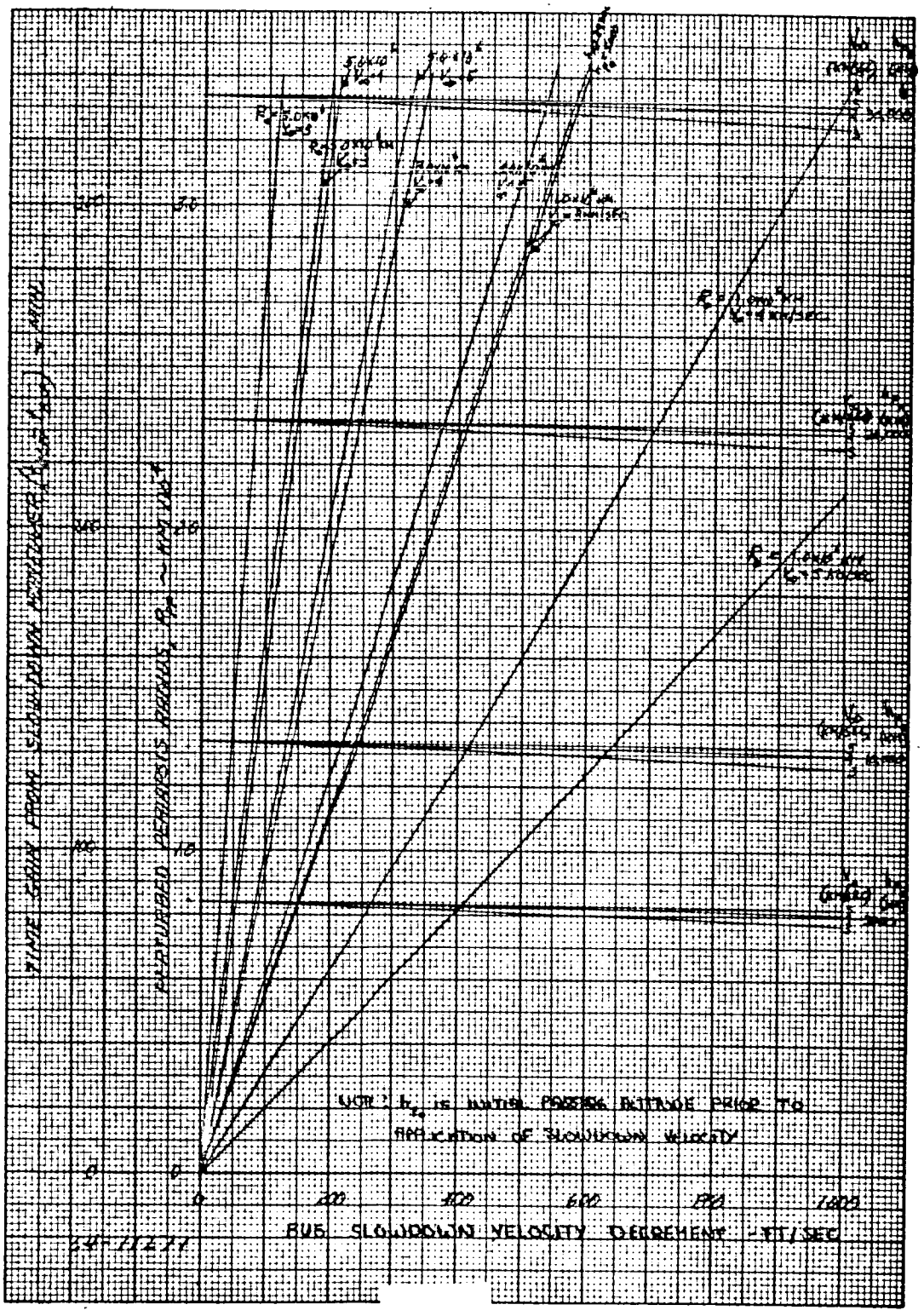

Figure 118 TIME GAIN FROM SLOWDOWN AND PERTURBED PERIAPSIS VERSUS PERTURBING VELOCITY

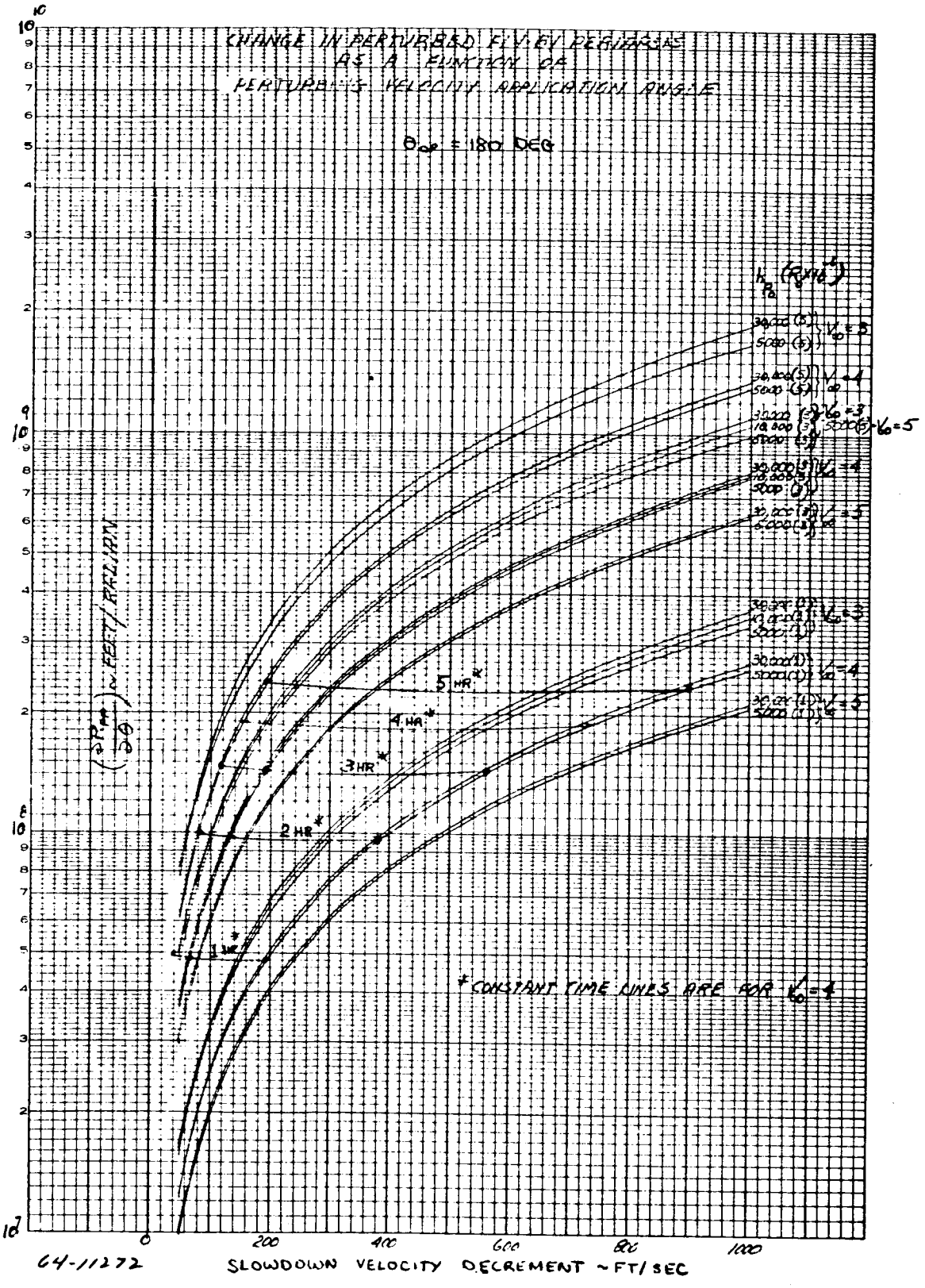

Figure 119 CHANGE IN PERTURBED FLYBY PERIAPSIS AS A FUNCTION OF PERTURBING VELOCITY APPLICATION ANGLE

RE-ORDER No. 64-522

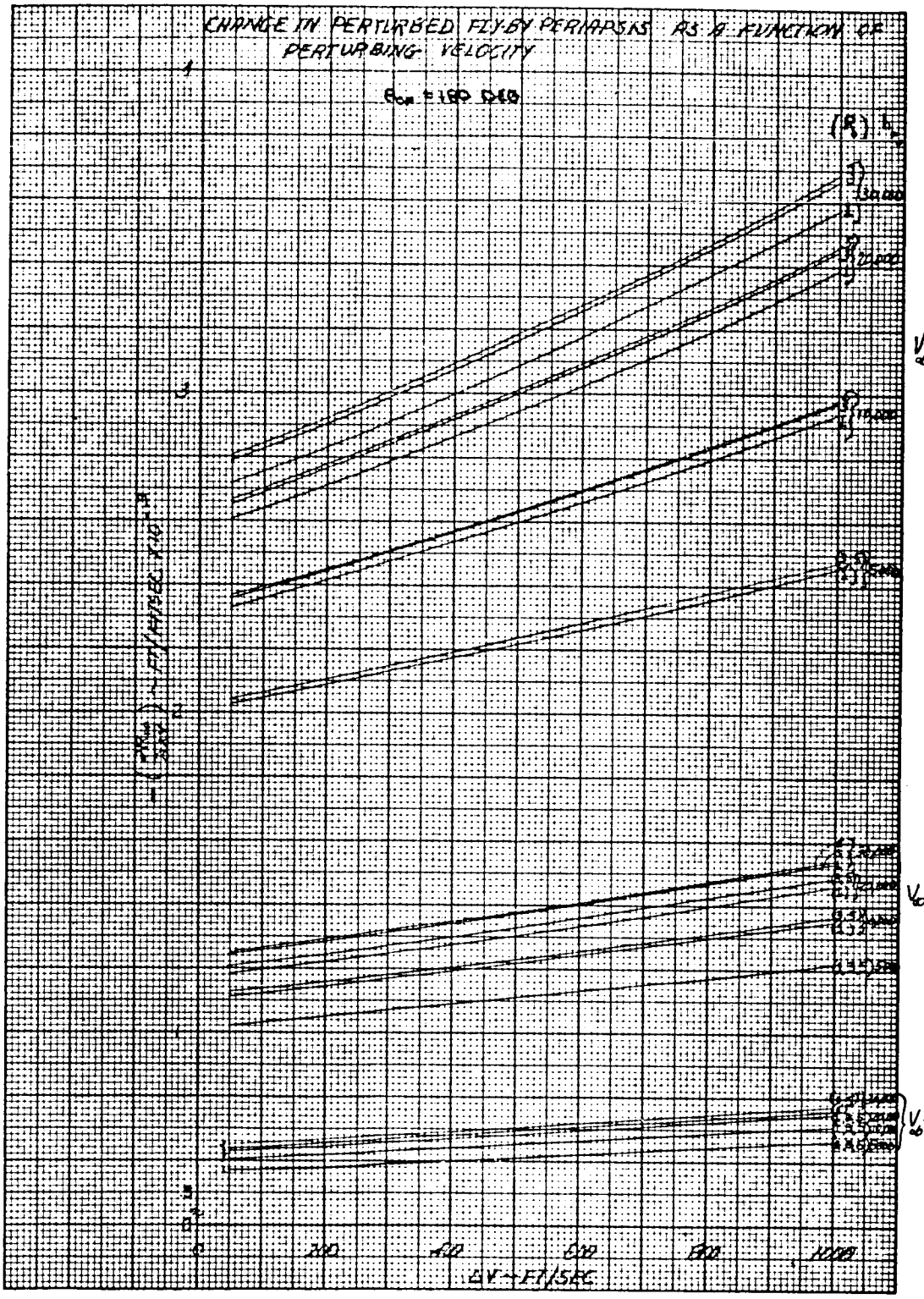

Figure 120 CHANGE IN PERTURBED FLYBY PERIAPSIS AS A FUNCTION OF PERTURBING VELOCITY

RE-ORDER No. 64-522

gain. For an approach velocity of 4 km/sec, the variation in periapsis altitude is approximately 0.4 km for a 1 ft/sec uncertainty in velocity. This indicates that slowdown velocity errors can be neglected as an appreciable error source producing perturbations in the periapsis altitude when the thrust application angle is 180 degrees.

For the same error sources, a similar analysis was conducted to determine the variation in time to periapsis, $\partial t/\partial \theta$ and $\partial t/\partial \Delta V$, and these results presented in figures 121 and 122 indicate that for normal errors, i.e., 1 percent error in separation velocity and 1 degree uncertainty in the thrust application angle, the variation in time is about 5 minutes with the velocity error the major contributor to the uncertainty.

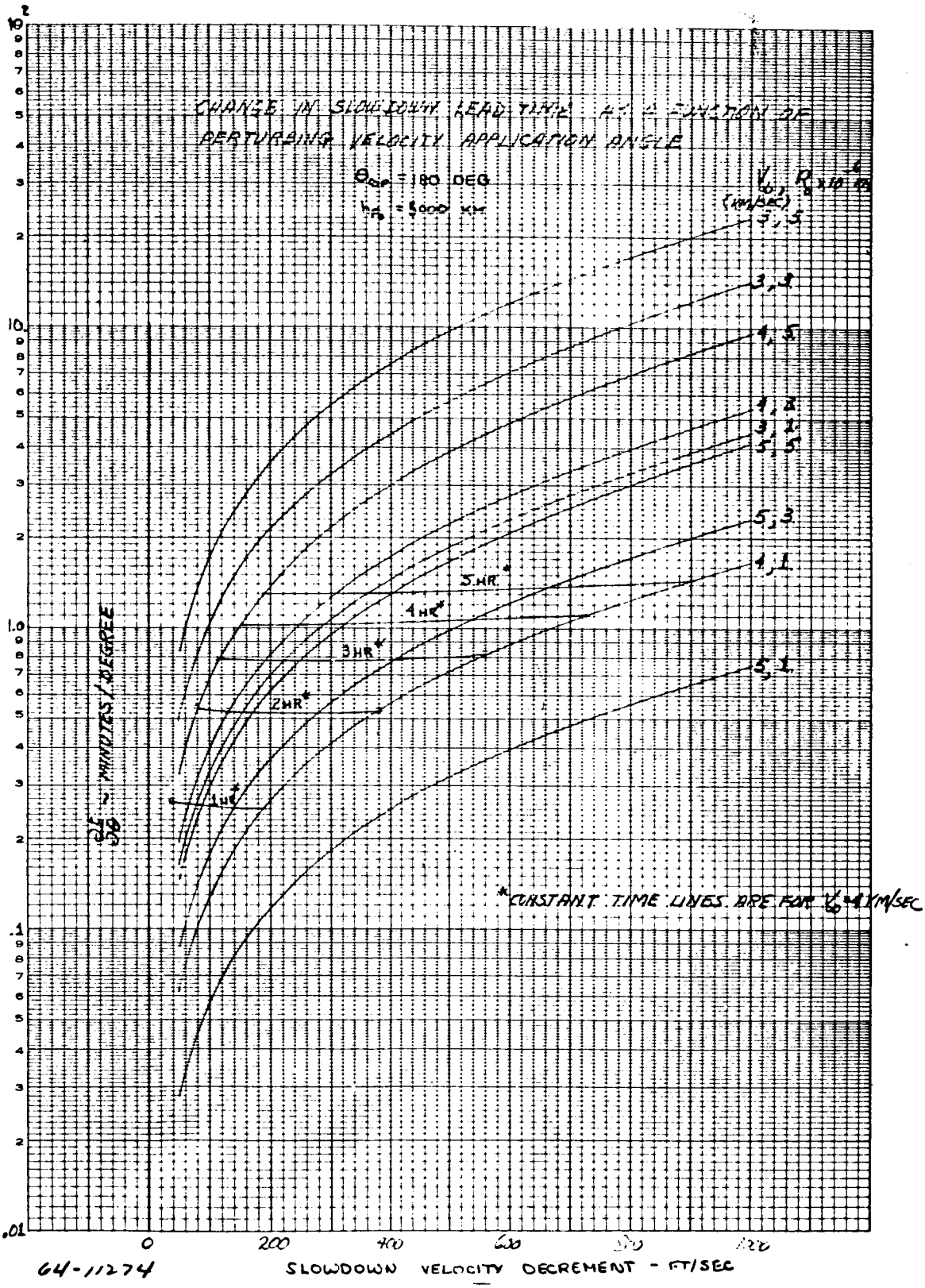

Figure 121 CHANGE IN SLOWDOWN LEAD TIME AS A FUNCTION OF PERTURBING VELOCITY APPLICATION ANGLE

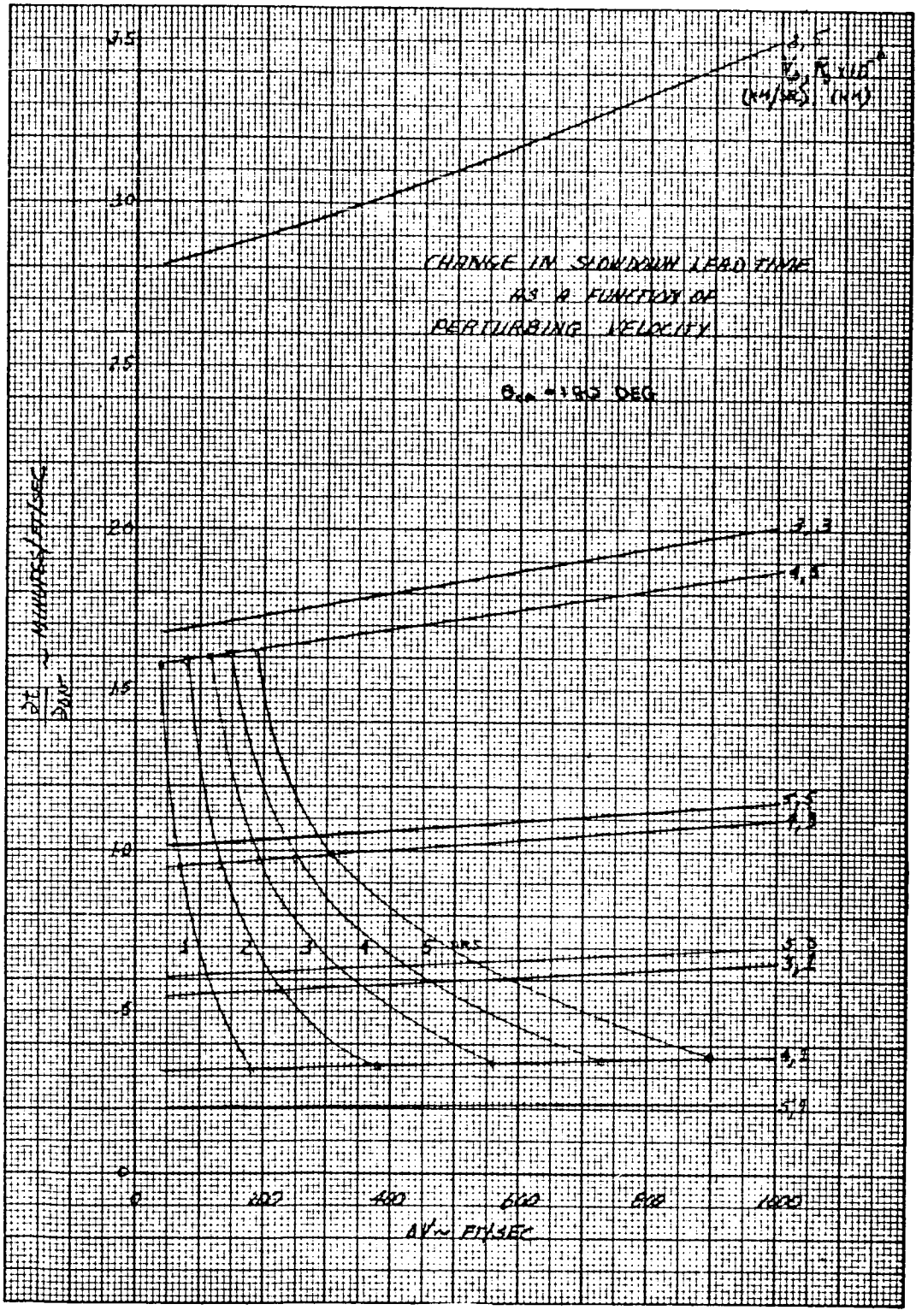

64-11275

Figure 122 CHANGE IN SLOWDOWN LEAD TIME AS A FUNCTION OF PERTURBING VELOCITY